



THE GEOLOGY OF THE ADELAIDEAN-KANMANTOO GROUP
SEQUENCES IN THE EASTERN MOUNT LOFTY RANGES

by

Stephen Toteff

B.Sc. (Hons.), University of Adelaide

Department of Geology and Mineralogy,
University of Adelaide.

November, 1977.

Awarded December 1978

CONTENTS (cont'd)

	<u>Page</u>
3. NAIRNE-MT. BARKER CREEK AREA	35
3.1 Introduction	35
3.2 Sturt Group	35
3.2.1 Tapley Hill Formation	35
3.2.2 Brighton Limestone Equivalent	37
3.3 Marino Group	37
3.3.1 Unit 1	37
3.3.2 Unit 2	40
3.3.3 Unit 3	41
3.3.4 Unit 4	46
3.3.5 Mt. Barker Quartzite	47
3.3.5.1 Stratigraphic position of the Mt. Barker Quartzite	50
3.3.6 Comparison with the Marino Group Stratotype	50
3.4 Normanville Group	51
3.5 Kanmantoo Group	52
3.5.1 Carrickalinga Head Formation	52
3.5.2 Backstairs Passage Formation	53
3.5.3 Talisker Calc-siltstone Equivalent	56
3.5.4 Tapanappa Formation	58
3.6 Conclusions	59
4. BIRDWOOD-BRUKUNGA AREA	60
4.1 Introduction	60
4.2 Precambrian	60
4.2.1 Torrens Group	60
4.2.1.1 Stoneyfell Quartzite	60
4.2.1.2 Saddleworth Formation	61
4.2.2 Sturt Group	63
4.2.2.1 Belair Sub-group	63
4.2.2.2 Tapley Hill Formation	64
4.2.2.3 Brighton Limestone	65
4.2.3 Marino Group	65
4.3 Cambrian	67
4.3.1 Carrickalinga Head Formation	68
4.3.2 Backstairs Passage Formation	70
4.4 Structure	73
4.5 Conclusions	74

CONTENTS (cont'd)

	<u>Page</u>
5. NATURE OF THE PRECAMBRIAN-KANMANTOO GROUP BOUNDARY	75
5.1 A comparison with previous work advocating an unconformity	77
PART II <u>FOLDING AND METAMORPHISM IN THE NAIRNE-MT. BARKER CREEK AREA</u>	
A: FOLDING	83
B: METAMORPHISM	86
1. INTRODUCTION	86
2. MINERAL ASSEMBLAGES AND INTERPRETATION OF TEXTURES	88
2.1 Metasiltstones	89
2.2 Metasandstones	92
2.3 Metashales	95
2.3.1 The less alluminous metashales	95
2.3.2 Peraluminous metashales	96
2.3.2.1 Phase rule considerations	97
2.3.2.2 Origin of andalusite and staurolite	99
2.3.2.3 The sillimanite problem	100
2.3.2.4 Textures in peraluminous schists	105
2.3.2.4.1 General	105
2.3.2.4.2 Textures involving andalusite and staurolite	106
2.3.2.4.3 Pressure shadows	110
2.3.2.4.4 Textures involving garnet	112
2.3.2.4.5 Textures related to the formation of fibrolite	113
2.3.2.4.5.1 Polymorphic inversion	113
2.3.2.4.5.2 The association of fibro- lite, biotite and quartz	114
2.3.2.4.5.3 The role of muscovite	117
2.3.2.4.5.4 Conclusions	122
2.3.2.4.6 Staurolite-fibrolite relations	122
2.3.2.4.7 Post-F ₃ features	124
2.4 Calc-silicates	124
2.4.1 Group one	125
2.4.2 Group two	127
2.4.3 Other assemblages	128
2.5 Marbles	129
2.6 Meta-Calcsiltstones and Calcshales	130
2.7 Quartz-Biotite Segregations	132
2.8 Basic Dykes (Meta-Dolerites)	135

CONTENTS (cont'd)

	<u>Page</u>
2.8.1 General	135
2.8.2 Textures	136
2.8.3 Minor Constituents	138
2.8.4 Comparison with the Metadolerite dykes of the Woodside area	139
2.8.5 Conclusions	141
2.9 Pegmatites	142
3. TYPE AND CONDITIONS OF METAMORPHISM	142
3.1 P-T Estimate	142
3.2 Cordierite	145
3.3 Comparisons with other Metamorphic Belts	146
4. METAMORPHIC HISTORY	147
C: FOLDING AND METAMORPHISM - ITS RELATION TO THE MOUNT LOFTY RANGES IN GENERAL	149
D: ROCK AND MINERAL ANALYSES	154
1. ANALYTICAL TECHNIQUES	154
2. META-SHALES, META-SILTSTONES AND META-SANDSTONES	155
2.1 Rock Chemistry	155
2.2 Rock Composition and Mineral Assemblages	157
2.3 Mineral Chemistry	159
2.3.1 Garnet	159
2.3.2 Biotite	161
2.3.3 Staurolite	162
2.3.4 Muscovite	163
2.4 Distribution of Elements between Coexisting Phases	163
2.4.1 The distribution of Mg and Fe between Garnet and Biotite	165
2.4.2 The distribution of Mn between Garnet and Biotite	168
2.4.3 The distribution of Mg between Staurolite and Biotite	168
2.5 Mineral Chemistry and Metamorphic Grade	169
2.5.1 The distribution of Mg between Garnet and Biotite	169
2.5.2 Muscovite composition	172
3. CALC-SILICATES	173
3.1 Rock Compositions and Mineral Analyses	173
3.2 Mineral Chemistry	174
3.3 Hornblende Composition and Metamorphic Grade	174

CONTENTS (cont'd)

	<u>Page</u>
4. CHEMICAL COMPARISON OF TYPE MARINO GROUP SEDIMENTS AND THEIR METAMORPHOSED EQUIVALENTS.	175
5. SUMMARY AND CONCLUSIONS	177
PART III <u>CONCLUSIONS</u>	180
TABLES A - 0	
Figure 1	Preceding page 1
APPENDIX I. DESCRIPTION OF THE SEQUENCE ALONG PART OF MT. BARKER CREEK.	
APPENDIX II. STRUCTURAL MAPS OF THE MOUNT LOFTY RANGES IN THE VICINITY OF THE STUDY AREA (after Fleming, 1971).	
APPENDIX III. AFM PLOTS OF ROCKS IN THE DAWESLEY-KANMANTOO AREA (after Fleming, 1971).	
APPENDIX IV. SUMMARY OF TEXTURES RELATED TO THE FORMATION OF FIBROLITE (after Fleming, 1971).	
APPENDIX V. MAGNETIC SURVEY OVER METADOLERITE DYKES	

REFERENCES

Volume 2

Figures 2 - 35

Plates 1 - 46

Maps 1 and 2

SUMMARY

The metamorphosed sedimentary sequence of the Precambrian Adelaide Supergroup in the eastern Mt. Lofty Ranges closely resembles its lower grade stratotype in the western Mt. Lofty Ranges. Although rocks have been metamorphosed from biotite to high andalusite grade, the nature of the original succession can still be deduced. Stratigraphic thicknesses in the eastern and western sequences differ, however. The thickness of the Torrens Group metasediments in the eastern sequence above the Stoneyfell Quartzite equivalent is over four times that found in its type area. In contrast, the overlying Sturt Group is less than half the thickness of the stratotype whilst the Marino Group is only slightly thinner in the eastern sequence.

In the region between Birdwood and Mt. Barker Creek, the Lower Cambrian Kanmantoo Group is in fault contact with the Adelaide Supergroup, the lower levels of the basal unit of the Kanmantoo Group (the Carrickalinga Head Formation) being absent. A conformable succession of Kanmantoo Group strata, closely resembling the lithologies in the type area on the south coast of Fleurieu Peninsula, occurs to the east of this contact. Evidence for a fault contact disproves earlier interpretations that the Kanmantoo Group unconformably overlies older strata in parts of this region and confirms the existence of the Nairne Fault. Furthermore, it is doubtful whether the Kanmantoo Group unconformably overlies older strata elsewhere in the eastern Mt. Lofty Ranges. Where there is a break in the normal Kanmantoo Group succession (which exhibits a remarkable constancy of facies), faulting is probably the cause.

A well developed penetrative schistosity (S_2) occurs throughout the Nairne-Mt. Barker Creek area, being related to a deformation phase F_2 which produced tight asymmetric folds with easterly-dipping axial planes (paralleled by S_2) during the Early Palaeozoic Delemarian Orogeny. An earlier deformation (F_1) with accompanying metamorphism, earlier than generally recog-

nized in the Mt. Lofty Ranges is evident in the schists. Metadolerite dykes in the area were probably emplaced pre-S₂ to early syn-S₂.

Petrological examination of the metasediments in the Nairne-Mt. Barker Creek area revealed that critical minerals present in metashales of appropriate bulk composition are andalusite, staurolite and almandine whereas cordierite is absent. The origin of andalusite and staurolite is unresolved. Fibrolite (\pm minor coarse sillimanite) is present in all andalusite-bearing rocks. The sillimanite problem is examined through the well developed textures in peraluminous schists.

Green hornblende, diopside and scapolite occur in calc-silicates. Green hornblende, high-An plagioclase and minor epidote are present in the metadolerite dykes.

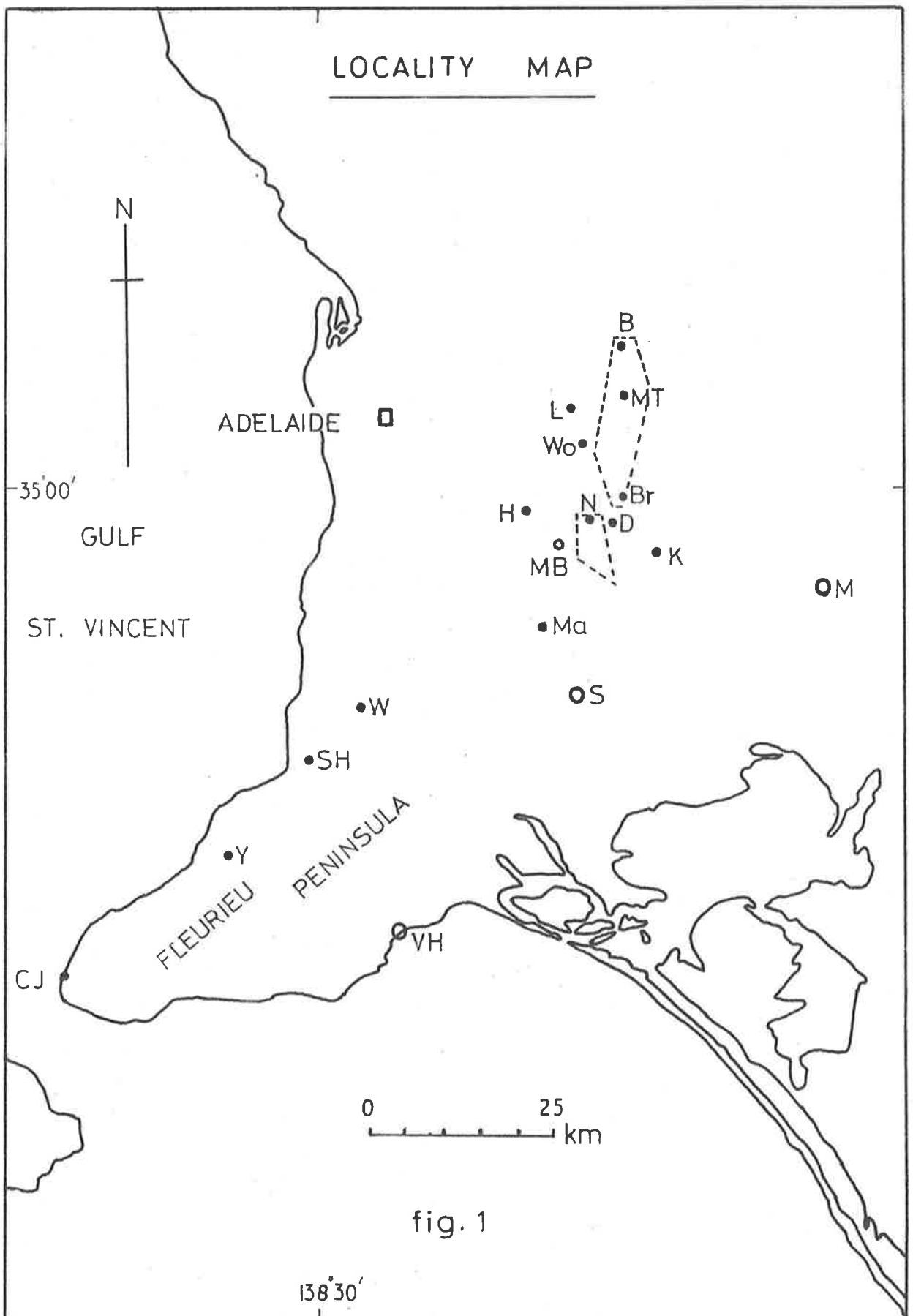
P-T conditions at the peak of metamorphism (based on mineral assemblages and metamorphic textures) were probably around 3.5 to 3.75 kb and 500 to 550°C (close to the andalusite-sillimanite phase boundary and near the Al₂SiO₅ triple-point). Temperatures of metamorphism deduced from the garnet-biotite geothermometer and more generally from muscovite compositions are compatible with this range. Fibrolite probably formed just within the upper limits of the andalusite stability field. It is uncertain, however, if fibrolite formed as a stable mineral under these P-T conditions or whether it formed metastably, perhaps as a result of rapid reactions induced by sudden temperature increases.

This thesis contains no material which has been accepted for the award of any other degree or diploma in any university and to the best of my knowledge and belief, the thesis contains no material previously published or written by another person, except when due reference is made in the text.

Stephen Toteff.

ACKNOWLEDGEMENTS

The author is indebted to Dr. B. Daily and Dr. R.L. Oliver for their supervision of this project and their invaluable criticisms of the first draft of the thesis. Special thanks to Dr. S.K. Sen who most willingly gave his time to read a portion of the thesis, and offered most constructive criticisms. Thanks go also to Dr. K. Turnbull for his guidance in the analytical work, to Miss A.M. Swan for helpful suggestions with regard to the drafting of maps and diagrams, and to Mr. R. Barrett for his dedication in reproducing my photographs. The ESSO Scholarship which covered part of the study period was most gratefully received. The use of the electron probe equipment at the Department of Earth Sciences, Melbourne University under the initial guidance of Dr. D. Sewell is gratefully acknowledged. Finally, the writer would like to thank Mrs. J. Brumby for her fastidiousness in typing the thesis.



B	BIRDWOOD	K	KANMANTOO	S	STRATHALBYN
Br	BRUKUNGA	L	LOBETHAL	VH	VICTOR HARBOUR
CJ	CAPE JERVIS	M	MURRAY BRIDGE	W	WILLUNGA
D	DAWESLEY	Ma	MACCLESFIELD	Wo	WOODSIDE
H	HAHNDORF	SH	SELICK HILL	Y	YANKALILLA
		N	NAIRNE		

INTRODUCTION AND AIMS

The broad distribution of the Precambrian Adelaide Supergroup and Cambrian stratigraphic sequences in the Mt. Lofty Ranges trends approximately north-south, enclosing Archaean anticlinal cores which form inliers along the central axis of the ranges. The thick succession of Adelaidean strata rests unconformably on the Archaean (clearly shown on the ADELAIDE and BARKER 1:250,000 map sheets, Thomson (1969); Thomson and Horwitz (1962) respectively).

On the western side of the ranges Lower Cambrian fossils have identified the basal Cambrian strata (Daily, 1963; Daily, 1976) which are transgressive onto the Adelaidean Marino Group (Thomson and Horwitz, 1961). The basal formation of the Kanmantoo Group (also of Lower Cambrian age) is the Carrickalinga Head Formation which conformably overlies the dominantly calcareous basal Cambrian Normanville Group (Daily and Milnes, 1971), the youngest formation of which is the Heatherdale Shale (Abele and McGowran, 1959; Daily, 1963). The bulk of the Kanmantoo Group, however, occurs on Fleurieu Peninsula and in the eastern Mt. Lofty Ranges. Its type area is along the south coast of Fleurieu Peninsula (Daily and Milnes, 1971).

The nature of the boundary between the Adelaidean and Cambrian strata in the eastern Mt. Lofty Ranges has been a controversial problem since the mapping of the Adelaide 1:63,360 map sheet by Sprigg, Whittle and Campana (1951). In the legend, the term "Kanmantoo" Group (actually Series) was first used to describe the bulk of the very thick sequence of dominantly clastic Cambrian metasediments in the eastern Mt. Lofty Ranges. The boundary between this sequence and the older Precambrian strata to the west was first interpreted as a fault. Subsequent work by others led not only to different interpretations of the nature of the boundary but also to unsubstantiated correlations of the strata underlying the typical Kanmantoo Group sequence, resulting in confused relations between inferred older ("basal") Cambrian strata and the Kanmantoo Group. Confusion resulted in interpretation of the

boundary as a fault, unconformity and a conformable contact, the problem being compounded by conflicting interpretations as to the stratigraphic positions of strata on either side of the boundary.

A lack of knowledge of the Kanmantoo Group stratotype (Sprigg and Campana, 1953) in earlier studies undoubtedly resulted in these incorrect correlations. This is particularly obvious with regard to correlations of pyritic metasilstone bands within the Kanmantoo Group with the two prominent units which occur in the vicinity of Brukunga, the lower of which is termed the "Nairne Pyrite Member" or "Nairne Pyrite Horizon". Similarly, conflicting correlations were made between the Type Adelaidean in the western Mt. Lofty Ranges and the metamorphosed strata to the east, the problems associated with correlating high-grade strata being accentuated in most areas by poor outcrop.

The region between Birdwood and Mt. Barker Creek (Fig. 1) which covers approximately 32 km in strike length of the Kanmantoo sequence is well situated for the purpose of examining the conflicting hypotheses regarding the nature of the Precambrian-Kanmantoo Group (or Precambrian-basal(?) Cambrian) boundary. This region embraces portions of the areas mapped by the proponents of all three hypotheses. Almost continuous exposures in Mt. Barker Creek and along excavations for the Mannum-Onkaparinga River pipeline between Dawesley and Hahndorf provided excellent sections (summarized in Table N) through the upper Adelaidean and lower Kanmantoo Group sequences which are unequalled elsewhere on the eastern side of the ranges. Comparison of these strata with the Type Adelaidean and Kanmantoo Group sequences provided a valuable background for mapping of the sequences and their relationships with the ultimate aim of resolving the nature and location of the Precambrian-Kanmantoo Group boundary in the eastern Mt. Lofty Ranges.

The grade of metamorphism in the Mt. Lofty Ranges increases from west to east, covering the interval chlorite to sillimanite zones. The

region studied occurs within the Andalusite-Staurolite Zone delimited by Offler and Fleming (1968). This zone is characterized by the presence of andalusite and staurolite in rocks of appropriate bulk composition. Fibrolite is sporadic in its occurrence through this zone and the problem of its origin has not as yet been fully resolved (Offler and Fleming, 1968; Fleming, 1971). Furthermore the nature of the reactions leading to the formation of andalusite and staurolite in the Mt. Lofty Ranges is also unknown (Fleming, 1971).

The petrology of the metasediments in the Nairne-Mt. Barker Creek area was studied with the aim of gaining some insight into the origins of these minerals (fibrolite in particular). In addition, minerals and rocks were analysed in order to determine whether chemical equilibrium was attained during the peak of metamorphism, which is of pertinence to the nature of the metamorphic reactions and estimates of the P-T conditions. Further study of mineral compositions was made through the examination of Mg-distributions, with special attention to garnet-biotite pairs which are of use in estimating metamorphic grade. More general determinations of grade were based on the compositions of other minerals for the purpose of comparison with data from the garnet-biotite geothermometer and the broader estimates of grade based on the mineral assemblages and metamorphic textures.

A consistent change in bulk composition with increasing grade of metamorphism has been reported in the literature (Engel and Engel, 1958; Miyashiro, 1964). Having distinctive lithologies in the Marino Group stratotype (Adelaidean) which permit close correlation with the high-grade sequence on the eastern side of the ranges, the opportunity existed to test these observations. With this aim, rocks from the lower grade western sequence were analysed for comparison with their relatively unweathered metamorphosed equivalents in the Nairne-Mt. Barker Creek area.

PART I
STRATIGRAPHY

A: SECTION THROUGH THE METAMORPHOSED
ADELAIDE SUPERGROUP, EASTERN MT. LOFTY RANGES



1. INTRODUCTION

The Adelaide Supergroup was first subdivided and described in detail by Mawson and Sprigg (1950) in its type area in the western Mt. Lofty Ranges near Adelaide. The equivalent sequence in the eastern Mt. Lofty Ranges, lying on the eastern limb of the major north-trending anticlinorium has been metamorphosed to biotite and andalusite grades (Offler and Fleming, 1968). Excavations for the Mannum-Onkaparinga River pipeline provided an almost continuous section through the metamorphosed Adelaidean strata, excluding the lower levels of the Torrens Group. There is virtually no outcrop of Torrens and Sturt Group strata within approximately 1 km north and south of the pipeline section aside from occasional very poor exposures of quartzites along ridges which are usually of limited extent. Consequently the unique exposures offered by the pipeline excavations are critical in the understanding of the geology of this portion of the eastern Mt. Lofty Ranges.

Unfortunately most rocks were extremely kaolinized which, combined with the rarity of peraluminous schists (except in the higher grade upper levels in the east), did not permit the location of the upper (eastern) limit of Offler and Fleming's "Biotite Zone".

The Adelaidean sequence as exposed in the pipeline excavations is described below¹, comparison being made with the lower grade type Adelaidean. The Marino Group, which occurs in the western part of the Nairne-Mt. Barker Creek area is described in a later section on the stratigraphy of that area. Boundaries of the major units indicated in the text are shown by encircled numbers (eg. ②) in Fig. 2.

¹Representative samples indicated bear the accession number prefix A405/- in the collections of the Geology Department, University of Adelaide.

The succession, from older to younger, encountered in an easterly traverse from the Onkaparinga River near Hahndorf is as follows:

2. TORRENS GROUP

An estimated 200 m of well laminated dark-grey fine metasiltsstones and minor phyllites were exposed below the Stoneyfell Quartzite equivalent. Paler laminae are sandy (L1). These fine sand layers are generally less than 1 cm thick (L2) (and occasionally to 1.5 cm), the thicker beds tending to be lenticular and being restricted to certain horizons. Some beds have been scoured out in their upper parts. Occasional thin very dark grey to black horizons are present, these probably being carbonaceous and possibly pyritic (L5, L9). The strata become imperceptibly less micaceous up the sequence, being predominantly laminated fine metasiltsstones (K2) with rare phyllites.

2.1 Stoneyfell Quartzite Equivalent

The Stoneyfell Quartzite equivalent is 54 m thick. Its base ① is marked by the first appearance of fine feldspathic metasandstones which are quartzitic in parts (K6, K9). The metasandstone units are generally thin (to 0.75 m), the thickest being restricted to the uppermost and basal portions of the formation. The upper and lower boundaries of these beds are generally gradational, passing into metasiltsstones over a few centimetres. The interval consists predominantly of dark grey metasiltsstones (phyllitic in parts) with common very fine sand laminae resulting in a generally well developed lamination. There are intervals which are virtually identical to the underlying sequence of metasiltsstones. Commencing 36 m above the base is a 12 m thick interval of metasiltsstones with occasional scapolite-bearing horizons giving the rocks a finely spotted appearance. Metasandstone beds are absent.

The eastern equivalent of the Stoneyfell Quartzite (type area in the vicinity of the Stoneyfell Quarries near Adelaide, (Mawson and Sprigg, 1950)) is considerably more pelitic, with metasiltsstones predominating

(c.f. Mawson and Sprigg, 1950, p.71). The Type Stoneyfell Quartzite however, consists of a very thick sequence (to 250 m (Heath, 1963)) of predominantly massive quartzites with variable feldspar contents and minor units (to several m) of very fine sandstones and siltstones ("feldspathic greywackes" of Heath, 1963) which are laminated in parts and contain minor scapolite in some beds.

2.2 Unit 2

Above the Stoneyfell Quartzite equivalent is a very thick sequence of metasiltsstones (estimated as 1980 m) which can be subdivided into three members.

Member a. This is a thick succession of approximately 490 m consisting mainly of well laminated dark grey fine metasiltsstones which are phyllitic in parts. Paler laminae (to 0.5 cm) are characteristically slightly coarser, to very fine sand size (K1, K7A, C4). Rare lenticular fine to medium-grained metasandstone beds (to 8 cm), (K8) are also present. Occasional small-scale low angle cross bedding is evident, sets being generally less than 3 cm. Some almost black carbonaceous horizons occur (K7,C6). As most rocks are highly weathered, however, it is uncertain whether much of the paler rocks were also originally as dark (and carbonaceous(?)). About 186 m above the base, a thin (2.75 m) more psammitic interval breaks the monotony of the sequence. Included are many fine to medium-grained metasandstones, generally around 1 cm but up to 10 cm in thickness, especially in the upper parts. Minor scapolite-bearing intervals occur in the upper levels of the sequence, giving the rocks a characteristic spotted appearance. The scapolite aggregates are occasionally up to 0.5 cm across.

Member b. This is an interval of predominantly dark grey non-laminated metasiltsstones and phyllites about 150 m thick. The contact ② with the underlying strata is concealed by alluvium but is presumed to be conformable.

Resistant metasiltstones, which are the major rock type (J4), grade into phyllites in some horizons (J1; Plate 1, Fig. (a)). There are few distinct beds although occasional resistant coarser metasiltstone and some very fine metasandstone beds to 10 cm (rarely to 25 cm) occur, these being more common in the lower levels (J2, J5; Plate 1, Fig. (b)).

Some metasiltstones are laminated in the less micaceous horizons (J8; Plate 1, Fig. (c)). There is a well developed cleavage showing obvious refraction through the more competent metasiltstones which are often boudinaged (Plate 1, Fig. (d)). It is probable that some of these beds were originally lenticular. In the more micaceous rocks the cleavage gives way to a schistosity. Kinking is well developed in some phyllites (Plate 2, Fig. (a)).

The upper contact ③ is gradational. In the upper levels lamination increases (I34) and occasional small-scale low angle cross-bedding is present (I32). Very dark grey to black horizons occur which are probably carbonaceous (I35). Phyllites and distinct resistant metasiltstone beds gradually disappear.

Member c. A sequence of finely laminated fine metasiltstones follows. Common small mesoscopic folding and abundant faulting (Plate 2, Fig. (b)) preclude an exact estimate of the thickness of this interval but it is approximately 1340 m.

The rocks are extremely weathered and are generally pale grey in colour and have degenerated to clays (mainly kaolin) and very fine silts, still retaining the fine laminations (I1, I7; Plate 2, Fig. (c)). The less altered horizons are very dark grey (I20, I31). Lamination is due to colour variations, paler (almost white or pale yellow) beds (to 1 cm) being generally coarser, often up to fine sand size. Thicker fine metasandstone beds often grade into metasiltstones and are rarely more than a few cm thick (to 25 cm at most). They are generally concentrated in certain horizons

less than 6 m thick (I28, I38, I19), these being particularly common in the lower levels, to about 230 m from the base. Some of the thicker metasandstone beds are interbedded with dark metasiltstones. Occasionally fine metasandstones and metasiltstones intertongue on a small scale (I21A). The occurrence of fine metasandstone beds and the presence of thin phyllite intervals in the lower 230 m distinguishes a more variable basal portion from the bulk of the interval which is very uniform in lithology. Variations are subtle and minor weakly or non-laminated horizons (to 14 m) are the most significant units present.

Sedimentary structures such as small-scale ripples, convolute bedding (I11) and low angle cross-lamination (I10) are present in some horizons but they are not characteristic of the interval. Thin (to 2 cm) dark clay lenses (originally fine silts or muds) are common, being interbedded with evenly laminated strata (Plate 2, Fig. (c)).

Occasional phyllitic intervals (very micaceous fine metasiltstones), rarely to 40 m thick help to break the monotony within the member. These are most common in the uppermost and basal portions of the member. The more micaceous lithologies are typically least well laminated and phyllitic strata are only laminated in thin horizons (I4, I17). A schistosity is well developed throughout, being the axial plane structure to the common mesoscopic folds (I3, I16).

Minor thin very dark grey to black horizons (15-60 cm) occur, these being characteristically very altered and reduced to clays. They were probably originally carbonaceous mudstones or very fine siltstones (I13, I40)¹. These units sometimes contain coarser laminae but are generally poorly laminated. Paler grey rocks found to pass laterally into these almost black rocks suggests that a much greater proportion of the interval was originally

¹Rock A405/I13 has retained a carbon content of 1.1%; rock A405/I40 has a carbon content of 0.2%. The carbon content was probably higher prior to deep weathering. Carbon was determined by combustion in a LECO furnace, and gravimetric determination by absorption of the CO₂.

carbonaceous prior to deep weathering. The only other rock type encountered in this member is scapolite-bearing metasilstone (I18), occurring in the basal 290 m. Most scapolite-bearing horizons are less than 1.5 m in thickness and are uncommon. A 2 m thick unit, the thickest present, occurs at the top of the scapolite-bearing interval.

Tertiary conglomerates and sands to over 3.5 m in thickness cover much of the eastern part of the sequence. Rocks below these deposits are typically kaolinized and usually iron-stained.

2.3 Unit 3

A coarser interval, 255 m thick, conformably overlies the monotonous metasilstone sequence described above. Its lower contact ④ is marked by the first appearance of medium-grained metasandstone.

The basal 40 m consist predominantly of dark grey metasilstone grading to very fine metasandstone. Both are generally laminated (G82) and contain occasional scapolite-rich intervals frequently associated with actinolite. Thin fine to medium-grained metasandstone beds (to 1 cm) and laminae occur in most rocks, with occasional thicker medium to coarse-grained metasandstone units (to 5.75 m) near the base (G85). These coarser units are usually interbedded with finer metasandstones and metasilstones up to 1 m in thickness. Minor thin units (to 0.75 m) of very micaceous metasilstones grading to mica schists are present, these being more common in the upper part of this basal interval.

Metasilstones and very fine metasandstones in the overlying 146 m are weakly laminated (with thin well laminated horizons) and interbedded with thin fine to medium (and occasionally coarse) grained poorly sorted feldspathic metasandstone units, to 0.75 m in thickness, these being less common in the upper and lower levels of the interval (Plate 9, Fig. (a)). Coarse metasandstone beds as little as 1 cm thick are not uncommon. Some metasandstones are lenticular and commonly contain rounded quartz pebbles to 3 mm (G74, G74A). Occasionally rounded very coarse sand grains occur

scattered through the weakly laminated very fine metasandstones and metasiltstones (G68B, G69) indicating an absence of sorting. The interval may possibly be of fluvio-glacial or shallow glacio-marine origin although no Torrens Group rocks have previously been interpreted as having formed in such environments.

Above is a 27 m interval with numerous horizons (exceptionally to 8.5 m) of poorly sorted fine to coarse feldspathic metasandstones (G64) with interbedded thin metasiltstones. The coarser metasandstone units (to 4 m) commonly contain rounded quartz pebbles of up to 1 cm (G65). Elongate grains have their long axes aligned in the bedding.

The uppermost strata consist of weakly laminated dark grey coarse metasiltstones and fine metasandstones (G61A, G63). Well laminated horizons to 1.5 m thick are present. Interbedded poorly sorted fine to medium (and some coarse) grained feldspathic metasandstones and occasional metaarkoses to 1.5 m in thickness (this being exceptional) are common (G61B, G62; Plate 8, Fig. (c)).

The top ⑤ of Unit 3 is defined by the disappearance of medium to coarse-grained metasandstones.

2.4 Unit 4

A very thick succession, estimated to be approximately 875 m thick overlies the metasandstones of Unit 3. It consists of dark grey scapolite-bearing metasiltstones. Variations in the proportion of fine metasandstone and black carbonaceous beds and the degree of lamination permits some subdivision of this monotonous sequence. The lower levels are very weathered and rocks are generally pale grey.

Member a. The basal 260 m contain occasional black very fine metasiltstone or metashale beds (G42A) which are probably carbonaceous and may have originally been pyritic but are now weathered to black clays. These rocks are typically either weakly laminated or non-laminated. Scapolite occurs in

some beds, in the lower levels of the sequence (G58). The uppermost 7 m of this interval contains abundant soft black interbeds (G42A)¹ which vary from about 2.5 cm to 15 cm in thickness, forming variable proportions of the strata which consist predominantly of pale grey weakly laminated metasiltstones. In one exceptional interval the carbonaceous beds formed 50% of the rock (Plate 6, Fig. (b)).

The relatively unweathered metasiltstones are dark grey (G46B) and may have a well developed bedding parting. Variations in mica content are generally subtle and distinct bedding is not always present. In addition, there are minor less micaceous, resistant beds (G46A, G52; Plate 7, Fig. (c)). Occasional very micaceous metasiltstone intervals are generally weakly laminated (Plate 7, Fig. (a)) and some grade into fine quartz-micaschists. Scapolite-bearing horizons are common throughout the member (Plate 6, Fig. (c)). They are usually less than 1.5 m in thickness and generally preferentially weathered (Plate 8, Figs. (a & b)). These rocks are typically weakly laminated, well laminated metasiltstones not usually containing scapolite. Actinolite is present in some beds.

In the upper levels of the member, fine metasandstone laminae are common. Occasional sandy lenses occur in the evenly laminated rocks and although some tectonic thinning may have occurred, it is probable that these were originally lenticular (Plate 7, Fig. (b)).

Sedimentary structures are few. Some medium-scale low angle cross-bedding is evident in occasional well laminated intervals (Plate 8, Fig. (a)) and rare ripple marks occur near the base.

Member b. The overlying interval is more uniform lithologically. Rocks are predominantly dark grey commonly laminated metasiltstones, grading to very fine metasandstones in parts and containing scapolite-bearing intervals. There

¹Rock A405/G42A has retained a carbon content of 1.1% following weathering.

are few distinct units and variations in lamination and scapolite content are subtle. A 65 m interval, commencing 25 m above the base of the member is, however, conspicuously more heterogeneous, with marked variations in scapolite-rich and fine metasandstone beds. Also present are rare fine to medium-grained metasandstone beds (to 10 cm, rarely to 20 cm thick (G30D)). These are usually strongly lenticular and appear boudinaged, usually being enveloped by very micaceous metasiltstones and micaschists suggesting some metamorphic segregation, resulting in quartz enrichment of the original sedimentary sand beds (Plate 5, Fig. (c)). In the upper levels the only conspicuous variation in the otherwise uniform sequence is a weakly laminated 27 m interval containing only rare scapolite horizons, to 1.3 m thick (G24). This interval occurs 445 m above the base of the member (Plate 5, Fig. (a)).

Most rocks of the member are well laminated (G25B, G25C, G41A) and often have a well developed bedding parting, with occasional flaggy intervals (G39; Plates 4, Fig. (b), 6, Fig. (a)). Minor scapolite-rich micaschists are present but are generally very thin (to 1.5 cm). Thicker micaceous intervals occasionally break the monotony but these are also few; an 18 m interval, 88 m from the base consisting of very micaceous metasiltstones grading to micaschists (G30A, Plate 5, Fig. (b)) is the thickest dominantly pelitic interval present.

Scapolite-rich rocks (G14A) are typically selectively weathered and usually poorly laminated. Most contain a variable proportion of actinolite (G37; Plate 5, Fig. (d)). Rocks rich in actinolite are rarely bedded although occasional less weathered beds show some lamination (G32, G34). Scapolite-actinolite rocks (calc-silicates) are usually less than 10 cm thick and often occur in units (to 3 m, usually less) where they are interbedded with metasiltstones and very fine metasandstones having little or no scapolite. Rare almost pure actinolite lenses are present, these being up to 12 cm thick in exceptional cases (G38).

Member c. The uppermost 48 m of Unit 4 consist of dark grey meta-siltstones to very fine metasandstones (G14). Lamination is generally less well developed than in the underlying strata. The interval is distinguished by the presence of occasional fine to medium-grained metasandstone and some meta-arkose beds (G5) up to 20 cm thick (Plate 3, Fig. (c)), these being most common in the upper levels. Both weakly laminated and non-laminated varieties occur and are often boudinaged (Plate 4, Fig. (a)). The occasional scapolite-bearing units (G12) are up to 3 m thick and are often well bedded. Rare large scale, low angle (to 15°) cross-bedding is present.

Approximately 10 m of dark grey weakly laminated very fine metasandstones and metasiltstones (G3; Plate 3, Fig. (a)) form the youngest strata west of the large macroscopic folds which repeat the underlying sequences to the east, as shown on the Echunga 1:63,360 map sheet. Younger rocks are again encountered in the vicinity of locality B1 (Fig. 2). The youngest 10 m are very similar to the strata directly underlying Member c, described above. There are intervals of resistant well bedded to flaggy metasiltstones and minor very micaceous phyllitic rocks (G-1). Well laminated intervals are thin (Plate 3, Fig. (b)) and scapolite-bearing rocks are common (G1A, G2). Some large-scale low angle cross-bedding is evident.

It was not possible to closely compare the repeated succession with the upper levels of Unit 4 seen west of the synclinal core as distinctive marker beds are absent in this interval. Part of Member c, however, could be recognized at three other localities along the section to the east (these are indicated in Fig. 2)¹. Minor faulting and mesoscopic folds locally complicate the succession (Plate 10, Figs. (a & d)). In general, the repeated strata appeared virtually identical although scapolite seems to be less abundant and rocks are more pelitic, particularly in the upper levels, where very micaceous metasiltstones grade into micaschists (Plate 10, Fig. (b), locality B5, Fig. 2; specimens B136, B139). Intensely deformed zones occur

¹The base and top of Member c are indicated in Fig. 2 as (6a) and (6b) respectively.

in these rocks in the vicinity of locality B5 (Plate 10, Figs. (b & c)).

The less weathered zones provided excellent exposures of the typical dark grey laminated metasiltsstones to very fine metasediments (representative samples indicating the range of metasiltsstone and fine metasediment types are: D17A, D100C, D6A, D7, D7A), (Plate 9, Figs. b, c & d), localities D2, D3, D5 respectively). Scapolite-bearing intervals are typically more weathered, although some relatively unaltered rocks remain (D7B). Another notable difference is the greater abundance of actinolite in the eastern exposures, reflecting different compositions of the original carbonate-rich sediments. The proportion of actinolite varies considerably in the originally calcareous strata, typically from a few percent (D9A) to almost pure actinolite beds (with minor scapolite and plagioclase (D31)). Commonly in actinolite-rich rocks, (which often occur in horizons up to 2.75 m thick) the actinolite has been remobilized into discordant veins where it has recrystallized as very coarse fibrous aggregates in the typical actinolite habit (D14G). Actinolite is very common in metasiltsstones and micaschists in the upper levels of Unit 4 (D2). A 2 m thick unit of medium-grained dolomitic marble (D14B) occurs at locality D6, some 11 m below the metasediment interval considered to be equivalent to part of Member c. Minor thin dolomites also occur about 9 m lower in the sequence and are associated with actinolite-rich metasiltsstones. Occasional thin tremolite-rich beds are also present (D14).

Minor thin beds (usually less than 5 cm) of fine to medium-grained metasediments are still present in the sequence. Rare coarse metasediment beds (D8, D15) also occur but are only 3 cm thick at most. Black carbonaceous beds also persist in the repeated sequence (D19C; Plate 10, Fig. (a), locality D5). An exceptionally thick metasediment interval of over 6 m (just east of locality D3) was equated with part of Member c (which is 48 m thick in the western section), the difference in thickness being attributed to facies change. The dominant lithologies near locality D3 are fine to

medium-grained metasandstones whereas the western equivalent is predominantly metasiltsstones with occasional interbedded metasandstones.

Further east along the macroscopic fold, near the western end of the summit cutting (locality B1, Fig. 2) there is, however, a thicker metasandstone interval (20 m) which is also equated with Member c. The basal portion is predominantly fine metasandstones with minor metasiltsstone interbeds. Occasional fine to medium-grained metasandstone beds occur near the base (B119A), these being generally less than 13 cm thick but in rare cases, up to 0.4 m thick. Rocks in the upper half are mainly metasiltsstones, grading to fine metasandstones in some horizons (to 1.5 m) in the upper levels. Thin (to 3 cm) fine to medium-grained metasandstone beds are common in parts.

Between localities B6 and B7 (Fig. 2), Member c is exposed again. Lithologies are similar, although very coarse metasandstone beds between 1 cm and 13 cm are present in some horizons.

2.5 Unit 5

The metasiltsstone interval overlying the uppermost metasandstones of Unit 4 is estimated as 206 m thick.

Member a (90 m). The strata immediately overlying Member c, Unit 4 are predominantly finely laminated metasiltsstones (Plate 11, Fig. (a)) with minor thin weakly laminated horizons. The subtle changes in mica content and grainsize (to very fine metasandstones) does not generally permit the distinction of individual units (specimens B70, B71, B72, B80, B91A, B96, B100 reflect the variations in mica content and lamination). The paler laminae are characteristically coarser (to very fine sand size) and more feldspathic (Plate 11, Fig. (b)). More pelitic metasiltsstones are usually only weakly laminated. Rare micaschists occur, (B94), these being less than 8 cm thick in general whereas occasional horizons of very micaceous metasiltsstones (grading to micaschists) are commonly thicker (B68, B82), to 1.25 m.

Minor thin fine to medium-grained (and rare coarse-grained) metasand-

stone beds occur in the basal portions of the member. Some are up to 1 m thick with the coarse beds usually less than 15 cm in thickness and often lenticular (B108A; Plate 12, Fig. (b)). Feldspar content varies, meta-arkoses to slightly feldspathic quartzites being present. Some small-scale low angle cross-bedding is evident in the better laminated strata (Plate 11, Fig. (a)).

In the vicinity of locality B4, the strata are extensively kaolinized and ferruginous. Irregular zones of opal¹ (\pm actinolite) have formed (B111, B61). Minor magnesioriebeckite² occurs along fractures and bedding planes (Plate 11, Figs. c & d) in the zones of opal development.

A minor low angle fault (Plate 12, Fig. (a)) breaks the succession at locality B2. To the east, strata are macroscopically deformed and dip to the west then south until locality B4, where an easterly dip is resumed, the easterly traverse again passing up through the sequence (Fig. 2).

Member b. A thin (11 m) interval is distinguished by the presence of common actinolite-rich metasiltstone and micaschist interbeds, to 30 cm in thickness. Thin fine metasandstone beds also occur.

Member c. A thick sequence (105 m) of kaolinized metasiltstones and minor fine feldspathic metasandstones follows ⑦. In the lower 50 m metasiltstones grade into fine metasandstones which are only slightly feldspathic in parts and occasionally grade into quartzites. There are flaggy intervals (Plate 12, Fig. (c)) but the metasandstones are generally massive and rarely laminated. The metasiltstones are mostly weakly laminated in the lower 50 m,

¹Identified by X-ray diffraction. Quartz is present with the opal which shows patterns of cristobalite (c.f. Deer et al. (1963, Vol. 4, p.210).

²Identified by Dr. A.W. Kleeman by petrological examination; X-ray diffraction inconclusive. The magnesioriebeckite may be authigenic (c.f. Milton and Eugster (1959)). The P-T range of this mineral is very large and its stability is also dependent on PO_2 and PH_2O (Ernst (1960)). Its distribution, however, suggests it does not belong to the main metamorphic paragenesis (see also Mount (1975) pp. 110-119).

becoming predominantly well laminated higher in the sequence. Minor thin actinolite-rich beds are present in the lower and upper levels of the member (B55B), and medium to coarse-grained metasandstones (rarely to 28 cm thick) are occasionally found in the lower half of the sequence.

2.6 Unit 6.

A more variable sequence of approximately 215 m in thickness overlies Unit 5. Minor folding and faulting precluded a precise determination of the thickness of this interval. The base ⑧ and top ⑨ are shown in Figure 2.

The basal 14 m consist of micaceous fine feldspathic metasandstones with less micaceous and feldspathic quartzitic interbeds generally less than 10 cm thick. Minor thin (to 15 cm) actinolite and scapolite-rich very fine metasandstones (grading into calc-silicates) are present in some horizons. These are extremely weathered.

This interval of metasandstones is followed by laminated metasiltsstones with thin micaschist horizons, to 15 cm in thickness (B49A, B50B). Some small scale cross-bedding is evident. Thin (to 1.5 m) fine to medium-grained metasandstone units are common near the top and scapolite is common in the lower 160 m. A thin (3 m) pale grey fine metasandstone (B48) marks the top of the unit.

2.7 Unit 7

This is a thick interval of approximately 1,020 m resembling Unit 2 and much of Unit 4, consisting of a monotonous sequence of laminated metasiltsstones. It is the uppermost unit of the Torrens Group. The metasiltsstones are mostly kaolinized and laminated in most horizons, and scapolite-rich horizons are common. Subdivision could be made on the basis of the proportion of micaceous intervals and calc-silicates.

Member a. Commencing 24 m above the base is a 41 m thick more micaceous interval consisting of relatively unweathered laminated very micaceous metasiltsstones (B45A) with thin interbeds of micaschists (B45B). Thin (to 15 cm) more resistant metasiltsstone interbeds occur through the sequence.

Member b. Above Member a are 238 m of typical grey laminated meta-siltstones (B39), with common scapolite-rich horizons which are restricted to the upper levels of the member. Scapolite-bearing horizons are generally less than 0.75 m thick. There are minor thin very micaceous intervals (B41A) which are generally poorly laminated. One exceptionally thick (10 m) more pelitic interval, 190 m above the base of the member, breaks the otherwise uniform sequence.

Occasional metasiltstones are rich in actinolite (B40) and grade into calc-silicates, up to 10 cm in thickness. These rocks are usually poorly laminated and highly weathered.

Member c. A thin (32 m) well laminated interval follows. Thin (to 15 cm) actinolite-rich beds are common and occasional thin resistant meta-siltstone and very fine metasandstone beds are also present.

Member d. This monotonous sequence of kaolinized metasiltstones persists to the top of the Torrens Group. There are variations in lamination from fine, distinct laminae (B30, B33) to poor, diffuse and non-laminated horizons (B36). The basal 60 m of the member is predominantly poorly laminated. Scapolite-rich horizons (to 1 m) occur in some intervals, there being virtually no scapolite in the basal portion. Occasional very fine meta-sandstone beds to 30 cm in thickness occur in the upper levels and a highly altered mineral (possibly andalusite) occurs in some poorly bedded meta-siltstones near the top.

2.8 Comparison with the Torrens Group Stratotype

A comparison with the thickness of the Type Torrens Group sequence above the Stoneyfell Quartzite, determined by Mawson and Sprigg (1950) as being approximately 910 m, indicates an enormous thickening to the east as the metamorphosed equivalent interval is estimated as some 4,550 m in thickness. Even considering most of the Type Stoneyfell Quartzite (which is approximately 250 m thick (Heath, 1963)) as equivalent to the interval of metasiltstones directly overlying its much thinner eastern equivalent, little

alters the magnitude of this thickening.

With due regard to the metamorphism, it is evident, however, that the lithologies in the eastern sequence are virtually identical to the type sequence above (and immediately below) the Stoneyfell Quartzite, described as "slates and phyllites including numerous dolomitic bands and thin quartzites" by Mawson and Sprigg (1950, p.71). Although only rare relatively pure carbonate beds are present (Unit 4), calc-silicates are common and the common occurrence of scapolite and actinolite-bearing metasilstones attests to the original dominantly calcareous nature of much of the sequence. The black carbonaceous beds encountered however, are not mentioned in the subdivision devised by Mawson and Sprigg (1950), nor on the Echunga 1:63,360 map sheet legend (Sprigg and Wilson, 1954). The presence of carbonaceous bands in some dolomites are mentioned by Sprigg (1946), however these occur below the Stoneyfell Quartzite in the type area. The interval above the Stoneyfell Quartzite on both sides of the ranges is referred to as the "Saddleworth Formation " (Riverton 1:63,360 map sheet (unpublished), Thomson) on the ADELAIDE 1:250,000 map sheet (Thomson, 1969) and a carbonaceous shale (the "Bethel Shale Member") is shown to occur in the northern part of the Adelaide sheet, principally on the western side of the ranges. This unit, however, occurs at the top of the Saddleworth Formation whereas carbonaceous beds were not found in this interval of the Torrens Group along the pipeline excavations.

Although the gross lithology is insufficient to delineate the nature of the depositional environment, the nature of the strata and the few relict sedimentary structures is not incompatible with deposition in a shallow marine environment, the inferred general depositional conditions of the Type Torrens Group (Thomson in Parkin, 1969; Forbes in Twidale et al., 1976).

3. STURT GROUP

3.1 Belair Sub-group

A predominantly psammitic interval some 438 m thick marks the base of the Sturt Group¹ (10) as in the western Mt. Lofty Ranges (Mawson and Sprigg, 1950). Variations in the proportion of metasandstones and meta-arkoses in the eastern sequence permitted further subdivision into five units.

Unit 1. The lowest 61 m of the Belair Sub-group consist predominantly of white (kaolinized) poorly bedded and feldspathic fine metasandstones (B21) and minor metasiltsstones. The metasandstones are occasionally cross-bedded and well laminated in parts. Some scapolite-rich fine metasandstones (to 1.75 m) and lenticular medium to coarse meta-sandstones and meta-arkoses (to 60 cm) are present (Plate 13, Fig. (a)). The latter are uncommon and usually thinner near the base where pale grey metasiltsstones with scapolite-rich horizons form the dominant rock type (Plate 12, Fig. (d)).

Unit 2. This is a dominantly pelitic interval which is 165 m thick, consisting of grey metasiltsstones which are mostly very micaceous. About 125 m above the base of the unit is a 2.5 m thick coarse metasandstone which separates the differing upper and lower portions. Below the metasandstone, the metasiltsstones are generally poorly laminated, and interbedded with minor micaschists in the basal 60 m. Above the metasandstone, subtle variations in mica content rarely distinguish individual units (B16). Occasional fine to medium-grained metasandstone beds (to 1 cm thick) and minor lenticular medium to coarse-grained metasandstones (to 12 cm thick) are present.

Unit 3. A thin (55 m) but highly variable psammitic interval overlies Unit 2. In the basal 4.5 m, medium-grained metasandstones are the dominant lithology, there being occasional coarse and fine metasandstone

¹Mawson and Sprigg (1950) used the term Belair "Group" as the basal unit of the Sturtian Series in the original time-stratigraphic subdivision of the Adelaide System.

interbeds. Some medium scale cross-bedding is evident. With a gradual coarsening, lithologies pass up into mainly coarse feldspathic metasandstones which are weakly laminated, usually massive (B14) and generally poorly sorted. Cross-bedding with sets up to 1.5 m is present.

Approximately 16 m above the base, the metasandstones become fine-grained and laminated with thin interbeds of medium to coarse metasandstone. Small scale cross-bedding occurs in the finer rocks and thin lenses of quartzite are present.

This interval (which is 17 m thick) is followed by predominantly medium-grained metasandstones which are well bedded and laminated. There are occasional coarse interbeds to 60 cm in thickness. Minor faulting disrupts the sequence (Plate 13, Fig. (b)).

The uppermost 9 m of the unit are coarse feldspathic metasandstones and quartzites (B12) which are poorly bedded and weakly laminated. The strata are commonly cross-bedded with sets up to 3 m.

Unit 4. This is another predominantly fine-grained interval. The lowest 43 m are metasiltsstones grading into fine metasandstones with flaggy horizons. Some small scale cross-bedding is present. The overlying rocks are mainly weakly laminated very micaceous metasiltsstones and micaschists (B8) with interbedded more resistant very fine metasandstones and metasiltsstones (B9). Minor andalusite occurs in the schists (B9A).

The uppermost 29 m are laminated metasiltsstones which are scapolite-bearing near the top. Some 19 m from the top, a weathered calc-silicate-rich horizon (2 m thick) breaks the otherwise uniform sequence.

Unit 5. This unit comprises the uppermost 60 m of the Belair Subgroup. Rocks pass upwards from metasiltsstones to fine metasandstones (B5) in the lower 40 m. Small-scale cross-bedding is abundant. Traces of scapolite (B6A) occur in more pelitic intervals which decrease in thickness up the sequence. Slightly feldspathic fine to medium-grained metasandstones dominate the upper levels and persist to the top (contact ⑪, Fig. 2).

3.1.1 Comparison with the Belair Sub-Group Stratotype

Lithologically, this interval is very similar to the type strata of the Belair Sub-group which are described as "slates and quartzites". Unit 1 is considered by the author to be a more pelitic equivalent of the arkosic Mitcham Quartzite (Mawson and Sprigg, 1950), the basal unit of the Sub-group. With an estimated thickness of approximately 300 m (Mawson and Sprigg, 1950), however, the type sequence is considerably thinner than its eastern counterpart which is approximately 440 m thick.

Deposition in shallow marine and tidal flat environments of the type strata has generally been envisaged (Coats, 1967; Thomson in Parkin, 1969). Although the eastern sequence appears compatible with a shallow marine origin, no sandstone dykes, mudcracks or other features were visible which might indicate periods of exposure to the air, in contrast to the type strata (Coats, 1967). The possible destructive effects of metamorphism and weathering on such features must be considered, however.

3.2 Sturt Tillite

Howchin (1929) first recognized the kaolinized Sturt Tillite equivalent in a railway cutting immediately to the south of the pipeline excavations (locality B11a, Fig. 2). Here the tillite is 58 m thick, however true tillite is restricted only to some portions of this interval.

The lower 31 m consist of very fine metasandstones and metasilts with occasional coarse poorly sorted metasandstone interbeds, generally less than 0.75 m thick. Scapolite-rich horizons occur in some metasilts, less commonly in metasandstones. Sub-rounded quartz pebbles to 4 cm across (this being exception) are present in some thin tillite intervals.

A massive tillite interval about 16 m thick follows. The rock consists of sub-rounded quartz and rare kaolinized metasandstone and quartzite pebbles (B3H, B3G) set in an unsorted matrix of metasilts to very fine metasandstone (Plate 14, Fig. (b)). Occasional rounded boulders up to 20 cm across are present in this fine matrix (Plate 14, Fig. (a)). Minor inter-

beds of fine to coarse poorly sorted metasandstones occur in the tillite interval. These are laminated in parts and are interpreted as reworked till deposits formed in a shallow glaciomarine environment (Link, 1976).

The uppermost interval consists of poorly bedded, weakly laminated metasiltsstones and fine to medium-grained metasandstones (B3C), some of which are quartzitic (these beds being less than 15 cm thick). Occasional thin (to 8 cm) coarse metasandstone beds are also present.

3.2.1 Comparison with the Sturt Tillite Stratotype

Thickness of the whole interval is much less than the estimated 220 m of the Type Sturt Tillite in the Sturt Gorge (Link, 1976). In the type area, Coats (1967) has interpreted the contact between the Tillite and the underlying Belair Sub-group as a disconformity, however no evidence of such a relationship was seen in the pipeline excavations.

The lithologies are similar except that the range of rock types represented in the pebbles and boulders of the tillite are not evident in the metamorphosed equivalent. Exposure is limited, however, and kaolinization may have virtually obliterated the presence of originally feldspar-rich rocks. Link (1976) interpreted the massive tillite of the Sturt Gorge as having been deposited beneath a floating ice sheet; the metamorphosed equivalent did not reveal anything contradictory to such an origin.

3.3 Tapley Hill Formation

The base (12) of the metamorphosed Tapley Hill Formation is marked by the appearance of finely laminated metasiltsstones (B2) which are scapolite-bearing in most horizons. The scapolite is weathered out of the kaolinized rocks as distinctive white granules (E30; Plate 14, Figs. (c & d)). Minor thin calc-silicates occur in the lower levels (E37A).

Just 4 m above the base is a 3 m thick horizon of kaolinized but very dark grey laminated metasiltsstone in an otherwise pale grey sequence. It is possible that this is the equivalent of the carbonaceous and pyritic "Tindelpina Shale Member" shown to occupy the basal portion of the Tapley

Hill Formation in the northern half of the ADELAIDE 1:250,000 map sheet area (Thomson, 1969).

Although the formation consists predominantly of a uniform succession of laminated metasiltsstones, there are variations (particularly in the upper levels) besides variations in the scapolite content of the rocks. In a 130 m interval which is approximately 380 m above the base, there are occasional fine metasandstone beds to 1 m thick. The following 68 m contains occasional quartz-micaschist interbeds (E35A) with traces of andalusite. Some strata are cross-bedded on a small scale (E32B) although the sequence is predominantly flat-bedded. An exceptionally thick (4.5 m) weakly laminated fine metasandstone unit (E31) occurs some 95 m from the top of the formation, the upper 30 m of which is predominantly weakly laminated and contains virtually no scapolite.

Overlying the laminated metasiltsstones (contact ⑬, Fig. 2) is a 70 m thick interval of scapolite-bearing metasiltsstones and fine to coarse-grained metasandstones and meta-arkoses which may be interpreted as shallow glaciomarine deposits (c.f. Link, 1976). It is suggested herein that this interval is the equivalent of the finer grained Eudunda Arkose Member of the Tapley Hill Formation which is developed in its upper levels further north, in the vicinity of Eudunda (ADELAIDE 1:250,000 map sheet (Thomson, 1969)). Still further north, lenticular psammitic intervals persist in the uppermost levels of the Tapley Hill Formation, (Burra 1:63,360 map sheet (Johnson, 1964); Wilmington area (Binks, 1966)).

In the vicinity of Nairne, the lower 27 m of the interval consists mainly of feldspathic fine metasandstones passing rapidly up the sequence into medium-grained metasandstones which are laminated in parts (E28) and occasionally cross-bedded. Some poorly sorted coarse metasandstone and meta-arkose interbeds (to 30 cm thick) are present (E28B) and minor thin metasiltsstones occur in the upper few metres. Coarse meta-arkose beds are particularly common in the lower levels and contain very large rounded

grains of relict siltstone or claystone.

Overlying an 8.5 m thick interval of scapolite-bearing metasiltstones which follows, are kaolinized poorly sorted fine to medium-grained feldspathic metasandstones and meta-arkoses (E26A) with medium to coarse-grained horizons (E26B) in the lower levels. Occasional weakly laminated metasiltstones (which are rich in scapolite in the upper levels) break the dominantly psammitic interval. Some weak ripple marks could be distinguished in the finer metasandstones.

3.3.1 Comparison with the Tapley Hill Formation Stratotype

The thickness of the eastern equivalent of the Tapley Hill Formation is much reduced (being some 910 m thick) compared with the 3,200 m originally estimated for the type sequence (Sprigg, 1942; Mawson and Sprigg, 1950), or the revised estimate of 2,000 m (Love, 1972). The arkosic interval described above has no counterpart in the vicinity of the type area (Sprigg, 1942; Love, 1972). Furthermore, there is no trace of the thin limestone beds which are common in the upper part of the Type Tapley Hill Formation, however, because of the deeply weathered nature of the lithologies it is unlikely that thin limestones would be preserved. In the Birdwood-Brukunga area, however, calc-silicate bands appear quite common in this interval (see section B.4.2.2.2).

Bearing in mind the effects of metamorphism, the sequence of laminated metasiltstones and metashales is identical to the laminated calcareous slates which constitute the bulk of the Type Tapley Hill Formation. The depositional environment of these rocks has been generally interpreted as shallow marine (Forbes in Twidale et al. (1976)).

3.4 Brighton Limestone

The arkosic interval marking the top of the Tapley Hill Formation is overlain by laminated scapolite-bearing metasiltstones, similar in appearance to the underlying metasiltstones (14). On the basis of observations along Mt. Barker Creek some 5 km to the south, the Brighton Limestone Equivalent

(a coarse white marble), which is the uppermost unit of the Sturt Group, should occupy a horizon immediately above the arkosic interval. It is possible that this unit has lensed out between Mt. Barker Creek and the pipeline section. Alternatively, it may be extremely reduced in thickness and may have been overlooked in the spoil adjacent to the pipeline trench (which had already been filled in this interval). Had the marble originally been present, however, it would undoubtedly have been weathered away to considerable depths, as indicated by the carious weathering of the exposed meta-siltstones and metasandstones which were originally calcareous. The marble (which is approximately 55 m thick in Mt. Barker Creek) bears no resemblance to the partly oolitic limestone in its type locality at the Brighton Quarries on the outskirts of Adelaide, where it is 30 m thick (Mawson and Sprigg, 1950). Such difference is believed to be due to facies changes.

The estimated total thickness of the Sturt Group exposed in the pipeline excavations is approximately 1400 m, considerably less than the equivalent sequence in the western Mt. Lofty Ranges, estimated by Mawson and Sprigg (1950) as being in excess of 3800 m thick.

4. MARINO GROUP

Strata of the Marino Group overly and are presumably conformable with the uppermost strata of the Sturt Group. This interval which was mapped in detail in the Nairne-Mt. Barker Creek area, will be described in a following section, however thicknesses will be compared here. Estimated thickness of the Marino Group in the pipeline section is approximately 1480 m whereas along Mt. Barker Creek, the Group is some 1120 m thick. This is in close agreement with the estimated 1800 m in the type area (Mawson and Sprigg, 1950).

PART I

STRATIGRAPHY (cont'd)

B: THE NATURE OF THE ADELAIDEAN KANMANTOO GROUP BOUNDARY1. INTRODUCTION

The history of the controversy relating to the nature of the boundary between Precambrian and Cambrian strata in the eastern Mt. Lofty Ranges is well documented by Daily and Milnes (1971) and only an outline of previous work will be given here. The earliest interpretation of the boundary was given on the Adelaide 1:63,360 map sheet (Sprigg, Whittle and Campana, 1951) which showed Precambrian strata lying to the west and the Kanmantoo Group sequence to the east of an approximately north-south fault (the Nairne Fault), thus explaining the obvious discordance between Adelaidean rocks and younger strata in the vicinity of Mt. Charles. This interpretation was carried through to the adjoining Gawler 1:63,360 map sheet (Campana, 1953) to the north and onto the Echunga 1:63,360 map sheet (Sprigg and Wilson, 1954) to the south, where Kanmantoo Group rocks are shown as being in fault contact with Adelaidean and Lower Cambrian strata (including some belonging to the lower levels of the Kanmantoo Group).

Campana and Horwitz (1956) first considered the Kanmantoo Group as a transgressive sequence, lying on rocks ranging from Archaean to Lower Cambrian age. Later, Horwitz, Thomson and Webb (1959) closely examined the region between Mt. Magnificent (Milang 1:63,360 map sheet) and Mt. Charles (Adelaide 1:63,360 map sheet), a distance of approximately 45 km, in an attempt to resolve the problem and locate the base of the Cambrian. They concluded that basal Cambrian strata (which were correlated with Lower Cambrian strata in the western Mt. Lofty Ranges up to and including the Heatherdale Shale) are conformably overlain by the Kanmantoo Group sequence. In the north and south of this region, the entire Cambrian sequence in the eastern Mt. Lofty Ranges was interpreted as being transgressive over rocks of the Adelaide Supergroup ranging from the upper levels of the Torrens Group up to and including the Marino Group (Horwitz, Thomson and Webb, 1959 Plates I and II), the boundary in the vicinity of Mt. Charles being an angu-

lar unconformity, transgression having occurred over previously folded Adelaidean strata. Between these two areas (including the Nairne-Mt. Barker Creek area), the Precambrian and Cambrian sequences were believed to be conformable. These interpretations were subsequently largely retained on the Milang 1:63,360 map sheet (Horwitz and Thomson, 1960), the BARKER 1:250,000 map sheet (Thomson and Horwitz, 1962) and the ADELAIDE 1:250,000 map sheet (Thomson, 1969). A modification of the original hypothesis of Horwitz, Thomson & Webb (1959) is shown by Thomson (1969) on the ADELAIDE 1:250,000 map sheet where the basal Cambrian sequence is bounded above and below by unconformities which truncate the basal Cambrian strata just north of Mt. Torrens. The younger Kanmantoo Group is shown persisting to the north, overlying progressively older Torrens Group rocks, the contact being interpreted as an angular unconformity.

Kleeman and Skinner (1959) mapped an area between Strathalbyn and Harrogate and disproved the existence of the Nairne Fault in the Macclesfield area as shown on the Echunga 1:63,360 map sheet (Sprigg and Wilson, 1954) by tracing marker horizons and structural features across the inferred fault. Conflicting with the original definition of the Kanmantoo Group by Sprigg and Campana (1953), Kleeman and Skinner (1959) proposed that the base of the Nairne Pyrite Member define the base of the Kanmantoo Group, suggesting that rocks immediately below are Marinoan. Their revised definition of the Kanmantoo Group was dismissed by Daily and Milnes (1971), giving priority to the original definition. Furthermore, the strata which lie immediately below the Nairne Pyrite Member can be correlated with the Backstairs Passage Formation of the Kanmantoo Group (Daily and Milnes, 1972). Finding no evidence for a sedimentary break or an angular unconformity, Kleeman and Skinner (1959) considered that the Precambrian and Cambrian formed an entirely conformable succession. This, however, was not in conflict with the work of Horwitz, Thomson and Webb (1959) as the proposed unconformities lie to the north and south of the area examined by Kleeman and Skinner.

The prominent but lenticular Mt. Barker and Macclesfield Quartzites were originally considered as Cambrian (but pre-Kanmantoo Group) by Sprigg and Wilson (1954, Echunga 1:63,360 map sheet). Subsequently these units were correlated by Horwitz, Thomson and Webb (1959) and shown as occupying a horizon immediately below the Heatherdale Shale equivalent. Later, however, Thomson and Horwitz (1962) indicated on the legend of the BARKER 1:250,000 map sheet that their stratigraphic position is uncertain but both were placed in the Cambrian (but pre-Kanmantoo Group). Earlier, Kleeman and Skinner (1959) were of the opinion that the Macclesfield and Mt. Barker Quartzites occupied different horizons within the same unit, this being termed the Inman Hill Formation (Kanmantoo Group) on the adjoining ADELAIDE 1:250,000 map sheet. Thomson in Parkin (1969) however proposed that these quartzites occur within the Strangway Hill Formation which Thomson (1969) indicated on the ADELAIDE 1:250,000 map sheet as being the basal unit of the Kanmantoo Group. The variability of these interpretations demonstrates the early confusion in the terminology and the stratigraphic scheme for this interval. More recently, Daily and Milnes (1972) revised the stratigraphic scheme for the Kanmantoo Group in the Nairne-Mt. Barker Creek area based on observations on the south coast of Fleurieu Peninsula. In a comparison with the terminology given on the BARKER 1:250,000 map sheet, the term Strangway Hill Formation was discarded (Daily and Milnes, 1971) owing to confusion as to its stratigraphic position. In the new stratigraphic scheme, the Backstairs Passage Formation is equated with the Inman Hill Formation and the lower portion of the overlying Talisker Calc-siltstone with the Nairne Pyrite Member. The present study, however, suggests that the Nairne Pyrite Member should more appropriately be equated with the upper levels of the Talisker Calc-siltstone.

Following the earlier dismissals of the Nairne Fault concept, Daily and Milnes (1971) again advocated a fault separating the Kanmantoo Group and Precambrian rocks in the eastern Mt. Lofty Ranges, indicating a number of

localities¹ on both the western and eastern sides of the ranges in which the interpretations presented by the proponents of an unconformity are incorrect. Working on excellent exposures on the south coast of Fleurieu Peninsula, Daily and Milnes (1971) demonstrated that the contact between the Kanmantoo Group and older "basal" Cambrian metasediments (collectively termed the Normanville Group (Daily and Milnes, 1973)) is conformable, not unconformable as proposed by Campana and Horwitz (1956) and more recently by Thomson in Parkin (1969).

Recently Marlow (1975) proposed that in the vicinity of the Strathalbyn Anticline (BARKER 1:250,000 map sheet), the boundary between the Kanmantoo Group (down to the lower levels of the Tapanappa Formation) and the Adelaidean sequence is a fault and that the uppermost Adelaidean unit is the Macclesfield Quartzite (upper Marino Group). These deductions were based primarily on the rock relations on the complementary Macclesfield Syncline to the west where "basal" Cambrian and lower Kanmantoo Group strata (possibly a portion of the Carrickalinga Head Formation) were interpreted as striking into the underlying Macclesfield Quartzite, thus disproving the unconformity proposed by Horwitz, Thomson and Webb (1959). This work showed that the Nairne Fault probably does exist in this area but is folded in the Macclesfield syncline - Strathalbyn anticline structure. Hence the earlier mapping of Kleeman and Skinner (1959) does not necessarily conflict with the existence of the fault in this area but only with its location

¹These localities include (i) the vicinity of Yankalilla Hill (Yankalilla and Jervis 1:63,360 map sheets); (ii) the vicinity of Angaston (Truro 1:63,360 map sheet (Coats and Thomson, 1959)); (iii) near Inman Hill (Milang 1:63,360 map sheet (Horwitz and Thomson, 1960)).

2. FACIES CHANGE WITHIN THE KANMANTOO GROUP

The formations of the Kanmantoo Group exposed in the Nairne-Mt. Barker Creek and Birdwood-Brukunga areas are remarkably similar to their counterparts in the Kanmantoo Group stratotype on the south coast of Fleurieu Peninsula, considering the large distances (in excess of 75 km of strike length) separating these areas. Some facies change, however, is detectable in the units examined and is summarized below, more detailed descriptions and comparisons being given in the following section.

The most distinctive unit, the Backstairs Passage Formation, consisting of laminated feldspathic metasandstones and meta-arkoses is easily recognized, although in the Nairne-Mt. Barker Creek area the upper portion of the formation is laterally variable and passes into a more pelitic facies where the rocks are rarely laminated. In both the Nairne-Mt. Barker Creek and Birdwood-Brukunga areas there are also considerable lateral and vertical variations within the basal portions of this formation, from dominantly psammitic to more pelitic facies. The upper levels of the underlying strata exposed in the Mt. Charles-Birdwood area recall the gross characteristic features of the upper member of the Carrickalinga Head Formation as described by Daily and Milnes (1971). The metasediments below these are equated with the middle member of this formation although the lithologies are more psammitic, particularly in the upper parts.

The Type Backstairs Passage Formation is conformably overlain by the Talisker Calc-siltstone, the equivalents of which in the areas examined consist of dominantly pelitic metasediments which are pyritic, except in their lower levels in part of the Nairne-Mt. Barker Creek area. In general, the characteristic banding of the Type Talisker Calc-siltstone is not prominent and sulphides are more common reflecting sedimentation in an environment more favourable to their formation.

The thick sequence of impure metasandstones of the overlying Tapanappa Formation appears to be almost identical to its equivalent in the Kanmantoo

Group stratotype, the presence of numerous sulphide bands being a characteristic feature. There is, however, in the Nairne-Mt. Barker Creek area, a marked basal portion in which there is a greater prevalence of fines.

3. NAIRNE-MT. BARKER CREEK AREA

3.1 Introduction

The metamorphosed sequence mapped in the Nairne-Mt. Barker Creek area can be correlated with rocks of the upper Adelaidean and lower Kanmantoo Group stratotypes. The Precambrian strata mapped include the upper levels of the Tapley Hill Formation which is conformably overlain by the Brighton Limestone Equivalent and Marino Group metasediments, these broad correlations being made earlier by Sprigg and Wilson (1954) on the Echunga 1:63,360 map sheet. A break in the sequence is followed by a conformable succession of Kanmantoo Group strata. Based on the stratigraphic scheme for the Kanmantoo Group in its type section on Fleurieu Peninsula (after Daily and Milnes, 1971), further subdivision of the Cambrian sequence could be made, with the recognition of strata from the upper levels of the basal Carrickalinga Head Formation to the lower levels of the Tapanappa Formation.

Description of the sequence given below is based primarily on the lithologies observed in a stratigraphic section measured along Mt. Barker Creek (Appendix I). This is supplemented by an examination of rocks exposed in excavations for the Murray Bridge-Onkaparinga River pipeline immediately north of Nairne and general mapping by the author. Rocks in Mt. Barker Creek are relatively unweathered permitting chemical analysis, however, in the vicinity of Nairne (particularly to the south-west) rocks are extensively kaolinized and rarely outcrop. The degree of alteration decreases rapidly to the south, however, permitting easier recognition of rock types.

Representative samples are indicated where appropriate while a more extensive collection accompanies Appendix I. From older to younger the sequence is:

3.2 Sturt Group

3.2.1 Tapley Hill Formation

Metamorphosed equivalents of the Tapley Hill Formation (termed Tapley Hill Slates in the original subdivision of the Adelaide System by

Mawson and Sprigg (1950)) are typically well laminated calcareous meta-siltstones grading into metashales (quartz-micashists and micaschists), (A405/BC1). Varying mica content between the layers is primarily responsible for the lamination seen in hand specimen. Scapolite, which is present in most horizons gives rocks a spotted appearance, while its variation in abundance is controlled by bedding. Kaolinized scapolite-rich rocks (A405/E37A) are well exposed in railway cuttings just west of Nairne. In the upper portion of the Tapley Hill Formation, pipeline excavations revealed a few fine metasandstone units (to 1.5 m in thickness) and minor andalusite in a quartz-micaschist horizon (A405/E35A).

With a gradual increase in grain size accompanied by a decrease in lamination over several metres, rocks pass into fine to medium-grained feldspathic metasandstones and meta-arkoses with interbedded metasilstone units. This interval, which is approximately 70 m thick, is interpreted as a possible equivalent to the finer grained "Eudunda Arkose Member" of the formation developed further north (ADELAIDE 1:250,000 map sheet), as mentioned in section A.3.3.

The contact (which is gradational), has been mapped as the horizon where metasandstones first appear, which is usually a few metres above the level of disappearance of lamination in the metasilstones, these becoming massive forming rounded, featureless outcrops. Outcrop is generally poor and the coarser lithologies are generally highly weathered, however they form a weakly defined ridge which can be traced from Mt. Barker Creek to the vicinity of Nairne.

The siltstone units are commonly laminated and contain scapolite (A405/BC3(1)). Fine metasandstones are also laminated in some horizons, however lamination in this interval is generally much weaker than in the underlying equivalents of the Tapley Hill Slates. Restricted to certain horizons are interbeds (to 30 cm) of coarse feldspathic metasandstone and meta-arkose in which grains are rounded and show a wide range in size indi-

cating poor sorting in the original sediment. Rounded quartz and relict claystone pebbles (to 1 cm) occur in some medium to coarse-grained beds (A405/E28B, BC4) and often indicate a complete absence of sorting.

3.2.2 Brighton Limestone Equivalent

The metamorphosed Brighton Limestone outcrops only in the vicinity of Mt. Barker Creek where it is approximately 55 m thick. Owing to lack of outcrop, the nature of the contact with underlying and overlying strata cannot be determined but is presumed to be conformable as in the stratotype. The unit is a massive coarse white marble interbedded with minor weakly laminated calcareous metasiltsstones grading into quartz-micaschists or meta-shales (A405/BC6) and impure marbles. Bands of relatively pure marble (A405/BC5) are up to 10 m thick.

Recrystallization has produced wholly crystalloblastic textures and there is no evidence of oolitic bands or stromatolitic structures which are found in the comparatively unmetamorphosed limestone in its type locality at the Brighton quarries. Bedding has been largely obliterated in the pure marble where only diffuse colour variations remain, with some parting along silty bedding planes.

To the north, the unit was mapped as approximately occurring a short distance above the uppermost outcrops of metasandstone and meta-arkose which overly the metasiltsstones of the Tapley Hill Formation.

3.3 Marino Group

Close correlation was possible between the sequence in the lower portion of the Marino Group stratotype and similar distinctive lithologies in the metamorphosed sequence. A correlation diagram showing thicknesses of the rock units is shown in Fig. 3.

3.3.1 Unit 1

This unit varies between 330 m and 390 m in thickness across the area. Overlying the Brighton Limestone is an interval of variable thickness (40-100 m) consisting of poorly outcropping feldspathic metasiltsstones which

are extensively kaolinized in the northern part of the area. Relatively unweathered rocks are usually calcareous.

In the vicinity of Mt. Barker Creek, the unit is seen as consisting of feldspathic metasiltstones with variable mica content which are well laminated in parts and contain occasional scapolite-rich horizons (A405/BC16, BC17). Scapolite-rich metasiltstones and metashales are most common in the upper levels of the unit and are correlated with laminated calcareous fine siltstones and shales which occur above the Hallett Arkose in the Marino Group stratotype (Fig. 3). Near the top of the unit, scapolite-rich rocks pass into calc-silicates (A405/BC18, BC23) which have a variable mineralogy (summarized as quartz + biotite + hornblende + scapolite \pm calcite \pm plagioclase). These calc-silicates and scapolite-rich metasiltstones and metashales are extremely lenticular, however three intervals could be traced for several kilometres north of Mt. Barker Creek. Scapolite-rich bands show a complex intertonguing with originally less calcareous rocks which is seen even on hand specimen scale (Plate 15, Fig. (a)). Minor cross-bedding (sets to 1 m) was noted at the top of this sequence in Mt. Barker Creek.

Two laterally variable arkose intervals persist across the area. The lower is correlated with the Hallett Arkose, which in the vicinity of Mt. Barker Creek is distinguished from enclosing strata by slightly coarser lithologies (metasiltstones to fine metasandstones) with lower mica content (A405/BC11(1), BC12) and minor thin interbeds of fine to medium-grained feldspathic metasandstone and meta-arkose. Outcrops are generally more resistant than those of enclosing lithologies. To the north, coarser lithologies become more common and fine to coarse feldspathic metasandstones and meta-arkoses form a major portion of the strata. Pipeline excavations revealed four arkose bands within these levels of Unit 1 in the vicinity of Nairne. These consist of medium to coarse poorly sorted feldspathic metasandstones and meta-arkoses (A405/E15A, E18B) with minor thin interbeds of fine metasandstone and metasiltstone. The coarser units are parted by horizons of

feldspathic metasilstone and minor fine metasandstone (A405/E16A, E19, E20) which are scapolite-bearing in parts and generally laminated.

The upper arkose marks the top of Unit 1 and is correlated with the "upper Arkose" in the Marino Group stratotype. The lower contact is sharp in some localities and gradational in others (eg., localities 23-24). In the vicinity of Mt. Barker Creek it is composed of micaceous fine to medium-grained, slightly feldspathic metasandstones (A405/BC22) grading into quartzites which form resistant outcrops. There are minor interbeds (to 1 m) of laminated metasilstones with scapolite-rich horizons in the upper parts. Some metasilstones pass into thin (to 30 cm) metashales (A405/BC22(1)). Occasional thin (to 5 cm) medium to coarse meta-arkoses occur near the top. To the north, with a general increase in grain size and feldspar content, rocks become predominantly poorly sorted medium to coarse meta-arkoses and feldspathic metasandstones with thin interbedded units of weakly laminated scapolite-bearing metasilstones and fine metasandstones. Due to lateral variations and poor outcrop it was impossible to trace individual arkose bands.

In the southern part of the area, the contact with the overlying schists of Unit 2 is more sudden than in the north. Over several metres, medium-grained metasandstones with minor thin beds of coarse arkose pass up into metasilstones followed by metashales (quartz-micaschists and mica-schists). In the north, the change is less marked and the metasandstones and meta-arkoses are overlain by at least 50 m of weakly laminated scapolite-rich feldspathic metasilstones and fine metasandstones (Plate 15, Fig. (b)) having at some localities (eg. locality 173) minor interbedded units of feldspathic quartz-micaschists and thin interbeds (to 50 cm) of fine to medium-grained feldspathic metasandstone and meta-arkose (concentrated in bands up to 4 m thick). There is obviously a considerable thickening of the upper arkose from south to north.

3.3.2 Unit 2

This unit varies between 260 m and 290 m in thickness (Fig. 3) and consists predominantly of distinctive andalusite schists which persist across the whole area in a belt some 250 m wide. Outcrop is generally poor and of low relief, however even the smallest, highly weathered exposures reveal the typical resistant granules composed of andalusite, quartz and micas which give outcrops their characteristic knotted appearance.

In addition to andalusite, other Al-silicate minerals (namely staurolite, garnet and fibrolite (A405/BC34,E8)) are developed along peraluminous beds of appropriate bulk composition in a sequence of thinly interbedded quartz-micaschists and micaschists (Plate 15, Figs.(c,d)). Andalusite porphyroblasts are large, occasionally to 1 cm across (A405/BC27,BC37). Laminae or beds commonly range from a few mm to 2 cm and rarely to 5 cm while finer laminae are seen in thin section. The sharp boundaries between quartz-rich and mica-rich layers (even on thin section scale) suggests that metamorphic segregation has considerably accentuated the original sedimentary layering.

More resistant beds of coarser metasilstone to very fine metasandstone occur in some intervals. These are usually weakly laminated and less than 10 cm thick although some up to 25 cm in thickness have been recorded. Within the less micaceous beds, lenses of quartz-biotite segregations often occur (A405/BC30, Plate 15, Fig. (d)), these being usually 3 to 10 cm thick. The form and orientation of these metamorphic structures is controlled primarily by bedding (S_0) and to a lesser extent by schistosity (S_2). Other features will be described in more detail in a later section.

A schistosity is well developed in these rocks, being sub-parallel to bedding in the schists whereas refraction through the less micaceous beds has resulted in a larger angle between these surfaces. The schistosity is the axial plane structure to folds which belong to the major phase of deformation in the area (Plate 16, Fig. (a)). A later set of crenulations

is commonly developed on schistosity surfaces (Plate 16, Fig. (b)) while crenulations are often found to emanate from porphyroblasts (Plate 16, Fig. (c), A405/BC34).

A transition interval at the top of the unit is less micaceous in general, marking a passage to the overlying less pelitic strata. Rocks consist predominantly of weakly laminated metasiltsstones with minor meta-shales. Andalusite and staurolite are less common than in the schists below, with beds up to 4 m thick in which these minerals are absent. Occasional interbeds of more resistant metasiltsstones to micaceous fine metasandstones (A405/BC33) are laminated in parts and up to 50 cm in thickness while quartz-biotite segregations (to 5 cm) occur in some of these less micaceous lithologies. The interval varies in thickness and thins to several metres north of Mt. Barker Creek (where it is 51 m thick), while a transition passage of similar thickness was found to overly the andalusite schists exposed in the pipeline excavations at Nairne.

3.3.3 Unit 3

Above the schists of Unit 2 is a sequence of metasiltsstones with minor metashales and some micaceous fine metasandstones (which grade into metasiltsstones). As a whole, this interval is less micaceous than the strata below. Exposure is often better and the lithologies generally make bolder but often featureless outcrops. Subtle variations in mica content and in abundance and thickness of resistant fine metasandstone and metasiltsstone beds has enabled a subdivision into five members. The two lower members can be traced across the map area although there is often uncertainty as to the location of their boundaries, due to poor outcrop. The three upper members could not be delimited in the northern part of the area, again due to poor outcrop. Unfortunately the pipeline trench had mostly been filled to the east of Member (b), consequently a comparison of lithologies with those in Mt. Barker Creek was impaired, although spoil alongside the trench gave a fair indication of the types of lithologies and their approximate thicknesses. There is a considerable increase in

thickness of the unit from south to north, from approximately 520 m to 800 m. Mapping indicated that most of this additional thickness is in the upper levels.

Member (a) The lowest member of the unit can be further subdivided into four distinct intervals which can be traced across the area.

(i) This consists of very micaceous metasiltsstones (beds to 1.5 m) passing into quartz-micaschists with less micaceous interbeds (to 1 m) which appear to be more common in the south. These more resistant beds tend to be lenticular and occasionally beds are completely pulled out into distinct lenses indicating that this is a tectonic feature produced by the boudinage process. Beds of the more micaceous lithologies (Quartz-micaschists) are generally thin (to 30 cm) and some layers contain andalusite and staurolite (A405/BC38).

(ii) This is a thin interval of more massive and resistant lithologies marked at the base by common resistant metasiltsstones to fine metasandstones (A405/BC35) which are weakly laminated and occasionally boudinaged. Thin (to 0.75 m) interbedded more micaceous metasiltsstones (grading to quartz-micaschists) are also present. The interval is 17 m thick in the vicinity of Mt. Barker Creek. While the marked decrease in mica content from intervals (i) to (ii) can be traced from south to north across the area, outcrop does not usually permit exact location of the boundaries. In the vicinity of Nairne, however, a corresponding thicker sequence (approx. 30 m) of resistant metasiltsstones and fine metasandstones (A405/E7A) was revealed in the pipeline excavations (Plate 16, Fig. (d)). Lithologies become gradually more micaceous in the upper levels, with interbeds of quartz-micaschist to 2.5 m. Minor andalusite occurs in the schists, mainly in the north.

(iii) Pelitic metasediments become more common in this interval. Rocks are predominantly weakly laminated micaceous metasiltsstones and minor quartz-micaschists (Plate 17, Fig. (a)) with interbedded less micaceous meta-

siltstones and fine metasandstones (A405/BC40) to 1.5 m thick, which are also weakly laminated. These less micaceous beds are again commonly boudinaged. Rocks are commonly thinly bedded and flaggy in parts. The few true quartz-mica schists are usually less than 20 cm thick and rarely to 1 m thick. Some schists contain andalusite. Quartz-biotite segregations (occasionally to 13 cm) occur throughout the interval and are commonly folded (A405/E4F(2)). Minor sedimentary structures (ripple marks, cross-bedding (A405/E5B)) were found in the strata exposed in the pipeline excavations near Nairne.

(iv) Mapping distinguished a fourth interval which is less obvious in Mt. Barker Creek. It is characterized by a greater abundance of resistant metasilstone and fine metasandstone beds (to 2.5 m) which are well laminated in parts (A405/E5, Plate 17, Fig. (b)). Their thickness rapidly decreases towards the top of the interval. Numerous quartz-biotite segregations (to 30 cm) occur, these being particularly common in the vicinity of Nairne.

Member (b) An overall increase in mica content of the rocks marks the base of the dominantly pelitic Member (b) which consists mainly of very micaceous metasilstones which grade into quartz-micaschists. This member can be further subdivided into three intervals, primarily on the basis of the proportion of resistant less micaceous interbeds.

(i) The lowest interval of this member consists of very micaceous metasilstones and quartz-micaschists (A405/E4B, Plate 17, Fig. (c)) with common interbedded less micaceous and coarser metasilstones. More resistant metasilstone to fine metasandstone interbeds as found in Member (a) are rare, and those present are under 0.75 m in thickness. Minor andalusite occurs in quartz-micaschists although some beds (to 2 cm) contain abundant andalusite porphyroblasts, often in addition to staurolite and garnet (A405/E4, E4E). In the vicinity of Nairne, however, andalusite-rich bands to 1.5 m are present (e.g., locality 196). Commonly metasilstones contain

quartz-biotite segregations (A405/E4A,E4D) to 15 cm thick (in rare cases to 30 cm) whereas these are rarely developed in the most micaceous lithologies.

(ii) Within the dominantly pelitic sequence of Member (b) is a thick interval (approx. 45 m) of less micaceous rocks which are very resistant and well laminated in parts. A sudden increase in the proportion of resistant metasilstone beds (to 2 m) marks its base. Lithologies pass upwards into predominantly massive, resistant metasilstones (grading to fine metasandstones) with thin (to 1 m) interbeds of more micaceous metasilstones (grading in parts into quartz-micaschists). The massive strata constitute about 65% of this interval. Owing to poor outcrop, its delimitation was not possible in the northern half of the area.

(iii) Overlying the boldly outcropping strata of interval (ii) is another dominantly pelitic interval similar to interval (i). The minor interbeds of resistant metasilstones generally range from 10 cm to 0.75 m in thickness. Andalusite is present in some quartz-micaschists and micaschists (A405/BC42).

Member (c) A significantly less pelitic interval (about 40 m thick) follows. Poor outcrop does not permit delimitation of Member (c) in the northern part of the area. However, an equivalent interval of similar thickness was apparent from the spoil alongside the pipeline excavations near Nairne.

The member is distinguished by the abundance of resistant metasilstone to fine metasandstone beds (A405/BC43,E3) which are most common and thickest (to 1.5 m) in the upper levels. The least micaceous rocks are generally weakly laminated whereas the more pelitic metasilstones (A405/E2A) are commonly well laminated. With increasing mica content some metasilstones pass into quartz-mica schists. Occasional thin calc-silicate beds (to 1 cm) were observed at locality 375 (A405/M11).

Quartz-biotite segregations are present throughout the member and are at most 30 cm thick. In the central part of the area, however, are

thick bands (to 2.5 m) of slightly micaceous, medium to coarse-grained quartz-rich rocks which are interpreted as exceptionally thick segregations. Some of these could be followed uninterrupted for up to 150 m, while in the upper levels of the member, where these bands are most common, individual segregations appear to be developed along horizons which persist for distances of up to a few km.

Member (d) A thick interval of dominantly pelitic metasediments overlies Member (c). This consists of very micaceous metasiltsstones grading to quartz-micaschists with minor less micaceous, weakly laminated metasiltstone interbeds which are usually less than 10 cm thick (A405/E2). In the upper levels of the member, however, resistant metasiltstone beds are occasionally thicker, up to 60 cm and rarely to 1.5 m (locality 111). Often these beds are lenticular, probably the result of boudinaging. Occasional andalusite-rich bands occur in thinly interbedded quartz-micaschists and micaschists (A405/BC44, E1; Plate 17, Fig. (d)). These are generally less than 30 cm thick, however rare bands of up to 4 m have been noted. Some quartz-biotite segregations (usually less than 10 cm) are developed in the metasiltsstones.

Member (e) More common resistant metasiltstone interbeds and better developed bedding distinguishes Member (e) from the underlying strata. Rocks are flaggy in parts, particularly in the upper levels (Plate 18, Fig. (a)) and are usually laminated. The common less micaceous interbeds (A405/E1A) are generally less than 10 cm thick (rarely to 50 cm) and mostly weakly or non-laminated. Thin andalusite schists occur, their proportion varying through the member.

The member thickens considerably from south to north. Poor outcrop however does not permit the precise location of its boundaries in the vicinity of Mt. Barker while a total absence of outcrop is encountered to the north. At the equivalent interval in the vicinity of Nairne, however, similar lithologies were recognized from the spoil adjacent to the pipeline

trench and at isolated locations along the trench where strata remained uncovered at the time of inspection.

3.3.4 Unit 4

Conformably overlying the metasiltsstones of Unit 3 is an originally carbonate-rich interval which is highly variable both laterally and vertically. The characteristic lithologies could be traced across the map area except for a small area due south of Mt. Barker. Due to the lateral variability of the strata, the descriptions given below are supplemented by a number of detailed stratigraphic sections examined along Mt. Barker Creek and immediately north of Mt. Barker (Fig. 4).

In the vicinity of Mt. Barker Creek, lithologies consist of massive to well bedded layered calc-silicate units (A40/BC47, BC45, BC52) which grade laterally and vertically into metasiltsstones (sections C to G, Fig. 4). The lateral variations result in widely variable thicknesses of calc-silicate-bearing strata, ranging from 38 m (section D) to about 10 m (section G) as the lower calc-silicates pass into metasiltsstones. In the vicinity of Mt. Barker, only massive, highly resistant layered calc-silicates outcrop, these units having thickened considerably, reaching over 100 m in thickness near the southern end of the Mt. Barker ridge (see Map 1). These calc-silicates rapidly change facies towards the northern end of Mt. Barker where excavations for the South-East freeway revealed some 15 m of scapolite-bearing metasiltsstones (A405/MCS2a) becoming rapidly richer in calc-silicate minerals up the sequence, with the occurrence of a thin (4 m) layered calc-silicate at the top of the sequence (Section B, Fig. 4; A405/MCS2c,2b). To the north, in an area of sporadic outcrop, some 80 m of scapolite-bearing metasiltsstones with minor micaschists occur above Unit 3 and are equated with the calc-silicate-bearing interval (Unit 4) in Mt. Barker Creek. The base of Unit 4 has obviously no time significance as the calc-silicate-bearing strata inter-finger with the upper metasiltsstones of Unit 3. Its base is therefore diachronous.

3.3.5 Mt. Barker Quartzite

The Mt. Barker Quartzite forms the prominent ridge which rises to the peak of Mt. Barker where the unit attains its maximum thickness, in excess of 40 m. A conformable contact between the Mt. Barker Quartzite and calc-silicates of Unit 4 revealed by excavations for the South-East freeway suggests probable conformity between these units elsewhere in the area (Plates 18, Fig. (c), 19, Fig. (a)).

In the Mt. Barker Creek, lenses of massive white orthoquartzite (Plate 18, Fig. (b)) overly the calc-silicates and metasilstones of Unit 4 (sections C to G, Fig. 4). Although the contact with the strata above and below is not seen (except at locality 130 (section G)), metasilstones outcrop to within a few metres of the quartzite at some localities. The lenticular outcrop pattern of the formation may be an original sedimentary feature or it may be the result of faulting along its eastern margin, or a combination of both. Two minor faults obviously displace the quartzite band between localities 103 and 119 (Map 1; Plate 18, Fig. (b)).

At locality 130 in Mt. Barker Creek (section G, Fig. 4) a lens of pure quartzite 1.5 m thick passes laterally into layered calc-silicates. The association of thin quartzite beds with scapolite-bearing metasilstones in the lower 2 m of the Quartzite at the northern end of Mt. Barker (section B, Fig. 4) suggests that this lens may in fact be equivalent to one of these thin quartzites which are stratigraphically below the main quartzite interval (which has probably been faulted out). Stratigraphically above the lens and some 30 m to the north are over 6 m of poorly outcropping layered calc-silicates. Whether these belong to the same interval as those immediately in (conformable) contact with the quartzite lens or whether they represent the basal Mt. Terrible Formation (Normanville Group) or are within the Kanmantoo Group, possibly the Carrickalinga Head Formation (c.f. section E, Fig. 4), cannot be resolved. It is suggested, with some reservation, that the uppermost calc-silicates at least may be in the Carrickalinga Head Formation on the basis of the occurrence of scapolite-bearing metasilstones in this formation at the

northern end of Mt. Barker (in the freeway excavations) and in section E (Fig. 4) where calc-silicates also overly the quartzite and are interpreted as belonging to the Kanmantoo Group. These lithologies will be further described in the following section.

The Quartzite in Mt. Barker Creek is a glassy orthoquartzite exclusively and lamination is only weakly developed in parts. To the north after an interval of about 0.5 km with no outcrop, the Quartzite reappears at the southern extremity of Mt. Barker. Here the rocks are white, fine to medium-grained, slightly feldspathic quartzites (A405/MQ-1) with thin silty interbeds. Rocks are generally well bedded and weakly laminated with occasional small-scale low angle cross-bedding. In this area the top of the Quartzite does not outcrop, however there are some poor outcrops of extremely weathered quartzites in the upper levels in addition to common more feldspathic and sometimes coarser metasandstone beds which are very friable (e.g. at locality 542). The quartzites generally have a silicified crust and bedding is not discernible and some outcrops may in fact be large fallen blocks buried in finer scree material and Tertiary sediments as seen in the freeway excavations. The more feldspathic rocks are tentatively interpreted as belonging to the Kanmantoo Group. However, it is feasible that they may belong to a more feldspathic facies of the Mt. Barker Quartzite as seen further north along the Mt. Barker ridge, as there is a general increase in grain size to the north, particularly in the upper levels of the Quartzite. The rocks are very weathered as they contain a considerable feldspar content (being feldspathic metasandstones rather than quartzites) resulting in friable outcrops. Cross-bedding is still present in some strata. Irregularly shaped patches of recrystallized quartz are common, grains being very coarse (up to 4 mm).

About 400 m south of Mt. Barker summit, lithologies pass laterally into white massive orthoquartzites with a characteristic glassy appearance, resembling the unit in Mt. Barker Creek. Occasional fine to medium-grained

slightly feldspathic interbeds occur, some of which show small-scale ripple marks. The rocks are generally weakly laminated or non-laminated. Individual massive beds are up to 4 m thick. The base of the quartzite is covered with scree along the entire length of the ridge. The lower levels are generally more feldspathic, fine-grained and fairly well bedded, passing upwards into less feldspathic beds, then into typical glassy rocks over a few metres. Occasional irregular patches of recrystallized quartz occur within some feldspathic beds.

The base of the quartzite is only exposed in the South-East freeway excavations at the northern end of the Mt. Barker ridge (section B, Fig. 4; Plates 18, Fig. (c), 19, Fig (a)). In this cutting, the predominantly massive orthoquartzite is seen to show some variations. Massive units are up to 2 m thick, parted by very thin, more silty interbeds. In the lower 10 m these are up to 5 cm thick, consisting of fine micaceous meta-sandstones and metasiltsstones, occasionally interbedded with quartzites of similar thickness. Small-scale cross-bedding is evident in the common laminated intervals (Plate 19, Fig. (b)). The basal 1 to 2 m of the formation consists of kaolinized scapolite-bearing metasiltsstones with thin (to 20 cm) interbedded quartzites, locally passing laterally into predominantly massive quartzite (Plate 18, Fig. (c), 19, Fig. (a)).

The eastern slope of Mt. Barker is covered with scree which overlies ferruginous Tertiary sandstones and conglomerates with rounded boulders which are up to 0.6 m across, consisting of Mt. Barker Quartzite. The underlying strata are highly weathered and the top of the Mt. Barker Quartzite is only visible in the freeway cutting. Here there is a sudden change from typical glassy orthoquartzite to kaolinized metasiltsstones of the Kanmantoo Group. The contact between these lithologies is a fault zone (Plates 19, Fig. (c), 20, Fig. (a)) some 3 m wide which dips steeply to the east at a higher angle than the strata on either side. Within the fault zone are undistorted blocks of both rock types bounded by faults which para-

11el the fault zone. Further description of this contact is reserved for a later section (B.5).

Approximately 1 km north of Mt. Barker summit (immediately north of the freeway excavations) the quartzite disappears, either due to marked sedimentary lensing or more likely, due to faulting, the unit being truncated by the Nairne Fault. Outcrop is poor between Mt. Barker and the northern extremity of the map area. It is unknown whether the quartzite is absent in this area or is reduced in thickness and fails to outcrop. Also the level of the Mt. Barker Quartzite in relation to the outcropping strata in this area is not entirely certain. Its estimated position is shown in Map 1 and section A, Fig. 4.

3.3.5.1 Stratigraphic position of the Mt. Barker Quartzite

A comparison with the Marino Group sequence in the western Mt. Lofty Ranges indicates a possible equivalent interval to the Mt. Barker Quartzite. Daily (1963, p.586) considered the upper limit of the Marino Group in the western sequence as being marked by a "sequence of thin light coloured massive quartzites interbedded with rippled siltstone and flaggy quartzites" which "form bold outcrops along the front of the Willunga Scarp". The Mt. Barker Quartzite may be equated with these quartzites, while the Macclesfield Quartzite horizon in the south (considered to be in the upper levels of the Marino Group by Marlow (1975)) may also belong to this interval (but not necessarily at the same stratigraphic level as the Mt. Barker quartzite.)

3.3.6 Comparison with the Marino Group Stratotype

In general, the metasediments were probably very similar to the rocks seen in the Marino Group stratotype, prior to the Delamerian metamorphism and deformation. Metamorphic reconstitution of the fabric and mineralogy would have undoubtedly largely masked the smaller scale sedimentary features which occur in the type section, such as mud cracks, ripples and clay galls in the more pelitic rocks (now schists) and oolites, intraclasts and cross-lamination in the limestones (now layered calc-silicates and marbles).

Broad correlations within the Marino Group are possible, however (summarized in Fig. 3), chemical analyses of the rocks being compatible with correlatives in the lower levels of the sequence (see section IID). It is probable therefore that the depositional environments were very similar to those of the stratotype: supratidal and shallow marine (low to high energies).

No evidence was found of the red to brown coloured, poorly developed diamictite interval which occurs at Hallett Cove (Fig. 3). This interval (termed the Reynella Siltstone Member by Thomson, 1966) is recognizable north and east of the Hallett Cove area. However, this facies has not been mapped elsewhere as yet in the western Mount Lofty Ranges (Madigan, 1927; Sprigg, 1942; Thomson, 1966). A glacial origin has been suggested for the diamictite (an interpretation earlier dismissed by Sprigg, 1942); it has been equated with the "more obviously tillitic sequences" such as the Elatina Formation of the Flinders Ranges by Thomson (1966) and Forbes in Twidale et al. (1976). Earlier, however, Mawson (1949) and Mawson and Sprigg (1950) suggested that the Type Hallett Arkose is equivalent to the Elatina glacial interval. Except for the possibility of a glacial origin for parts of the eastern Hallett Arkose equivalent (and possibly the "upper arkose" also), there is no evidence of glacial sedimentation in the eastern Marino Group sequence in the area studied, although an upper glacial horizon is quite evident in the Kapunda region where tillites have been recorded (Kapunda 1:63,360 map sheet (Dickinson and Coats, 1957)).

3.4 Normanville Group

The Normanville Group (Daily and Milnes, 1973), a dominantly calcareous sequence conformably below the Kanmantoo Group on the western side of the Mt. Lofty Ranges, does not occur in the study area due to the effects of the Nairne Fault¹.

¹ See sections B3.6, B4.5 and B5 for discussion of the Nairne Fault in the Birdwood-Mt. Barker Creek region.

3.5 Kanmantoo Group

The distinctive lower formations of the Kanmantoo Group were easily recognized in the study area.

3.5.1 Carrickalinga Head Formation

The uppermost member of the Carrickalinga Head Formation, the Campana Creek Member (Daily and Milnes, 1971) is represented in the Nairne-Mt. Barker Creek area. In the Kanmantoo Group stratotype, this unit consists of well laminated metasiltsstones with common sedimentary structures (Daily and Milnes, 1971, p. 204). Exposed by excavations for the South-East freeway at Mt. Barker is a 95 m thick interval of finely laminated feldspathic metasiltsstones which are in fault contact with the Mt. Barker Quartzite. This interval, which is overlain by metasandstones of the Backstairs Passage Formation, is correlated with the Campana Creek Member, its basal portions presumably being absent. Scapolite-rich beds are common in the upper levels.

The only other exposures of possible Carrickalinga Head Formation strata are along Mt. Barker Creek where the interval (if present) is much reduced in thickness due to faulting. In section E (Fig. 4) is an interval some 10 m thick which might be equated with the top of the Campana Creek Member. The lithologies consist of scapolite and hornblende-bearing metasiltsstones passing laterally and vertically into layered calc-silicates. A very lenticular pale grey impure marble lens (A405/BC49(2)) is also present. From its maximum of 4 m this unit passes into calc-silicates over just a few metres (Plate 18, Fig. (b)). On the basis of the abundance of scapolite-rich beds in the lower part of the Campana Creek Member at Mt. Barker and the common occurrence of calc-silicates in this interval in the area between Mt. Torrens and Birdwood (see section B.4.3.1), it is suggested that these rocks also belong to the Carrickalinga Head Formation. This interpretation is only tentative, however, as it is also possible that the calc-silicates are in the basal portion of the Backstairs Passage Formation (as observed in

the Birdwood-Brukunga area). As mentioned earlier, the upper calc-silicates in section G (Fig. 4) in Mt. Barker Creek may also belong to the Carrickalinga Head Formation.

3.5.2 Backstairs Passage Formation

The Backstairs Passage Formation rests conformably on the laminated metasiltsstones of the Carrickalinga Head Formation, the contact being marked by the first appearance of resistant metasandstone beds. Where the Carrickalinga Head Formation is absent, the Backstairs Passage Formation is in fault contact with Marino Group strata (Fig. 4).

The Type Backstairs Passage Formation on the south coast of Fleurieu Peninsula consists of a thick sequence of laminated and cross-bedded and commonly slumped metasandstones with a more silty basal portion which has bioturbated intervals (Daily and Milnes, 1971). Although the bulk of the formation in the Nairne-Mt. Barker Creek area closely resembles the type strata, the upper and lower levels are quite variable. In the vicinity of Mt. Barker Creek (where exposure is good) a basal member can be distinguished while in the southern half of the area, lithologies in the upper levels also differ sufficiently to warrant the distinction of an upper member.

(i) Basal member. The basal member is distinguished from the overlying strata primarily by its much thicker pelitic intervals. Consequently where outcrop is poor (as is the case to the north of Mt. Barker Creek) it is virtually impossible to delimit the member or detect any lateral changes. From the exposures available north of Mt. Barker, it appears that there are no significant differences between the lithologies in the lower levels and the overlying bulk of the formation, however exposures in the highway cutting at the northern extremity of Mt. Barker (section B, Fig. 4) show that the lithologies immediately above the contact with the Carrickalinga Head Formation are significantly more pelitic.

In the vicinity of Mt. Barker Creek, the basal member is approximately 320 m thick. It consists of a sequence of fine-grained and occasionally less

micaceous medium-grained feldspathic metasandstones (Plate 20, Fig. (b)) with thick more pelitic intervals (exceptionally to about 35 m) of very micaceous fine metasandstones grading into metasiltsstones and some quartz-micaschists (to 3 m). The degree of lamination in the dominantly more pelitic intervals is variable, however a large proportion of the strata are well laminated (A405/BC53(1)). The quartz-micaschists generally show little lamination however. Occasional thin (to 1 m) less micaceous and more resistant weakly laminated metasiltsstone and fine metasandstone interbeds are present (A405/BC53(2),BC56).

The metasandstones of the coarser, less micaceous intervals are only weakly laminated or non-laminated in general (A405/BC57) although occasional well laminated horizons do occur, these being usually less than 1 m in thickness. Thin metasiltsstones (normally less than 1 m thick) part the more massive metasandstones. They are commonly better laminated and often flaggy, however the most micaceous horizons (quartz-micaschists) rarely show any lamination. Small to medium scale cross-bedding with sets up to 0.75 m occurs in some metasandstone units (Plate 20, Fig. (c)).

(ii) Middle member. The overlying interval (distinguished as a middle member in the vicinity of Mt. Barker Creek) constitutes the bulk of the Backstairs Passage Formation in this area and consists of pale grey, weakly to well laminated feldspathic metasandstones and meta-arkoses which are fine to medium-grained (A405/BC60,A1). These are interbedded with darker more pelitic metasediments which consist predominantly of well laminated very micaceous fine metasandstones and metasiltsstones (A405/A3,A10) (grading into quartz-micaschists (A405/BC61)) which are commonly flaggy. The more pelitic intervals are rarely over 0.75 m thick and often occur as mere partings between the coarser metasandstone and meta-arkose units, which are usually less than 1.5 m in thickness. The metasandstones are occasionally thinly interbedded with pelitic layers resulting in flaggy outcrops (Plate 20, Fig. (d)). Rare very thick metasandstone units (to 5 m) usually show little lamination.

Low angle cross-bedding (usually under 25°) is common in these strata, with sets of over 0.75 m being recorded. Slumping is common in the metasandstones (Plate 21, Fig. (a); A405/A4,A13). The slumps commonly have a simple form and are probably current induced (Dr. B. Daily, pers. comm.), coming mainly from the south-east. There are, however, occasional chaotic intervals with very irregular slumps which have probably formed by mass slumping of over-saturated sediments, possibly induced by shock or loading. One such interval, some 2 m thick, was found to persist over 100 m along strike (locality 170, Mt. Barker Creek). Occasional ripple marks and scours to 15 cm in depth also are present in some intervals.

Deposition was probably rapid in general, perhaps in a high energy regime as suggested by Daily and Milnes (1971) with regard to the laminated metasandstones of the type sequence. The sedimentary structures are consistent with deposition at shallow to moderate depths (Heckel in Rigby and Hamblin, 1972; Reineck and Singh, 1973) and it is suggested that the sea bed had a considerable gradient, which combined with rapid sedimentation, would present a favourable situation for chaotic slumping.

(iii) Upper member. The sequence of laminated feldspathic metasandstones and meta-arkoses persists to the top of the formation in the northern half of the area, however at the northern-most extremity of the map, the upper levels rarely outcrop and the precise nature of the lithologies is uncertain.

A facies change to the south is reflected in the increasing mica content and decreasing lamination of the metasandstones. The more pelitic interval in the south constitutes the thin upper member which is more uniform lithologically than the rest of the formation. Rocks which were originally poorly sorted clay-rich feldspathic sandstones (and minor siltstones) typically form rounded featureless outcrops as well developed lamination is rare and bedding parting is either poor or absent.

In the vicinity of Mt. Barker Creek, where the member is about 60 m

thick, the contact between the underlying cleaner laminated metasandstones and the mainly non-laminated very micaceous metasandstones (A405/BC66) is gradational over a few metres. To the north, however, the intergradations become greater until approximately 3.5 km from Mt. Barker Creek where typical laminated Backstairs Passage Formation metasandstones become dominant. Strata exposed in the pipeline excavations between Dawesley and Nairne indicated some differences between the upper levels (about 30 m) of the Backstairs Passage Formation and the underlying metasandstones and meta-arkoses. Lithologies at the top have a slightly greater proportion of fines and lamination is generally weak (A405/F1). Bedding parting, however is well developed and the strata are too similar to warrant the distinction of an upper unit. The slight differences would not be obvious in the areas of poor outcrop immediately to the south of the pipeline excavations.

No surface exposures of calc-silicates were found in the Backstairs Passage Formation, however, two thin calc-silicate bands (A405/F1A,F1B) were exposed in the pipeline excavations. These occur approximately 45 m and 20 m from the top of the formation.

3.5.3 Talisker Calc-siltstone Equivalent

In its type section, the Talisker Calc-siltstone consists of banded calc-phyllites with numerous sulphide-rich zones (Daily and Milnes, 1971). Two prominent sulphide-rich bands with an approximately north-south trend have been mapped in detail by Kleeman and Skinner (1959) and are shown on the ADELAIDE and BARKER 1:250,000 map sheets. The lower band is referred to as the "Nairne Pyrite Member" which until recently was mined as a source of sulphur at Brukunga and its nature is well documented (Skinner 1958; George, 1967). The sulphide-rich metasediments were interpreted as shallow marine deposits, probably forming in a series of basinal depressions, sulphides being chemically precipitated (La Ganza, 1959; George, 1967).

The pyritic metasiltsstones and metashales form typical gossanous outcrops and have been equated with the pyritic zones of the Talisker Calc-

siltstone by Daily and Milnes (1972). In the Nairne-Mt. Barker Creek area the pyritic metasediments are underlain by a variable thickness of non-pyritic metasiltsstones and metashales which become subordinate to the north across the area as the strata become progressively more pyritic down the sequence.

In the vicinity of Mt. Barker Creek, where the Talisker Calc-siltstone is about 100 m thick, the contact with the Backstairs Passage Formation is marked by a gradation over several metres from very micaceous feldspathic metasandstones to metasiltsstones (A405/BC67) which are well laminated in parts. The metasiltsstones vary in their mica content, grading into quartz-micaschists, to 1.5 m (A405/BC68) and are interbedded with occasional more resistant, commonly laminated metasiltsstones to fine metasandstones (to 0.5 m). Quartz-micaschists and micaschists (some containing andalusite) become more common up the sequence. A thick unit (approximately 45 m) of poorly laminated fine metasandstones (A405/BC69) and metasiltsstones (with minor quartz-micaschists) occurs within the more pelitic strata at Mt. Barker Creek (e.g., localities 208 to 209). Minor pyritic schists and metasiltsstones (A405/BC71) appear in this unit about 180 m to the north of the section (locality 214).

Typical iron-stained gossanous outcrops of laminated metasiltsstones and metashales (A405/BC70, BC70(1)) overly the predominantly non-pyritic strata. Some pyrite still remains, however most sulphides have been leached out leaving "boxwork" structures. Jarosite veins are common in some horizons. The acid solutions released during breakdown of the sulphides have commonly altered the underlying non-pyritic (or less pyritic) schists for several metres, leaving them bleached or iron-stained.

The pyritic rocks are confined to one distinctive band which thickens from south to north as the underlying schists become progressively more pyritic. In Mt. Barker Creek (localities 210-211) the pyritic band is approximately 38 m thick whereas in the vicinity of localities 599 and 600

(about 3 km to the north), the band is just over 50 m thick. Further north (e.g. locality 615) only a few metres of non-pyritic metasediments occur between the typical laminated metasandstones and meta-arkoses of the Backstairs Passage Formation and the "Nairne Pyrite Member". Due east of Nairne the pipeline excavations revealed similar pyritic strata and jarosite veins to 2 cm thick were encountered in the altered metasiltsstones (A405/F2, F3, F4).

3.5.4 Tapanappa Formation

Directly overlying the pyritic strata of the Talisker Calc-siltstone is a thick sequence of impure metasandstones termed the Tapanappa Formation of which only the lower levels were examined in this study. The strata in the Nairne-Mt. Barker Creek area resemble the Type Tapanappa Formation described by Daily and Milnes (1971) although the lithologies are slightly finer grained with thicker, more common pelitic intervals in the lower levels.

The feldspathic metasandstones are typically very micaceous and fine to medium-grained (A405/BC74(1)). Lamination is generally weak although some thin horizons (usually less than 0.5 m) are well laminated. Cross-bedding (at least near the base), is not as common as in the type area. In the vicinity of Mt. Barker Creek, the good exposures reveal that the basal lithologies are predominantly fine metasandstones grading into metasiltsstones with common quartz-micaschists (to 40 cm). The occasional interbeds of micaceous fine to medium-grained metasandstones are usually thin (to 20 cm) except near the base where these form the dominant lithology. About 125 m above the base, metasandstones again become the major rock type and sedimentary structures such as small-scale slumping and cross-bedding are present. The occasional metasiltsstone (to quartz-micaschist) interbeds are generally thin (usually to 30 cm) although there are certain thicker intervals in which fine metasandstones grade into metasiltsstones (A405/BC75).

Sulphide bands occur in the Type Tapanappa Formation (Daily and Milnes, 1971; 1972) and in the Nairne-Mt. Barker Creek area, the first sulphides

occur quite low in the formation. Spoil alongside the pipeline excavations revealed a thin sulphide band approximately 20 m above the base. The leached metasediments (A405/F6B) contained "boxwork" structures and occasional jarosite veins resembling the pyritic strata of the "Nairne Pyrite Member". In Mt. Barker Creek, about 165 m above the base is a sulphide band which is several metres thick, consisting of thinly interbedded metasiltsstones and micaschists (A405/BC76) which are leached and iron-stained. About 11 m above is another sulphide band which is 7 m thick (A405/BC77). Earlier work by Kleeman and Skinner (1959) showed that this is the same band which occurs about 450 m above the Nairne Pyrite in the vicinity of Brukunga where it is 15 m thick. The much greater thickness of strata between this band and the "Nairne Pyrite Member" may be attributed possibly to deformation rather than sedimentary thinning. Additional sulphide bands mapped in the Tappanappa Formation by Kleeman and Skinner were of more limited extent.

3.6 Conclusions

Detailed stratigraphic mapping in the Nairne-Mt. Barker Creek area has shown that the Marino and Kanmantoo Group sequences can be equated directly with their respective stratotypes. It is now clear that the thick interval of pre-Kanmantoo Group Lower Cambrian (or "basal Cambrian") strata, the Normanville Group, is absent. The Mt. Barker Quartzite, previously interpreted as belonging to the basal Cambrian sequence is in fact within the upper levels of the Marino Group.

The bulk of the Carrickalinga Head Formation, the basal unit of the Kanmantoo Group, is also absent while its distinctive upper portion, the Campana Creek Member, is recognized at the northern extremity of Mt. Barker; to the south this interval is mainly absent. The missing intervals and the disappearance of the younger strata along the Marino Group-Kanmantoo Group contact are definite evidence for a fault contact, which is evidenced at the South-East freeway cutting at the northern end of Mt. Barker. This fault is the Nairne Fault.

4. BIRDWOOD-BRUKUNGA AREA

4.1 Introduction

The sequence of metasediments in the area mapped between Birdwood and Brukunga (Fig. 1; Map 2) consist of a conformable succession of Precambrian strata from the Stoneyfell Quartzite of the Torrens Group through to rocks of the upper Marino Group, all of which as shown below, are in fault contact with lower Cambrian metasediments of the Kanmantoo Group along an approximately north-south line. The lower member of the Kanmantoo Group as defined in its type section along the south coast of Fleurieu Peninsula (Daily and Milnes, 1971), is absent. Conformably overlying the Carrickalinga Head Formation is the thick Backstairs Passage Formation followed by the sulphide-rich Talisker Calc-siltstone equivalent which embraces the "Nairne Pyrite" in the vicinity of Brukunga (Daily and Milnes, 1972).

Although the Precambrian sequence outcrops poorly, lithologies can be equated directly with those exposed in the Dawesley-Onkaparinga River pipeline excavations and those shown on the Echunga 1:63,360 map sheet (Sprigg and Wilson, 1954) and the Adelaide 1:63,360 map sheet (Sprigg, Whittle and Campana, 1951).

4.2 Precambrian

Passing up through the sequence, the Precambrian stratigraphic units in fault contact with Cambrian strata are from oldest to youngest:

4.2.1 Torrens Group

4.2.1.1 Stoneyfell Quartzite (Mawson and Sprigg, 1950)

The Stoneyfell Quartzite (upper levels) in this area consists of a sequence of poorly outcropping metasiltstones with thick interbedded quartzite units. These fine to medium-grained white quartzites are feldspathic, usually well bedded and often flaggy. Minor interbedded feldspathic metasiltstones have been kaolinized.

The uppermost quartzite intertongues with a thick layered calc-

silicate which appears on the western limb near the hinge of a small anticlinal structure, immediately north of Birdwood. The calc-silicate is absent on the eastern limb where the quartzite is thicker and interbedded with metasiltsstones. The tight hinge zone (which does not outcrop), is close to the contact with Kanmantoo Group strata, the nearest outcrop of which occurs about 0.25 km to the north-east in a railway cutting.

4.2.1.2 Saddleworth Formation (Thomson, Riverton 1:63,360 map sheet (unpublished))

Overlying the Stoneyfell Quartzite is a sequence of laminated metasiltsstones referred to as the Saddleworth Formation (Thomson, 1969). Interbedded quartzites occur in the lower portion of the formation, with two thick units occurring in the vicinity of Mt. Torrens township, the lower of which forms a prominent ridge which rises to form the peak of Mt. Torrens. Outcrops are poor and the units are best examined in the small quarries situated along the eastern slopes of this ridge and at the southern extremity of the small, poorly defined ridge which marks the upper quartzite (situated just off the Lobethal-Mt. Torrens road). The quartzites are medium to coarse-grained and flaggy in parts, and the lower quartzite contains interbeds of calc-silicate (seen only in float). Both quartzites appear to lens out to the south-west in the vicinity of the Lobethal-Mt. Torrens road. To the north-east, the units disappear on the western side of the disused Adelaide-Mt. Pleasant railway line just before they are cut off at a low angle by the younger Kanmantoo Group strata.

Several minor quartzites, all less than 5 m thick, occur above these two quartzites on Mt. Torrens. These are glassy orthoquartzites which are medium to coarse-grained, poorly bedded and lack lamination. They have an approximately east-west strike, and either lens out to the west or fail to outcrop. To the east the quartzites are abruptly truncated in the vicinity of the contact with Kanmantoo Group rocks. The exposed contact of a truncated quartzite with (probable) Kanmantoo Group metasiltsstones appears to

be a fault with a slickensided surface (locality 31a; Plate 21, Fig. (b)). This surface dips steeply east with a strike of approximately 320° , thus having a similar trend to the mapped contact between the Precambrian and Cambrian strata.

The laminated metasiltsstones of the formation outcrop rarely and most occurrences are in road or railway cuttings and creek beds. These rocks are predominantly very fine-grained and their constituent minerals have not undergone significant grain growth during metamorphism. Lamination and bedding parting are very well developed and thin calc-silicate bands (<10 cm) are common. Thin quartz-mica schist interbeds are also present, in which micas are typically coarser than in the more resistant and less micaceous metasiltsstones. Near the base of the formation are lenticular intervals with interbedded calc-silicates to 1.5m thick (A405/M27, M28), containing diopside + scapolite + plagioclase + calcite \pm hornblende \pm quartz. Interbeds of resistant fine metasandstone (to 2 m) channeled into the underlying metasediments also occur.

An indeterminate thickness of quartz-mica schists and very micaceous laminated metasiltsstones occurs almost immediately above the upper Mt. Torrens Quartzite unit. Fibrolite and muscovite porphyroblasts occur in some of the more pelitic metasediments (A405/M39). Outcrop is restricted to a small area just south of Mt. Torrens summit, near the Lobethal-Mt. Torrens road. Similar lithologies also occur above a thin quartzite which overlies this unit, however outcrop is again limited to this small area.

Generally, the metasiltsstones are coarser in the upper levels of the formation. They are normally laminated but the associated occasional quartz-micaschists (to 4 m) rarely show any lamination. Some finer metasiltsstones contain abundant scapolite and thin calc-silicates are present. Minor interbeds of resistant coarse metasiltsstone to medium-grained metasandstone (A405/M35, M36) also occur.

The uppermost quartzite unit of the Saddleworth Formation occurs near

a small quarry about 0.7 km north-west of Mt. Charles East. This is medium to coarse-grained, slightly feldspathic and only a few metres thick. It strikes at right angles towards the contact with Kanmantoo Group strata which lies approximately 0.25 km to the east. Within the quarry are exposed massive feldspathic metasiltsstones with occasional quartz-micaschist interbeds. These rocks have been kaolinized and only certain thin horizons show good lamination. At locality 40 (about 0.5 km SW of Mt. Charles East) there are outcrops of andalusite-rich metasiltsstones (A405/M40, M40a) and metashales which are reminiscent of the upper levels of this formation as seen in the Dawesley-Onkaparinga River pipeline excavations. Rocks are predominantly massive and weakly laminated in the lower parts with interbedded units of resistant massive metasiltsstones with little or no andalusite. The upper parts are mainly well bedded, with interbedded units of massive andalusite-rich metasiltsstones and metashales. Lamination is present in some more micaceous intervals. These strata have a similar orientation to that of Kanmantoo Group strata immediately to the east due to small macroscopic folding in the Adelaidean sequence. This is reflected in the occurrence of small mesoscopic folds which plunge at 10° towards 180° and have a well developed axial plane schistosity with a steep easterly dip (A405/M41, Plate 21, Fig (c)). Similar lithologies which have been kaolinized are exposed in a road cutting about 0.25 km to the east of the small quarry referred to above. Small mesoscopic folds in these strata plunge at a shallow angle towards 35° . The folds have an almost similar style and shearing has occurred along some limbs, while their axial plane structure strikes about 50° with steep south-easterly dips.

4.2.2 Sturt Group

4.2.2.1 Belair Sub-group

As in the Dawesley-Onkaparinga River section, the base of the Sturt Group sequence is marked by units of medium to coarse-grained feldspathic

metasandstone and quartzite which are interbedded with laminated fine metasandstones and scapolite-bearing feldspathic metasiltsstones. This interval is equivalent to the Belair Sub-group (termed the Belair Group in the original subdivision of the Adelaide System on the western side of the ranges by Mawson and Sprigg, (1950)).

The quartzites clearly define the western limb of a macroscopic syncline which plunges at a low angle to the SSE, with a closure in the vicinity of Mt. Charles (mapped earlier by Sprigg and Wilson (1954)). These quartzites strike into and are truncated at the "contact" with Kanmantoo Group metasediments just south-west of Mt. Charles East. The upper quartzite passes up into laminated scapolite-bearing metasiltsstones with fine feldspathic metasandstone interbeds. In the Nairne area, the Sturt Tillite occurs above fine metasandstones and metasiltsstones of the basal Sturt Group sequence, however in the Birdwood-Brukunga area this formation fails to outcrop and no conclusive erratics could be found in the rare float to verify its existence.

4.2.2.2 Tapley Hill Formation

Outcrop of the overlying Tapley Hill Formation is scarce and restricted to the upper portion of the unit. Rare patches of float material however identify the formation over some of the area. Rocks are typically well laminated fine feldspathic metasiltsstones with common scapolite-rich bands. Minor interbeds of non-laminated and slightly coarser metasiltsstones occur near the top while layered calc-silicates are common in the upper levels also. The mineralogy of these is diopside + hornblende + plagioclase + scapolite + quartz + epidote + calcite. Although the calc-silicate intervals are of considerable thickness (2-15 m) individual units could not be traced with certainty due to poor outcrop. Furthermore, it is possible that these intervals are lenticular. They may be equated with the thin limestones which occur in the Tapley Hill Formation stratotype, described by Sprigg (1942) and Mawson and Sprigg (1950).

4.2.2.3 Brighton Limestone

In the Nairne-Mt. Barker Creek area, the Tapley Hill Formation meta-siltstones are overlain by fine to coarse meta-arkoses and metasandstones with pebble-rich horizons. This interval is possibly a coarser facies equivalent of the Eudunda Arkose Member of the Tapley Hill Formation (ADELAIDE 1:250,000 map sheet) as previously suggested. Overlying these rocks is the metamorphosed Brighton Limestone, a coarse white marble. In the Birdwood-Brukunga area, arkosic lithologies immediately overlying the laminated metasiltstone sequence discussed above outcrop sporadically along the western limb of the macroscopic syncline. These rocks are poorly bedded, white, fine to coarse-grained feldspathic metasandstones, meta-arkoses and feldspathic quartzites with common fine to medium-grained grey metasandstones which are less feldspathic and more micaceous. In the southern part of the area this interval is overlain by a layered calc-silicate (determined from float) which is correlated with the marble at Mt. Barker Creek. Outcrop in the hinge of the syncline to the north is poor and mainly isolated outcrops of layered calc-silicates occur. It is tempting to correlate the thickest outcropping calc-silicate (not shown on the Echunga 1:63,360 map sheet) with the Brighton Limestone, however no meta-arkoses were found below or in close proximity to this unit. Although outcrop is rare, some trace of these resistant lithologies might be expected. The first feldspathic quartzites occur as float material near one of the uppermost calc-silicate outcrops and this association alone is used to correlate this calc-silicate with the Brighton Limestone, particularly as the Brighton Limestone is of variable facies on Fleurieu Peninsula (Daily, 1963). A poorly outcropping unit of massive grey feldspathic metasandstone overlies these rocks.

4.2.3 Marino Group

Overlying the proposed Brighton Limestone is a sequence of laminated feldspathic metasiltstones and fine metasandstones comparable to that marking the lower part of the Marino Group in the Nairne-Mt. Barker Creek

area. Thick interbedded units of fine to coarse meta-arkoses, feldspathic quartzites and grey micaceous feldspathic metasandstones occur through the sequence. These include the Hallett Arkose and an overlying "upper arkose" as recognized in the Marino Group stratotype in Waterfall Creek and in the Nairne-Mt. Barker Creek area. Mapping in the latter area has shown that these units are quite variable laterally and in the Birdwood-Brukunga area the equivalent of the "upper arkose" is represented by metasiltsstones with thin interbedded fine to medium-grained feldspathic quartzites which form a poorly defined ridge along the western limb of the macroscopic syncline. In the hinge zone of the syncline, however, the uppermost outcrops are of massive, micaceous and feldspathic metasandstones which are fine to medium-grained. It is uncertain whether these represent the "upper arkose" or whether the quartzites seen on the limb merely fail to outcrop. In the hinge area immediately below these micaceous metasandstones is a thick (about 8 m) layered calc-silicate unit (A405/M23) having the mineralogy hornblende + diopside + plagioclase + scapolite \pm epidote \pm quartz \pm calcite.

The above-mentioned marker units define small macroscopic folds in the hinge area of the larger synclinal structure to which they are related. These folds plunge at shallow to moderate angles to the SSE. The lower arkosic units strike into the contact with Kanmantoo Group strata, while the calc-silicate is deformed in a small anticline just west of this contact and disappears under alluvium which covers the contact area. Kanmantoo Group metasandstones (A405/M36) occur about 1/3 km to the south, just to the east of the inferred contact.

Outcrop of the overlying more pelitic interval of the Marino Group sequence is very scarce, but road cuttings show that the sequence is very similar to that mapped in the Nairne-Mt. Barker Creek area. The lower half to one third of the interval consists of thinly interbedded quartz-mica schists and andalusite schists (A405/M22) with occasional thin interbeds of less micaceous metasiltsstones. As in the Nairne-Mt. Barker Creek area,

quartz-mica schists become prominent towards the top. The upper half to two thirds of the interval is composed of metasiltstones with variable mica content which pass into quartz-mica schists in some horizons. Interbedded thin units of quartz-mica schists with andalusite schists occur through the sequence. On the whole, lamination in the metasiltstones is generally poor but it tends to be well developed in some of the more micaceous intervals.

Mesoscopic folds in andalusite schists within the hinge zone of the major syncline plunge at low angles to the SSE. The syncline is probably tight as schists outcropping on the east limb near the hinge are vertical whereas those on the western limb have a similar strike and dip at moderate to steep angles to the east. The presence of a minor fault is indicated by andalusite schists on the eastern limb striking into the underlying feldspathic metasandstones and calc-silicates.

In the south of the area the top of the Marino Group sequence is marked by the Mt. Barker Quartzite equivalent which outcrops as an almost pure, white medium-grained quartzite about 10 m thick. The quartzite lenses out abruptly to the north and south, striking parallel to the proposed contact between Marino Group metasiltstones and andalusite schists, and Kanmantoo Group metasandstones. No trace was found of the calc-silicates or scapolite-rich metasiltstones which underly the Mt. Barker Quartzite in the Nairne-Mt. Barker Creek area. Outcrop of upper Marino Group strata is rare, however. Also, as calc-silicates were found to pass laterally into scapolite-rich metasiltstones in the vicinity of Mt. Barker, it is possible that further facies change to the north has eliminated or greatly reduced the thickness of scapolite-bearing strata.

4.3 Cambrian

The Cambrian is represented in the study area by the Kanmantoo Group, the older Normanville Group being absent due to faulting, as discussed later.

4.3.1 Carrickalinga Head Formation

The lowest Cambrian unit in this area is the Carrickalinga Head Formation of the Kanmantoo Group. It extends north from the Mt. Charles area towards Birdwood, occupying low undulating land between ridges formed by the Mt. Torrens quartzites to the west and younger Cambrian metasandstones to the east. Much of the area is under pasture and exposures are uncommon except in the area immediately north of Mt. Torrens township where two members could be distinguished. These are the Blowhole Creek Siltstone and the overlying Campana Creek Member, the two upper members in the three-fold subdivision of the formation described by Daily and Milnes (1971) on the south coast of Fleurieu Peninsula. The formation persists to the north of Birdwood, where outcrop is rare and the location of its boundaries can only be approximated.

(a) Blowhole Creek Siltstone. In the type section this member consists of grey laminated phyllites with common fine sand and silt interbeds in the upper parts (Daily and Milnes, 1971). Correlation of strata in the Birdwood-Brukunga area with this unit is primarily based on their stratigraphic position immediately below the more distinctive lithology of the Campana Creek Member.

The thicker lower portion consists of very micaceous metasiltstones and quartz-micaschists (phyllitic in parts) with occasional andalusite schist interbeds (to 30 cm). Lamination is generally poor but is well developed in some horizons. A small outcrop of layered calc-silicate (a minimum thickness of 2 m) occurs in the lower levels near the contact with Adelaidean strata, just east of Birdwood. South-east of Mt. Torrens summit is another calc-silicate (now covered with soil but shown on the ADELAIDE 1:250,000 map sheet) and a coarse white marble is exposed in a small excavation about 1.5 km to the north of this. It is probable that these carbonate-rich metasediments occur along the same stratigraphic level.

In the upper portion, resistant interbeds (to 2 m) of massive feldspathic metasiltstones to micaceous fine metasandstones are common. These

less pelitic lithologies are laminated in parts and form the major rock type in some intervals, individual beds or units being separated by more micaceous metasiltstones and occasional thin quartz-mica schists. No evidence of worm casts was found in the less pelitic rocks whereas these have been noted in the type section (Daily and Milnes, 1971, p.204).

Due to lack of outcrop, the location of the contact with the underlying Precambrian strata is approximate, except for locality 31a where a probable fault contact exists between metasiltstones and quartz-mica schists interpreted as belonging to the Blowhole Creek Siltstone and quartzites of the Saddleworth Formation, as mentioned earlier. The trend of the contact is more certain, however, particularly in the area between Mt. Torrens and Birdwood. Here the Cambrian metasiltstones mostly strike into the contact at low angles. South of Mt. Torrens, the strata generally strike sub-parallel to the contact.

(b) Campana Creek Member. Conformably overlying the Blowhole Creek Siltstone is a distinctive sequence of finely laminated very micaceous metasiltstones with minor quartz-micaschists and thin micaschists (metashales). Within the more pelitic horizons are occasional layers rich in andalusite (to 10 cm thick). Thin less micaceous laminated metasiltstone to micaceous fine metasandstone interbeds (to 30 cm) occur, particularly near the top of the unit. The rocks show abundant small-scale sedimentary structures such as current bedding, slumps and possible ripples. Layered calc-silicates occur in the upper parts of the member (A405/M31). These can occur as thin beds (about 1 cm thick) associated with scapolite-rich metasiltstones (to 40 cm) or more commonly as thicker units from 10 cm to 12 m. Their mineralogy is hornblende + diopside + plagioclase + quartz \pm calcite \pm scapolite. These units are lenticular and pass laterally into weakly laminated metasiltstones with variable amphibole and scapolite content, consequently it is unsafe to correlate bands over any large distances. Calc-silicates have not been reported in the type section on Fleurieu Peninsula, presumably due to facies

changes.

4.3.2 Backstairs Passage Formation

The lower portion of the overlying Backstairs Passage Formation shows considerable lateral and vertical variation in this area and on the whole, lithologies are more micaceous than in the upper levels. In the area between Birdwood and Mt. Charles East a distinct lower member can be recognized which is overlain by the typically more resistant metasandstones and meta-arkoses of the formation which characterize this unit in its type section (Daily and Milnes, 1971). The contact with the underlying laminated metasiltsstones of the Carrickalinga Head Formation is marked by the first appearance of resistant, massive fine to medium-grained feldspathic meta-sandstone units which are generally less than 2 m in thickness (A405/M33). Rocks are predominantly very micaceous fine feldspathic metasandstones grading into metasiltsstones. Lamination is commonly developed but some intervals are poorly bedded and not laminated, forming rounded featureless outcrops. Interbedded units of less micaceous, often laminated, fine to medium feldspathic metasandstones and meta-arkoses (to 3 m thick) form a variable but minor proportion of the sequence and commonly grade laterally into more micaceous lithologies. Occasional thick metasiltsstone units (to 10 m) occur which are interbedded with minor quartz-mica schists. Layered calc-silicates (A405/M29,M30) are common in this interval and have the mineralogy hornblende + diopside + plagioclase + scapolite + quartz [±] calcite. Thicknesses are usually less than 4 m, but a 10 m band of limited extent occurs near the top of this member just south-east of Birdwood. Also, a lenticular unit (locally to 14 m thick) occurs near the base of the formation and appears sporadically from just south-east of Birdwood to the Mt. Charles area. About 0.5 km north of Mt. Charles East where this band attains its greatest thickness, the lower part of the calc-silicate passes into a white fine-grained quartzite up to 6 m thick. Immediately east of the truncated Mt. Charles quartzites occurs an isolated outcrop of another white

lenticular quartzite (at least 5 m thick) which may correlate with the above-mentioned unit which lies about 1 km to the north.

South of Mt. Charles East, lithologies become less micaceous in the upper part of the member and pass into metasandstones and meta-arkoses, the upper boundary becoming indefinable. Four bands of layered calc-silicate, two of which are also associated with quartzites, occur about 2.5 km south of Mt. Charles East, passing laterally into scapolite-bearing metasiltstones. They occur in very micaceous fine metasandstones, metasiltstones and minor meta-arkoses which recall the basal portion of the formation in the north. The lowest calc-silicate is 15 m thick while 10 m above is a 9 m calc-silicate band directly overlain by a thin lenticular almost pure quartzite which passes laterally into micaceous metasandstones. Several metres above is another thinner (4-5 m) calc-silicate band which is also overlain by a lenticular white quartzite. This in turn is overlain by a few metres of metasandstones and metasiltstones followed by a 6 m thick calc-silicate (A405/M37). Diopside is more common in these rocks than in calc-silicates to the north and extensive recrystallization has occurred, particularly in the uppermost band. Below the lowest calc-silicate are poorly outcropping metasiltstones and quartz-micaschists with minor andalusite which are tentatively correlated with the upper levels of the Carrickalinga Head Formation. Just over 1 km to the south are two small calc-silicate outcrops. The lower possibly occupies a similar stratigraphic level to those immediately to the north whereas the location and orientation of the upper outcrop suggests it occurs some distance above the four bands. In this area, the basal portion of the formation is truncated at the Precambrian-Cambrian boundary.

South of Mt. Charles, facies change in the strata immediately overlying the basal member confuses the location of the upper boundary of this unit. The overlying lithologies pass from predominantly medium-grained metasandstones and meta-arkoses in the Birdwood-Mt. Charles East area to

mainly laminated very micaceous fine metasandstones and metasiltsstones about 3 km south of Mt. Charles East. Then over another 4 km to the south, rocks pass into typical resistant Backstairs Passage Formation metasandstones and meta-arkoses which persist to the southern extremity of the map area.

The lowest Cambrian strata in the southern part of the map area, extending approximately 2 km north of the Mt. Barker Quartzite lens, are predominantly very micaceous fine feldspathic metasandstones and metasiltsstones which are well laminated in parts. These strata are overlain by coarser, less micaceous lithologies characteristic of the Backstairs Passage Formation and are correlated with the basal member of the formation as recognized in the north. Calc-silicates if present, do not outcrop. The northerly extent of this basal portion of the formation is uncertain due to poor outcrop and facies change to the north of the overlying metasandstones and meta-arkoses to predominantly more micaceous lithologies. It is proposed that the base of the formation has been faulted out where the Precambrian and Kanmantoo Group metasediments are in contact over a distance of about 5.5 km in the southern part of the map area, reappearing a short distance north of the most southerly calc-silicate outcrop.

In the southern part of the Birdwood-Brukunga area, fine to medium-grained metasandstones and meta-arkoses persist upwards to the overlying conformable pyritic metasiltsstones and metashales of the "Nairne Pyrite Member", the sulphide-enriched equivalent of part of the Talisker Calc-siltstone (Daily and Milnes, 1971). This marker unit defines a macroscopic syncline which extends south-east to the Dawesley-Kanmantoo area (Kleeman and Skinner, 1959; Fleming, 1971).

To the north, the Backstairs Passage Formation thickens considerably as indicated by the position of the "Nairne Pyrite Member", although some of the apparent increase in thickness is due to deformation within the formation. More pelitic strata become dominant at certain levels. These rocks are predominantly fine to medium-grained very micaceous feldspathic

metasandstones and metasiltstones with minor interbedded less micaceous arkosic horizons. Rocks are commonly well bedded and laminated although some form rounded featureless outcrops, showing little or no lamination. Only one distinctive lithology, a layered calc-silicate unit about 11 m thick, was found in the sequence overlying the basal member.

4.4 Structure

Offler and Fleming (1968), Pain (1968) and Fleming (1971, Fig. 11) suggest that the structure of the Woodside-Brukunga area (Map 2) is dominated by a macroscopic syncline, the axial plane of which is presumed to extend from just west of Mt. Charles, through the vicinity of Murdock Hill and Brukunga, turning south-east towards the Dawesley-Kanmantoo area where Fleming (1971) has classified it as an "F₃" structure. As alluded to earlier, however, mapping in this study shows that there are two major synclinal structures involved, one on each side of the Precambrian-Kanmantoo Group boundary.

The eastern structure, outlined by the "Nairne Pyrite Member" has an axial plane trace which trends approximately 330-340° and extends south-east to the Dawesley-Kanmantoo area (Kleeman and Skinner, 1959). The axial plane to crenulations in metashales of the "Nairne Pyrite Member" has a similar orientation, dipping steeply east. Crenulations plunge at a moderate angle to about 150° and are presumably related to the "F₃" structure of Fleming (1971) recognized in the Dawesley-Kanmantoo area. The syncline dies out to the north-west within the Backstairs Passage Formation. Other structures east of the Precambrian-Kanmantoo Group boundary are rare in the map area. Two small poorly defined mesoscopic structures in Backstairs Passage Formation metasandstones have moderate plunges to the ENE and SSE, and on the basis of orientation may possibly belong to Fleming's "F₂" and "F₃" deformations respectively. Mesoscopic structures (possibly "F₃") also occur in the Carrickalinga Head Formation just north of Mt. Charles East, where folds plunge at about 25° towards ESE and axes of crenulations associated with

these folds have a similar plunge to SE.

The western syncline, with associated parasitic folds has an axial plane which trends SSE from just west of Mt. Charles past Murdock Hill to the Precambrian-Kanmantoo Group boundary where the structure is truncated (Map 2). Small folds indicate the structure plunges at a shallow angle towards 160° . The axial plane structure of small mesoscopic folds in andalusite schists is a well defined schistosity (dipping steeply east) which is locally weakly crenulated (locality 22). As the axial plane structure (if developed) of Fleming's "F₃" folds is a crenulation cleavage (Fleming, 1971), it seems likely that the western syncline is not an "F₃" but an "F₁" structure (denoted F₂ in the Nairne-Mt. Barker Creek area in this study) in which the axial plane structure is characteristically a schistosity. The structure of older strata to the north outlined by the Mt. Torrens quartzites is possibly also related to this deformation. West of the Precambrian-Kanmantoo Group boundary the only mesoscopic structures found occur near Mt. Charles East. Here, small folds in highly weathered metasiltstones have shallow plunges to the NE and are possibly "F₂" structures. About 0.75 km to the south are shallow south-plunging folds which are probably "F₁" structures as the fold axis is paralleled by strong axial plane schistosity-bedding intersections in andalusite schists (locality 41).

4.5 Conclusions

Mapping in the Birdwood-Brukunga area on the basis of a detailed knowledge of the Adelaidean and lower Kanmantoo Group sequences has confirmed the existence of the Nairne Fault. To the west are folded Adelaidean strata which are truncated along the fault. To the east of the fault, all rocks belong to the Kanmantoo Group, the lower levels of which disappear and reappear along the contact with the Adelaidean sequence. The Kanmantoo Group is folded in the vicinity of Brukunga by a deformation which probably post-dates that which macroscopically folded the Adelaidean.

5. NATURE OF THE PRECAMBRIAN-KANMANTOO GROUP BOUNDARY

Mapping in the Birdwood-Mt. Barker Creek region provides evidence which indicates that the boundary between the Precambrian Adelaide Super-group and Kanmantoo Group strata is a fault. The presence of a break seems obvious in the Birdwood-Brukunga areas from the discordance between these strata, but the angular relation between the underlying Adelaidean rocks and the boundary could also be explained as an unconformity (Horwitz, Thomson and Webb, 1959; Thomson, 1969). The evidence for a fault rests on detailed stratigraphic mapping of the Cambrian sequence and its relationship to the contact.

(1) Mapping has shown that the two upper members of the Carrickalinga Head Formation are truncated in the vicinity of Mt. Charles East, with the uppermost portion of the upper member reappearing about 2 km to the south for some 1.5 km and again disappearing into the boundary. The lower levels of the Backstairs Passage Formation are also truncated and re-emerge along this boundary. Further south in the Mt. Barker area, laminated metasiltstones characteristic of the upper levels of the Carrickalinga Head Formation reappear alongside the boundary (obviously a fault; see below) exposed at the northern end of Mt. Barker, thinning rapidly again to the south and disappearing into the boundary. This sudden appearance and disappearance of overlying strata at the boundary cannot be explained by the unconformity hypothesis.

(2) In the Birdwood-Mt. Torrens area, the Blowhole Creek Siltstone strata strike into the contact with the underlying Adelaidean Saddleworth Formation, at low angles to it. Only a fault contact can explain this relationship.

(3) Direct evidence for a fault contact locally.

(i) Freeway excavations at the northern extremity of Mt. Barker revealed a fault contact between the upper levels of the Carrickalinga Head Formation and the Precambrian Mt. Barker Quartzite. There is a fault zone

varying between 3 m and 4 m in width within which are angular blocks of undeformed Mt. Barker Quartzite and possible Carrickalinga Head Formation metasiltsstones which are extremely weathered to kaolin and stained by iron oxides (Plate 19, Fig. (c)). The fault zone has a steep easterly dip (strike 350° , dip 58°) which is greater than that of the strata on either side of the fault (the Mt. Barker Quartzite has the orientation strike 340° , dip 35° about 30 m west of the fault).

Brecciation is evident within the fault zone but is not present at the western margin of the fault where the Mt. Barker Quartzite is abruptly truncated. The apparent paucity of fine fault breccia explains why the fault, which trends sub-parallel to the strike of strata in the Mt. Charles-Mt. Barker Creek area, is not apparent even in areas of good outcrop. An isolated patch of possible fault breccia was, however, found in Mt. Barker Creek a few metres east of the Mt. Barker Quartzite and within the Backstairs Passage Formation (locality 119, Map 1; A405/M43). Outcrop is poor, however, and it is uncertain whether this is a minor fault or a splinter of the Nairne Fault.

In the freeway cutting, there is obvious drag of the strata on either side of the fault (Plate 19, Fig. (c)), (drag of the Mt. Barker Quartzite was noted by Dr. B. Daily). It is conceivable that there may have been drag and minor reorientation of the strata on a larger scale elsewhere along the contact, possibly explaining the near-parallelism of the Kanmantoo Group strata with the fault through most of the Birdwood-Mt. Barker Creek region.

(ii) Observations in the freeway excavations at Mt. Barker recall a similar situation near the Mt. Torrens ridge in the vicinity of the proposed Kanmantoo Group-Torrens Group boundary (locality 14a, Map 2). Here a probable fault breccia zone (A405/M44) on the eastern limits of the lower Mt. Torrens Quartzite unit is also overlain by ferruginous conglomerates with rounded quartzite pebbles and boulders.

(iii) The contact between a Torrens Group Quartzite at locality 31a (Map 2) and probable Kanmantoo Group metasiltsstones is best interpreted

as a fault. The exposed surface marking the eastern limit of the east-west trending quartzite is a possible fault plane (strike 320° , dip 80°E).

Assuming the western syncline is an " F_1 " structure (using the terminology of Fleming, 1971) then the fault must have developed either syn-" F_1 " or post-" F_1 ". In both the Nairne-Mt. Barker Creek and Birdwood-Brukunga areas the fault deviates significantly from its mean north-south orientation. Immediately north-west of Mt. Charles East, the marked deviation in the fault appears to be the result of later (possibly " F_2 ") folding which is evident in Precambrian strata near the contact. It is proposed that the lesser deviations in the orientation of the fault elsewhere are also due to post-" F_1 " deformation. The relatively low degree of brecciation along the fault at Mt. Barker is compatible with its development while the rocks were still in a ductile state, as indicated by the style of post-" F_1 " (i.e. post-fault) deformations.

The relationship of the fault to the Kanmantoo Group strata through most of the Birdwood-Mt. Barker Creek region indicates that the fault is not a true strike fault as the Cambrian sequence strikes into the fault at variable but low angles. The relation between strata on either side of the boundary reveals that it is a normal fault with relative downward movement on the eastern side. Orientation of the exposed fault at Mt. Barker (see above) is compatible with these observations and the sense of drag on either side of the fault is also consistent with relative downward movement to the east.

5.1 A comparison with previous work advocating an unconformity

Detailed stratigraphic mapping in the region between Birdwood and Mt. Barker Creek has led to conclusions which differ from the interpretations made by the proponents of an unconformable or conformable boundary between the Kanmantoo Group and older strata. Those differences pertinent to the problem of the boundary are outlined below:

(1) No trace was found of a lenticular "basal quartzite" which is shown as occurring about 1 km south of Nairne (Horwitz, Thomson and Webb, 1959, Plate I).

(2) The strata below the level of the Mt. Barker Quartzite between Mt. Barker Creek and approximately 1 km north of Murdock Hill mapped as "basal Cambrian" by Horwitz, Thomson and Webb (1959) (also on the ADELAIDE and BARKER 1:250,000 map sheets) are considered to be within the upper levels of the Marino Group (Units 3 and 4, this study). To the north of Murdock Hill, the limits of "basal Cambrian" strata approximately correspond to the sequence herein interpreted as being equivalent to the upper portion of the Carrickalinga Head Formation (Kanmantoo Group). The upper levels of this sequence are correlated with the Campana Creek Member of the Carrickalinga Head Formation¹ and consist of finely laminated metasiltsstones commonly exhibiting small-scale sedimentary structures, which are quite different to the less laminated and more variable metasiltsstone sequence to the south with which they were equated by Horwitz, Thomson and Webb (1959). There is no evidence for the lensing out of the "basal Cambrian" immediately to the north of Mt. Torrens township as shown on the ADELAIDE 1:250,000 map sheet. On the contrary, the strata in this area are within the Kanmantoo Group and conformable with the overlying strata (not unconformable as indicated on the ADELAIDE 1:250,000 map sheet legend) which have been correlated with the upper levels of the middle member of the Carrickalinga Head Formation (shown as belonging to the basal portion of the Strangway Hill Formation (Kanmantoo Group) on the ADELAIDE 1:250,000 map sheet). To the west, the strata have a slightly more westerly orientation and strike into the contact with the Adelaidean rocks, disproving the existence of an unconformity.

¹Further north, on the Truro 1:63,360 map sheet, Coats and Thomson (1959) have described the strata underlying a thick arkose unit (the Backstairs Passage Formation equivalent) as a sequence of "rapidly alternating grey-wacke and siltstone with small-scale cross-bedding" and occasional marble lenses. This interval is reminiscent of the Campana Creek Member and demonstrates the constancy of facies exhibited by most units of the Kanmantoo Group over large distances.

(3) The Mt. Barker Quartzite is within the upper levels of the Precambrian Marino Group, rather than in the Cambrian ("basal Cambrian" (Horwitz, Thomson and Webb, 1959); Kanmantoo Group (Thomson in Parkin, 1969)).

(4) In the area between Mt. Charles East and Inverbrackie Creek, there are thin lenticular quartzite units, some of which are associated with calc-silicates. These have been correlated with the "basal Cambrian" Mt. Barker and Macclesfield Quartzites by Horwitz, Thomson and Webb (1959) whereas they should be included in the Kanmantoo Group, in the basal portion of the dominantly more pelitic basal member of the Backstairs Passage Formation (Map 2). Approximately 0.75 km north of Mt. Charles East, it can be seen that a white quartzite and associated calc-silicates in a sequence of micaceous metasandstones directly overly the distinctive finely laminated metasiltsstones belonging to the upper member of the Carrickalinga Head Formation. Horwitz, Thomson and Webb (1959), however, mapped these strata as "basal Cambrian".

(5) North of the vicinity of Mt. Torrens township, the area shown on the ADELAIDE 1:250,000 map sheet as being occupied by the Strangway Hill Formation (described as "grey-green metamorphosed siltstone-greywacke, arkosic small-scale cross-bedded siltstone") corresponds to the well bedded, finely laminated metasiltsstones of the upper member of the Carrickalinga Head Formation described in this study. To the south, however, the term Strangway Hill Formation embraces both these laminated metasiltsstones of the Campana Creek Member and the distinctly different basal portion of the Backstairs Passage Formation which consists predominantly of massive metasiltsstones grading to micaceous fine metasandstones and less micaceous fine to medium-grained meta-arkoses and metasandstones in which lamination is generally poorly developed. The contact between these two units passes immediately to the west of Mt. Charles East. In this respect, the interpretation presented by Horwitz, Thomson and Webb (1959, Plate I) is in best agreement with this study, with strata immediately above the "basal Cambrian"

being shown as occurring immediately to the east of Mt. Charles East and interpreted as a more pelitic facies ("greywackes") within the main "arkose" sequence (i.e. the Backstairs Passage Formation) which persists up to the "Nairne Pyrite Member".

South of Inverbrackie Creek, the situation becomes more confused. Much of the "basal Cambrian" interval of Horwitz, Thomson and Webb (1959) described as "phyllite and greywacke" between Inverbrackie Creek and a point approximately due west of Brukunga belongs to the basal portion of the Backstairs Passage Formation, with the remaining lower part being in the upper levels of the Marino Group. It appears that the facies changes within the basal portion of the Backstairs Passage Formation are responsible for these conflicting interpretations, however there are occasional fine to medium-grained meta-arkose beds in the lower levels of the Backstairs Passage Formation but not in the underlying Marino Group, permitting location of the boundary. Horwitz, Thomson and Webb (1959) indicate an "arkose" facies at the base of the interval now termed the Backstairs Passage Formation, as occupying an area between Inverbrackie Creek and a point approximately 1 km west of Brukunga, with strata grading north and south into more pelitic lithologies ("greywackes"). This interval is in fact more variable both laterally and vertically than previously envisaged, with micaceous fine metasediments and metasiltsstones being common in different horizons throughout the lower half of the Backstairs Passage Formation in this area.

(6) Horwitz, Thomson and Webb (1959) originally proposed a conformable succession from the Adelaide Supergroup, through "basal Cambrian", to Kanmantoo Group strata in the area between Ashbourne and Murdock Hill (Horwitz, Thomson and Webb, 1959, Plates I and III; also BARKER 1:250,000 map sheet). On the ADELAIDE 1:250,000 map sheet, however, Thomson (1969) proposed that two unconformities break the succession, the Mt. Barker Quartzite being immediately below the upper unconformity. The hypothesis of conformity is obviously incorrect as mapping has indicated that almost the entire

Carrickalinga Head Formation (the basal unit of the Kanmantoo Group) is absent between Mt. Barker Creek and Mt. Charles East. This situation cannot be interpreted as conformity (involving facies change or sedimentary thinning) or even as being due to unconformity (non-deposition of most of the Carrickalinga Head Formation) since:

(i) the strata immediately beneath the Backstairs Passage Formation are of identical facies to the Type Campana Creek Member (upper Carrickalinga Head Formation) which occurs over 75 km to the south. It is therefore extremely unlikely that the underlying bulk of the Carrickalinga Head Formation was not deposited resulting in only a very thin upper member as the representative of this formation in this area.

(ii) There is a marked lensing of these characteristic strata along their lower boundary (which is immediately above the Mt. Barker Quartzite level in the Murdock Hill-Mt. Barker Creek area). This boundary cannot therefore be a conformable contact or an unconformity.

PART II

FOLDING AND METAMORPHISM IN THE

NAIRNE-MT. BARKER CREEK AREA

A: FOLDING

Large macroscopic folds are absent in the Nairne-Mt. Barker Creek area and mesoscopic structures are uncommon, hence the tectonic history was largely deduced from the study of thin sections. In the following outline of deformation in the area, tectonic elements will be referred to by the standard nomenclature¹.

A relict schistosity (S_1) observed in some rocks will be discussed in detail in Section B.2.2. The later regional schistosity, S_2 , parallels the axial planes of microscopic and mesoscopic F_2 folds. These folds are asymmetric with east-dipping axial planes which are usually inclined at 50° to 60° to the horizontal. The west limbs of anticlines are shorter and steeper than the east limbs and are commonly overturned. Mesoscopic folds, often with associated parasitic folds in the more micaceous rocks, have an almost similar style with characteristic thickening of the hinges and thinning of the limbs. Some folds appear almost isoclinal and in these S_2 is sub-parallel to S_0 (bedding) in the limbs. Folds in more competent (less micaceous) rocks tend to be more open in style. Thin sections of microscopic F_2 folds show the bedding sliced up by the axial plane schistosity which has the appearance of a shear surface (Plate 22(a)). S_2 is characteristically refracted through the more competent layers, a feature which, combined with other observations of F_2 folds, suggests a mechanism of internal deformation by a combination of layer boundary slip and tangential longitudinal strain as described by Ramsay (1967, pp. 403-406).

The plot of poles to S_0 (Fig. 5) shows only a partial spread along a great circle since most readings are taken on east-dipping strata. The partial spread is along a great circle with pole β_2 lying within the field

¹Tectonic phases and groups of folds are denoted by the symbol "F". Corresponding axial surfaces or schistositities formed during these phases are denoted by the symbol "S" and bedding (the pre-tectonic planar structure) is denoted as S_0 . Lineations are given the symbol "l".

of plotted F_2 fold axes and l_2 lineations defined by biotites which lie in S_0 and which parallel the axes in some folds. These axes and lineations are observed in the field to plunge at shallow angles to SSE (Fig. 5). Rare crude small-scale folds in S_0 with axes parallel to the S_2 - S_0 intersection at locality 198 are presumed to be F_2 structures. The orientation of S_2 shows considerable variation through the area, strikes ranging from 340° to 010° and dips from 37° to 60° . The spread of the F_2 elements might be due to one or all of the following;

- (i) inhomogeneous strain;
- (ii) effects of later deformation;
- (iii) effects of F_2 overprinting an already folded bedding surface.

The last possibility is supported by the presence of an earlier schistosity S_1 , presumably related to an earlier deformation F_1 , which can be recognized in many of the schists. The orientation of S_1 relative to S_2 is variable and is usually defined by inclusion trails of elongate quartz and opaque minerals in andalusite and staurolite porphyroblasts. In rare cases S_1 , defined by fine biotites, is seen within S_2 augen structures.

In addition to the l_2 biotite lineation on S_0 surfaces mentioned above, another lineation defined by aligned biotites is commonly developed on S_2 surfaces, often accompanied by fine crenulations. Thin section examination reveals that this biotite lineation which is seen on most S_2 and also S_0 surfaces, is considered due to the elongation of crystals in the direction of "maximum finite extension" (Ramsay, 1967, Fig. 5-2) and is related to the development of S_2 during the F_2 deformation. This "down-dip" lineation is approximately perpendicular to the strike of strata which constitute the limbs of the F_2 structures and is denoted l_2' . The crenulations are a later F_3 structure, denoted l_3 , which are microfolds deforming S_2 (Plate 16(a,b)). These are commonly observed also on bedding surfaces as S_2 is inclined at very low angles to S_0 in pelitic strata not mesoscopically folded. The l_3 lineation is observed on both limbs of some small mesoscopic F_2 folds (localities 187A, BC96) and defines the intersection of S_2 and S_3 where S_3 is the

axial plane of the F_3 crenulations. Crenulation of S_2 is observed in the most micaceous lithologies (schists) whereas the biotite lineation l_2' is more widely developed and may occur in impure metasediments. The F_3 axes of crenulations have shallow plunges to the east and are therefore almost at 90° to l_2 and virtually parallel to l_2' (Figs. 6,7) since S_3 is almost vertical and nearly perpendicular to S_2 . No mesoscopic F_3 folds were found.

In a few localities a fourth phase of deformation appears to exist. Mesoscopic F_4 folds plunge at moderate angles to the NE and NNE (Fig. 6). These structures appear to overprint small mesoscopic F_2 folds and F_3 crenulations which have developed on their limbs, at one locality (BC96). In the Nairne railway cutting (locality 198) fine crenulations with a similar orientation are found in close proximity to F_3 crenulations on some S_2 and S_0 surfaces. These crenulations were rarely found to coincide on the same portion of the surface, however, and although the " F_4 " crenulations possibly overprint the E-W F_3 crenulations, their time relation is regarded as uncertain. Rare crenulations which plunge at shallow angles to SE (localities 198, BC63) appear to be overprinted by the NE crenulations. Their relation to the F_3 crenulations also is uncertain.

The present study differs from previous interpretations of the tectonic history of the Mount Lofty Ranges in the recognition of a phase of deformation which is earlier than generally recognized elsewhere. Consequently the F_1 deformation with accompanying penetrative schistosity S_1 described in earlier work are herein denoted F_2 and S_2 (Table 0).

B: METAMORPHISM1. INTRODUCTION

Metamorphic mineral assemblages observed in the Nairne-Mt. Barker Creek area and along the water pipeline trench excavated between Dawesley and Hahndorf indicate that regional metamorphism represents a low to intermediate pressure metamorphic series, as defined by Miyashiro (1961a, 1973 Table 7-A). This becomes evident when assemblages are compared with those formed in metapelites characterizing low and intermediate pressure metamorphic series of other metamorphic belts. The presence of kyanite just 3 km to the NE of the area, at Brukunga (Skinner, 1958), indicates that the pressure conditions approached the upper limits of low pressure metamorphism (as classified in relation to the stability fields of the Al_2SiO_5 polymorphs by Miyashiro (1973, Fig. 3-3)).

Critical minerals formed in metapelites of the Nairne-Mt. Barker Creek area, representing these conditions, are almandine, staurolite, andalusite, low An-plagioclase and sillimanite (both as fine needles of fibrolite and less common coarser prismatic crystals). In metamorphosed basic rocks, minerals such as high An-plagioclase, green hornblende and minor epidote characterize the Amphibolite Facies (Turner, 1968; Miyashiro, 1973). Calcite, diopside, hornblende and epidote occur in calc-silicate rocks. The Greenschist Facies assemblages actinolite + calcite and prograde chlorite + quartz are characteristically absent. All chlorite present in the rocks belongs to a later paragenesis, often as a retrograde mineral after biotite and less commonly, hornblende.

The lower grade assemblage albite + epidote + hornblende which elsewhere characterizes the Epidote-Amphibolite Facies in basaltic compositions (Turner, 1968) was not encountered in rocks west of the Nairne-Mt. Barker Creek area as might be expected in keeping with the lower metamorphic grade shown by pelitic rocks. This may be because the absence of suitable rock types and extreme weathering and kaolinization were detrimental to proper

petrological examination, but it is doubtful whether an Epidote-Amphibolite Facies zone would in any case exist below the Amphibolite Facies (or at most it would be narrow) in a region metamorphosed under the relatively low pressure conditions estimated (see Miyashiro, 1973, p.300).

The Nairne-Mt. Barker Creek area is situated within the extensive "Andalusite-Staurolite Zone" of Offler and Fleming (1968) (Fig. 8). This zone extends along the east side of the Mount Lofty Ranges, its lower limit being defined by the first appearance of andalusite and staurolite and the disappearance of these minerals marking the upper limit. The andalusite and staurolite isograds are commonly almost coincident and in places cross (Offler and Fleming, 1968) and these two minerals appear to have formed almost synchronously in the metamorphic history. Their derivation and the nature of reactions leading to their formation are problems encountered in other metamorphic terrains, for example the transitional low to intermediate pressure metamorphics of the Appalachians, U.S.A. (Green, 1963; Woodland, 1963, 1965; Thompson and Norton, 1968). Sillimanite (mainly in the form of fibrolite), which occurs sporadically throughout the Andalusite-Staurolite Zone (Offler and Fleming, 1968), is common in the schists of the area studied. The problem of the origin of fibrolite in this zone has not yet been fully resolved (Fleming, 1971) and is one which has been encountered by workers in many areas. Descriptions of the textural relationships of fibrolite with micas and quartz in these areas are remarkably similar to the features observed in the Nairne-Mt. Barker Creek schists (e.g., Tozer, 1955; Chinner, 1961; Woodland, 1963; Green, 1963). These schists exhibit various textures which give some insight into the possible modes of origin of fibrolite.

A lower grade "Biotite Zone" (Offler and Fleming, 1968) extends along the length of the Mount Lofty Ranges west of the Andalusite-Staurolite Zone (Fig. 8). The boundary between these zones could not be determined precisely from observations along the Dawesley-Hahndorf excavations due to ex-

tensive weathering and kaolinization.

2. MINERAL ASSEMBLAGES AND INTERPRETATION OF TEXTURES

Prograde metamorphism has increased the grainsize of the original sedimentary rocks to a variable degree which seems to be largely related to the mica content of the rocks (reflecting the clay content of the original sediments). The effects of this are important in the classification of observed metaclastic rocks, as the distinction between coarse and fine meta-sandstones, metasiltsstones and metashales is not only dependent on grainsize. The assumption that finer sediments contained a higher proportion of clay minerals (hence a higher proportion of micas in their metamorphic equivalents) than coarser sediments permits the use of mica content as the primary criterion for classifying the various metamorphosed clastics. Thus resistant metasiltsstones can be distinguished from soft, friable more micaceous metashales, although the grainsize of the metasiltsstones is usually much finer. A classification on this basis is: metasandstones (all clastic rocks with originally sand grainsize), less than 20% micas; metasiltsstones, 20 to 45% micas; metashales, greater than 45% micas.

Although the extent of recrystallization and grain growth in the rocks is variable, it is generally observed, with some exceptions, that the more micaceous rocks have undergone the most recrystallization and have textures showing a maximum attainment of physical equilibrium. Decreasing mica content is accompanied by a lesser degree of recrystallization and equilibrium textures become rare. The irregular nature of recrystallization even within single beds, has largely obliterated any fine sedimentary features such as silt-shale laminae, graded bedding etc. The results of differential recrystallization and grain growth are that, generally, quartz and plagioclase are only slightly coarser in the less micaceous lithologies than in the most micaceous. Micas, however, are usually much coarser in mica-rich rocks than in those poor in mica. The original difference in grainsize of quartz, plagioclase and biotite between psammitic and pelitic sedimentary

layers has been largely obliterated. This has often been replaced by a virtual reversal of grainsize of the respective layers.

Some metasandstones and metasilts have undergone only minor recrystallization (e.g., A405/F12, E12A, E12C). Recrystallization within these rocks is variable and often lenses and beds remain very fine, their component quartz, plagioclase and biotite being markedly finer than in adjacent beds of very similar composition. Fine mica-rich lenses are commonly observed in these rocks (e.g., A405/E12A) where the micas (biotites) are an exception to the usual observations and tend to be finer than the enclosing less micaceous lithology. Possibly different compositions of these layers resulted in different reactions to the metamorphic conditions.

2.1 Metasilts

The representative mineral assemblages are: quartz, plagioclase, biotite \pm muscovite \pm garnet \pm chlorite. These are dark grey fine to medium-grained rocks, the more micaceous being quartz-mica schists. Many of these rocks are only slightly recrystallized but grain growth has produced coarser than silt grain sizes in most. The typical range in grain size within a rock is 0.04-0.35 mm. In the less recrystallized rocks the grain size is considerably finer (max. to 0.12 mm).

In laminated rocks, variation in biotite content is responsible for the layering seen in hand specimen whilst slight grain size variations are visible in thin sections of those rocks not extensively recrystallized. These variations reflect primary sedimentary differences in grain size. Layers of metasandstone and metashale to less than 1 cm are common and relict clay layers are seen as laminae of abundant biotite crystals as little as 0.5 mm in thickness. In the recrystallized rocks, layering this fine is almost certainly not entirely primary and metamorphic differentiation must have played a substantial role in its development. Accessory minerals are distributed along the bedding, opaque minerals being most common in the more micaceous layers. In addition to lamination which defines bedding, other

sedimentary features are preserved such as small-scale current bedding and less commonly, ripple marks. Other relict sedimentary features are:

(i) relict sedimentary grains of quartz which are conspicuously larger than the average recrystallized matrix grainsize (Plate 22(b)). These quartz grains are equant and usually have slightly irregular boundaries. They have undergone little recrystallization as suggested by their form and biotite crystals in the bedding schistosity tend to pass around these grains (e.g. A405/F12). Rocks with good lamination and current bedding were probably well sorted and do not contain such distinctly large grains whereas these are common in some non-laminated rocks which were poorly sorted (e.g. A405/E12A).

(ii) Sandy lenses associated with ripple-marked and cross-laminated rocks (e.g. A405/E4B(2)).

(iii) Relict "heavy mineral bands" with magnetic, zircon, sphene.

(iv) Thin lenses of fine biotites defining relict clay layers (Plate 22(c)).

Physical equilibrium is most fully developed in the textures of the more micaceous metasiltsstones where recrystallization and grain growth have resulted in even-grained quartz and plagioclase crystals elongated in the schistosity formed by a continuous network of coarser elongate subidioblastic biotite crystals. With decreasing mica content, biotites become dispersed (Plate 22(d)), the least micaceous rocks showing a tendency for crystals to become elongate aggregates parallel to the schistosity (e.g. A405/A6). Also, the difference in grainsize between biotite and the equidimensional quartz and plagioclase becomes less marked with decreasing mica content. The grainsize of component minerals becomes more variable, intergranular boundaries more irregular and few triple points are formed between adjacent quartz or plagioclase grains. The biotite schistosity is weakly refracted through the more layered, inhomogeneous rocks. Patchy recrystallization of quartz to coarse equant grains in mica-poor beds has produced equilibrium textures.

The mineralogy of the metasiltsstones is:

Quartz 35-75%. This is xenoblastic, equant to elongate, with the less micaceous rocks exhibiting a large grainsize range, usually of the order 0.03-0.55 mm with the exclusion of the most micaceous metasiltsstones and coarsely recrystallized patches where grainsize tends to be more even.

Plagioclase 12-40%. Plagioclase is xenoblastic and finer than quartz. Some grains show albite twinning. Often there is partial alteration to sericite or clay minerals. Composition of the plagioclase was determined as oligoclase, based on 2V and RI relative to adjacent quartz grains.

K-feldspar trace -20%. This mineral is most common in plagioclase-rich rocks. It is untwinned but could be distinguished on stained rock slabs¹.

Biotite 15-45%. Biotite is subidioblastic and elongate, generally coarser than quartz and feldspar. Maximum grainsize is 0.6 mm. It is pleochroic, from red-brown, dark brown to pale yellow-brown and pale brown. Later stumpy subidioblastic and idioblastic plates of the same colour lie across earlier biotite, quartz and plagioclase.

Muscovite trace -20%. Muscovite is thin, very elongate crystals being parallel to biotite and as intergrowths in the more micaceous rocks where it is more abundant. Grainsize is similar to biotite. Later subidioblastic and ragged xenoblastic stumpy plates lie across the schistosity.

Garnet (almandine²) trace -4%. This mineral is pale pink, idioblastic to xenoblastic, grainsize being 0.08-0.6 mm, to 1 mm in more pelitic layers.

Chlorite trace -2%. Chlorite has low birefringence and is pleochroic, coloured pale green, dark blue-green or blue-grey. It is very fine (to 0.12 mm); xenoblastic and subidioblastic crystals lie across earlier minerals. Some chlorite replaces biotite with liberated magnetite distributed along cleavage.

¹Rock slabs were first etched with 40% HF for 15 seconds at room temperature and then stained with sodium cobaltinitrite solution by immersion in a saturated solution at room temperature for 1 minute.

²Determined by X-ray diffraction and electron probe analysis.

Accessory minerals commonly present are:

Opagues (mostly magnetite with minor ilmenite or graphite) trace -22%.

These are generally abundant only in thin very micaceous beds. Magnetite is idioblastic to xenoblastic. Tabular opaques (possibly ilmenite or graphite) are elongate along the schistosity. Grainsize is highly variable, from very fine to 0.5 mm. Magnetite is generally coarser than the platy opaques.

Rutile is rare, very fine, subidioblastic to xenoblastic.

Tourmaline (<1-3%) occurs in very micaceous beds. It is subidioblastic to xenoblastic, pleochroic dark blue-green and pale green; 0.05-0.1 mm is the maximum variation in grainsize. Some crystals are zoned.

Apatite (trace -1%) is subidioblastic to xenoblastic, 0.02-0.1 mm, average commonly 0.04 mm.

Zircon (trace -2%) is colourless, subrounded, 0.025-0.3 mm. Some crystals are zoned (Plate 23(a)).

Sphene (trace -5%) is idioblastic to xenoblastic. Average grainsizes are around 0.025 mm. It possibly formed after ilmenite. Sphene is pleochroic red-brown and colourless; it is concentrated in bands with magnetite and zircon.

Rare accessories are:

Calcite (trace-<1%) is xenoblastic, av. 0.05 mm.

Sillimanite. A radial cluster of fibrous sillimanite was found in one rock (A405/E12C).

2.2 Metasandstones

Mineral assemblages observed are:

quartz, plagioclase plus:

- (i) biotite, muscovite \pm garnet \pm K-feldspar \pm chlorite
- (ii) biotite
- (iii) biotite, garnet, chlorite
- (iv) hornblende, epidote
- (v) biotite, muscovite, phlogopite

(vi) muscovite, chlorite, calcite.

Assemblages (iv), (v), (vi) are rare and (iii) is only of minor occurrence.

Bedding lamination in these rocks is defined by the variation in biotite content. Bands of opaque minerals, generally most common in the more micaceous layers, parallel bedding and are responsible for fine lamination in some rocks.

Except for coarsely recrystallized patches in some rocks, recrystallization and grain growth has not been extensive and textures of the metasandstones do not generally show physical equilibrium. Grainsize is very variable, common ranges being 0.03-0.5 mm and few triple-point junctions are formed. Some sedimentary grains are preserved (e.g. A405/H11, F10, BC74¹). Rocks of finer grainsize (0.025-0.25 mm) are marginal and possibly were originally coarse siltstones or very fine sandstones. As with metasiltstones, the more micaceous metasandstones contain quartz, plagioclase which are finer than the micas present. Thin bands, generally 1 mm or less with 20-30% mica content show near textural equilibrium with elongate quartz and plagioclase grains formed along the schistosity defined by subidioblastic biotite crystals (to 0.5 mm). This schistosity is refracted through layers of different mica content, being generally sub-parallel-15° to bedding in more micaceous beds and at relatively higher angles (to 25°) in quartz-rich beds.

As most rocks have a low biotite content (<15%) a schistosity is poorly developed, defined by weakly oriented biotite crystals which are slightly coarser than the quartz and plagioclase. In the least micaceous rocks (<5% micas) biotite tends to be finer than quartz. Here biotites are deflected by the coarser grains, deviating at high angles from the mean schistosity orientation. In rocks which are more micaceous (originally clay-rich impure sandstones), schistosity is better developed and a discontinuous network of oriented micas is formed, whilst in some rocks elongate aggregates of biotite crystals have resulted in a finely speckled or "salt and pepper"

appearance. Subidioblastic muscovite often forms parallel intergrowths with the biotite. Late subidioblastic and ragged xenoblastic muscovite and chlorite cut across earlier minerals. Pale pink idioblastic to xenoblastic garnet is present in minor amounts in some rocks, usually most common in the more micaceous layers. Coarser crystals cut across the biotite schistosity.

The mineralogy is summarized below:

Quartz 25-85% xenoblastic. 0.01-0.6 mm.

Plagioclase 5-60% xenoblastic. Grainsize similar to quartz. Mostly un-twinned. Commonly partly altered to sericite or clays.

K-feldspar trace -35% xenoblastic. Some crystals show carlspad twinning. Grainsize similar to quartz.

Biotite 3-30% subidioblastic. 0.02-1 mm.

Muscovite trace -4% subidioblastic, xenoblastic. 0.025-1 mm.

Chlorite trace -1% idioblastic to xenoblastic, very fine -0.4 mm. Some replacing biotite.

Garnet (almandine?) trace -3% idioblastic to xenoblastic, pale pink. 0.04-0.25 mm.

Accessory minerals commonly present are:

Magnetite trace -20%. Concentrated in mica-rich bands less than 0.5 mm thick. Idioblastic to xenoblastic. 0.01-0.35 mm.

Opaque minerals (possibly graphite or ilmenite) trace -3%. Concentrated in biotite-rich layers. Tabular, aligned in the schistosity.

Tourmaline trace. Subidioblastic to xenoblastic. Pleochroic, often zoned. To 0.25 mm.

Zircon trace -2% colourless. Subrounded to rounded. Commonly to 0.12 mm, rarely to 0.3 mm. Some crystals zoned. Concentrated with magnetite.

Apatite trace -2%. Subidioblastic, very fine -0.12 mm.

Rare accessories are:

Hornblende <1% subidioblastic, green.

Phlogopite trace <1%. Xenoblastic. Very fine, very low 2V-nearly uniaxial. Colourless.

2.3 Metashales

These are dark grey micaschists, some of which are peraluminous and characterized by the appearance of large porphyroblasts giving the rocks a rough or knotted appearance (Plate 15(c)).

2.3.1 The less aluminous metashales

Mineral assemblages of the less aluminous metashales are similar to those of metasiltsstones and are summarized as:

quartz, plagioclase, biotite, muscovite [±] garnet (almandine)¹ [±] chlorite.

In the less aluminous metashales, sedimentary layering down to 1 mm is defined by variations in mica content. Thin quartz-rich layers occur (e.g. A405/E6, H8a) which have undoubtedly been accentuated by metamorphic segregation (Plate 23(b)). Bands of opaque minerals commonly follow the bedding lamination. The fabric of these rocks is simple and similar to that of the more micaceous metasiltsstones. Coarse subidioblastic plates of biotite and muscovite (av. grainsizes from 0.1 to 0.5 mm) are aligned to form a continuous network defining S₂ (the regional schistosity). In less micaceous metashales muscovite is less abundant than biotite but with increasing mica content muscovite increases in proportion and in rocks with greater than 70% micas, muscovite is usually in excess of biotite and coarser. Quartz, 3-50% is variable in its average grainsize (0.1-0.25 mm) depending on mica content (commonly being finer in the more micaceous layers) and extent of metamorphic segregation and recrystallization. Plagioclase, 6-10% is generally finer than quartz and untwinned. Quartz and plagioclase

¹The garnet in these rocks is approximately 70% almandine, determined by electron probe analysis.

are xenoblastic and elongate in the schistosity but with decreasing mica content become more equidimensional. Most metashales show equilibrium textures.

Small-scale crenulations occur exclusively in metashales. A secondary layering of fine biotite-quartz enriched bands (about 5 mm thick) has been locally observed to parallel the S_2 schistosity in both peraluminous and less aluminous rocks (c.f. Fleming, 1971).

Accessory minerals present are summarized below:

Magnetite trace -5%, idioblastic to xenoblastic. To 0.2 mm.

Ilmenite and/or graphite trace -5% as aligned plates in S_2 schistosity, av. about 0.15 mm.

Apatite <1% subidioblastic to idioblastic. To 0.08 mm.

Tourmaline <1% subidioblastic to idioblastic. To 0.1 mm.

2.3.2 Peraluminous metashales

Peraluminous metashales contain one or more of the minerals andalusite, fibrous sillimanite (fibrolite) and staurolite and are commonly thinly interbedded with less aluminous metashales or very micaceous metasiltsstones. They generally occur as layers less than 3 cm thick with a range from several mm to 5 cm. Mineral assemblages present are:

Quartz, plagioclase, biotite, muscovite plus

- (i) andalusite, sillimanite \pm garnet \pm chlorite
- (ii) sillimanite, chlorite \pm staurolite
- (iii) andalusite, staurolite, sillimanite \pm garnet
- (iv) staurolite.

In almost all sillimanite-bearing rocks some trace of andalusite occurs. For the remainder, evidence from textures (described later in this section) indicates that some andalusite preceded the sillimanite. Also, some sillimanite can be found in all andalusite-bearing rocks. Hence for simplicity, the number of assemblages can be reduced by considering these two minerals as just Al_2SiO_5 and not distinguishing between them in the

mineral assemblages. Furthermore, as chlorite is a much later mineral unrelated to the earlier paragenesis and rather sporadic in its occurrence, it need not be included in the assemblages formed in the earlier metamorphic episodes. With these restrictions, the number of assemblages can be reduced to:

I Quartz, plagioclase, biotite, muscovite, (andalusite/sillimanite)
± garnet ± staurolite.

This can be subdivided into:

Ia (garnet only), Ib (staurolite only), Ic (garnet + staurolite),
Id (no garnet or staurolite).

II Quartz, plagioclase, biotite, muscovite, staurolite.

Assemblage II is rare.

Textures and fabrics of the peraluminous metashales are more complex than those of the less aluminous metashales and record the structural and metamorphic history of the area. The descriptions and interpretations of these textures are summarized in section 2.3.2.4. Sedimentary lamination is largely obliterated where large porphyroblasts have formed, however the distribution of andalusite and staurolite still follows bedding, defining primary aluminous clay layers.

2.3.2.1 Phase rule considerations

Most assemblages encountered contain no more than the maximum of 3 phases (in addition to muscovite) in Thompson's AFM projection, this being the maximum allowed by the mineralogical phase rule for equilibrium assemblages. As chlorite does not belong to the high-grade paragenesis, it is not included as a phase. Assemblages tend to comply with Fleming's (1971) AFM representation of aluminous assemblages in the Andalusite-Staurolite Zone of the Mount Lofty Ranges, which is reproduced in Appendix III. As mentioned, most assemblages contain both the aluminium silicates, andalusite and sillimanite and are therefore anomalous, as observed elsewhere in the Mount Lofty Ranges by Fleming (1971) and others, and in other areas (e.g.

the northern New Hampshire area (Green, 1963)). It is proposed that this anomaly is the result of either (i) the incomplete transition of andalusite to sillimanite or (ii) the premature formation of sillimanite in the form of fibrolite, as proposed by Fleming (1971). In addition, two other anomalous assemblages (Ia,Ic) occur which are also observed elsewhere in the Mount Lofty Ranges and in northern New Hampshire. For assemblage Ic the anomaly is due to an excess in the number of phases in the AFM projection (biotite, andalusite, staurolite, garnet), resulting from (a) disequilibrium through non-completion of the reaction $\text{staurolite} + \text{quartz} \rightleftharpoons \text{garnet} + \text{sillimanite}$ or (b) from an inadequacy of the AFM projection to allow for the variations in the composition of garnet (Green, 1963; Phinney, 1963; Hess, 1969; Fleming, 1971). In the Nairne-Mt. Barker Creek area textures indicate that garnet has formed after at least some staurolite. There is, however, no textural evidence for the formation of this garnet as a product of the breakdown of staurolite which seems to have a separate and unrelated distribution from any garnet in the same rock. This rules out disequilibrium as the cause of the anomaly. Also Green (1963) has noted that in some rocks with this assemblage, staurolite is "fresh, euhedral, unmantled". In the Nairne-Mt. Barker Creek rocks, garnets contain 5 to 10% MnO, hence do not strictly belong to the plane of the AFM projection and MnO must be treated as an additional component.

The critical phases of assemblage Ia in the AFM projection are biotite, andalusite, garnet. There are no excess phases but reference to figures 30 and 31, and Appendix III, shows that staurolite should not be absent in a rock whose composition would plot in the andalusite-biotite-garnet portion of the AFM projection. As mentioned above, MnO is an extra component in the garnet. The absence of staurolite from the assemblage of a rock of appropriate bulk composition could possibly also be explained by the dependence of the staurolite stability field on factors other than P-T conditions. Ganguly (1968) and Hoschek (1969) have demonstrated the dependence of staurolite stability on oxygen fugacity. Local reducing conditions (such as may

be imposed by the presence of graphite in the original sediment) would be unfavourable to the formation of staurolite, yet favourable to the formation of almandine with little spessartine or pyrope components (Hsu, 1968). Ganguly (1968) has also indicated that the presence of considerable MnO or CaO in the rocks could restrict the stability of staurolite, and almandine may form instead. There is a suggestion of this from the rock analyses; staurolite-bearing rocks with no almandine have slightly lower MnO contents (0.11-0.13%) than garnet + staurolite-bearing rocks (0.16, 0.19%) and garnet-bearing rocks without staurolite (0.15, 0.27%). There is no relation, however, between rock CaO contents and the presence of garnet or staurolite. In Section D (Rock and Mineral Analyses), the anomalous assemblages Ia and Ic will be discussed in greater detail.

2.3.2.2 Origin of Andalusite and Staurolite

The origin of andalusite and staurolite is a problem in the Mount Lofty Ranges. A number of generalizations made by Fleming (1971) concerning the lack of evidence for reactions leading to the formation of these two minerals appear to hold true for rocks of Andalusite-Staurolite and Biotite grades observed in the Nairne-Mt. Barker Creek area and along the line of the excavated Nairne-Hahndorf section of the Murray Bridge-Onkaparinga River pipeline. In relation to the origin of andalusite:

(i) No alkali feldspars occur in aluminous metashales, therefore the reaction muscovite + quartz \rightarrow K-feldspar + Al silicate could not be responsible for the formation of andalusite.

(ii) Only minor amounts of iron oxide minerals occur in the pelitic rocks of the Biotite Zone. Hence the reaction quartz + magnetite + muscovite \rightarrow Al silicate + annite + haematite is not feasible in this area.

(iii) Pyrophyllite was not found in the lower grade rocks which seems to preclude the reaction pyrophyllite \rightarrow andalusite + quartz + H₂O.

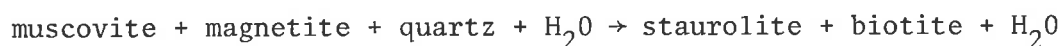
(iv) The reaction chlorite + muscovite + quartz \rightarrow andalusite + biotite + H₂O can also be dismissed as prograde chlorite does not seem to occur in the Biotite Zone.

For the formation of staurolite:

(i) No chloritoid was found in the lower grade rocks and could not have been a source of staurolite.

(ii) As mentioned, chlorite does not occur in the Biotite Zone except as a retrograde mineral, and only in very small amounts. This precludes Fe-rich chlorite as a source of staurolite (Ganguly, 1968; Hoschek, 1967, 1969).

Hence staurolite has formed by some reaction not involving chloritoid or Fe-rich chlorite. Ganguly (1968, p.291) states that other equilibria which can account for the formation of staurolite require higher temperatures than those involving chloritoid. The first appearance of staurolite in these rocks was likely therefore, at a higher grade than would be required had chloritoid been the source of staurolite. For the assemblages observed in these metapelites, the most likely alternative reaction (of those proposed by Ganguly (1968) and Hoschek (1969)) involves muscovite and magnetite at high oxygen fugacities:



(unbalanced equation).

A major problem with this reaction is that magnetite is relatively rare in the metapelites of the Biotite Zone. Fleming (1971) has also raised other arguments unfavourable to this reaction.

In conclusion, the origin of andalusite and staurolite in the area studied is not resolved. The high extent of weathering in the lower-grade rocks studied was a major disadvantage in attempting to solve this problem.

2.3.2.3 The sillimanite problem

The mode of origin of sillimanite is a problem encountered throughout the Andalusite-Staurolite Zone in the eastern Mount Lofty Ranges. The direct inversion of andalusite to prismatic sillimanite is relatively uncommon when compared with the more extensive but irregular development of the fibrolite form. Due to the sporadic occurrence of fibrolite, which is

occasionally accompanied by minor quantities of the coarser prismatic sillimanite, Fleming (1971) has placed the boundary between the Andalusite-Staurolite and Sillimanite Zones at the disappearance of andalusite rather than the first appearance of sillimanite.

The Nairne-Mt. Barker Creek area lies about 3 km south of Brukungu where the isolated occurrence of kyanite has been noted by Skinner (1958) and George (1967). Here kyanite, andalusite and minor fibrolite occur together. Skinner (1958, p.554) concluded andalusite and kyanite are a stable pair having formed at or near the andalusite-kyanite transition¹. This is a situation similar to that noted in many other areas where the three Al-silicate polymorphs occur in close proximity, e.g. Idaho Batholith, Idaho (Hietanen, 1956, 1969); Donegal Granite, Ireland (Pitcher and Read, 1960); northeast Vermont (Woodland, 1963; Albee, 1968); Kwoiek area, British Columbia (Hollister, 1969). Relations between the coexisting polymorphs are often confused and the problem of metastability arises. These conditions of metastability and the resulting confused relations between the polymorphs near the phase boundaries are believed to be consequences of the thermodynamics of the equilibria (Richardson *et al.* 1969, p.268; Holdaway, 1971). The relatively small differences in the free energy (ΔG) between the polymorphs at the P-T conditions around the triple point and the ΔG for the dehydration reactions which commonly produce these minerals do not provide each polymorph with a sufficiently high energy barrier to prevent its partial replacement and the crystallization of another polymorph in its own stability field. In addition to these complexities around the triple point it has been suggested by Strens (1968) that the polymorphs may contain extra components which can stabilize them in the field of another polymorph. Cameron and Ashworth (1972), however, suggested that the effects of these "impurities" is almost negligible. If, however, the polymorphs can have different structural states, the position of the triple point will be uncertain and the polymorph stability field, will vary (Zen, 1969; Beger,

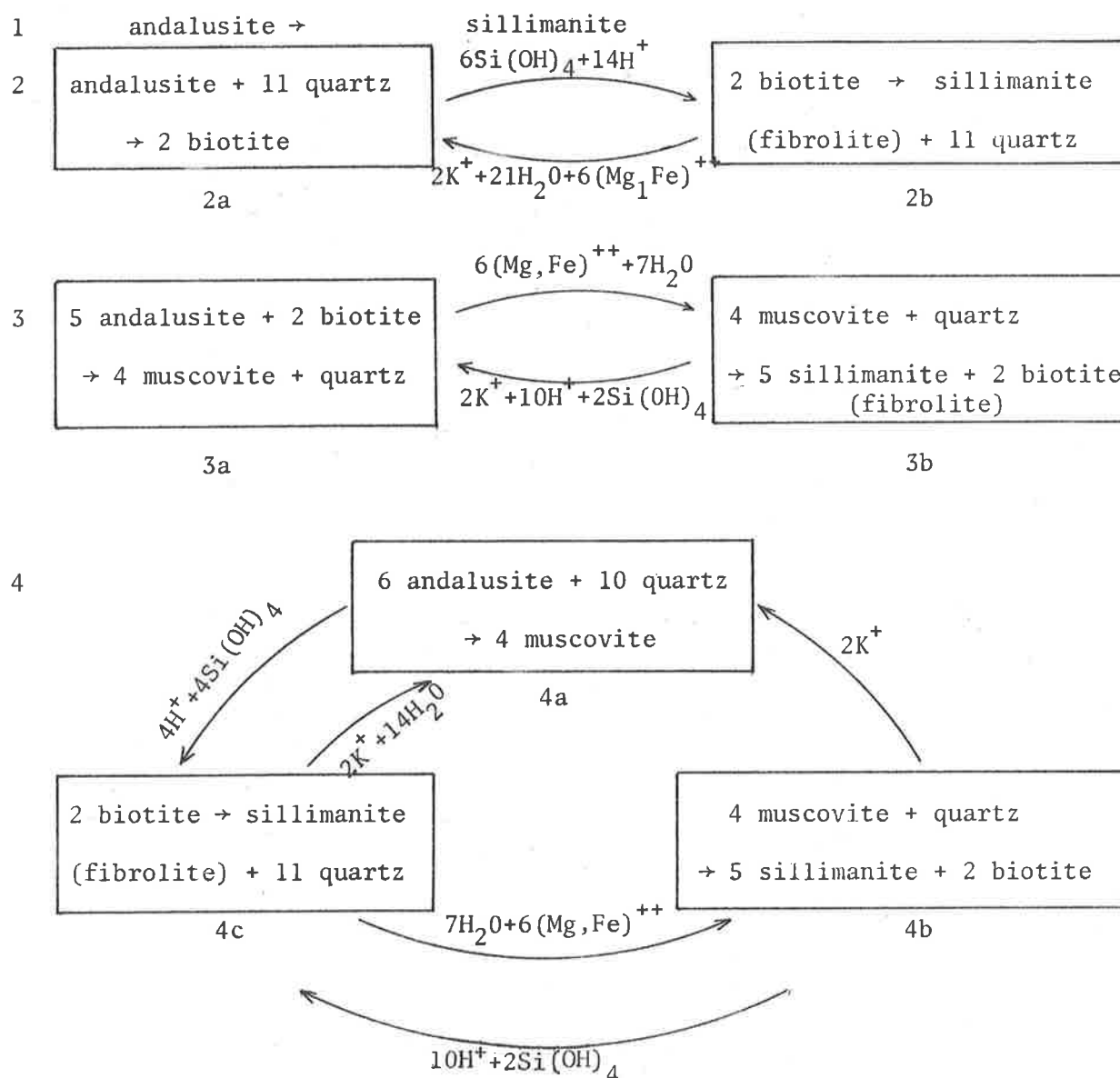
¹It is possible that the kyanite at Brukungu may have formed within the andalusite field in response to locally reduced partial pressure of water at some time during metamorphism. Alternatively, directed stress may have resulted in a local pressure "high", promoting the formation of kyanite.

et al. 1970). If fibrolite has, in fact a structural state different from the coarser prismatic form of sillimanite and hence a different stability range, it would significantly affect the interpretation of fibrolite-bearing rocks. However this difference in structural state and composition has not yet been proved (Zen, 1969) and there is some evidence to the contrary (Cameron and Ashworth, 1972). Yet fibrolite has contrasting habits to the prismatic form and a spatial distribution which is distinct from the coarser sillimanite, which is noted also in other metamorphic belts (Green, 1963; Hollister, 1969). This would support the view that these two forms of sillimanite have differing stability ranges. Although the coarser prismatic form is present in the Andalusite-Staurolite Zone in the Nairne-Mt. Barker Creek area, it is relatively rare and probably metastable. Most of this sillimanite directly replaces andalusite, however some also occurs in close association with fibrolite alone.

Holdaway (1971) has noted that fibrolite has a free energy of up to 150 kcal/mole above that of the prismatic form of sillimanite (presumably because of its Al-Si disorder as suggested by Zen (1969)). Holdaway invokes that to form fibrolite requires overstepping of the equilibrium boundaries, by 200°C or more when derived from andalusite, up to 55°C when derived from kyanite and only by approximately 9°C when derived from muscovite. This would explain why fibrolite is often associated with muscovite but does not form from andalusite. Holdaway suggests that fibrolite is always a metastable mineral forming in a disequilibrium process "from the reaction of a mineral or mineral assemblage which has been made very unstable by overstepping of the equilibrium boundary". A rapid reaction is believed to favour the formation of fibrolite rather than the coarser crystalline sillimanite. Fibrolite, however, is commonly believed to occur prior to sillimanite grade rocks in the kyanite stability field (e.g. Hollister, 1969) and is found well within the Andalusite-Staurolite Zone prior to the higher grade appearance of prismatic sillimanite in the Sillimanite Zone of the

Mount Lofty Ranges (Fig. 4), (Fleming, 1971). If P-T conditions in the Nairne-Mt. Barker Creek area were near the andalusite-sillimanite phase boundary, possibly brief increases in temperature into the sillimanite stability field induced rapid reactions involving muscovite and possibly biotite, resulting in the indirect breakdown of andalusite to fibrolite (as discussed later). As reaction rates dropped, sillimanite crystallized as the coarser prismatic form (it is noted in some rocks that fibrolite passes directly into this form). As fibrolite precedes the Sillimanite Zone, however, it seems more likely that the rate of reaction induced rather than the amount of over-stepping was the driving force of fibrolite formation. If fibrolite has a stability field which overlaps the andalusite and possibly kyanite fields, it would not be necessary to invoke sudden over-stepping of phase boundaries with a return to lower temperature conditions.

The possible mechanisms of indirect transformation from one Al-silicate polymorph to another are suggested by the work of Carmichael (1969) involving kyanite and sillimanite. These hypothetical mechanisms have been based on textures observed in rocks of the Whetstone Lake area, south Ontario. The reaction models based on sets of cation exchange reactions have been modified by Fleming (1971) to explain the breakdown of andalusite to sillimanite, consistent with textures observed in the Dawesley-Kanmantoo area (Appendix IV). The Dawesley-Kanmantoo (and Nairne-Mt. Barker Creek) textures show that plagioclase was not involved in the transition from andalusite to sillimanite as postulated by Carmichael for the Whetstone Lake rocks. Textures instead show fibrolite associated with poikiloblastic andalusite, coarse muscovite plates, biotite and quartz. Because of this difference, the reactions formulated by Fleming for the rocks of the Andalusite-Staurolite Zone in the Dawesley-Kanmantoo area differ from those of Carmichael (1969). Fleming's reaction models explain much of the textural associations encountered in the Nairne-Mt. Barker Creek area. These reaction models are given below (after Fleming, 1971) and the corresponding textures from which they were derived are summarized in Appendix IV.



While textures involving fibrolite in the Nairne-Mt. Barker Creek rocks show evidence of the transformation of andalusite along these reaction paths, uncertainty arises in many cases in the recognition of which particular reaction set has produced a particular textural association. This is due to the coincidence of two or more reaction paths leading to the formation of fibrolite in the same rock. Furthermore, it appears that the cycle of cation exchange is often incomplete and textures show the incomplete development or absence of a component reaction from a reaction system recognized in a particular rock. In addition, these reaction models alone do not

adequately explain all textures involving fibrolite and biotite.

2.3.2.4 Textures in peraluminous schists

Textures of the peraluminous schists will be outlined below, numerical reference being made to Fleming's postulated reactions outlined above.

2.3.2.4.1 General

The regional schistosity S_2 defined by micas is deformed about augen-like structures which have originated in either of two ways:

(i) The first of these is as pre-existing aggregates of quartz, biotite and minor plagioclase and opaque minerals forming poorly to well developed augen structures (Plate 23, (c,d)). These aggregates usually contain poikiloblastic andalusite and staurolite porphyroblasts with inclusions which are much finer than the matrix which encloses the augen.

The paucity of fine micas in these augen, particularly of muscovite, may be due to their involvement in the decomposition of andalusite to fibrolite. These augen probably originated as a result of metamorphic segregation of quartz-rich beds or lenses prior to F_2 folding. (ii) The second mode of occurrence is as extensive pressure shadow areas (Spry, 1969, p.246) developed about pre- S_2 andalusite and staurolites. These structures are by far the most common. It is not always possible to determine the origin of the augen-like structures. Pressure shadows have probably formed about earlier matrix and variable recrystallization of this pre- S_2 matrix has occurred in some rocks. Although the occurrence of augen with a grain size considerably finer than that of the enclosing matrix is not common, evidence of a pre- S_2 matrix is best seen where no pre-existing porphyroblast is associated with the augen (e.g. A405/E6(2)), Plate 24, (a). Where the grain size of the augen has remained finer than that of the enclosing matrix, pressure shadows in the S_2 plane can be distinguished (Plate 24, (a)). Elsewhere the earlier matrix is often extensively recrystallized (possibly syn- S_2 or post- S_2) yet the augen structure is still clear (Plates 23, (d), 35 (a)).

Recrystallization has commonly produced grainsizes which are coarser than the enclosing matrix (Plate 40, (c)). Quartz is the major component in these recrystallized augen. Its grainsize is highly variable (to 2.5 mm) due to irregular recrystallization. Physical equilibrium does not seem to have been attained; triple point junctions are uncommon. Coarse biotite (to 0.6 mm) and muscovite (to 1.5 mm) are often present in the augen; most are randomly oriented and have probably crystallized post- S_2 . In some rocks (e.g. A405/BC44) finer patches of quartz and biotite occur within the large recrystallized areas of the augen and amongst the coarse muscovite plates. The fine biotites are often aligned and define a relict schistosity S_1 (Plate 24, (b,c)). Recognition of S_1 is possible where it is inclined at a high angle to S_2 ; in cases where S_1 might be inclined at low angles to the enclosing schistosity, its identification is uncertain as it is conceivable that some syn- S_2 biotites may form within the augen, particularly if part of the augen is composed of a quartz-rich pressure shadow.

Pre- S_2 to early syn- S_2 metamorphic segregation is common, with concomitant quartz enrichment of the mica-poor layers and the formation of coarse quartz-biotite segregations (these are described in a later section). In some rocks (e.g. A405/E6(2)) it is evident that quartz-rich layers, formed by syn- S_2 segregation, pass into partially developed augen which probably formed earlier (Plates 23, (d); 24, (a)).

2.3.2.4.2 Textures involving andalusite and staurolite

Poikiloblastic andalusite porphyroblasts are associated with these augen-like structures in most rocks. These andalusites have formed pre- S_2 since definite quartz-filled pressure shadows are developed in the S_2 plane and the inclusions in these xenoblastic porphyroblasts are distinctly finer than the grainsize of the enveloping matrix which defines S_2 . In some cases the andalusites are set in a variably recrystallized matrix which composes some of the augen as mentioned earlier. Staurolite is commonly found in these augen structures also. Less commonly, staurolite and andalusite

occur as isolated porphyroblasts or as aggregates of crystals which are not enclosed by a pre-existing quartz-biotite matrix but are usually accompanied by quartz-filled pressure shadows (Plates 24(d), 25(a), 40(b)).

Andalusite crystals typically have very irregular or ragged margins and are commonly elongate, generally ranging from 0.75 mm - 1 cm (Plate 37, (b)). Inclusions consist mainly of quartz with minor plagioclase and opaque minerals, occasionally forming up to 25% of the crystal. In most cases, the variation in size, parallel orientation and abundance of these (and occasionally biotite) inclusions across andalusites seems to reflect an earlier layering (e.g. A405/BC34C) and/or schistosity S_1 (Plates 25(a,b,c,d), 37(b,c), 24(c), 26(a,b,c)). In some porphyroblasts the inclusions are equidimensional (Plate 41(c)) yet they often form bands which define relict bedding S_0 and/or S_1 (Plate 25(d)). In some cases andalusites are obviously elongate in S_0 , commonly paralleled by bands of opaque inclusions which are occasionally also elongate (Plates 24(c), 26(a,b,c), possibly reflecting an earlier schistosity S_1 which may have formed sub-parallel to the bedding.

Some andalusites show evidence of multistage growth (e.g. A405/MD5, E2A) seen as overgrowths of crystals with relatively coarse inclusions on cores with very fine equidimensional inclusions. The inclusions in some overgrowths are elongate and probably define relict S_1 (Plate 26(d)). Individual rocks contain both crystals with equidimensional or random inclusions and crystals with aligned elongate inclusions. Andalusites commonly have also a narrow rim which contains far fewer but usually coarser inclusions than the rest of the crystal. These rims probably represent overgrowths which grew at a slower rate than the earlier portions.

Andalusites in some rocks appear to have grown syn- S_2 (e.g. A405/H8a, H8b) and are elongate in S_2 with no evidence of pressure shadow areas (Plate 23(b)). Syn- S_2 andalusites are rare but have been observed in the axial plane schistosity of F_2 microfolds. Typically these andalusites

contain inclusions which are commonly slightly finer than the enclosing matrix yet appear continuous with S_2 (Plate 27(a)). Some are partly rotated, with inclusion trails still continuous with S_2 and have probably formed early during F_2 (Plate 27(b,c)). The slightly finer grain size of the inclusions is consistent with this. In the same rocks S_2 in places is partly deformed around some andalusites which also have considerably finer inclusions than the matrix and have probably formed either pre- S_2 or early syn- S_2 . Elsewhere post- S_2 rotation of some crystals has probably been responsible for discontinuity of inclusion patterns with the matrix schistosity. Commonly the syn- S_2 andalusites show evidence of multistage growth where overgrowths of early syn- S_2 origin occur on crystals with very fine equidimensional inclusions which have formed pre- S_2 (Plates 27(d), 41(b)). While some of the andalusites believed to be syn- S_2 might be considered as having formed post- S_2 by partly pushing aside the matrix in the manner suggested by Misch (1971), the continuity or near continuity of the slightly sigmoidal inclusion patterns with the matrix schistosity would preclude this in most crystals.

Staurolite is generally more equidimensional than andalusite and typically contains fewer but coarser inclusions. These are generally opaque minerals and less commonly quartz. The inclusions are commonly finer than the matrix and in some appear to define relict S_1 . Some staurolites have cores choked with fine inclusions and rims, which probably grew at a slower rate, with few inclusions (Plate 37(d)). Crystals are generally less than 3 mm across and are xenoblastic to sub-idioblastic. In some rocks aggregates to 3.5 mm occur. The interlocking staurolite crystals contain inclusions which are occasionally seen to form a sigmoidal pattern defining a relict pre- S_2 schistosity (Plates 28 (a,b), 40 (b)). Less commonly single crystals exhibit a pre- S_2 sigmoidal inclusion pattern.

Where andalusite and staurolite occur together (e.g. A405/MD5, BC37, BC37a), staurolite is usually seen to cut across andalusite (Plate 28(c)).

These staurolites appear to have formed either slightly later than or synchronously with andalusite (Dr. R.L. Oliver, pers.comm.). The occurrence of occasional idioblastic staurolite crystals within the poikiloblastic andalusites is not conclusive evidence of staurolite forming before andalusite. Rather these staurolites have probably formed synchronously with or possibly later than the andalusites as evidenced by crystal boundaries of the staurolite being usually perfectly sharp and often cutting across quartz inclusions in the andalusites (Plate 28(d)). Some staurolites contain abundant quartz inclusions of similar size to the quartz in the enclosing matrix, resulting in a skeletal appearance (e.g. A405/E4,E8). The time relation between the growth of these crystals and the development of the S_2 -schistosity is uncertain; these staurolites, however, occur most commonly together with andalusite porphyroblasts, occasionally with associated pre- S_2 matrix in the augen structures which formed as large syn- S_2 pressure shadow areas. In some rocks (e.g. A405/E4E,BC37,BC34a) staurolites appear to cut across S_2 micas and hence appear to have crystallized after the formation of the schistosity (Plates 29(a), 38(d), 39(c)). Commonly close examination shows that the syn- S_2 biotites intersect the boundaries of the staurolites, which contain inclusions aligned in a direction discordant with S_2 and (or) which are oriented parallel to S_1 recognized in nearby andalusite porphyroblasts (Plates 28(b), 29(a)). Also, in some cases there is apparent disintegration along boundaries of staurolite porphyroblasts where they are in contact with S_2 biotites (Plate 29(b)). This suggests that these porphyroblasts may be earlier than S_2 (Dr. R.L. Oliver, pers. comm), even though the inclusions in the staurolite are aligned in S_2 . This situation occurs in rock A405/E4E(Plate 29(b)) where S_2 parallels S_0 and the inclusions may reflect bedding layering or define S_1 which is of similar orientation to bedding, as suggested by the pattern of inclusions in nearby andalusites. An alternative interpretation of the above is indicated by intergrown biotites (oriented in S_2) and staurolite (Plate 29(c)). The staurolite is more

likely to have formed post- S_2 , the biotites being merely inclusions. While the relative time of formation of some staurolites is uncertain (Plate 46(c)) some crystals have clearly formed post- S_2 (Plate 38(d)). Hence, there seems to be evidence of both pre- S_2 and post- S_2 crystallization of staurolite in the same rock (e.g. A405/BC37a).

The ambiguity of the textural relations at porphyroblast margins has been recently stressed. Observations by Ferguson and Harte (1975) and others show that truncation of the matrix schistosity by a porphyroblast occurs not only where the porphyroblast post-dates the schistosity but may in fact occur if the porphyroblast antedates that schistosity (Ferguson and Harte, 1975 p.476-478). This is in strong contrast to the work of Misch (1971) in which truncation with variable degrees of deflection are interpreted as evidence of post-tectonic porphyroblast growth. It is now widely believed (eg. Ferguson and Harte, 1975) that truncation of the matrix schistosity (with much less but variable deflection) is insufficient evidence for post-tectonic growth. Commonly inclusions in the Nairne-Mt. Barker Creek staurolites do not offer additional information required to supplement the ambiguous textural patterns at the crystal margins. Often the inclusions are slightly finer but not significantly different from the matrix grain size and do not display any obvious relationships (Plate 46(c)).

2.3.2.4.3 Pressure shadows

Pressure shadow areas about porphyroblasts and augen are usually well developed in the S_2 plane, with strongest development in a direction perpendicular to the F_2 axis and l_2 (Plates 26(b), 28(a); compare 23(d), 24(d) with 24(a), 29(d) respectively). This direction is perpendicular to the "direction of maximum finite contraction" (Turner and Weiss, 1963) or along the "direction of maximum extension" (Ramsey, 1967, Fig. 5-2) and are analagous with the extension of oolites, with their longest axes lying perpendicular to the fold axis (Cloos, 1947). The pressure shadows consist predominantly of quartz which is mobile, and minor biotite. The quartz is

coarse, (to 2 mm in some augen), generally irregular in outline and often shows strain shadows. Few triple point boundaries are formed, the grain-size is highly variable and in general, physical equilibrium has not been attained. Biotite is of similar size to that in the matrix and is commonly disoriented. Where the pressure shadow effect is not as severe, biotite is more common and continuous with S_2 , tending to fan out about the pre-existing obstruction (e.g. A405/E4,E8,E2A).

The biotite lineation l_2' formed in the S_2 plane and approximately perpendicular to l_2 and the F_2 axis is evident in thin sections cut parallel to l_2' , perpendicular to S_2 (e.g. A405/BC27(2a),BC38a) and in sections in the S_2 plane (e.g. A405/BC37a(1),BC34a(1),BC29(1),M21A,BC38(1),E2A(1),E4(1),M21(1),BC44) in which the biotite (001) plane has formed and is elongate in the direction of maximum extension (as for the direction of strongest development of pressure shadows). Deformation of S_2 around porphyroblasts and augen has resulted in a variable local orientation of l_2' . Sections perpendicular to l_2' and S_2 are almost perpendicular to F_3 and S_3 (Fig. 7) and show well developed F_3 crenulations of S_2 micas. These crenulations commonly emanate from the margins of porphyroblasts or augen (Plate 35(d)) and generally penetrate less than a few mm into the matrix (Plates 26(a), 30(a), 40(a,c)). Besides crenulating S_2 micas, the F_3 crenulations are observed in fibrolite also, with later fibrolite needles growing in the S_3 plane (Plate 30(b,c)). Biotites formed along S_3 are not common and usually occur in the less micaceous layers of the metashales (e.g. A405/E10,BC29) or within the pre- S_2 augen where S_2 is weakly developed or absent (e.g. A405/BC29,BC37, Plates 25(b), 30(d), 31(a,b,c)). Within the augen, subidioblastic S_3 biotites (generally finer than 0.5 mm) are found to form at high angles to S_2 in the enclosing matrix, occasionally cutting across any relict S_1 biotites and through any S_2 micas formed in the outer extremities of the augen. At the boundaries of the augen these S_3 biotites usually tend to partly align along S_2 where the effects of this schistosity are stronger than within the augen (Plate 30(d)). In some cases, however, the F_3 biotites

can be seen to cut across biotites of the enclosing S_2 schistosity (e.g. A405/E10, BC37; Plate 31(b,c)). There is rare evidence of the development of crenulations in S_2 , with axial planes sub-parallel to S_2 (e.g. A405/BC34C & possibly A405/E4).

2.3.2.4.4 Textures involving garnet

Idioblastic pale pink almandine garnets occur in mica-rich layers. Crystals up to 2.5 mm occur but most commonly they are under 1 mm. In quartz-rich layers or segregations, garnets are much finer and usually have a poorly developed form. This compositional control on garnet size and form is particularly obvious in well layered rocks (Plate 31(d)). Inclusions are mainly opaques with some quartz. In quartz-rich layers, quartz inclusions tend to be more common and some garnets have a skeletal appearance in consequence. Crystallization of garnet occurred both during and after the development of S_2 . Syn- S_2 garnets are identified by sigmoidal inclusion trails with patterns continuous with the external schistosity ("Snowball" structures (Spry, 1963; Rast, 1965), Plate 32(a)). Post- S_2 idioblastic crystals cut across S_2 micas (Plates 26(b), 31(d)). In these the S_2 schistosity is usually preserved as undeflected inclusion trails in the garnet crystal (e.g. Plate 31(d)). There is some suggestion in these garnets of a forcing aside of the matrix to various degrees as suggested by Misch (1971) (e.g. A405/E4, E2A, Plates 32(b), 39(b); but c.f. Ferguson and Harte, 1975). Some garnets, however, show virtually no deflection of the matrix schistosity at the crystal margins (Plate 46(d)) and it seems probable that the slight deflections observed may have formed by later flattening. An alternative explanation for this deflection is suggested, however, by the pattern of inclusions within one particular post- S_2 garnet (Plates 32(b), 39(a)). Though showing some deflection of S_2 , the inclusion pattern in this garnet is also continuous with the deflected schistosity. It is proposed that garnet crystallization began syn- S_2 with inclusions aligning in S_2 . As the garnet grew the schistosity was deflected about the obstruction. Post- S_2 growth

of the crystal passively replaced the deflected schistosity.

The time relation between garnet and the other phases (fibrolite and coarse muscovite plates) which formed in the period syn S_2 -post S_2 (as shown later), is uncertain. In a few cases fibrolite mats appear to pass around garnet (e.g. A405/E8(2)) and it is probable that the garnet is earlier than some but not necessarily all, fibrolite. The latest garnet and most coarse muscovite crystallized post- S_2 but are rarely found to co-exist in thin section. In one case garnet appears to be pre-coarse muscovite (Plate 41(a)) and it is likely that muscovite formation continued after all garnet crystallization ceased. The typically short extent of F_3 crenulations does not permit a conclusive time relation between garnet and F_3 .

2.3.2.4.5 Textures related to the formation of fibrolite

The indirect transformation of andalusite to fibrolite has produced textures which can mostly be interpreted in terms of the reactions outlined earlier (Section 2.3.2.3). Not all textural features described by Fleming (1971) are recognized, however.

2.3.2.4.5.1 Polymorphic inversion

The direct inversion of andalusite to prismatic sillimanite is relatively rare. Porphyroblasts of poikiloblastic andalusite containing numerous prisms and coarse needles of sillimanite with characteristic diamond-shaped cross sections occur in over 10% of andalusite schists (e.g. A405/E2A, H8a, BC27(4), MD5, M21'; Plates 32(c,d), 33(c), 40(d)). The orientation of these sillimanite crystals can often be resolved as growth in S_2 or S_3 as with most of the fibrolite. Commonly these prismatic crystals are not restricted to the limits of a single andalusite host and may transect nearby crystals. Also, fibrolite is occasionally seen to pass directly into coarse blades of sillimanite (Plate 39(d)), (c.f. Vernon, 1975). This would suggest that not all coarse sillimanite has formed by direct polymorphic inversion of andalusite and that there must have been a redistribution of the Al_2SiO_5 before it recrystallized as this form of sillimanite. Possibly more definite

evidence of direct inversion is seen where the orientation of the sillimanite is not related to the schistosity in the matrix but is controlled by the orientation of the andalusite crystal.

2.3.2.4.5.2 The association of fibrolite, biotite and quartz

Textural evidence for Fleming's reaction system 2 can be seen in a large proportion of andalusite schists. The net reaction is andalusite \rightarrow fibrolite. The formation of fibrolite from biotite has occurred as a result of the diffusion of mobile cations between a different microscopic domain of the rock to one where biotite replaces andalusite. Reaction 2(a) explains textures showing this replacement of andalusite by biotite, where post- S_2 disoriented fine to coarse biotites and fine syn- S_3 biotites cut across and fill embayments in ragged xenoblastic andalusites (e.g. A405/BC37, BC29, BC27(3), BC27(4)). Biotites are generally xenoblastic to subidioblastic. Mutual boundaries are often diffuse and andalusite is commonly skeletal in appearance (Plates 32(d), 33(a,b,c), 36(d)). In the vicinity of these andalusites fibrolite needles occur as sprays emanating from biotite into quartz, commonly growing parallel to S_2 or S_3 -oriented biotites as products of reaction 2(b) (Plates 30(b), 33(a,c), 37(c), 38(c), 40(d)). Studies in other metamorphic belts have revealed very similar textural features involving fibrolite, biotite and quartz (Tozer, 1955; Green, 1963; Woodland, 1963; Hollister, 1969).

Where the alignment of fibrolite needles is strong and there is little random tendency, it is probable that crystallization occurred during the same tectonic phase as the biotites and that the needles are not merely mimicing their orientation. Commonly fibrolite occurs, together with variable amounts of biotite, as mats in the matrix. The fibrolite needles are aligned to varying degrees in S_2 . F_3 crenulations commonly intersect these mats (Plate 30(b), 33(d), 34(a)). Although quartz, also a product of reaction 2(b), is rare or absent in these mats, this can be explained by its high mobility relative to the other components. Where there is ample evidence of

reaction 2(a) such mats can be considered as results of reaction 2(b), particularly in rocks showing little evidence of any other reaction than the replacement of andalusite + quartz by biotite (e.g. A405/E2A,BC29). Imperfect alignment of most fibrolite in S_2 has probably resulted from post- S_2 crystallization, with needles mimicing the orientation of the S_2 biotites. That most biotite which replaces andalusite (reaction 2(a)) can usually be recognized as having formed post- S_2 seems to support this. Much fibrolite has formed syn- S_3 also. This is observed where F_3 crenulations of fibrolite mats are accompanied by the growth of fibrolite needles in the axial planes of the crenulations, passing into neighbouring quartz grains (Plates 30(b,c), 33(d), 35(a), 38(b,c)). Possibly some fibrolite also formed post- S_3 , mimicing the orientation of the F_3 biotites.

In conclusion, it seems that the reaction model can explain the association of fibrolite and biotite, and also the mimicing of the biotite orientation which is obvious in many rocks where fibrolite emanates from biotites of all orientations (e.g. A405/MD5). The strong biotite cleavage has controlled the orientation of fibrolite needles produced from their breakdown which is initiated by the replacement of andalusite by biotite in another microscopic domain of the rock. While this adequately explains the situation in some rocks, many show that the amount of biotite and associated fibrolite is far in excess of the amount of biotite in contact with and presumably replacing andalusite, since in the reaction model formulated, the volume of fibrolite formed is less than 1/6 of the volume of biotite involved in the replacement of andalusite. Although the reaction biotite \rightarrow sillimanite + quartz can also occur in reaction system 4 and textures involving biotite and sillimanite also occur as a result of reaction system 3, many rocks do not contain sufficient volume of muscovite replacing andalusite (which characterizes these two reaction models) to account for the large volumes of rock containing fibrolite mats (e.g. A405/M21' b, BC29; Plates 30(b), 34(b)).

Whereas andalusite usually occurs in rocks with associated fibrolite,

biotite and quartz (e.g. Woodland, 1963), Tozer (1955) has noted that rocks in the Glen District, Co. Donegal, Ireland, often show only incipient fibrolization of biotite and that there was obviously no Al_2SiO_5 polymorph present before the formation of sillimanite. In such cases, the formation of fibrolite is probably the result of the breakdown of biotite, accompanied by the release of K, Mg, Fe and OH. Tozer (1955) and Woodland (1963) have noted the bleaching of biotite associated with fibrolite, with the concomitant release of iron oxides. In addition, however, Tozer and Woodland report the presence of fibrolite needles in quartz grains (Tozer's type (ii) sillimanite), suggesting that the reaction $\text{biotite} \rightarrow \text{sillimanite} + \text{quartz}$ (2(b)) also played a role in the formation of fibrolite. Tozer (1955, p.318) has suggested that this feature is due to some diffusion of the elements of which sillimanite is composed. It is also possible, however, that the large granite bodies present in that area acted as external source and sink for ions required for reaction 2(b) to proceed without the presence of an earlier Al_2SiO_5 mineral being involved in the complementary reaction 2(a). In the Nairne-Barker Creek rocks some bleaching of biotite has occurred but this appears to be a weathering effect and is not restricted to biotite associated with fibrolite. Magnetite is common in some rocks but is not usually present in fibrolite mats, although there are some exceptions (Plate 37 (a)). It is therefore doubtful that biotite alone was a source of fibrolite in these rocks and the only likely mode of origin of fibrolite associated with biotite in some rocks as an alternative to Fleming's model is a process of nucleation of fibrolite on biotite as proposed by Chinner (1961) (see also Rast, 1965, p.81). In Chinner's model, the Al and Si are derived by solution of the unstable Al_2SiO_5 polymorph (andalusite) to form as fibrolite over the nucleating agent, biotite. This process, however would require a considerably greater mobility of Al than that proposed by Carmichael (1969), (c.f. Rast, 1965).

2.3.2.4.5.3 The role of muscovite

In a large proportion of rocks where andalusite and fibrolite are present, coarse muscovite is found to cut across and replace andalusite and neighbouring biotite and quartz grains (Plates 24(b), 29(b), 34(c,d), 35(a,b), 40(a)). This muscovitization can be explained by the metasomatic cation exchange reaction 3(a) and 4(a) outlined earlier (Section 2.3.2.3). The presence or absence of abundant quartz inclusions within the muscovite serves to differentiate between these two reactions (Plate 35 (c)). Similar textures have been described by workers in other regions (e.g. Green, 1963; Woodland, 1963, Figs. 4,5; Thompson and Norton, 1968).

The muscovite plates referred to are xenoblastic to idioblastic with crystals commonly up to 3 mm. Replacement of the andalusite has occurred to varying degrees leaving skeletal remnants and isolated grains in optical continuity enclosed by diversely oriented muscovite plates (Plates 34(d), 35(c)). In some rocks no andalusite remains but the presence of aggregates of disoriented muscovites and the occurrence of nearby fibrolite is a strong indication of its earlier presence (Plate 35(a,d)). Isolated patches of fine to coarse biotites and remnant patches of quartz-biotite aggregates from the augen occur within these muscovites (Plates 24(b), 35(b)). Some muscovite crystals retain opaque mineral inclusion trails from replaced andalusite, defining relict S_1 or S_0 (e.g. A405/E4E; Plate 35(c)). Replacement of andalusite consistent with reaction systems 3 and 4 occurred primarily during the post- S_2 metamorphic phase as the muscovites are nearly always disoriented. Although these are mainly restricted to areas immediately around andalusites and hence usually within augen structures, crystals occasionally transect S_2 micas beyond the augen margins. In some rocks (e.g. A405/E4) muscovite plates are found to align in S_2 at the margins of the zone of andalusite replacement but these may in some cases be mimicing this schistosity and have not necessarily crystallized syn- S_2 . Since there is evidence for the breakdown of andalusite via reaction system 2 during the syn- S_2 period however, it is probable that some replacement by muscovite

also began at this time. Some finer muscovites are found to align in S_3 but are generally confined to the augen structures as with most S_3 -oriented biotites. The coarse muscovite plates are not usually found in association with F_3 crenulations of S_2 or with fibrolite mats which have been crenulated, although there is some evidence that coarse muscovite plates cut across the crenulations and have therefore formed post- S_3 as well but this observation is not conclusive (e.g. A405/BC42, BC38; Plate 30(a)). Rarely, do pre- S_3 muscovites appear to be deformed by the F_3 crenulations and some muscovites cut across S_3 -oriented biotites (Plate 36(d)).

The occurrence of textures composed of randomly oriented muscovites with inclusions of very fine disoriented fibrolite and minor biotite can be interpreted as the breakdown of muscovite to fibrolite and biotite as shown by reactions 3(b) and 4(b) (e.g. A405/E6, BC42, BC44; Plates 36(a), 40(a)). Crystallographic control of the orientations of these inclusions however, is possibly more conclusive evidence of their origin as products of the breakdown of their host crystals. This is seen in the rare occurrence of fibrolite inclusions whose orientation is controlled by the cleavage of the muscovite host (Plate 36(a,b)). Often the fibrolite needles only approximately follow the cleavage and it is uncertain as to whether the crystallography of the muscovite has indeed controlled their orientation. Although there is little definite evidence for reactions 3(b) and 4(b) they can explain most textures observed adjacent to andalusites replaced by muscovite plates. Biotite present together with fibrolite as inclusions in these muscovites is xenoblastic and fine. Individual crystals cannot always be distinguished. Its distribution is very uneven and biotites may be concentrated in one muscovite host with little or none present in adjacent crystals. The orientation of these biotites follows that of the associated fibrolites.

Another pattern of distribution of fibrolite inclusions in coarse muscovite is seen in some rocks. Small amounts of biotite are generally present but these are mostly restricted to the boundaries of the muscovites

which are diffuse, implying instability of this particular association (Plate 36(c)). In these textures, aligned fibrolite needles are discordant with the cleavage of the muscovite host and must have formed earlier by a different mechanism. These needles commonly pass into quartz grains in the enclosing matrix without changing orientation and are often aligned in S_1 and S_2 (e.g. A405/E4) or in S_3 (e.g. A405/BC44). The absence of crystallographic control of their orientation is clearly seen where needles pass un-deviated through muscovites of diverse orientations. Such discordance has also been noted by Wiltshire (1975) where inclusions of fibrolite needles in muscovite porphyroblasts form fold patterns identical to those occurring in fibrolite and biotite in the surrounding matrix. It seems that these textures must be due to the replacement of the typical fibrolite-biotite-quartz associations described earlier, by coarse muscovites which mostly formed under static conditions. In the Nairne-Mt. Barker Creek rocks fibrolite formed in alignment with S_1 , S_2 or S_3 and thus possible later replacement by muscovite of remaining andalusite as well as biotite and some quartz occurred during the post- S_2 and possibly post- S_3 periods. This solution can also be applied to the above-mentioned assemblage of disoriented fibrolite needles in muscovite where the sillimanite can in places be seen to transect the boundaries of the muscovite hosts. The replacement of biotite from which fibrolite sprays commonly emanate by later muscovite plates, leaving the fibrolite unaffected as inclusions, could conceivably result from such a process.

The above-mentioned muscovitization is undoubtedly related to the replacement of andalusite, and replacement of biotite or quartz resulting from reactions 3(a) or 4(a) respectively. This interpretation is supported by the presence of relict disoriented coarse biotites which are obviously not syntectonic and have presumably partially replaced andalusite (reaction 2(a)) prior to the replacement of remaining andalusite and these biotites by muscovite.

These textures involving muscovite with fibrolite and quartz inclusions are noted in other areas. Within randomly oriented muscovite porphyro-

blasts, Tozer (1955) has noted small sillimanite prisms which are generally oblique to the muscovite cleavage but are oriented approximately parallel to the schistosity in the enclosing matrix. Also present in and in close proximity to the muscovites of Tozer's rocks are large quartz grains which are commonly crowded with randomly oriented fibrolite needles. Carmichael (1969) has proposed that this texture is the result of the reaction;

$$2 \text{ muscovite} + 2\text{H}^+ \rightleftharpoons 3 \text{ sillimanite} + 3 \text{ quartz} + 2\text{K}^+ + 3\text{H}_2\text{O} \text{-(i)}$$

In formulating a corresponding reaction which with (i) would give the net reaction kyanite (or andalusite) \rightarrow sillimanite, Carmichael has suggested the reactions

$$\text{kyanite} + \text{quartz} + \text{K}^+ + \text{H}_2\text{O} \rightleftharpoons \text{muscovite} + \text{H}^+ + \text{Si}(\text{oH})_4 \text{-(ii)}$$

or alternatively;

$$4 \text{ kyanite} + 3 \text{ quartz} + 2\text{K}^+ + 3\text{H}_2\text{O} \rightleftharpoons 2 \text{ muscovite} + \text{ sillimanite} + 2\text{H}^+ \text{-(iii)}$$

These are deduced from a texture described by Chinner (1961) where inclusions of relict kyanite and quartz occur in muscovite porphyroblasts which also contain oriented fibrolite needles which cut across the cleavage of the host. Reaction (iii) fails to explain why the fibrolite is aligned but not controlled by the muscovite cleavage if the two minerals formed simultaneously. Similarly, (i) and (ii) seem inadequate in explaining Chinner's observations. A comparison with the virtually identical textures in the Nairne-Mt. Barker Creek rocks suggests a common origin for the textures in the two occurrences, viz. that of coinciding textures resulting from two or more reaction systems operating in the same microscopic domain of the rock. Although in rare cases rocks of the Nairne-Mt. Barker Creek area contain some muscovite porphyroblasts with quartz inclusions containing small disoriented sillimanite needles (e.g. A405/BC27(4)), it is not necessary to explain this by an additional reaction system involving the reaction

$$\text{muscovite} \rightleftharpoons \text{ sillimanite} + \text{ quartz}$$

These inclusions are probably products of the reaction biotite \rightarrow sillimanite + quartz (2(b)) which were encased in muscovite during the replacement of andalusite. Such an origin might also explain Tozer's observation of sillimanite needles which "crowd the pools of enclosed quartz" (Tozer, 1955, p.315). It seems significant that Tozer

(p.315) has noted that thin sections displaying these textures "sometimes show fine sillimanite needles similar in their mode of occurrence to those described.....as type (ii)" (that is, fibrolite enclosed in quartz which is associated and probably contemporaneous with "fibrolite derived directly from biotite"). Fleming (1971) also has not found evidence for reaction (i), above, in an extensive study of andalusite and sillimanite-bearing rocks in the Mount Lofty Ranges.

In many rocks containing coarse muscovite which has partly or wholly replaced andalusite, mats of fibrolite and biotite are seen in the matrix, in the proximity of the muscovites. Fibrolite needles are generally aligned in S_2 and quartz is virtually absent. Fine-grained muscovite which usually forms about 50% of the matrix in mica-rich layers is greatly depleted or absent where fibrolite has formed. This suggests that the matrix enclosing the andalusites has played a role in the formation of fibrolite and that syn- S_2 muscovite has broken down to biotite and fibrolite, the products of reactions 3(b) and 4(b). Cation exchange has occurred with the microscopic domain in which muscovites replaced andalusite. In most rocks the breakdown of this matrix muscovite is greatly in excess of the breakdown of the coarse disoriented muscovite to biotite and fibrolite.

The occurrence of fibrolite closely associated with biotite and quartz (as described earlier) in rocks where the andalusite is primarily replaced by muscovite can be explained in terms of reaction 4(c) (e.g. A405/BC44). Though reaction 4(c) is identical to reaction 2(b) this texture represents part of reaction system 4 which is characterized by the replacement of andalusite and quartz by muscovite (Plate 38 (b)). The occurrence of fibrolite-biotite mats is not, however, diagnostic of any one reaction system. Due to the mobility of quartz such mats can form from either the reaction biotite \rightarrow fibrolite + quartz (2(b) or 4(c)) or the reaction muscovite + quartz \rightarrow sillimanite + biotite (3(b), 4(b)), particularly where the matrix muscovite is involved. Identification of the reaction system responsible for the formation of these mats in a particular rock depends on the recog-

nition of the minerals involved in the replacement of the andalusite porphyroblasts.

2.3.2.4.5.4 Conclusions

The breakdown of andalusite to fibrolite via interacting microscopic sub-systems as envisaged by Fleming (1971) on the basis of earlier work by Carmichael (1969) is largely substantiated in the Nairne-Mt. Barker Creek rocks. Some textures, however, could only be explained by the superimposition in time of these sub-systems.

There is, in addition, evidence for the breakdown of andalusite and the nucleation of Al and Si on biotite to form fibrolite in the manner proposed by Chinner (1961). This situation occurs in textures which consist predominantly of interwoven biotite and fibrolite, there being little or no evidence of the replacement of andalusite by biotite or muscovite, a feature which characterizes the reaction systems proposed by Fleming (1971).

2.3.2.4.6 Staurolite-fibrolite relations

Most staurolite-fibrolite associations give the impression of mutual stability. Certain textures, however, are not clear.

Staurolite is intersected by fibrolite in some rocks (Plate 41 (d)) and also occurs as islands in large mats of fibrolite. Usually this staurolite retains good crystal form with sharp margins indicating stability (Plate 38(a)). Some staurolite crystals are cut by coarse muscovite plates or occur as islands within these. Fibrolite and biotite occur nearby commonly forming typical mats. These textures may be interpreted in terms of a reaction proposed by Chinner (1965), viz. Mg-rich biotite + staurolite + muscovite + quartz \rightarrow Fe-rich biotite + Al silicate + H₂O. Guidotti (1968) has noted the rimming of decomposing staurolite by muscovite. Also, Chakraborty and Sen (1967) describe textures where ragged staurolites are in contact with muscovite crystals and surrounded by masses of intergrown sillimanite and biotite. These writers suggest a decomposition reaction for staurolite, viz. 3 staurolite + muscovite + quartz \rightarrow 7 sillimanite + biotite

+ 3H₂O. In the Nairne-Mt. Barker Creek rocks, however, where staurolite is associated with muscovite, it is usually included in muscovite crystals or enclosed by masses of muscovites which appear to be related to the decomposition of adjacent unstable andalusites (Plates 42(a,b), 35(c)). The staurolite margins are generally sharp and often straight. Textures of muscovite relics in biotite and "scums" of biotite on muscovite as noted by Chakraborty and Sen (1967) are not seen in the Nairne-Mt. Barker Creek rocks. There is also no evidence for the breakdown of staurolite to sillimanite and garnet, as proposed by Hoschek (1969), viz. staurolite + muscovite + quartz → Al silicate + biotite + garnet + vapour. No textural evidence was found for the breakdown of staurolite by the mechanism proposed by Carmichael (1969). This mechanism is based on an interpretation of textures characterized by the embayment of staurolite by quartz and oligoclase and various intergrowths in the same rock involving garnet, biotite, muscovite and plagioclase.

Although textures are unclear in portions of some rocks (Plate 42(c)) and despite the association of staurolite with biotite and fibrolite mentioned above, there is no definite evidence that the staurolite is anywhere decomposing to fibrolite. The absence of fibrolite and coarse muscovite plates in a rare staurolite schist (A405/BC34) in which no trace of andalusite occurs, strengthens the argument for the stability of staurolite, assuming of course that conditions of oxygen fugacity and PH₂O were similar to those in the rocks containing staurolite, andalusite and fibrolite, as the stability of staurolite shows a dependence on these factors (Hoschek, 1969). Had prograde Mg-chlorite been present in these rocks it is possible staurolite would have been close to decomposition by the reaction: staurolite + chlorite + muscovite → Al-silicate + biotite + quartz + vapour (Hoschek, 1969, p.217, Fig. 2) under the proposed metamorphic conditions of the area (see section 3.3.1).

2.3.2.4.7 Post-F₃ features

Small kinks, often in conjugate form are developed in the S₂ micas at various orientations to S₂ and S₃. These are not penetrative over more than a few mm and are not visible in hand specimen. Their time relation to S₃ is uncertain but is most likely post-S₃. Retrograde reactions are of minor importance. Most rocks contain chlorite which varies from fine to very coarse (to 2.5 mm) and usually containing exsolved magnetite along cleavage planes resulting from the replacement of biotite. Crystals vary from ragged xenoblastic to idioblastic, occurring as individuals, large rosettes and masses of fine xenoblastic crystal aggregates (Plates 36(a), 42(d), 45(a)). Partial alteration of andalusite to sericite is not uncommon (e.g. A405/BC27(2), MD5).

2.4 Calc-Silicates

Mineral assemblages encountered in the various stratigraphic units are:

- (i) plagioclase, biotite, hornblende, scapolite ± diopside;
- (ii) quartz, plagioclase, hornblende, clinozoisite, garnet;
- (iii) quartz, biotite, hornblende, scapolite ± calcite ± plagioclase;
- (iv) quartz, plagioclase, biotite, hornblende, scapolite, diopside;
- (v) quartz, plagioclase, hornblende, epidote;
- (vi) plagioclase, hornblende, scapolite, diopside ± biotite;
- (vii) biotite, hornblende, scapolite ± plagioclase;
- (viii) quartz, plagioclase, biotite, scapolite ± calcite.

Although the actual number of assemblages can be reduced by incorporating one assemblage within another (e.g. (i) with (ii)), these are kept separate to aid descriptions. Whilst the mineralogy of two calc-silicates can be the same, the relative proportions of the minerals and the textures can differ greatly resulting in completely different appearances in hand specimen.

Two major groups of calc-silicates can be distinguished on the basis of appearance in the field and the mineral assemblages present. Other assem-

blages are rare and only occur in isolated zones. Assemblage (ii) which contains garnet (Plate 43(a)) was observed only in one locality, occurring as a thin calc-silicate band in a metasandstone.

2.4.1 Group one

Assemblages (iv), (v) and (vi) form the first group. All these rocks show a characteristic pale yellow-dark olive green layering. Assemblages (iv) and (v) occur in the southern part of the area, the latter in calc-silicates below the Mt. Barker Quartzite and the other immediately above the Quartzite. They consist of a fine granoblastic mass (commonly av. 0.03 mm), with quartz as a minor constituent. Rocks with assemblage (iv) pass into meta-calc-siltstones and shales to the north of Mt. Barker Creek. These rocks are described in a later section (2.6). A facies change to the north has also resulted in a replacement of assemblage (v) by assemblages (vi) and (iv), i.e. diopside and scapolite in place of epidote. The calc-silicate rocks in the southern part of the area also differ from their northern equivalents in the finer grain size of the former. These appear to have undergone far less recrystallization and the finer textural features are preserved. Lamination is finer and intertonguing on hand specimen scale is visible (e.g. A405/BC52, BC45). Layering is chiefly the result of mineralogical variations, consisting of pale yellow to white diopside or epidote-rich layers (commonly together with high-An¹ plagioclase (untwinned)) and dark green hornblende-rich layers (Plate 43(b)). The layering is paralleled by bands of accessory minerals (magnetite, sphene and minor zircon).

Although this variation in the relative amounts of calc-silicate minerals is probably the result of original variations in the composition of the calcareous sediment, there has undoubtedly been considerable enhancement of layering (= bedding) by metamorphic segregation. This segregation is evident where enrichment of certain minerals has produced lenses (to 1 cm thick) of hornblende and granoblastic aggregates of scapolite and diopside (\pm plagioclase) or epidote (\pm plagioclase, hornblende). The grain size of many of these segregations is distinctly finer than the rest of the

¹ Plagioclase composition was determined as approximately An80 (Bytownite) by electron probe analysis.

rock.

As biotite is uncommon or absent in these rocks, a strong schistosity is not usually developed. Within the fine granoblastic mass, however, coarser, elongate, subidioblastic hornblende crystals define the regional schistosity S_2 . The degree of development of this schistosity is variable and largely related to the abundance of hornblende but there is variation even in layers of similar hornblende content (e.g. A405/BC52). In those portions of the rocks where a schistosity has formed (presumably when recrystallization occurred during tectonism), plagioclase and quartz are partly elongated in S_2 as well. Here also epidote or diopside have commonly recrystallized into elongate aggregates of coarse crystals roughly parallel to the schistosity. Any biotite present tends to be aligned in S_2 also. Some coarse subidioblastic hornblendes cut across the schistosity, having crystallized post- S_2 . The formation of segregations appears to have commenced pre- S_2 as the oriented hornblende crystals which define S_2 tend to be deflected around these in some cases (e.g. A405/BC49').

Textures in mineralogical units (iv) and (vi) in the north manifest extensive recrystallization and segregation (A405/MCS 2b, MCS 2c). Layering is mainly defined by a variation in abundance of coarse crystals of hornblende and scapolite and to a lesser extent, diopside. The fabric is almost isotropic and granoblastic (Plate 43 (c)), yet the hornblende, scapolite and diopside tend to be xenoblastic and porphyroblastic and set in a highly variable matrix. This matrix is composed of fine plagioclase and diopside (av. 0.03 mm typically) \pm fine biotite, hornblende and rare quartz. Matrix diopside and biotite seem to be mutually exclusive which may be an original sedimentary feature, diopside (a low-Al mineral) forming in the less aluminous calcareous beds and biotite in the more aluminous, and potassium-rich

beds. A matrix is commonly absent in many layers, these being composed almost entirely of coarse scapolite and diopside with lesser amounts of hornblende.

The scapolite and hornblende crystals contain variable amounts of inclusions. Inclusions in scapolite are mainly plagioclase, biotite and occasionally minor hornblende while those in hornblende are generally plagioclase only. Scapolite with variable amounts of diopside form almost pure layers up to 2.5 cm thick. Here the scapolite and diopside are typically coarser than elsewhere (to 1.2 and 2 mm respectively) and scapolite contains few inclusions. Hornblendes are also coarsest (to 1 mm) in bands where the mineral is most abundant. Where individual scapolite and hornblende crystals and crystal aggregates are set in a matrix, they tend to be skeletal and ovoid in form, the longest dimension paralleling the layering along the bedding. Where a matrix is present, aligned biotites and to some degree, hornblendes define a schistosity (S_2) which is sub-parallel to the bedding. In the coarsely recrystallized portions where no matrix is visible, a definite schistosity cannot be recognized although the alignment of ovoid hornblende porphyroblasts and aggregates is in this direction and may represent S_2 . The inclusion patterns of scapolites set in a matrix are parallel to this schistosity and these crystals probably formed either syn- S_2 or post- S_2 .

2.4.2 Group two

The second major group of calc-silicate is common in the lower Marino Group and is characterized by assemblage (iii); this grades into meta-calc-siltstones and shales with thin calc-silicate bands of assemblage (viii). Typically the lithologies containing assemblage (iii) have a spotted appearance, due to the presence of aggregates of poikiloblastic scapolite and show considerable intertonguing with metasiltstones on all scales. Assemblage (iii) contains little biotite and occasionally minor plagioclase, which is rarely twinned. Coarse poikiloblastic hornblende and scapolite commonly

produce a near granoblastic texture with minor fine quartz and twinned calcite which is irregularly recrystallized in patches of coarse crystals (to 0.5 mm) discordant with the layering (e.g. A405/BC23). This layering is crude but overall it parallels relict bedding defined by bands of opaque minerals, sphene and zircon. Biotite is mostly disoriented and commonly poikiloblastic although some crystals are aligned along bedding. The relative amounts of amphibole and scapolite are highly variable even within the same layer over distances as little as a few centimetres. Rocks with no hornblende (assemblage (viii)) contain considerably more biotite. These calc-silicates are merely scapolite-rich layers with minor biotite (less than 20%) in spotted meta-calc-siltstones and shales with the same mineral assemblage but richer in quartz and biotite and are described in section 2.6.

The well layered calc-silicates of the first group change facies along strike to the north and with decreasing carbonate content pass into calc-silicate lithologies characterized by assemblages (iii) and (viii) and calc-siltstones and shales and then into non-calcareous lithologies.

2.4.3 Other assemblages

Rocks with assemblage (i) are of minor occurrence and are observed in the Backstairs Passage Formation in the vicinity of Nairne. They are unique in consisting almost entirely of calc-silicate minerals (plagioclase <10%, no quartz, biotite <4%). Scapolite, unusually not poikiloblastic, is abundant. Physical equilibrium is well advanced with a granoblastic mass (averaging 0.12-0.05 mm) of anhedral scapolite and minor plagioclase, crystals being slightly elongate forming a weak schistosity which is partly paralleled by subidioblastic and idioblastic hornblende crystals. This schistosity follows a crude layering which probably defines bedding as it is paralleled by bands of accessory minerals. Late stage recrystallization of hornblende to very coarse subidioblastic to idioblastic crystals (to 1 cm) along bedding and in veins disrupts much of the layering.

Rocks with assemblage (vii) contain up to 30% biotite in some thin layers which might be considered calc-shales. These rocks show evidence of retrograde reactions, with xenoblastic chlorite replacing biotite and hornblende, liberating magnetite. Replacement of hornblende by chlorite is uncommon in the other assemblages.

Accessory minerals present in the various calc-silicates are similar. These are:

Zircon is present in traces, subidioblastic to rounded, to 0.12 mm typically. These are primary grains.

Sphene (to 8%) is pleochroic pale red-brown-colourless. It is subidioblastic to idioblastic, typically from 0.04 to 0.16 mm in size and in aggregates of xenoblastic crystals or granules. Some is partly altered to leucoxene. Usually sphene is concentrated with opaques in thin bands.

Opaques (probably magnetite), to 3%, occur in bands or associated with hornblende where they are probably secondary.

Apatite is present in traces, being very fine, subidioblastic to idioblastic.

2.5 Marbles

Mineral assemblages are:

- (i) calcite, quartz, plagioclase \pm biotite;
- (ii) calcite, plagioclase, hornblende, scapolite, diopside.

Assemblage (i) is found in the pale grey-white marbles of the metamorphosed Brighton Limestone. Non-carbonate content is variable; nearly pure calcite rocks pass into schistose quartz and biotite-rich rocks. A typical marble is composed of a mosaic of interlocking xenoblastic calcite crystals, which are typically coarse-grained (av. about 2 mm) and twinned. The calcite crystals tend to be elongate in the schistosity (which is sub-parallel to the bedding) and commonly crystals show strain shadows and deformed twin planes. Quartz and plagioclase are extremely variable in grain size (to a

maximum of 0.7 mm) and are scattered sporadically through the rock. The biotite is typically pale yellow-brown. Assemblage (ii) is developed in a coarse pale grey marble lens immediately above the Mt. Barker Quartzite horizon. Interlocking xenoblastic twinned calcite crystals which form around 80% of the rock are of very uneven grain size (to a maximum of 2 mm) and are disoriented (Plate 43(d)). Unevenly distributed amongst the coarse calcite are finer xenoblastic to subidioblastic scapolite and diopside which are poikiloblastic and generally closely associated, with maximum grain sizes of 1 mm and 0.5 mm respectively. Hornblende is rare, fine and xenoblastic.

2.6 Meta-Calcsiltstones and Calcshales

The mineral assemblage quartz, plagioclase, biotite, scapolite ± calcite is representative of these rocks. With decreasing scapolite and calcite content, these rocks pass into metasiltstones and the less aluminous metashales described earlier.

The rocks are dark grey and finely to coarsely spotted white due to ovoid aggregates and individual crystals of scapolite. Bedding lamination is fair to good and defined by the variation in biotite and scapolite content. The more recrystallized scapolite-rich rocks are less laminated due to the disruption of laminae by the abundant large aggregates of scapolite (over 0.25 cm in some rocks).

Microscopically, bands of opaque minerals also are found to parallel this lamination and in less recrystallized rocks some variation in grain size is preserved (e.g. A405/BC18). Scapolite-rich bands, with decreasing quartz and biotite, pass into lithologies which may be termed calc-silicates but which contain the same mineral assemblage. These are often lenticular and intertongue with scapolite-poor layers on all scales.

Recrystallization and grain growth in these rocks is very irregularly developed in the south of the area. As a rule, the scapolite-rich layers have undergone the most recrystallization and are consequently coarser.

The biotite contained in these recrystallized layers, is up to five times its size elsewhere. The maximum size of scapolite varies from 3.5 mm in the more recrystallized metashales (e.g. A405/BC16) to 1 mm in the more quartzitic metasiltsstones (e.g. A405/BC18). North of Mt. Barker these scapolite-rich rocks are usually coarsely recrystallized and spots of scapolite aggregates are very large (to 0.75 cm), e.g. A405/M20, E12D. The matrix of quartz, plagioclase and biotite is variable in grain size, ranging from 0.1-0.025 mm.

Most of the scapolite has been broken down during kaolinization of the weathered rocks in the vicinity of Nairne and in the areas of Sturt Group and lower Marino Group rocks south to Mt. Barker Creek. Some rocks with a very low scapolite content (<5%) still have a spotted appearance due to the segregation of fine xenoblastic scapolite and plagioclase + minor quartz (e.g. A405/E23B).

In the less recrystallized rocks, inclusions of quartz and plagioclase in scapolite result in skeletal crystals. The scapolite of more recrystallized rocks is less poikiloblastic and in some meta-calc-shales some scapolites have no inclusions (e.g. A405/M20, Plate 44(a)). Scapolites may show a large variation in the proportion of inclusions in a single rock. In specimen A405/MCS2a, for example, some ovoid porphyroblasts contain abundant inclusions whereas the scapolites forming the bulk of the common large aggregates have relatively few. The cores, however, of these ovoid aggregates, which are composed of a radial arrangement of crystals are choked with very fine inclusions (Plate 44(b,c)). Presumably the poikiloblastic single porphyroblasts and the cores of the aggregates grew rapidly, trapping matrix material before it could diffuse away.

Inclusions of biotite in poikiloblastic scapolite parallel the S_2 schistosity developed in interbedded metashales whereas quartz and plagioclase are not elongated (e.g. A405/BC16, MCS2a). The inclusions are of similar size to the matrix grains. Individual ovoid scapolites tend to be elongate in the schistosity (defined by biotite) which is not markedly deformed

about them. Most scapolites exhibit these features and probably crystallized during the syn-S₂-post S₂ period. Some rocks show more definitely that scapolites crystallized both syn-S₂ and post-S₂. In specimen A405/M20, for example, aggregates of early pre-scapolite matrix are enclosed in the scapolite aggregates and have oriented biotites aligned in S₂ (defined by coarser biotites of the enclosing rock). This would suggest an early syn-S₂ formation of this scapolite (Plate 44(a)). Later post-S₂ subidioblastic and idioblastic scapolite crystals cut across the S₂ schistosity.

Except for scapolite and calcite, the mineralogy of these rocks is very similar to that of the metasiltsstones and less aluminous metashales. The abundance of these two minerals is extremely variable. Typical features are summarized below:

Scapolite (trace -50%), varies from 0.02 to 1 mm in grainsize. Coarsest crystals are commonly very poikiloblastic; individual non-poikiloblastic subidioblastic to idioblastic crystals are less than 0.5 mm across. Aggregates of scapolite are generally coarse (to 1 cm).

Calcite (trace -20%) is most common in scapolite-rich layers. Interlocking fine xenoblastic crystals to 0.025 mm form straight boundaries with quartz and plagioclase producing a granoblastic mass transected by scapolite and biotite. Calcite and some quartz recrystallized late in the metamorphic history along veins up to 0.75 cm thick composed of coarse interlocking crystals to 0.8 mm. Small vughs remain only partly filled with calcite (e.g. A405/BC18).

Accessory minerals are similar to those in metasiltsstones and form less than 1% of the rock. They are mainly tourmaline, zircon, apatite and magnetite.

2.7 Quartz-Biotite Segregations

Metamorphic segregations of quartz and biotite have formed throughout the area in the more micaceous metasandstones, metasiltsstones and quartz-rich metashales (Plate 15(d)). They are especially common in the upper parts

of the Marino Group. Typically segregations vary from about 0.5 to 6 cm in thickness and often the thicker segregations extend for several metres or more along strike. Commonly the thinner ones persist for only a few cm.

Shape and orientation are controlled by bedding and the regional schistosity S_2 . Tongues extend from the segregated layers where the schistosity intersects bedding at an angle. The schistosity is refracted and markedly weakened through the more competent quartz-rich portions of the segregations. Segregations have been folded in some cases, with the S_2 schistosity as their axial plane structure (e.g. A405/E4B,E4A) which suggests that their development began pre- S_2 and continued syn- S_2 . These segregations probably originated as quartz-rich beds or lenses with migration and segregation of quartz and biotite accentuating the primary differences.

Most segregations thicker than about 1 cm show a characteristic development of three zones. In the majority of these segregations, textures indicate that equilibrium is well advanced although some (e.g. A405/BC27', Plate 45(a)) have irregular shaped quartz crystals of variable grain size forming few triple point boundaries and have not reached a state of physical equilibrium (possibly due to rapid recrystallization).

The characteristic zones recognized are summarized below:

(1) Outer zone forming about 25-50% of the thickness, sharply bounded against the enclosing lithology (Plate 44(d)). It consists of medium to coarse-grained quartz and plagioclase which sharply increase in grain size near the margins of the second zone in some segregations. The crystals are generally equant and interlocking forming a mosaic texture, although locally irregular patches of coarsely recrystallized quartz may occur. Poikiloblastic garnet is common in some. In a minority of cases a thin envelope of very coarse biotite crystals is partially formed in this zone, crystals being of similar size to those in zone (2) and aligned to define a schistosity. Typical mineralogy is:

Quartz 70-85%. Interlocking equant grains, maximum range 0.05-0.25 mm commonly observed.

Plagioclase 10-20%. Grains interstitial to quartz, 1/4-1/2 av. grainsize of quartz. Untwinned, largely altered to sericite or clays.

Biotite 1-5%. Av. 0.1 mm, varying from very fine -0.3 mm. Moderately aligned in S_2 .

Garnet trace -4%. Xenoblastic, often poikiloblastic with quartz, magnetite inclusions. 0.17-1 mm common range, some to 1.25 mm.

Accessories:

Magnetite 2-4%. Subidioblastic to xenoblastic, 0.017-0.15 mm.

Apatite trace -2%. Subidioblastic, very fine.

Chlorite 0-1%. Xenoblastic, ragged to subidioblastic. To 0.4 mm. Some replacing biotite with magnetite exsolved along cleavage.

(2) A middle thin biotite-rich zone or envelope which is generally <1-3 mm thick, either with diffuse or sharp boundaries. Some idioblastic or subidioblastic garnet often forms in this zone. The mineralogy is:

Quartz 5-65%, 0.08-0.45 mm.

Plagioclase about 5%, similar grainsize as quartz.

Biotite 20-60%, to 2 mm typically. Subidioblastic, elongate and weakly to strongly aligned in S_2 .

Muscovite 0-1%, to 0.4 mm.

Garnet 0-2%, to 1 mm. Subidioblastic to idioblastic, some xenoblastic and poikiloblastic.

Accessories:

Magnetite 1-5%, to 0.4 mm, xenoblastic to subidioblastic.

Chlorite trace, replacing biotite.

Ilmenite and graphite trace, platy.

(3) Quartz-rich core with granoblastic texture resembling (1) but is coarser and garnet is uncommon. This zone may be absent in smaller segregations (Plate 45(a)). The mineralogy is:

Quartz about 90%, 0.05-0.4 mm maximum range observed. Equant, interlocking.

Plagioclase about 5%, <0.08-0.25 mm, interstitial to quartz.

Largely altered to sericite or clays.

Biotite 2-5%, 0.07-0.4 mm. Subidioblastic

Muscovite <1%, very fine

Garnet trace, xenoblastic. To 0-25 mm

Accessories:

Magnetite 1-2%, idioblastic to subidioblastic. To 0.4 mm.

Apatite trace-2%, subidioblastic to xenoblastic. To 0.17 mm.

Chlorite <1%, to 0.75 mm. Replacing biotite.

In the upper parts of the Marino Group where the development of segregations has been strongest, units rich in quartz are very common. These vary from <1 cm to 25 cm and occasionally up to 1.5 m thick. The quartz is medium to coarse-grained and mica content is very low (<5%). The thicker units can be traced for distances of up to 1.25 km. Presumably, these are larger scale developments of the segregations described above as weakly defined zones can sometimes be distinguished, with the quartz-rich core forming the bulk of the units.

2.8 Basic Dykes (Meta-Dolerites)

2.8.1 General

Metamorphosed basic dykes tend to follow the strike of the country rocks but are locally discordant; they are common in the Marino Group strata in the northern half of the area. They are medium-grained amphibolites or metadolerites, commonly under 3 m thick and invariably less than 5 m, having a typical very dark green colour.

The rocks are commonly composed of a near granoblastic mass of hornblende and plagioclase which form 50-60% and 40-45% of the rock respectively. Most dykes contain variable proportions of relict plagioclase phenocrysts in addition resulting in exceptional plagioclase contents of

up to 65%. Within a single dyke the proportion of phenocrysts commonly ranges from 0-25% although portions of some dykes contain up to nearly 50% phenocrysts (e.g. A405/E9S). The different degrees of recrystallization during metamorphism and the development of schistosity in some rocks has resulted in differing textures and fabrics. On the whole, the smaller dykes seem to have finer average grainsizes but variable recrystallization and grain growth has commonly altered the primary differences.

2.8.2 Textures

Dyke rocks with common relict plagioclase phenocrysts are lighter in colour, phenocrysts being clearly visible in hand specimen. These rocks largely retain their igneous fabric usually being the least recrystallized of the metadolerites; a schistosity is usually only weakly developed or absent altogether (Plate 45(b)).

Primary compositional differences between the phenocrysts and groundmass feldspars are still evident. These differences are obvious in weathered rocks where the phenocrysts have been preferentially altered to sericite or clay minerals (kaolinite?) whilst matrix feldspars remain relatively unaltered (Plate 45(d)), implying the relict phenocrysts are more calcic¹. Furthermore, some cores of phenocrysts appear to be more altered and hence more anorthitic, as is commonly the case in igneous rocks. The groundmass feldspars in some less recrystallized rocks are also commonly zoned in this way, as seen from their selective alteration. Unweathered inclusion-free plagioclase rims which occur on some phenocrysts (e.g. A405/A12,A14) may be overgrowths formed during metamorphism.

In the least recrystallized metadolerites, the groundmass feldspars still retain an elongate, subhedral to euhedral form and generally exhibit albite twinning. Together with decussate subhedral hornblendes they form a completely igneous texture with a nearly isotropic fabric (Plate 45(b)). The plagioclase is commonly coarser (av. 0.1 mm with crystals commonly to 0.2 mm) than in more recrystallized rocks. Hornblende (0.025-0.4 mm typically) is

¹Electron probe analysis showed that compositions of the relict phenocrysts are around An_{80-90} .

usually coarser than plagioclase but crystals are short or stumpy. The relict xenoblastic feldspars (0.6-5.5 mm) have largely retained their original subrounded forms (Plate 45(c,d)) and contain partly rounded plagioclase inclusions (to 0.5 mm) which can be seen in the less weathered rocks. These large inclusions have a different orientation to the host crystals providing more definite evidence of their igneous origin, and indicating that the hosts were probably present in the magma prior to intrusion. Carlsbad twinning is common and is usually combined with albite twinning, and occasionally pericline twinning also.

Rocks with a very low proportion of relict phenocrysts are richer in amphibole and have a more uniform grain size. These have generally undergone extensive recrystallization and exhibit a planar metamorphic fabric. Grain sizes vary considerably between individual dykes and within the dykes. While these phenocryst-deficient rocks constitute the larger proportion of the smaller dykes and often occur at the margins of the large dykes, it is uncertain whether or not they represent chilled zones as they are found also near the centres of many larger dykes where the grain size of the groundmass is similar in some cases, in both phenocryst-rich and phenocryst-deficient zones. Possibly these zones of differing relict phenocryst content are the result of a physical separation of the phenocrysts from the mass of liquid during emplacement. Alternatively, variable recrystallization may have been responsible for the differing contents of relict phenocrysts, these possibly having been obliterated in the more recrystallized zones. This interpretation is not feasible in all cases, however, as fine-grained phenocryst-deficient rocks with little evidence of a planar or metamorphic fabric have been observed. There are, in rare cases however, a few relict plagioclase phenocrysts in recrystallized rocks exhibiting a well developed planar fabric (e.g. A405/E7; Plate 45 (d)).

The planar fabric in the recrystallized rocks consists of aligned

hornblende crystals which define the same schistosity (S_2) developed in the enclosing metasediments. Plagioclase, however, is equidimensional and interlocking. In contrast to the phenocryst-rich rocks, it is rarely twinned; average grainsizes are commonly around 0.05-0.08 mm. The hornblende is much coarser, commonly up to 1 mm and occasionally to 2 mm in length; crystals are generally subidioblastic and very elongate, intersecting the finer, earlier metamorphic hornblende and plagioclase (Plates 45(c), 46(a)). These later hornblendes can be seen to partly trend around any relict plagioclase phenocrysts present (e.g. A405/MD1,E7(1); Plate 45(d)).

The hornblendes form a lineation in S_2 and sections parallel to this reveal a well developed planar fabric whereas sections perpendicular to this lineation show a more random distribution of stumpy crystals (e.g. compare A405/E7(2) with A405/E7(1)).

There is a suggestion of an earlier schistosity (S_1 ?) in some rocks (e.g. A405/MD1,E9,E9B) which appears to be truncated by the very elongate hornblendes which define S_2 (Plate 45(c)). Therefore it seems probable that the time of intrusion of the dykes was pre- S_2 and possibly early syn- S_1 .

2.8.3 Minor Constituents

Coarse xenoblastic pale yellow epidote (to 2%, 0.25-1 mm) and minor clinozoisite of similar grainsize occur in some rocks, usually associated with feldspar phenocrysts. Rare quartz occurs in some rocks (e.g. A405/A12) as irregularly distributed coarse xenoblastic crystals (to 0.25 mm), possibly the product of the breakdown of relict pyroxene to amphibole during metamorphism. Occasionally, however, quartz fills embayments in groups of plagioclase phenocrysts which might suggest an origin (of some quartz) as a late-stage crystallization from the igneous melt.

Fine scapolite (less than 0.25 mm) occurs in minor amounts in some rocks (e.g. A405/H14) as ragged xenoblastic crystals. It is abundant (12%) in one particular rock (A405/A11) which is extensively recrystallized, consisting of a near granoblastic intergrowth of xenoblastic interlocking plagioclase

clase, hornblende and scapolite. The abundance of scapolite might be attributed to contamination during emplacement. Plagioclase in this rock consists of (i) clear grains, largely equidimensional and occasionally twinned, averaging 0.17 mm and generally with straight boundaries, and (ii) contrasting completely altered xenoblastic to idioblastic, often elongate crystals which are coarser and form about 2/3 of the total feldspar. Some may be relict pheocrysts. Whether sericite alone or whether some very fine scapolite also replaced this feldspar could not be determined. Alteration is concentrated along cleavage planes. Contrasting degree of alteration of the two plagioclase types is probably the result of relict compositional differences as discussed above. Coarse xenoblastic epidote is present throughout the rock (5%), occurring as single crystals (to 1 mm) and aggregates (to 1.5 mm) which appear to transect the hornblende and plagioclase crystals. Rare inclusions of clear plagioclase occur in some crystals, while inclusions of hornblende are more common. There is some indication that epidote may be replacing hornblende, mutual boundaries being ragged, with epidote showing a tendency to occur in those portions of the rock richest in hornblende.

2.8.4 Comparison with the Metadolerite dykes of the Woodside Area

Similar amphibolite dykes which occur to the north in the Woodside area have been studied by Pain (1968) who has observed that the dykes tend to follow the prominent schistosity developed through the area. The schistosity developed in the dykes, defined by aligned hornblendes parallels this regional schistosity and presumably formed at the same time (Pain, 1968). Hence the dykes were intruded either pre- or syn- schistosity. Pain (1968) has suggested that the dykes are related to a single macroscopic synclinal structure dominating the area. The axial plane of this structure is presumed by Fleming (1971) to extend from the area just west of Mt. Charles, passing just north of Murdock Hill, trending SSE through Brukinga then SE to the Dawesley-Kanmantoo area where Fleming (1971) has classified it as an "F₃" structure. As mentioned in Section I2.4. however, mapping has shown that two large syn-

clinal structures occur. The westernmost structure has its axial plane passing from Mt. Charles to Murdock Hill, with parasitic folds indicating shallow plunges to 160° and a well developed schistosity parallel to the axial plane. This syncline is truncated to the east by the Nairne Fault.

The eastern structure, in Kanmantoo Group strata, is defined by the "Nairne Pyritic horizon" which forms a closure just north of Brukunga. This structure extends south-east to the Dawesley-Kanmantoo area and is presumed to be an " F_3 " structure (after Fleming, 1971). A non-penetrative planar surface (where developed) associated with " F_3 " folds in schists is interpreted as a crenulation cleavage by Fleming (1971). The planar surface with which the dykes are associated, however, is a schistosity which is uniformly penetrative through the rock. This schistosity strikes at about 350° , with a moderate to steep easterly dip throughout the area and is the planar feature " S_1 ", axial plane to Fleming's " F_1 " folding (denoted F_2 in this study in the Nairne-Mt. Barker Creek area). It is concluded that the dykes are not related to a single macroscopic structure (" F_3 " of Fleming) as suggested by Pain (1968) but that they have probably been emplaced synchronously with the regional schistosity as the dyke swarm is slightly discordant with bedding but follow " S_1 " on the large scale (Pain, 1968).

Chemical analyses by Pain (1968) on the dyke rocks have shown that the parent magma was tholeiitic, with Al_2O_3 around 12-15%. Nairne-Mt. Barker Creek dykes formed from a higher Al tholeiitic magma (A405/E9S, Table H). Yoder and Tilley (1962, Fig. 27) have found that at 5 kb water pressure a magma of this composition at $940^{\circ}C$ is composed of only amphibole + magnetite in equilibrium with the liquid and gas phases. Pyroxene and olivine have been consumed. With falling temperature further amphibole crystallizes with the first precipitation of sphene at $890^{\circ}C$ and plagioclase at $825^{\circ}C$. These temperatures are well above the highest reached during metamorphism (see section 3.1). These values are similar for a wide range of water pressures. At the time of intrusion therefore, the magma may have contained only amphibole, sphene and plagioclase (including the large phenocrysts) in equili-

brium with the melt. No relict pyroxene has been found in the dyke rocks in the Nairne-Mt. Barker Creek area. Some of the larger hornblendes present in the least recrystallized phenocryst-rich rocks might thus be of igneous origin but this must remain uncertain.

Accessories in the metadolerites are:

Biotite (0-1%) is subidioblastic to xenoblastic, 0.02-0.6 mm in grainsize. It is pleochroic red-brown - pale-brown.

Sphene (to 3%) is subidioblastic to idioblastic, 0.0025-0.05 mm in size commonly; rarely to 0.4 mm. It is probably secondary either after ilmenite or a product of the replacement of relict augite by hornblende.

Chlorite occurs in traces; it is very fine.

Opaques (<1%) probably consists of mainly fine magnetite and ilmenite.

No wall rock alteration was observed although thin 1 mm veins of plagioclase with minor idioblastic hornblende were found in an andalusite schist adjacent to one dyke (A405/MD5, Plate 46(b)).

A magnetic survey carried out by the author over some of these dykes using a fluxgate magnetometer revealed their high magnetic susceptibility. The results of this survey are in Appendix V.

2.8.5 Conclusions

Metadolerite dykes in the Nairne-Mt. Barker Creek area are oriented along the bedding and regional schistosity (which are sub-parallel). They are locally discordant, however. Textures of the dyke rocks suggest that they were probably emplaced prior to the F_2 phase of deformation and the development of the associated regional schistosity S_2 ; some emplacement may also have occurred early syn- F_2 . Similar dykes in the Woodside area described by Pain (1968) were probably emplaced during the early syn- F_2 period rather than during the later " F_3 " deformation¹ of Fleming (1971) as suggested by Pain (op.cit.).

¹The F_2 phase of deformation in this study is equivalent to the F_1 phase of Fleming (1971). The correlation of later deformations is shown in Table 0.

Metadolerite dykes on Dudley Peninsula (Kangaroo Island) and Fleurieu Peninsula, however, were emplaced post-"F₁" (F₁ of Fleming, 1971) and are discordant with the bedding (Milnes et al. 1977). This suggests at least two periods of dolerite dyke emplacement in the Mount Lofty Ranges.

2.9 Pegmatites

Major pegmatites in the area were mapped earlier by Sprigg and Wilson (Echunga 1:63,360 sheet, 1954). These pegmatites are very coarse-grained and are common in the vicinity of Nairne, occurring in both Sturt and Marino Group metasediments. Most pegmatites are sub-parallel to bedding on the macroscopic scale but are discordant on close examination. Thicknesses range from a few mm to 1 m. Thin pegmatites are commonly folded and recrystallized syn-S₂ (e.g. A405/E10B) and hence formed either pre-S₂ or early syn-S₂.

Plagioclase is the major constituent of the rocks, usually having well developed albite twinning and some pericline twinning (e.g. A405/BC72). Some plagioclases are perthitic. Crystals commonly range from 1-4 mm, with crystals up to 2.5 cm in some larger pegmatites. Xenoblastic muscovite and quartz are present in highly variable quantities; in some pegmatites muscovite constitutes over 15% of the rock. Biotite is present only in very minor amounts and appears to have partly segregated from plagioclase into irregular veins in which subidioblastic biotites have recrystallized and largely aligned in S₂.

3. TYPE AND CONDITIONS OF METAMORPHISM

3.1 P-T Estimate

Mineral assemblages and textures of the metashales in the area provide sufficient information concerning the relative stabilities of critical minerals to approximately determine the P-T conditions which prevailed at the peak of metamorphism. This seems to have occurred at some time during the F₂ to F₃ phases of folding. Observations pertinent to the determination of P-T conditions are:

(i) The direct replacement of some andalusite by prismatic crystals of sillimanite is not uncommon in rocks containing fibrolite.

(ii) Fibrolite is present in at least trace amounts in all rocks containing andalusite and occasionally fibrolite needles pass directly into coarse sillimanite crystals.

(iii) Andalusite is partly replaced in most rocks and textures indicate it is transformed to fibrolite.

(iv) The two forms of sillimanite, fibrolite and the coarse prismatic crystals, may have different stability fields (Zen, 1969; Beger et al. 1970). There is also evidence to the contrary, however (Cameron and Ashworth, 1972).

(v) Staurolite seems to be stable in most rocks; there is uncertainty in some cases.

(vi) Muscovite + quartz is a stable association.

(vii) Kyanite is absent but occurs sporadically within 3 km of the area in regionally metamorphosed rocks (Skinner, 1958; George, 1967).

Observations (i) - (iv) suggest the P-T conditions during the peak of metamorphism were within a field along or just on the low temperature side of the curve marking the boundary between the andalusite and sillimanite stability fields. Observations (v) and (vi) further limit the P-T field as lying between the experimentally determined staurolite-producing reactions and the reactions for the breakdown of staurolite and muscovite (Fig. 9). From (vii), the P-T field can be further narrowed. Thus it would seem that P-T conditions must have been close to the Al_2SiO_5 triple point and near the andalusite-sillimanite phase boundary.

The results of various workers show considerable variation in the P-T co-ordinates of the triple point and in the position of the andalusite-sillimanite phase boundary. The data of Althaus (1967) and Richardson et al. (1969) are compatible with the observations in the Nairne-Mt. Barker Creek area since these triple point estimates fall between the staurolite-producing

curves and the curves marking the breakdown of staurolite and muscovite (Fig. 9)¹. The Richardson et al. (1969) triple point² is situated around 622°C, 5.5 kb whilst that of Althaus (1967) is at 600°C, 6.5 kb and that of Newton (1966) at around 520°C, 4 kb. The range in possible P-T values is therefore considerable as values depend on which triple point is chosen. With the phase diagrams of Newton (1966) and Holdaway (1971) (triple point at 501°C, 3.76 kb similar to Newton (1966)) the "standard" staurolite-producing curves fall on the high-temperature side of the triple points (Fig. 9). The choice of which staurolite-producing curve is difficult, however, because (a) the origin of staurolite is unknown and (b) the curves showing the formation of staurolite from chloritoid or chlorite assume $P_{H_2O} - P_{TOTAL}$. If P_{H_2O} were considerably less than P_{TOTAL} , the equilibrium curves may shift to lower temperatures (as suggested by Holdaway (1971) for the reaction Fe-chloritoid + sillimanite = Fe-staurolite + quartz + H₂O; also see Hoschek, 1969, Fig. 9). Hence the phase diagrams of Newton (1966) and Holdaway (1971) could also be considered.

Studies by Scott (1976) on the sphalerite geobarometer applied to the nearby Brukungu sulphide ore deposit suggest pressures of about 4.4 kb which are not incompatible with Holdaway's (1971) phase diagram. Furthermore, estimates of temperature based on the garnet-biotite geothermometer (see section IID) indicate temperatures considerably lower than those deduced using the Richardson et al. (1969) or Althaus (1967) triple points, but are in closer agreement with Holdaway's data. Using the latter, the approximate P-T range for the Nairne-Mt. Barker Creek area is 3.5-3.75 kb, 500-550°C.

¹For this reason Fleming (1971) used the data of Richardson et al. (1969) in preference to that of Newton (1966) in the P-T estimates for the Dawesley-Kanmantoo area, eastern Mt. Lofty Ranges.

²The sillimanite used by Richardson et al. (1969) contained fibrolite which Holdaway (1971, p.101) has shown can raise the experimental andalusite-sillimanite phase boundary by 200°C.

3.2 Cordierite

In the Mount Lofty Ranges, cordierite occurs only in rocks of the highest metamorphic grades, occurring just west of the Sillimanite Zone, where it replaces andalusite and staurolite, and coexists stably with sillimanite in the Sillimanite Zone (Fleming, 1971). Experimental estimates of the stability fields of cordierite and the Al_2SiO_5 diagrams of Richardson et al. (1969) and Holdaway (1971) are shown in Fig. 10 where the proposed P-T field for metamorphism in the Nairne-Mt. Barker Creek area is indicated relative to these two triple point estimates.

Experimental studies on the stability field of Mg-cordierite (Schreyer and Yoder, 1964; Hess 1969; Seifert and Schreyer, 1970; Green and Vernon, 1974) summarized in Fig. 10, show that under hydrous conditions pure Mg-cordierite would be stable in the P-T field estimated for the Nairne-Mt. Barker Creek area and in fact for the whole Andalusite-Staurolite Zone. Mg-cordierite, however, represents the maximum stability of natural cordierite and its formation is strongly dependent on the bulk compositions of the rocks (Schreyer and Yoder, 1964; Richardson, 1968; Hess, 1969; Seifert and Schreyer, 1970; Hensen and Green, 1971, 1973). The complete solid solution series of cordierites is considered to be stable only at very low pressures and high temperatures (Chinner, 1962; Richardson, 1968). Furthermore, the work of Schreyer and Seifert (1969) indicates that the upper stability range of Mg-cordierite is greatly reduced in muscovite-bearing rocks. This range, when superimposed on the phase diagram for Al_2SiO_5 polymorphs after Richardson et al. (1969) (Fig. 10) suggests that Mg-rich cordierite should be stable in the Nairne-Mt. Barker Creek area in rocks with sufficiently high Mg/Fe ratios. The phase diagram of Holdaway (1971), however, indicates that temperatures were too low and pressures too high for the formation of Mg-cordierite; the slope of the stability curve shows that temperature had the greater control on cordierite stability. This is consistent with field evidence (Fleming, 1971) and consequently the phase diagram of Holdaway is considered as the more appropriate.

3.3 Comparisons with other Metamorphic Belts

Within the temperature limits of the Andalusite-Staurolite Zone, assemblages in metapelites can be compared with those formed in a number of areas. Closest agreement is found with rocks belonging to low-pressure metamorphic series which are merging into the intermediate pressure types (Miyashiro, 1973, Table 7-A). Temperatures in the Nairne-Mt. Barker Creek area were insufficiently high for the formation of cordierite and the breakdown of staurolite or muscovite. Comparison with a few areas will be made in Table M but no exact duplication of an area occurs, since regional metamorphism shows great diversity, depending on factors such as P_{H_2O} , P_{O_2} , P_{CO_2} and the chemical composition of sediments in addition to P_{TOTAL} and T. In addition, geothermal gradients will vary and no two areas can be expected to show exactly the same sequence of progressive mineral changes.

4. METAMORPHIC HISTORY

The time relationships between crystal growth and folding are summarized below:

1. Syntectonic with the first phase of deformation F_1 and accompanying planar structure S_1

Quartz, plagioclase, opaque minerals and biotite formed a matrix. Some andalusite and staurolite possibly crystallized during this period. S_1 is manifested as fine aligned biotites, opaques and quartz inclusion trails in andalusite if it formed at this time. Hornblende, epidote and possibly diopside crystallized in calc-silicates.

2. Post- F_1 and Pre-second phase of deformation F_2 with related penetrative schistosity S_2

Quartz, plagioclase and biotite continued to crystallize and quartz-biotite segregations began to develop. Poikiloblastic andalusite and staurolite with quartz and opaque mineral inclusions crystallized, exhibiting the inherited S_1 structure through their inclusion patterns. Andalusites formed along bedding S_0 reflecting differences in bulk composition of the sedimentary layers. Fine hornblende, epidote and diopside crystallized in calc-silicates.

3. Syntectonic with the second phase F_2 and schistosity S_2

Quartz, plagioclase and aligned biotite, muscovite and opaque minerals crystallized forming the matrix. Quartz-biotite segregations developed further, with new partial segregation of layers rich in quartz. Some coarse muscovites possibly replaced andalusite at this time. Andalusite with sigmoidal inclusion trails continuous with S_2 , and possibly staurolite with quartz inclusions of similar size to the matrix crystallized in this period. In addition, almandine with sigmoidal inclusion trails formed. Fibrolite and possibly some coarse prisms of sillimanite probably crystallized late syn- S_2 . Epidote, diopside, scapolite and hornblende (which is aligned in S_2) recrystallized in calc-silicates; hornblende recrystallized and aligned in S_2 in metadolerites.

4. Post- F_2 and Pre-third phase of deformation F_3 with S_3 as axial plane to micro-crenulations.

Some staurolite and idioblastic almandine with inclusion trails continuous with S_2 probably formed in this period. Coarse muscovite and biotite replaced andalusite with the formation of new biotite and quartz as products of reactions producing fibrolite indirectly from andalusite. Fibrolite formed as disoriented sprays and some mimicing S_2 . Prismatic crystals of sillimanite probably directly replaced andalusite in this period. Muscovite and rare biotite formed with other post- S_2 minerals such as coarse idioblastic to ragged xenoblastic opaque minerals (mainly magnetite); these transect the S_2 schistosity. Scapolite, hornblende and calcite recrystallized in calc-silicates, and possibly some hornblende recrystallized in the metadolerite dykes.

5. Syntectonic with the third phase of deformation F_3 which produced microcrenulations of S_2 to which S_3 is the axial plane.

Biotites formed along the S_2 - S_3 intersection and some muscovites formed in S_3 . Common fibrolite crystallized, needles passing into coarser crystals of sillimanite which are aligned in S_3 . Some coarse prismatic sillimanite possibly directly replaced andalusite during this period. Some muscovite and biotite probably replaced andalusite, resulting in the indirect transition to fibrolite.

6. Post- F_3

Rare coarse muscovites apparently transecting F_3 crenulations possibly crystallized post- F_3 . Some muscovite and biotite may have replaced andalusite at this time. Later, with diminishing grade, chlorite replaced biotite and minor hornblende.

C: FOLDING AND METAMORPHISM -
ITS RELATION TO THE MOUNT LOFTY RANGES IN GENERAL

The general structural maps of the Mount Lofty Ranges by Fleming (1971, Figs. 9,11, reproduced herein as Figs. A,B, Appendix II) suggest that the major macroscopic structure prevailing in the Nairne-Mt. Barker Creek area is either predominantly "F₁" of Fleming and Offler (1968) and Fleming (1971), possibly modified by "F₃" folding developed as the Strathalbyn Anticline to the south, and trending north to the Meadows-Mt. Kitchener Fault. Alternatively, from their map it could be concluded that the area is situated on the east limb of this anticline which plunges steeply to the south, with "F₃" overprinting "F₁" and possibly "F₂" structures. The latter seems improbable due to the parallelism of regional schistosity¹-bedding intersections with the observed mesoscopic fold axes which plunge at very shallow angles to SSE. These axes are also in agreement with the approximate position of the determined β -axis from the π_{S_0} diagram (Fig. 5).

The deformations and associated planar structures observed in the Nairne-Mt. Barker Creek area can be related to those devised in the general synthesis of folding in the Mount Lofty Ranges by Fleming (1971); these relations are summarized in Table 0. The style of F₂ and features of its axial plane schistosity S₂ in the Nairne-Mt. Barker Creek area are very similar to those of Fleming's "F₁" and "S₁" structures. Fleming's "S₂" and "S₃" are crenulation schistositities, and the axis to microcrenulations in the Nairne-Mt. Barker Creek area, denoted F₃ herein, may be correlated with "F₂" of Fleming (1971) which has an ESE or SE trend in the vicinity of this area (Fig. B, Appendix II).

It appears that high-grade metamorphism and deformation F₁ with associated schistosity S₁ occurred prior to Fleming's "F₁" deformation. This

¹The regional schistosity is denoted S₂ in this study.

is supported by the following observations in a number of areas in the Mount Lofty Ranges:

(a) Poole (1969) noticed non-correspondence between a mineral streaking with associated fine crenulation on the " S_1 " schistosity surface and " F_1 " fold axes. This lineation is deformed and is presumed to be earlier than " F_1 ".

(b) Fleming (1971) has suggested the overprinting by " F_1 " on an already folded and therefore inhomogeneous surface to explain the variation in orientation of the " F_1 " axes.

(c) Daily and Milnes (1973) have recognized a pre-tectonic (pre-" F_1 ") bedding plane schistosity with an accompanying mineral streaking (designated L_1 ' by Daily and Milnes) in the Middleton area.

(d) In the South Hill area (near Kanmantoo) Spry (1976)¹ has noted the presence of an internal fabric in andalusite porphyroblasts which is discordant with the external schistosity " S_1 ", suggesting that the andalusites possibly crystallized pre-" S_1 ", preserving a pre-" S_1 " schistosity. Alternatively, a rotation of syn-" S_1 " andalusites with later deformation of " S_1 " about them was suggested, the latter interpretation being favoured.

Pre-" F_1 " metamorphism has been recognized in some areas, with the crystallization of "pre-tectonic" or "pre- F_1 " high-grade minerals:

(a) In the Strathalbyn area, Offler (1963) has observed "pre- F_1 " andalusite and augen containing disoriented micas in " S_1 ".

(b) In a number of areas Fleming and Offler (1968) and Fleming (1971) have recognized some andalusite, staurolite and cordierite as having crystallized "pre- F_1 ".

(c) South of Kanmantoo, Poole (1969) recognized "pre- F_1 " andalusites.

(d) On the south coast of Fleurieu Peninsula, Daily and Milnes (1973) have observed "pre- F_1 " cordierite and relict augen in " S_1 " consisting of

¹The work of Spry (1976) was submitted as a thesis for the degree of B.Sc (Hons) at the University of Adelaide approximately one year after the first draft of the present thesis was prepared in which pre-" F_1 " deformation and metamorphism was proposed.

quartz, plagioclase, mica and opaque minerals with random internal mica fabric.

It seems that the remnant in the Nairne-Mt. Barker Creek area of a clearly recognizable fold phase with accompanying metamorphism which are earlier than generally recognized in the Mt. Lofty Ranges is probably due to the lack of strong overprinting following the F_2 fold phase. F_2 and its associated schistosity S_2 are correlated with the major deformational phase " F_1 " and associated penetrative schistosity " S_1 " of Fleming and Offler (1968), Fleming (1971), Poole (1969), Daily and Milnes (1973) and Marlow (1975). Whereas Fleming (1971) has distinguished two later tectonic phases (" F_2 ", " F_3 ") with associated crenulations, Marlow (1975) believes the two crenulation cleavages associated with these crenulations to have formed synchronously in an area just south of Macclesfield (the Macclesfield syncline - Strathalbyn anticline structure). The E-W crenulation in that area recognized by Offler (1963) and Marlow (1975) can possibly be correlated with F_3 crenulations herein in the Nairne-Mt. Barker Creek area where the axial plane of these crenulations is also sub-vertical and E-W. The N-S crenulation with near-vertical axial planes, also related to the " F_2 " phase of Marlow is the axial plane structure to the Macclesfield syncline and Strathalbyn anticline (Marlow, 1975). Although this crenulation cleavage did not develop in the Nairne-Mt. Barker Creek area, there is evidence of crenulations with axial planes approaching this orientation (localities 198, BC63, where rare crenulations in S_2 plunge at shallow angles to the SE-SSE). Also crenulations in S_2 with moderate plunges to NE and NNE are found and are believed to be related to rare small mesoscopic folds tentatively denoted herein as F_4 (section IIA); these have moderate plunges to the NNE. These crenulations have a very restricted development and time relations are uncertain as is their relation to the well developed N-S crenulation cleavage of the Macclesfield area.

The existence of a pre-"F₁" deformation has interesting implications with regard to the time of emplacement of the Encounter Bay Granites. These granites intrude the youngest strata of the Kanmantoo Group in the Encounter Bay region and contain metasediment xenoliths of the enclosing lithologies (Milnes, Compston and Daily, 1977). Schistose granite sheets, both concordant and discordant with the bedding, occur near the margin of the pluton. The schistosity in these metamorphosed granite sheets parallels the schistosity "S₁" in the enclosing strata and has been interpreted as the same structure (Daily and Milnes, 1973; Milnes et al. 1977). Andalusite occurs in the regionally metamorphosed rocks and crystallized late syn-"F₁" and post-"F₁" (Daily and Milnes, 1973). Staurolite is absent, P-T conditions being inadequate for its formation (Milnes et al. op. cit.). Cordierite formed in proximity to the granite at Rosetta Head on the south coast of Fleurieu Peninsula. This mineral crystallized pre-"F₁" to early syn-"F₁" at the peak of metamorphism (Milnes et al. op. cit.). These authors concluded that the granites were emplaced in probably weakly deformed and metamorphosed strata (Daily in Twidale et al. 1976; Milnes et al. op. cit.), in the early stages of the first phase of deformation ("F₁"). During this time, the grade of metamorphism reached its peak. The major phase of the "F₁" deformation followed and in this respect the granites are pre-tectonic (Daily and Milnes, 1973; Milnes et al. op. cit.).

Although most metasediment xenoliths do not possess a tectonic fabric, some are found to contain a relict schistosity (Milnes et al. 1977) which as has been suggested may indicate the existence of a schistosity, possibly on a local scale, that is older than the "S₁" schistosity induced by the major phase of the "F₁" deformation. Evidence for this initial schistosity has also been noted in the Middleton area (Daily and Milnes, 1973, p.224) where three schistositities are evident. In addition there is clear evidence that the granites intruded strata that were already folded (Milnes et al. 1977).

Work in the Nairne-Mt. Barker Creek area now supports the earlier contention of Daily and Milnes (1973) that prior to the main phase of the "F₁" deformation there was a tectonic event, herein denoted F₁ (see Table 0), which produced an accompanying planar structure herein denoted S₁. It is suggested herein that F₁ should be regarded as distinct from "F₁" (see Table 0), and that the granites were intruded during the time span between these deformations rather than during the opening stages of the continuous "F₁" deformation envisaged by Milnes et al. (1977, Fig. 8). The weakly deformed strata which existed prior to granite emplacement, the presence of schistose xenoliths and the existence of pre-granite folds can be reconciled with the existence of the pre-"F₁" deformation. That only a few xenoliths are schistose can be explained if the pre-"F₁" deformation was inhomogeneous, only narrow zones of strata being deformed. Alternatively, this weakly developed schistose fabric may have been regional in extent, but may have been virtually obliterated by the main tectonic event, namely "F₁".

D: ROCK AND MINERAL ANALYSES1. ANALYTICAL TECHNIQUES

Rocks were crushed to <120-180 mesh size. Losses (H_2O , F_2 , CO_2 etc.) were determined by ignition of samples in silicon crucibles in an electric furnace at $1,000^{\circ}C$ for at least 6 hours. Ignited samples were then analyzed by X-ray fluorescence. Na_2O was measured, and the measurement of K_2O duplicated on an atomic absorption spectrometer. K_2O values determined by both methods were in close agreement.

Mineral compositions were determined by electron probe analysis on polished thin sections. A "Jeol" electron probe was used by the writer at the Department of Earth Sciences at Melbourne University. This probe was operated at 15KV with a 15μ X-ray beam directed onto the sample. Kaersutite was used as the standard for the nine major elements analyzed by the probe's computer program in which the spectrometers scan for a total of 12 elements Si, Ti, Al, Fe, Mn, Mg, Ca, Na, K, Cr, Ni, Ba.

Biotites were separated using heavy liquids and the Frantz magnetic separator. These were refined until at least 98% pure.

The Fe^{2+} and Fe^{3+} contents of a number of rocks and of those biotites separated were determined by a modification of Wilson's Method (after Whipple, 1974). Dissolution of a weighed sample in HF at room temperature in the presence of a known excess of vanadate solution (which oxidizes all Fe^{2+} to Fe^{3+}) is followed by the addition of excess Fe^{2+} . This solution is then titrated against a dichromate solution. The weight % FeO was then calculated using the relation

$$\frac{(\text{titration volume} - \text{blank}) \times 2.8738}{\text{weight of sample}} \times 100\%$$

Water contents of a number of rocks including those with very high ignition losses were determined by heating a weighed sample plus flux in a furnace to release the H_2O which was passed into a solution. The weight of water in this solution was then determined by the Karl Fischer titration

method (Turek et al. 1976).

2. META-SHALES, META-SILTSTONES AND META-SANDSTONES

2.1 Rock Chemistry

The compositions of rocks analyzed are given in Tables A and B. Differences between the compositions of these rock types are seen in their contents of SiO_2 , Al_2O_3 and total Fe (as Fe_2O_3). Metasandstones have the highest SiO_2 and Na_2O contents whilst metashales have the least. Metashales have the highest Al_2O_3 , total Fe and MgO contents, metasandstones being poorest in these elements. Metasiltstones analyzed have values intermediate between these rock types. The compositions of metasandstones and metasiltstones are comparable with those of average greywackes (Pettijohn, 1975) although the metasandstones are slightly poorer in Al_2O_3 and CaO and richer in SiO_2 . Compositions of the metashales are similar to those of average shales (Shaw, 1956; Pettijohn, 1975). The metashales analyzed here are peraluminous schists, and rocks have higher Al_2O_3 , total Fe, MgO and slightly lower CaO contents than average shales.

The oxidation state of the rocks is expressed as the "oxidation ratio" defined by Chinner (1960) as molecular $(\text{Fe}_2\text{O}_3 \times 100) / (\text{Fe}_2\text{O}_3 + \text{FeO})$. Chinner (1960) and others have found close correlations between rock oxidation ratios and compositions of ferromagnesian minerals. Examination of Figure 16 shows that there is no relation between rock oxidation ratio and rock $\text{Mg}/\text{Mg}+\text{Fe}_{\text{TOT}}$ in Nairne-Mt. Barker Creek rocks. There is a suggestion, however, of a correlation between rock oxidation ratio and rock $\text{Mg}/\text{Mg}+\text{Fe}^{2+}$, which is in contrast to the complete absence of a correlation found by Fleming (1971). The use of total Fe partly masks the effect of rock oxidation state on $\text{Mg}/\text{Mg}+\text{Fe}$ ratio.

Rock oxidation state appears to have had little control on mineral $\text{Mg}/\text{Fe}_{\text{TOT}}$ ratios, as shown in the plot of mineral $\text{Mg}/\text{Mg}+\text{Fe}_{\text{TOT}}$ against rock oxidation ratio (Fig. 15). The weak correlation between this ratio in biotite and rock oxidation ratio is presumably due to the greater tendency

for formation of opaque minerals (e.g. magnetite) rather than biotite with increasing rock oxidation state (Dr. R.L. Oliver, pers. comm.). With the formation of opaques, less Fe is available to biotite, consequently $Mg/Mg+Fe_{TOT}$ increases with increasing rock oxidation state. The low range in $Mg/Mg+Fe_{TOT}$ values in staurolite and garnet may preclude any relation becoming apparent. The use of Fe^{2+} in plotting $Mg/Mg+Fe$ ratios (estimated for three biotites) results in a closer correlation between this and rock oxidation ratio (Fig. 15). Fleming (1971), by contrast, found no correlation between rock oxidation state and compositions of the ferromagnesian minerals.

The oxidation ratios of the rocks all tend to be high when compared with Chinner's (1960) range of 6-75 for Glen Clova gneisses and Fleming's (1971) range of 8-29 for metagreywackes and schists in the Dawesley-Kanmantoo area. In metashales, metasiltstones and metasandstones from the Nairne-Mt. Barker Creek area values range from 48.0 - 66.5 (with one value of 32.4), as shown in Tables A and B, whereas in calc-silicates the range is 31.9 - 60.8 (Table H). These rather high values would suggest high and fairly uniform values of P_{O_2} during metamorphism. The graphite content of metashales is probably very low as its presence in significant concentrations is known to act as a redox buffer and maintain relatively low oxidation states (Miyashiro, 1964; French and Eugester, 1965). As values are high and of low range, subtle relations with other features of rock and mineral compositions would not be readily apparent. No correlation was found between rock oxidation ratio and total Fe or MnO (Figs. 14B and 17B respectively) in contrast to the excellent relation noted by Chinner (1960). Furthermore there is no apparent relation between mineral assemblage and rock oxidation ratios in the metashales. While it was expected that rocks containing garnet would tend to have the lower oxidation states, as almandine would be more stable under the more reducing conditions (Hsu, 1968), no such relationship was found. This discrepancy could be caused by the small range of values and the significant effects of experimental error. The bulk composition of the rocks, however, was probably a major factor in controlling

the crystallization of almandine, the small range in oxidation states (possibly with their variation controlled by a variation in graphite content) being relatively insignificant in affecting its stability.

Ignition losses of these metasediments vary between 0.07% and 2.24% (Tables A,B). This is presumably almost entirely as H₂O (see H₂O analysis on A405/BC27).

2.2 Rock Composition and Mineral Assemblages

Typically rocks containing andalusite (\pm fibrolite) are richest in Al₂O₃. Rock MnO contents in general are low (below 0.27%) but rocks with garnet tend to have the most MnO (0.15-0.27% compared with 0.1-0.13 for other metashales and metasiltsstones). The relation between bulk composition and mineral assemblage can be further examined with the aid of the Thompson AFM projection. This diagram demonstrates the major role that the Mg/Mg+Fe ratio of the rock plays in influencing the ferromagnesian mineral assemblage. Figures 30, 31, and 32 show that chemical equilibrium was attained, rock compositions plotting within the fields defined by the tie-lines of component minerals. A higher biotite Mg/Mg+Fe ratio is accompanied by a slightly higher garnet or staurolite Mg/Mg+Fe value with the result that tie-lines do not intersect even when the different assemblages are plotted on one diagram (Fig. 30).

Figure 33 portrays two 2-phase assemblages. The assemblage Al₂SiO₅ minerals + biotite is presumed to be an equilibrium assemblage as the rock plots almost on the Al₂SiO₅-biotite tie-line. The slight discrepancy could easily be attributed to analytical error. The garnet + biotite assemblage was examined in two rocks (A405/E4B,F10) and shows a large shift of the whole rock composition from the garnet-biotite tie-line. Rock A405/E4B is a metasiltsstone containing abundant garnets in layers near a zone of quartz enrichment and shows the greatest deviation. This displacement of rock compositions from the garnet-biotite tie-lines may partly be explained by the limitations of the projection in neglecting MnO which is a significant com-

ponent in both rocks. Rock A405/E4B contains 0.27% MnO, the garnet phase has around 10% and the biotite has 0.25% MnO. Rock A405/F10 contains only 0.12% MnO however the biotite phase contains 0.54% MnO. The garnet in this rock (which was not analyzed due to its rarity and fine grain size) is presumed to have a high MnO content also, as the value of the distribution coefficient for Mn between garnet and biotite is at least around 50 or over in these rocks (see section 2.4.2). In incorporating Mn with Fe^{2+} in garnet and rock in the AFM plot has virtually no effect on the relation between tie-line and whole rock composition (Fig. 34). Also a correction for magnetite in rock A405/E4B (Fig. 33) produces no significant change. The magnitude of the discrepancy, particularly in rock A405/E4B indicates some degree of disequilibrium, possibly between the garnet-bearing layers and the enclosing rock. That Mg-partitioning between garnet and biotite in A405/E4B is consistent with that between mineral pairs in other rocks, is not in disagreement with this suggestion as both minerals analysed were from the same layer. Although no Al_2SiO_5 minerals were found in these rocks, it is possible that traces of very fine fibrolite occur disseminated in the biotite-rich layers (particularly A405/E4B) in which case the anomalous situation would be greatly improved and the possible degree of disequilibrium reduced.

The anomalous assemblages: Al_2SiO_5 minerals + almandine + staurolite + biotite (rocks A405/E4E, M24) and Al_2SiO_5 minerals + almandine + biotite (rocks A405/E2A) mentioned earlier are shown in Figures 32 and 31 respectively. Figure 32 shows that while the rocks plot within the field defined by tie-lines from Al_2SiO_5 -biotite-almandine, they fall almost on the Al_2SiO_5 -biotite tie-lines. Examination of Figure 30 shows that these rocks plot in the bulk composition field which produced Al_2SiO_5 minerals + biotite + staurolite assemblages, which suggests that the almandine is an excess phase. This excess phase in the AFM plane has resulted from its high MnO content. From Figure 31 it can be seen that rock A405/E2A plots on the Al_2SiO_5 -biotite tie-line rather than in the Al_2SiO_5 -biotite-almandine field. This is also a consequence of the high MnO content of the garnet phase.

The bulk composition of the rock falls on the Al_2SiO_5 -biotite tie-line and hence was inappropriate to form staurolite whilst Mn-rich almandine was stabilized to accommodate the MnO component of the rock. Oxidation states of the rocks do not appear to have been significant in the formation of these two anomalous assemblages as they vary little between the different assemblages and are not lower in those containing garnet, as might be expected if the oxidation state of the rocks stabilized this phase (Hsu, 1968).

2.3 Mineral Chemistry

2.3.1 Garnet

Garnet analyses are shown in Table C. The garnet is almandine with considerable spessartine and pyrope components, MnO being between 5-10% and MgO between 2.7-3.2%. The MnO content is not directly a function of rock MnO (Fig. 19B), in contrast to the strong correlation between garnet composition and rock composition found by Atherton (1965). Hsu (1968) found that the composition of almandine garnet was dependent on fO_2 , in addition to other factors. The high MnO content of the almandine in the rocks being discussed is thus thought due partly to the P,T conditions (as found by Miyashiro (1953)), and partly to the relatively high oxidizing conditions of the rock. As shown in Table A, rocks with almandine garnet have the highest MnO contents, sufficient to stabilize almandine under high oxidation conditions (c.f. Hsu, 1968, p.79).

There is no correlation between rock oxidation ratio and the presence of almandine. Also, there is no relation evident between rock oxidation ratio and garnet MnO content (Fig. 19A). This contrasts with the good correlation found by Chinner (1960), with MnO in garnet increasing sharply with increasing rock oxidation ratio. The very small range of rock oxidation ratios in garnet-bearing assemblages does not, however, permit a proper examination of this relation as the effects of analytical errors are likely to be significant. Also, the MnO content of the almandine would have some degree of dependence on bulk composition and possibly PH_2O and the effects

of the compositions of other phases as well. Therefore a simple, close relationship between garnet MnO and rock oxidation ratio should not commonly occur (e.g. Fleming, 1971).

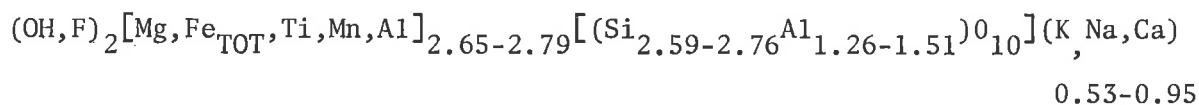
There appears to be some control of garnet $Mg/Mg+Fe_{TOT}$ ratios by the host rock $Mg/Mg+Fe_{TOT}$ ratio (Fig. 25B) though the range of these ratios is small. The position of A405/E4B in this plot is anomalous, though as suggested earlier, this rock may not be completely homogeneous with respect to garnet. In view of the absence of any correlation between rock oxidation ratio and rock $Mg/Mg+Fe_{TOT}$ (which has some control on that ratio in garnet), the absence of a strong relation between rock oxidation ratio and garnet $Mg/Mg+Fe_{TOT}$ ratio as shown in Figure 15 is not unexpected.

Electron microprobe analysis revealed that the compositions of garnet cores differ from their outer rims (Table C)¹. Whether this change is abrupt or gradational was not determined. As zoning is not evident optically, it is probable that the compositional change is gradational. Typically the change from core to rim is strongest in MnO which shows a decrease in that direction. There is also a slight decrease in CaO. MgO and FeO show slight increases from core to rim which is in agreement with the trend commonly observed (e.g. Miyashiro, 1953; Hietanan, 1969; Hsu, 1968). Whether this variation in composition is due entirely to increasing grade of metamorphism during crystallization of the garnet cannot be determined, and the cause of zoning in garnet will not be discussed here.

¹Rim compositions were determined as close to the margin of the garnet as possible, however, accurate analysis of the extreme outer edge or "skin" of the crystals was not possible.

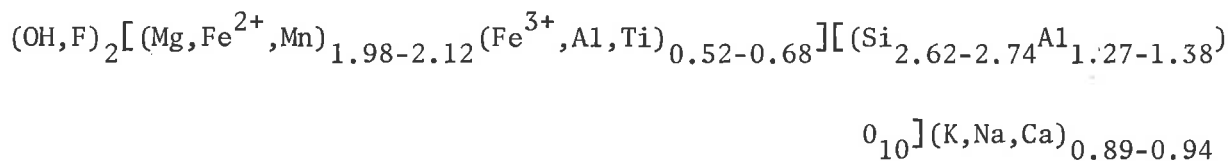
2.3.2 Biotite

Biotite analyses and formulae computed on the basis of 12 anions are shown in Table D. The formulae calculated for biotites in which only total Fe was determined can be expressed as:



These formulae were calculated using $\text{Fe}^{3+}/\text{Fe}^{2+}$ ratios¹ of biotites from similar assemblages and metamorphic grades given in the literature. Most emphasis was placed on the data of Fleming (1971) derived from rocks 10 km to the east of the Nairne-Mt. Barker Creek area.

For those biotites where Fe^{2+} and Fe^{3+} were determined (A405/E4E, E4B, M24), their formulae can be expanded further as:



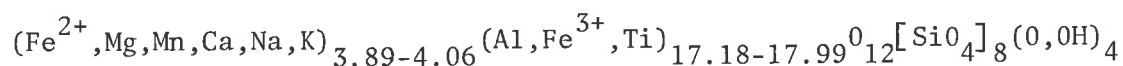
¹As the $\text{Fe}^{3+}/\text{Fe}^{2+}$ ratios were not determined by analysis, the $\text{Fe}^{3+}, \text{Fe}^{2+}$ values were not used in the formula, however these were needed to compute more accurately the total of the proportion of anions in the process of deriving the mineral formula.

There appears to have been some degree of control on biotite composition by the host rock chemistry. The absence of a correlation between biotite MnO content and rock MnO is evident from Figure 20A. Although a weak correlation may exist between biotite and rock $Mg/Mg+Fe_{TOT}$ ratios (Fig. 25A), the narrow range in values is a disadvantage and their relation is uncertain. There appears to be a slightly improved correlation between biotite and rock $Mg/Mg+Fe^{2+}$ ratios (Fig. 25A), however this is a plot of only three rocks (including A405/E4B in which the possibility of some disequilibrium has been suggested earlier) and an improved correlation might occur with other analyses. It is surprising that there is no stronger correlation evident between rock and biotite $Mg/Mg+Fe_{TOT}$ ratios in view of the evidence of equilibrium and the absence of crossed tie-lines in Figs. 30, 31 & 32. It seems that the biotite $Mg/Mg+Fe$ ratio is partly controlled by other factors, such as the composition of coexisting garnet (as shown in Figs. 11B and 12A). Such an influence would produce the scatter shown in Figure 25A. Neglecting rocks containing garnet does not, however, reveal any improved correlation and it is likely that the composition of associated staurolite and more certainly muscovite (e.g. Butler, 1967; Guidotti, 1969) could also affect the composition of coexisting biotite. Furthermore there is some correlation between rock oxidation state and biotite $Mg/Mg+Fe$ ratios, as mentioned earlier (Fig. 15), and Figure 18B suggests rock oxidation ratio has considerable control on that ratio in biotite.

2.3.3 Staurolite

The host rock $Mg/Mg+Fe$ and oxidation ratios appear to have little influence on the staurolite $Mg/Mg+Fe$ ratios (Figs. 25B and 15 respectively). The rather narrow range of $Mg/Mg+Fe$ values (less than 0.03) in these staurolites however, does not permit any correlation that may exist to be apparent.

The formulae for staurolite, computed from the analysis of five staurolites in Table E can be summarized as:



(calculated on the basis of 48 anions). Formulae were calculated using Fe^{3+}/Fe^{2+} ratios of staurolites from similar rocks given in the literature, particularly Deer, Howie and Zussman (1962).

2.3.4 Muscovite

Analyses for muscovite and calculated formulae are given in Table F. Some substitution of Mg, Fe, Mn, Ti for octahedral Al, Na for K and less substitution of Al for Si in tetrahedral sites has altered the composition of muscovite from its idealized formula $K_2Al_6Si_6O_{20}(OH,F)_4$ to that of $(K,Na,Ca)_{1.32-2.01}(Mg,Fe_{TOT},Al,Ti,Mg,Mn)_{3.79-4.49}Si_{6.12-6.71}Al_{1.29-1.88}O_{20}(OH,F)_4$

calculated on the basis of 24 anions.

As the Fe^{2+} , Fe^{3+} contents of muscovite were not determined, a survey of the literature (in particular Deer, Howie and Zussman (1962)) revealed the most probable Fe^{3+}/Fe^{2+} ratios. If these differ slightly from the true ratios, the formulae would be only marginally altered.

The formula computed shows that a small but significant phengite component is present.

Although the $Mg/Mg+Fe_{TOT}$ ratios of biotite and staurolite do not show a significant correlation with rock $Mg/Mg+Fe$, within any host rock, the minerals almandine, biotite, staurolite and muscovite still show the normal trend of increasing Mg/Fe ratio in the order almandine \rightarrow staurolite \rightarrow muscovite \rightarrow biotite (Fig. 26).

2.4 Distribution of Elements between Coexisting Phases

The study of the distribution of elements between coexisting phases at equilibrium utilizes a distribution coefficient K_D . The distribution coefficient with respect to element A in phases α and β is defined as

$$K_{DA}^{\alpha-\beta} = \frac{X_A^\alpha}{1-X_A^\alpha} \cdot \frac{1-X_A^\beta}{X_A^\beta} \quad (\text{Kretz, 1959, 1960})$$

where

α and β have the formulae (A,B)Y and (A,B)Z

where

A, B, Y, Z are chemical species with A-B exchangeable.

The compositions of the two phases are indicated by their molecular ratios X_A^α and X_A^β where $X_A = A/A+B$.

$$\begin{aligned} \text{For ideal mixtures, } K_D &= \exp [\Delta G/RT] \\ &= \text{constant at fixed P, T} \\ &= (A/B)^\alpha / (A/B)^\beta \end{aligned}$$

where ΔG is the change in free energy for the distribution of A between phases α and β i.e. $A(\text{in } \alpha) + B(\text{in } \beta) = B(\text{in } \alpha) + A(\text{in } \beta)$.

Plotting X_A^α against X_A^β produces a characteristic curve (Kretz, 1961, Fig. 6). Towards very low values of X_A^α and X_A^β the slope of this curve should approach a value equal to K_D . A plot of $X_A^\alpha / (1 - X_A^\alpha)$ against $X_A^\beta / (1 - X_A^\beta)$ produces a straight line of slope = K_D .

In the general case, where α and β are not ideal mixtures,

$$K_D = K_f \exp [\Delta G/RT]$$

where K_f is a value dependent on the activity coefficients of the chemical constituents AY, BY, AZ, BZ in phases α and β .

As K_f depends on the concentrations of A and B in α and β , K_D is not constant. A plot of X_A^α against X_A^β produces an irregular curve. A distribution which is based on a regular but not ideal solution model may produce a scatter of points about a smooth curve which should approximate the curve corresponding to the average K_D of the mineral pairs.

If one of the chemical species is present in small amounts in both phases, K_f is constant regardless of whether α and β are ideal mixtures or not. In this case $K_D \approx X_A^\alpha / X_A^\beta$.

For two phases α and β with the formula (A,B,C)Y and (A,B,C)Z, the relation

$$K_D = \frac{X_A^\alpha}{1 - X_A^\alpha} \cdot \frac{1 - X_A^\beta}{X_A^\beta} \quad \text{is still valid.}$$

where $X_A = A/A+B+C$.

Even if the two phases are ideal mixtures with reference to A,B and C, K_D for any one of the chemical species A,B or C will, in general, be dependent on the ratio of the other two species in one or both phases (Kretz, 1961).

2.4.1 The distribution of Mg and Fe between Garnet and Biotite

This distribution is examined by the determination of a distribution coefficient defined as

$$K_D^{G-Bi}_{Mg-Fe} = \frac{X_{Mg}^G}{1-X_{Mg}^G} \cdot \frac{1-X_{Mg}^{Bi}}{X_{Mg}^{Bi}} \quad \text{where} \quad X_{Mg} = \frac{Mg}{Mg+Fe}$$

The K_D 's for garnet-biotite pairs examined in these rocks are given in Table G and the ideal distribution curve, determined for the average $K_D = 0.199$ is shown in Figure 11A. The scatter about this curve is not large and the distribution is regular. The use of atomic ratios of Mg in biotite defined as $X_{Mg}^{Bi} = Mg/Mg+Fe+Mn$ and in garnet as $Mg/Mg+Fe+Mn+Ca$ in the determination of K_D (average = 0.148) does not reduce the scatter about the ideal distribution curve drawn for this K_D value (see Fig. 24A).

The degree of ideality is examined in Figure 12B where $X_{Mg}^G/(1-X_{Mg}^G)$ is plotted against $X_{Mg}^{Bi}/(1-X_{Mg}^{Bi})$. For ideal mixtures the points should fall on a line of slope = $K_D(0.148)$. It can be seen that while the distribution does not approach ideality, the points do fall about a line of this slope but with a considerable scatter.

The value of $K_D^{G-Bi}_{Mg}$ has been found to depend on the composition of garnet, biotite, PH_2O and mineral assemblage in addition to metamorphic grade (Albee, 1965). As K_D is influenced by these variables, its value at any particular grade will vary slightly between different garnet-biotite pairs even if equilibrium has been established. The effect of garnet composition in particular has been examined by Albee (1965) and more recently in greater detail by Sen and Chakraborty (1968). Mole fractions were calculated using Fe^{2+} whilst in this work only garnet total Fe was determined.

Figures 11B and 12A show the relation between garnet Ca/Ca+Mg+Fe and Mn/Mn+Mg+Fe respectively and Mg/Mg+Fe in garnet and biotite. In Figure 11B a relation is evident between garnet Ca/Ca+Mg+Fe ratio and the very narrow range of garnet Mg/Mg+Fe values; however it is such that garnet Mg/Mg+Fe increases (slightly) with increasing Ca content, which is opposite to the relation found by Sen and Chakraborty (1968). Also, the limited range in garnet Ca/Ca+Mg+Fe ratios (compared with those of Sen and Chakraborty) does not allow a proper examination of any relation between garnet Ca content and Mg/Mg+Fe in biotite. A broken line has been drawn which would show a relationship similar to that found by the above workers. In this case the garnet-biotite pair of rock A405/E4B appears anomalous.

With increasing Ca atomic ratio in garnet (Fig. 11B), the increase in garnet Mg/Mg+Fe and the greater rate of increase of that ratio in co-existing biotite seems to have resulted in a weak decrease in K_D (Fig. 27). This is the same relation between garnet Ca ratio and K_D found by Sen and Chakraborty (1968). Decreasing garnet Mg/Mg+Fe with increasing garnet Ca ratio as found by the above workers, is not necessary to maintain the relation between garnet Ca atomic ratio and K_D as outlined. Only the relative effects of the Ca ratio in garnet on garnet and biotite Mg/Mg+Fe are important in influencing K_D .

Figure 12A reveals a fairly close relation between garnet Mn content (as Mn/Mn+Mg+Fe) and Mg/Mg+Fe_{TOT} in garnet and biotite. Again, the slope of the line defining the relation between garnet Mn/Mn+Mg+Fe and garnet Mg/Mg+Fe is positive, but the relative degrees of influence on garnet and biotite Mg/Mg+Fe are such that the line relating garnet Mn/Mn+Mg+Fe and K_D (using Fe_{TOT}) has a negative slope (as found by Albeé (1965)), (Fig. 23A). This relation is little changed if Fe²⁺ is used in the determination of K_D (Fig. 23A). Sen and Chakraborty, however, found that in general, there is no definite relation between garnet Mn content and K_D (except for one set of analyses where they were related by a line of positive slope). In

Figure 12A it can be seen that the garnet-biotite pair of rock A405/E4B again does not fit the relation between garnet composition and biotite Mg/Mg+Fe ratio. From Figure 11B it seems unlikely that the garnet Ca atomic ratio is responsible for this discrepancy which is probably due to other factors which may influence biotite Mg/Mg+Fe (e.g. rock Mg/Mg+Fe, rock oxidation ratio). Hence rock A405/E4B is also anomalous in a plot of garnet Mn content and K_D (Fig. 23A) and does not obey the simple relation found by Albe  (1965). Such a relation should probably hold strictly true only if variables in biotite composition which may influence the Mg/Mg+Fe ratio do not vary greatly in a set of analyses.

The effects of garnet composition on K_D shown in Figures 23A and 27 are apparent in the Mg-distribution diagrams (Figs. 11A and 24A). The distribution diagrams also show the variation in the distribution of Mg between garnet cores or rims and biotite. The effect of differing MnO and CaO contents of the garnet cores and rims is to modify K_D to different degrees. It is presumed that the garnet rims are in equilibrium with the matrix biotite. If the cores did form at lower temperatures, however, the difference could not have been great as K_D determined between the cores and matrix biotite is very close to that between the rims and biotite. In rocks A405/E4E, M24 the K_D determined relative to the garnet rim is only marginally higher as expected, while in A405/E2A the difference, although in the same sense, is so small as to be insignificant.

The Mg-distribution coefficients of three garnet-biotite pairs have been calculated using Fe^{2+} rather than total Fe in an attempt to reduce the scatter on the distribution diagram. The result shown in Figure 21 is similar to that in Figure 11A, however, where total Fe is used. This variation from the ideal is to be expected of course, due to the significant effects of other variables on K_D as discussed above.

2.4.2 The distribution of Mn between Garnet and Biotite

The distribution of Mn between garnet and biotite is not regular (Fig. 23B). $K_{D_{Mn}}^{G-Bi}$ between individual mineral pairs varies from 49 to 116 (Table G). This variation contrasts with the regular distributions encountered by Hounslow and Moore (1967) and Sen and Chakraborty (1968). Also $K_{D_{Mn}}$ does not increase with increasing concentration of Mn in garnet as found by Fleming (1971). The irregularity of the distribution seems to be largely due to the effect of variation in garnet Ca content which influences $K_{D_{Mn}}$ (Fig. 29A). Furthermore, there is a dependence of garnet Mn content on factors including rock oxidation state and possibly PH_2O , and on the compositions of other phases (e.g. staurolite) also. These variable controls on Mn would also disturb its distribution and hence $K_{D_{Mn}}^{G-Bi}$.

As mentioned earlier, garnet composition (particularly Mn) varies considerably from core to rim. It is conceivable that the rim compositions determined may not have exactly the same composition as the extreme outer "skin" of the crystal, which is that portion of the garnet which is presumably in equilibrium with the matrix minerals. Hence minor discrepancies may arise not only in $K_{D_{Mn}}$ but also in the relationships between garnet Mn content and other chemical parameters.

2.4.3 The distribution of Mg between Staurolite and Biotite

The distribution coefficient $K_{D_{Mg-Fe}}^{St-Bi}$ was determined using mole fractions of Mg defined as $Mg/Mg+Fe_{TOT}$. The range of values is small (Table G) and the distribution curve (Fig. 24B) drawn for the average $K_D(0.262)$ reveals the almost ideal distribution in assemblages which do not contain garnet. The staurolite-biotite pairs from the two 4-phase assemblages (rocks A405/E4E, M24) do not fit the ideal distributions. This is also evident in the plot of $X_{Mg}^{St}/(1-X_{Mg}^{St})$ against $X_{Mg}^{Bi}/(1-X_{Mg}^{Bi})$ as seen in Figure 14A where staurolite-biotite pairs from assemblages without garnet fall very close to a line with slope = 0.262 (= Av. K_D). The

staurolite-biotite pairs from the Al_2SiO_5 -staurolite-biotite assemblages plot close to a line of slope 0.26 which is the value of the average K_D . This represents distribution of Mg in ideal mixtures. The distribution of Mg between the two minerals in the garnet-bearing assemblages is undoubtedly the result of garnet Ca and Mn influence on biotite Mg/Mg+Fe ratios (Figs. 11B,12A) and possibly on staurolite Mg/Mg+Fe ratios also.

2.5 Mineral Chemistry and Metamorphic Grade

2.5.1 The distribution of Mg between Garnet and Biotite

Ideally this distribution coefficient should be dependent on temperature only, however the use of K_D^{G-Bi} in geothermometry is complicated by its dependence on other variables, in particular the Mn and Ca contents of the garnet. The dependence of K_D on pressure is found to be very small, K_D changing only by about 2 1/2% per 1 kb (Albe , 1965, p.163). Perchuk (1967) has derived isotherms for the distribution of Mg between these two minerals using data on equilibrium temperatures taken from another geothermometer¹. X_{Mg} was defined as Mg/Mg+Fe+Mn. The dependence of K_D , however, on the additional factors mentioned above makes any temperatures concluded from these isotherms rather suspect. The use of Perchuk's isotherms, however, does give an equilibrium temperature around 550°C (Fig.13) which is of the order expected.

Saxena (1969) derived a "transformed K_D " by the use of eigenvectors and eigenvalues to correct for the dependence of K_D on compositional variables in garnet and biotite. This K_D is calculated as:

$$\begin{aligned}
 K_{D\text{TRANSF.}} &= 0.5013 K_D - 0.4420 X_{Fe}^G + 0.1506 X_{Fe}^{Bi} - 0.3474 X_{Mn}^G \\
 &+ 0.0865 X_{Ca}^G - 0.0333 X_{Al}^{Bi\text{iv}} - 0.3165 X_{Al}^{Bi\text{viii}} \\
 &+ 0.5488 X_{Ti}^{Bi}
 \end{aligned}$$

¹Equilibrium temperatures in the paragenesis amphibole+garnet+biotite+quartz+plagioclase were determined using the amphibole-garnet geothermometer.

where $X_{Fe} = Fe/(Fe+Mg)$

X_{Mn}^G, X_{Ca}^G = number of Mn or Ca ions on 12 anion basis.

$X_{Al}^{Bi\ iv}, X_{Al}^{Bi\ viii}$ = number of tetrahedrally or octahedrally coordinated Al ions (on 22 anion basis)

X_{Ti}^{Bi} = number of Ti ions.

The compositions on a basis of 22(0) are given in Table D. Values of $K_{D\ TRANSF.}$ from garnet-biotite pairs in Nairne-Mt. Barker Creek rocks are given in Table G. $K_{D\ TRANSF.}$ has been computed using total Fe and Fe^{2+} for three garnet-biotite pairs (A405/E4E, M24, E4B).

Saxena was able to estimate T approximately in equilibrium assemblages by plotting the linear relation between $K_{D\ TRANSF.}$ and $1/T$ (Saxena, 1969, Fig. 7). Transformed K_D 's from Nairne-Mt. Barker Creek rocks are plotted on this diagram in Figure 28. The equilibrium temperatures indicated are around 340-370°C, av. 360°C (using Fe^{2+}) and 350-400°C, av. 370°C (using total Fe). Although these values seem rather low as metamorphic temperatures were probably around the Al_2SiO_5 triple point (i.e. at least 500°C), it is now generally regarded that the temperatures obtained using Saxena's diagram tend to be low, possibly by as much as 100°C or more (Dr. S. Sen, pers. comm.). Saxena (1969, p.266) gives temperatures of around 400°C for epidote-amphibolite and staurolite zone rocks and about 500°C for high amphibolite facies rocks. Temperatures around these facies are, however, at least 100°C higher (Winkler, 1967, Fig. 40; Miyashiro, 1973, Fig. 3-12). Therefore it would be reasonable to add 100°C to the temperature estimates obtained from the transformed K_D of Saxena using Figure 28. This would give temperatures of the order of 475-500°C which approach the values proposed earlier in section B.3.1.

Due to the susceptibility of K_D values to compositional influences and other factors, the variation of K_D with metamorphic grade is compli-

cated and some overlap occurs between rocks of different grades. Ranges of K_D have, however, been established which tend to characterize the different metamorphic grades.

Lyons and Morse (1970) have calculated average $K_{D_{Mg}}^{G-Bi}$'s for a number of metamorphic zones, with values of 0.130 for the garnet zone, 0.151 for staurolite and kyanite zones and 0.277 for sillimanite and sillimanite-orthoclase zones. The average K_D for Nairne-Mt. Barker Creek rocks is 0.147 (using Fe^{2+}) which is consistent with metamorphic conditions concluded earlier.

Albe  (1965) made a correction for the Mn content of garnet as $K_D + 0.7 \text{ Mn/Mn+Mg+Fe}$ which is obtained from the straight line relation resulting from a plot of K_D against $(\text{Mn/Mn+Mg+Fe})^G$ (Albe , 1965, Figs. 3 and 8). The values of K_D corrected for the effect of Mn in garnet for different metamorphic zones are obtained by extrapolating this line to values of K_D where $\text{Mn/Mn+Mg+Fe} = 0$. Corrected K_D in garnet zone rocks is 0.2; in the staurolite zone 0.215; kyanite zone 0.23 and sillimanite zone 0.3-0.37. The average value of this corrected K_D in Nairne-Mt. Barker Creek rocks is 0.31 which is high. This could be the result of the high Mn contents of the garnets which may not entirely obey the relation formulated by Albe  using garnets with Mn/Mn+Mg+Fe values ranging from 0.01-0.2 compared with values of 0.2-0.25 from the Nairne-Mt. Barker Creek minerals. In fact the relatively straight line relation between K_D and garnet Mn/Mn+Mg+Fe shown by Albe  (1965, Figs. 3,8)) tends to curve upwards towards garnets with mole fractions of Mn higher than about 0.14.

Sen and Chakraborty (1968) have empirically correlated variations of K_D within metamorphic zones with the Ca/Mn ratios of garnets in the range 0.4-3.5. The relation found between Ca/Mn and K_D is:

$$\left(\frac{\text{Ca}}{\text{Mn}}\right)^G = -10.44 K_{D_{Mg-Fe}}^{G-Bi} + C$$

where C is found to vary systematically with grade.

In the garnet and staurolite zones, C varies from 2.0-3.4 whereas in the sillimanite zone it is greater than 3.4. The values of garnet Ca/Mn covered by Sen and Chakraborty (0.4-3.5) are above those of Nairne-Mt. Barker Creek almandines (0.17-0.24) and the value of C in these rocks is low, averaging 1.74 (Table G). It seems that with more Mn-rich almandines this empirical relation is also no longer accurate, as with the K_D correction of Albee (1965). Coin (1976, pers. comm.) has recognized an exponential dependence of K_D on Ca/Mn ratio in garnet following the relation $(\text{Ca/Mn})^G = a \cdot b^{K_D}$ (where a, b constants). A plot of the data from this study on a diagram of log Ca/Mn versus K_D indicates metamorphism of approximately low sillimanite grade, when compared with other data (C. Coin, pers. comm.).

2.5.2 Muscovite composition

The change in muscovite composition with grade is well documented (Velde, 1965; Butler, 1967; Guidotti, 1969; Miyashiro, 1973). With increasing grade, Al replacement of Si in tetrahedral sites and of Fe and Mg in octahedral sites increases, and compositions approach that of ideal muscovite as the phengitic component decreases. Butler (1967) has portrayed this marked change in Al_2O_3 and total Fe contents of muscovites in a simple plot of Al_2O_3 versus $\text{FeO} + \text{Fe}_2\text{O}_3$ (Butler, 1967, Fig. 4). This plot is shown in Figure 22 demonstrating the relatively small overlap of the composition fields of muscovites from different metamorphic grades. Muscovites from Nairne-Mt. Barker Creek metashales are plotted on this diagram. Whereas a considerable spread of compositions is revealed, the greater proportion of muscovites fall into the field defined by muscovites from rocks of staurolite and higher grade zones. Although only total Fe was determined in the analyses, and $\text{Fe}^{3+}/\text{Fe}^{2+}$ ratios common in the literature used, any difference between estimated $\text{FeO} + \text{Fe}_2\text{O}_3$ and the true value is not expected to significantly alter the muscovite plots on this diagram.

Within the same rock, decrease in Mg and Fe and corresponding increase in Al in coarse muscovites relative to finer grained matrix muscovite (Table F, Fig.22) reflects a higher temperature of crystallization of the former. Textural relations indicate that the coarse-grained muscovite post dates the matrix muscovite and is associated with the breakdown of andalusite and the formation of fibrolite at somewhat higher temperatures than the formation of the matrix. From Figure 22 it is evident that although the muscovite plates have compositions indicating higher temperatures than the matrix muscovites in the same rock, there is considerable overlap between muscovites from the different rocks. This overlap is most likely the effect of rock bulk composition and the compositions of the other phases, particularly biotite, on the muscovite composition.

3. CALC-SILICATES

3.1 Rock Compositions and Mineral Analyses

The layered calc-silicates of assemblages (v) and (vi), (Sect.B.24) do not differ greatly in their compositions (Table H). The main differences are in the slightly higher Al_2O_3 , Na_2O and K_2O contents of assemblage (vi). The relatively high Al_2O_3 content of this assemblage approaches that of the peraluminous schists.

The two analyses from rocks of assemblage (viii) are similar. The rock containing calcite (A405/BC18) is richer in CaO whereas the other, which contains more biotite, has a higher Al_2O_3 and K_2O content. The Al_2O_3 content of this rock (A405/MCS2a) also approaches those of the peraluminous schists.

A rare amphibole-rich metasandstone (A405/BC40) contains traces of epidote and should strictly be included in assemblage (v), however because of its entirely different appearance with a total absence of lamination and very different relative proportions of the component minerals, it should be considered as a separate assemblage. This rock has a very high SiO_2 content and low Al_2O_3 , MgO, Na_2O and K_2O (Table H). CaO and total Fe

are similar to the other calc-silicates.

Use has been made of the ACF diagram (Fig. 35) to determine whether chemical equilibrium has been established in these rocks. ACF diagrams have only been drawn for assemblages not containing a significant proportion of biotite as the Fe_2O_3 and FeO contents of this mineral must be known for a proper correction of the whole rock analysis. Equilibrium was achieved in rock A405/BC45 (assemblage (v)) as the rock composition falls well within the field defined by the epidote-hornblende-plagioclase tie-lines. Plagioclase was not analysed and is assumed to be high-An. Rock A405/MCS2c containing the assemblage hornblende+plagioclase+scapolite+diopside also falls within the field defined by the tie-lines. The presence of 4 phases is not in conflict with the phase rule as FeO and MgO can be considered as separate components. The composition of A405/BC40 falls on the tie-line between plagioclase and hornblende again indicating chemical equilibrium.

3.2 Mineral Chemistry

A comparison of the mineral analyses with those of mineral suites in Deer, Howie and Zussman (1962) reveals the identities of analysed hornblende, diopside, scapolite and plagioclase (Tables I,L) and indicates that the compositions are consistent with formation by regional metamorphism of Ca-rich sediments. Hornblende in A405/BC45, MCS2c is common hornblende, in A405/BC40 it is tchermakitic hornblende. This range in hornblende compositions is noteworthy as hornblendes of the amphibolite facies are generally common hornblende and extremes of composition are rare (Deer, Howie & Zussman, 1962). Plagioclase (A405/BC40) is bytownite (about An 80); in A405/MCS2c, diopside is salite and scapolite is dipyre.

3.3 Hornblende Composition and Metamorphic Grade

The increasing replacement of Si by Al in calciferous amphiboles with increasing temperature is well known (Harry, 1950). Hornblendes from Nairne-Mt. Barker Creek rocks (three calc-silicates and one amphibolite,

A405/E9S) have a considerable range in composition (Table I). When plotted on a simple diagram portraying the extent of Si replacement by Al (after Harry 1950, Fig. 1), three of these hornblendes (including one from the amphibolite) are found to have compositions consistent with metamorphism in the amphibolite facies (Fig. 20B). The remaining hornblende (A405/MCS2c) which is richer in Si, indicates a lower metamorphic grade. This inconsistency could arise from:

(i) Hornblende in rock A405/MCS2c formed out of equilibrium with its metamorphic environment. This would appear unlikely from the ACF plot of this rock and its mineral assemblage (Fig. 35).

(ii) The hornblende in A405/MCS2c is retrograde. There is no evidence for this from thin section study, however,

(iii) Hornblende composition is not strictly dependent on metamorphic grade and compositions of co-existing phases may influence its Si:Al ratio.

4. CHEMICAL COMPARISON OF TYPE MARINO GROUP SEDIMENTS AND THEIR METAMORPHOSED EQUIVALENTS.

Analyses of sedimentary rocks from the Marino Group stratotype on the western side of the Mount Lofty Ranges (Table J) indicate high ignition losses, ranging from 5.08 - 16.38%. The actual H₂O content, determined in rocks showing the highest weight losses, was found to be only a small fraction of the total ignition loss (H₂O 1.37-2.72 wt %). This large difference can be attributed to a high CO₂ loss from carbonate, visible in thin section. CO₂ contents were not specifically determined.

Oxidation states of the sediments, expressed as "oxidation ratio" defined by Chinner (1960) tend to be moderate to high (30.0-74.4) and values do not appear to characterize specific rock types, except that the maroon shales of the lowest Marino Group unit seem to have the highest oxidation states. Oxidation ratios vary between similar lithologies (e.g. A405/MS3a and MS3b have oxidation ratios of 53.4 and 30.05 respectively, even though in hand specimen they appear to be identical).

A comparison between metasediments in the eastern Mount Lofty Ranges and their sedimentary equivalents in the Marino Group stratotype is also given in Table J. Although correlation on the basis of stratigraphy is believed to be approximately correct, it is appreciated that a strict chemical comparison of the units is not possible. This is due to (i) the probability of minor sedimentary facies change and its effect on the bulk chemistry of the rocks and (ii) the variability of rock compositions within a stratigraphic unit at any one locality.

The sequence below the "upper arkose" can be correlated fairly closely with similar distinctive lithologies on the eastern side of the ranges. The sequence above this level, however, cannot be compared with certainty due to the differences in thickness and the absence of distinctive units.

The major differences between the proposed equivalents are evident in Table J. The metashales of Unit 2 (see also Table A) have slightly lower SiO_2 and considerably lower CaO and H_2O contents compared with their sedimentary equivalents A405/MS4a and MS4a'. The metashales also have higher Al_2O_3 and total Fe contents. Metasandstones of Units 2 and 3 are slightly richer in Al_2O_3 , total Fe and Na_2O , and poorer in CaO , H_2O than the sandstones from a similar stratigraphic level. Scapolite-rich metasiltstone A405/BC18 of Unit 1 is similar in composition to its sedimentary equivalents A405/MS3a and MS3b except for its slightly higher SiO_2 and considerably lower CaO and H_2O contents. No additional trends are evident if analyses are compared using loss-free data (Table K). There is some suggestion that the metamorphic equivalents have the higher oxidation ratios, the average oxidation ratio for metasediments being 52.32 (54.69 excluding calc-silicates) and the average for the sediments being 49.96. The difference, however, is small and its magnitude and sense may vary with another set of analyses.

In general it appears that there are compositional differences between the sediments and their metamorphosed equivalents which are consistent amongst

the different rock types. Metasediments are characteristically richer in Al_2O_3 and total Fe and poorer in CaO. As expected, the metamorphosed rocks also have lower H_2O contents. These differences, which may be attributed to metamorphism, are in agreement with the systematic correlation of bulk composition changes with metamorphic grade noted by Engel and Engel (1958) in progressively metamorphosed gneiss, except for the apparent decrease in CaO with grade which is the reverse of the observations of the above writers.

A comparison of the few metasediments and sediments with similar Si/Al ratios (Tables A,B,J and H) did not reveal any systematic changes in other compositional parameters. Wide variations in the composition of either sediments or metasediments with fixed Si/Al ratios is reflected in the variable Ca/Al ratios. Consequently comparison was further restricted to that between sediments with similar Ca/Al ratios and metasediments having Ca/Al values nearest to these. The few rock analyses which fulfilled these restrictions indicated little systematic compositional variation in other respects except that the metasediments have higher total Fe and lower H_2O contents than the sediments. The metasediments have similar or slightly higher oxidation ratios thus corroborating the trend mentioned above. This is the reverse of the trend of progressively increasing Fe^{2+} and decreasing Fe^{3+} with increasing grade noted by Engel and Engel (1958) and Miyashiro (1964).

A statistical comparison using a large number of analyses would be required to rigorously examine the changes in bulk composition but this is beyond the scope of this study. In any case, the metasediments and sediments represent strata originally deposited at great distances apart, and the influence of facies change on bulk composition would be a major problem to contend with even in such a more statistical comparison.

5. SUMMARY AND CONCLUSIONS

Analysis of mineral assemblages indicates that rocks have largely attained chemical equilibrium under metamorphic conditions of the amphibolite facies. A few anomalous assemblages appear on the Thompson AFM pro-

jection due to the presence of MnO as an additional component.

Within the limitations of the low range of values for certain chemical ratios, relations between host rock chemistry and chemical composition of the individual ferromagnesian phases are generally consistent with the findings of others. Oxidation ratios of the rocks are relatively high and have a restricted range, possibly accounting for the absence of a correlation between this ratio and several aspects of rock and mineral chemistry including rock total Fe and rock MnO content.

Garnet, which occurs in rocks having the highest MnO contents, contains a significant spessartine component, sufficient to stabilize the mineral under the high oxidizing conditions. The variable content of MnO in garnets (also dependent on a number of different factors including PH_2O , PO_2 and chemistry of the other phases) is found to have little or no correlation with rock MnO or rock oxidation ratio.

The presence of considerable MnO and CaO in the garnet disturbs the Mg distribution between garnet and biotite as recognized by a number of workers. Although the distribution is not ideal it is regular. This disruptive effect of variation of garnet composition is evident also in the Mg distribution between biotite and staurolite where the distribution is close to ideal for mineral pairs not associated with garnet but far from ideal in garnet-bearing rocks. Also, the irregular distribution of Mn between garnet and biotite appears to be largely the result of variation of garnet Ca content.

The numerical values of uncorrected $K_{D_{\text{Mg}}}^{\text{G-Bi}}$ are consistent with metamorphic conditions of the andalusite-staurolite zone. After various corrections to allow for the variable compositions of garnet or garnet and biotite, the values of K_D indicate temperatures around 500°C (Saxena, 1969) and metamorphic grades ranging from just below the staurolite zone to lower sillimanite zone (Sen and Chakraborty, 1968; Albeé, 1965). The wide range of metamorphic grade thus indicated is possibly due to inadequacies of the

corrections for MnO in garnets with regard to the calculation of K_D , the MnO content of the garnets being outside the range used in the formulation of the corrections.

Compositions of muscovites also indicate staurolite or higher grades and hornblende compositions are mostly consistent with metamorphism in the amphibolite facies. Hence, although there are minor discrepancies, mineral compositions and Mg-distribution coefficients are in agreement concerning the grade of metamorphism.

PART III

CONCLUSIONS

CONCLUSIONS

In the opening sections of this work it has been shown that the sequence of upper Adelaidean and lower Kanmantoo Group strata from the Stoneyfell Quartzite to the Tapanappa Formation can be equated directly with their respective stratotypes in the western Mount Lofty Ranges and on the south coast of Fleurieu Peninsula. Although metamorphism of the eastern Adelaidean sequence reached high andalusite grade in the youngest strata, the nature of the original succession can still be deduced. There are, however, marked differences in stratigraphic thickness between the Torrens and Sturt Group stratotypes and their metamorphosed eastern counterparts. Minor differences in facies between the Adelaidean strata and their respective stratotypes are evident, the most significant being:

(i) the eastern equivalent of the Stoneyfell Quartzite is of a predominantly more pelitic facies, quartzites forming only a portion of the interval;

(ii) above the Stoneyfell Quartzite is a pebbly metasandstone interval (Unit 3) which is interpreted herein as being possibly of shallow glaciomarine origin. Nowhere else in the Torrens Group has an equivalent interval been described;

(iii) pebbly arkoses and impure metasandstones mark the interval between the lenticular Brighton Limestone equivalent and the characteristic finely laminated metasiltsstones of the Tapley Hill Formation. This interval is absent in the Tapley Hill Formation stratotype and is herein equated with its Eudunda Arkose Member which occurs in the upper levels of the Tapley Hill Formation further north but has hitherto been unrecorded in the study area (BARKER and ADELAIDE 1:250,000 map sheets; Burra 1:63,360 map sheet).

The Kanmantoo Group exhibits a remarkable constancy of facies considering the large distances, in excess of 75 km, from the type area on the south coast of Fleurieu Peninsula. Although some facies change is evident, the formations could readily be distinguished and mapped. The major facies

changes evident are in the upper and lower levels of the Backstairs Passage Formation which show lateral variations from the typical laminated psammitic rocks into more pelitic facies. Variations in the basal portion of this formation have previously contributed to the confusion in interpretations of the stratigraphy in the vicinity of the Adelaidean-Kanmantoo Group boundary in the Birdwood-Brukunga area.

Detailed stratigraphic mapping by the author in the Birdwood-Mt. Barker Creek region has shown that the boundary between the Adelaidean and Kanmantoo Group is not an unconformity as shown on the BARKER and ADELAIDE 1:250,000 map sheets. The contact is a fault, originally termed the Nairne Fault in interpretations of the contact prior to the unconformity hypothesis (Sprigg, Whittle and Campana, 1954, Adelaide 1:63,360 map sheet). Furthermore, results of the present study are in conflict with earlier interpretations by Horwitz, Thomson and Webb (1959), Thomson and Horwitz (1962) and Thomson (1969) regarding the stratigraphy and distribution of "basal Cambrian" strata and the younger Kanmantoo Group in the vicinity of the fault. One major difference lies in the interpretation of the stratigraphic level of the Mt. Barker Quartzite. Earlier work by Sprigg and Wilson (1954); Horwitz, Thomson and Webb (1959) and Thomson and Horwitz (1962) assigned a Cambrian age to this unit whereas the Quartzite is herein reinterpreted as occupying the upper levels of the Precambrian Marino Group. Thus the Mt. Barker and Macclesfield Quartzites occupy similar stratigraphic levels, as Marlow (1975) included the latter to be in the upper parts of the Marino Group also. The relationship between these formations was hitherto uncertain.

Evidence for a fault rests in the Cambrian and its relationship to the contact with the underlying Adelaidean. There are two lines of evidence:

(i) A large part of the normal Cambrian sequence is missing in the study area. The missing interval includes (a) the Normanville Group which conformably underlies the Kanmantoo Group on the western side of the Mount Lofty Ranges (Daily, 1963; Daily and Milnes, 1973) and (b) the lower levels

of the basal unit of the Kanmantoo Group, the Carrickalinga Head Formation (Daily and Milnes, 1971).

(ii) The lower strata of the Kanmantoo Group are truncated along the fault; the distinctive upper unit of the Carrickalinga Head Formation termed the Campana Creek Member (Daily and Milnes, 1971) has a sporadic development adjacent to the fault. Locally, the angular discordance between the Kanmantoo Group and the fault is sufficient to reveal that the beds strike into the contact with the underlying Adelaidean.

Following interpretation of the Adelaidean-Kanmantoo Group boundary as being a fault, excavations for the South-East freeway at the northern extremity of Mt. Barker confirmed the existence of a fault contact between the Carrickalinga Head Formation and the Precambrian Mt. Barker Quartzite at that locality.

Mapping in the Birdwood-Brukunga area also shows that the structure of that area consists of a western and an eastern syncline, the boundary between the two folds being the Nairne Fault (Map 2). Previously the area was considered to be dominated by a single "F₃" syncline which extended south-east to the Dawesley-Kanmantoo area (Fleming and Offler, 1968; Pain, 1968; Fleming, 1971). To the north-west, this structure was shown to be truncated at the Meadows - Mt. Kitchener fault (Fig. B, Appendix II). The western syncline is herein interpreted as an "F₁" structure (see Table 0); whereas the eastern syncline which folds the Nairne Pyrite (part of the Talisker Calc-siltstone equivalent) is the structure which extends to the south-east and is probably the "F₃" structure of Fleming (1971). As the Nairne Fault truncates the western "F₁" structure, it is concluded that the main period of faulting occurred post-"F₁" but prior to subsequent deformations which appear to be responsible for the later flexuring of the fault. This is compatible with the findings of Marlow (1975) in the Macclesfield area to the south. It is suggested that detailed re-mapping of the strata in the vicinity of the Adelaidean-Kanmantoo Group contact north of Birdwood

will also indicate the existence of a fault relationship. Furthermore, the Carrickalinga Head Formation, hitherto un-recorded north of its stratotype, is expected to comprise a significant proportion of the Kanmantoo Group north of Birdwood.

Through detailed petrological examination of the metashales in the Nairne-Mt. Barker Creek area the present study has shown that a deformation phase (herein denoted F_1) with accompanying high-grade metamorphism occurred prior to that generally recognized elsewhere in the Mount Lofty Ranges. The development of the regional schistosity (herein denoted S_2) post-dated this deformation whereas this schistosity was previously interpreted as the planar structure accompanying the first tectonic event of the Delamerion orogeny in the Mount Lofty Ranges (Fleming and Offler, 1968; Fleming, 1971). The presence of a pre-" F_1 " deformation, which was possibly inhomogeneous, suggests a plausible explanation for the spread of " F_1 " axes noted in some areas (e.g. Fleming, 1971).

Milnes et al. (1977, Fig. 8) recently envisaged the emplacement of the Encounter Bay Granites during the opening stages of the " F_1 " deformation; their " F_1 " deformation embraced an earlier deformation (recognized earlier in the Middleton area by Daily and Milnes (1973)) and was continuous through to the end of the main phase of " F_1 " which followed. It is suggested herein that the granite emplacement occurred in the time span between the main phase of " F_1 " (herein denoted F_2 in the Nairne-Mt. Barker Creek area - Table 0) and a distinct earlier deformation which is denoted F_1 in the Nairne-Mt. Barker Creek area.

Metadolerite dykes in the Nairne-Mt. Barker Creek area were probably emplaced pre-" F_1 " to early syn-" F_1 ". They are aligned sub-parallel to the bedding and regional schistosity. Similar dykes in the Woodside area studied by Pain (1968) were probably emplaced early syn-" F_1 " and parallel the regional schistosity " S_1 "; their fabric is compatible with the orientation of " S_1 " in the metasediments. This interpretation differs from that of Pain (op.cit)

who suggested that the dykes were related to the later "F₃" deformation. Discordant metadolerite dykes on Kangaroo Island and Fleurieu Peninsula, however, have probably been emplaced post-"F₁" (Milnes et al. 1977). It is concluded therefore that there were at least two periods of dolerite dyke intrusion in the southern Mount Lofty Ranges.

Petrological examination and chemical analysis of the rocks and minerals has shown that chemical equilibrium was attained under metamorphic conditions of the Amphibolite Facies (Figs. 30 to 35). The peak of metamorphism probably occurred during the latter stages of the major deformation which produced the regional penetrative schistosity (herein denoted S₂), this being compatible with other studies (e.g. Fleming, 1971; Marlow, 1975; Milnes et al. 1977). P-T conditions deduced from critical minerals and metamorphic textures are 3.5 to 3.75 kb and 500 to 550°C - close to the andalusite-sillimanite phase boundary and near the Al₂SiO₅ triple point, using the data of Holdaway (1971). Temperatures of metamorphism deduced from the garnet-biotite geothermometer are compatible with this range.

Textures in the peraluminous schists have provided some insight into the sillimanite problem. The indirect breakdown of andalusite to fibrolite via interacting microscopic sub-systems as envisaged by Fleming (1971) following Carmichael (1969) is largely substantiated. Some complex textures can be explained by the superimposition in time of these sub-systems. In addition, there is also evidence for the breakdown of andalusite and the nucleation of the Al and Si on biotite in the manner proposed by Chinner (1961). No one mechanism can explain the textures involving andalusite, fibrolite, biotite, muscovite and quartz.

Fibrolite formed within the upper limits of the andalusite stability field as seen elsewhere in the Andalusite-Staurolite Zone delimited by Fleming (1971). It is suggested herein that the fibrolite may not necessarily have formed metastably but that it may have a stability field which partly overlaps that of andalusite under certain conditions. Further experi-

mental work on this problem is warranted. Alternatively it is suggested that fibrolite may indeed have formed metastably in the andalusite field as the result of rapid reactions, possibly induced by sudden temperature increases. However, there is no experimental data to verify this.

Chemical analysis of the rocks and minerals (section IID) revealed the following:

(i) Within the limitations of the low range of values for certain chemical ratios, the relations between host rock chemistry and composition of the individual ferromagnesian minerals are generally found to be consistent with the results of others (op.cit.).

(ii) Garnet is approximately 70% almandine and has a high spessartine component (5-10% MnO). The high MnO content of the garnets is considered to be related to the high oxidizing conditions which prevailed during its crystallization.

(iii) The distribution of Mg between garnet and biotite was examined and found to be regular, but not ideal. It is concluded that the presence of considerable MnO and CaO in the garnet has a disruptive effect on $K_{D_{Mg}}^{G-Bi}$, as reported in the literature (op.cit). This effect is also evident in the Mg-distribution between biotite and staurolite where the distribution is found to be almost ideal for mineral pairs not associated with garnet but irregular in garnet-bearing rocks. The irregular distribution of Mn between garnet and biotite is interpreted as being largely the result of variations in garnet Ca content.

The use of empirical corrections of $K_{D_{Mg}}^{G-Bi}$ as indicators of metamorphic grade has indicated grades ranging from just below the staurolite zone to the lower sillimanite zone using the corrections devised by Albee (1965) and Sen and Chakraborty (1968). It is suggested herein that the wide range of metamorphic grade indicated is due to inadequacies in the corrections in cases where Mn-rich garnets are under consideration, the MnO contents of the Nairne-Mt. Barker Creek garnets being outside the range used

in the formulation of these corrections. In general, however, it appears that while there are minor discrepancies, the mineral assemblages, textures, mineral compositions and Mg-distribution coefficients are in agreement concerning the grade of metamorphism.

TABLE A

ANALYSES OF METASHALES (all samples from the Marino Group (Unit 2) except A405/E4E and E2A)

Sample A405/ Assemblage	M24	E4E(Unit 3)	BC38	BC34a	BC37A	E2A(Unit 3)	M21	BC27
	Q,Pl,Bi,M,A/S,G,St	Q,Pl,Bi,M,A/S,G,St	Q,Pl,Bi,M,A/S,St	Q,Pl,Bi,M,St,S(tr)	Q,Pl,Bi,M,St,A/S	Q,Pl,Bi,M,A/S,G	Q,Pl,Bi,M,A/S	Q,Pl,Bi,M
SiO ₂	61.19	57.29	60.40	66.78	60.34	59.75	58.24	60.70
Al ₂ O ₃	16.40	19.76	17.76	14.82	19.98	17.66	19.42	15.82
(Fe ₂ O ₃)	(3.29)	(3.78)	(2.69)	(2.38)	(1.44)	(3.00)	(4.19)	(3.64)
Total Fe as Fe ₂ O ₃	8.37	8.70	8.39	6.76	8.11	9.82	8.88	8.27
(FeO)	(4.57)	(4.43)	(5.13)	(3.94)	(6.00)	(6.14)	(4.22)	(4.17)
MnO	0.16	0.19	0.13	0.11	0.13	0.15	0.10	0.12
MgO	3.11	2.93	2.96	2.55	3.25	2.82	3.15	3.71
CaO	1.99	0.54	0.73	1.47	1.02	0.35	1.06	2.57
Na ₂ O	1.92	1.39	1.44	2.81	1.21	0.87	1.11	2.15
K ₂ O	3.03	5.04	4.33	2.63	3.42	4.99	3.67	3.50
TiO ₂	1.04	1.35	1.21	1.14	1.17	1.05	1.21	1.08
P ₂ O ₅	0.21	0.17	0.21	0.16	0.17	0.14	0.23	0.22
Ignition Loss	1.20	2.24	1.85	1.02	1.24	1.81	2.08	1.38
Total	98.86	99.58	99.41	100.23	100.03	99.40	99.16	99.80
H ₂ O	n.d.	n.d.	n.d.	n.d.	n.d.	n.d.	n.d.	1.63
2+	0.578	0.544	0.514	0.538	0.494	0.455	0.576	0.616
Mg/Mg+Fe _{TOT}	0.417	0.400	0.412	0.427	0.443	0.362	0.412	0.470
"Oxidation Ratio" After Chinner (1960)	59.01	63.05	51.19	54.71	32.43	49.42	66.51	63.58
Si/Al(as SiO ₂ /Al ₂ O ₃)	n.d.	n.d.	n.d.	4.51	n.d.	n.d.	3.00	5.84
Ca/Al(as CaO/Al ₂ O ₃)	n.d.	n.d.	n.d.	0.10	n.d.	n.d.	0.05	0.16

Abbreviations: Q(Quartz); Pl(Plagioclase); Bi(Biotite); M(Muscovite); G(Almandine garnet); A/S(Andalusite and sillimanite); St(Staurolite); tr(trace)
n.d. = not determined.

TABLE B

ANALYSES OF METASILTSTONES AND METASANDSTONES

Sample A405/	E4B Marino Group, Unit 3	F10 L. Tapanappa Formation	BC33A Marino Group, Unit 2	BC43 Marino Group, Unit 3
Assemblage	Q,Pl,Bi,M,G	Q,Pl,Bi,G(tr)	Q,Pl,Bi	Q,Pl,Bi
SiO ₂	71.30	75.43	78.01	72.27
Al ₂ O ₃	11.80	10.81	9.38	11.55
(Fe ₂ O ₃)	(2.97)	(n.d.)	(1.37)	(2.34)
Total Fe as Fe ₂ O ₃	7.37	3.24	4.67	6.82
(FeO)	(3.96)	(n.d.)	(2.97)	(4.03)
MnO	0.27	0.12	0.08	0.12
MgO	2.08	1.28	1.48	2.17
CaO	2.04	0.99	1.71	1.41
Na ₂ O	3.06	2.93	2.81	3.65
K ₂ O	1.65	3.46	1.20	1.69
TiO ₂	0.97	0.49	2.38	0.97
P ₂ O ₅	0.15	0.14	0.26	0.05
Ignition Loss	0.24	0.26	0.36	0.87
Total	100.69	99.13	101.97	100.71
Mg/Mg+Fe ²⁺ _{TOT}	0.486 0.361	n.d. 0.438	n.d.	n.d.
"Oxidation Ratio" After Chinner (1960)	60.00	n.d.	47.99	53.73
Si/Al(asSiO ₂ /Al ₂ O ₃)	6.04	6.98	8.32	6.26
Ca/Al(asCaO/Al ₂ O ₃)	0.17	0.09	0.18	0.12

Abbreviations: Q(Quartz); Pl(Plagioclase); Bi(Biotite); M(Muscovite); G(Almandine garnet). nd = not determined.

TABLE C

GARNET ANALYSES AND FORMULAE

Sample A405/	E4E(c)	E4E(r)	M24(c)	M24(r)	E2A(c)	E2A(r)	E4B(c)	
SiO ₂	36.83	36.54	36.61	36.76	36.51	36.78	38.56	
Al ₂ O ₃	20.34	19.85	20.58	20.45	20.46	20.48	20.40	
TiO ₂	0.01	0.10	0.02	-	0.03	0.07	0.05	
Fe ₂ O ₃ ^Y	0.5	0.5	0.5	0.5	0.5	0.5	0.5	
FeO ^Y	28.49	28.26	25.29	25.95	30.07	31.14	26.08	
MgO	2.93	3.00	3.04	3.23	2.73	2.77	2.88	
MnO	8.70	8.18	10.13	9.75	6.60	5.44	10.66	
CaO	1.17	1.14	1.83	1.86	1.34	1.31	1.81	
Na ₂ O	0.04	0.06	-	0.07	0.04	-	0.01	
K ₂ O	-	-	-	-	-	-	-	
Total	99.02	97.73	98.09	98.59	98.38	98.56	101.07	
Cations The basis of 24 anions	Si	6.09	6.13	6.08	6.09	6.09	6.05	6.22
	Al	3.74	3.71	3.81	3.76	3.80	3.76	3.66
	Ti	0.001	0.01	0.002	-	0.004	0.01	0.006
	Fe ³⁺	0.06	0.06	0.06	0.06	0.06	0.06	0.06
	Fe ²⁺	3.95	3.96	3.51	3.59	4.19	4.28	3.52
	Mg	0.75	0.75	0.75	0.80	0.68	0.68	0.69
	Mn	1.22	1.16	1.43	1.36	0.93	0.76	1.45
	Ca	0.21	0.20	0.33	0.33	0.24	0.23	0.31
	Na	0.01	0.02	-	0.02	0.12	-	0.004
	K	-	-	-	-	-	-	-
Mg/Mg+Fe	0.153	0.157	0.173	0.179	0.138	0.136	0.161	
Mg/Mg+Fe+Mn	0.122	0.125	0.130	0.137	0.116	0.118	0.120	
Mg/Mg+Fe+Mn+Ca	0.118	0.122	0.123	0.130	0.112	0.113	0.114	
Mn/Mn+Mg+Fe	0.205	0.196	0.248	0.235	0.159	0.132	0.254	
Ca/Mg+Fe+Ca	0.042	0.041	0.071	0.069	0.046	0.043	0.068	
Ca/Mn	0.171	0.174	0.230	0.241	0.258	0.298	0.213	
%								
Andradite	1.16	1.15	1.03	0.99	1.06	1.18	1.11	
Almandine	65.25	65.22	58.58	59.34	69.72	72.29	59.28	
Pyrope	12.06	12.35	12.52	13.22	11.32	11.49	11.62	
Spessartine	20.15	19.11	23.87	22.48	15.48	12.84	24.42	
Grossular	1.73	1.56	4.01	3.97	2.33	2.11	3.54	

Abbreviations: c(garnet core); r(garnet rim)

^YFe₂O₃ is expected to be low in these garnets (Deer, Howie & Zussman, 1962).

Value arbitrarily set at 0.5%.

BIOTITE ANALYSES AND FORMULAE

Sample A405/	M21 (c)	F10(m)	BC37a(m)	BC54a(m)	BC38(m)	E2A(m)	E2A(c)	E4B(m)	E4E(m)	M24(m)
SiO ₂	36.05	34.52	35.47	33.86	34.65	35.84	34.24	36.71	34.09	35.63
Al ₂ O ₃	19.61	17.81	18.87	18.25	18.63	18.81	19.50	18.14	17.74	18.57
TiO ₂	1.47	2.82	1.56	1.61	1.29	1.81	1.29	1.90	1.48	1.55
(Fe ₂ O ₃) ^Y	(2.07) ^Y	(2.27) ^Y	(3.25) ^Y	(3.20) ^Y	(3.09) ^Y	(2.28) ^Y	(2.62) ^Y	(5.86)	(6.84)	(3.97)
Total Fe as FeO	15.68	19.52	19.18	18.91	18.23	21.03	19.86	19.45	19.51	16.34
(FeO) ^Y	(13.80) ^Y	(17.46) ^Y	(16.23) ^Y	(16.00) ^Y	(15.43) ^Y	(18.96) ^Y	(17.48) ^Y	(14.18)	(15.36)	(12.76)
MgO	12.13	9.67	9.92	10.62	10.90	8.58	8.91	9.75	9.79	11.66
MnO	0.10	0.54	0.11	0.08	0.11	0.08	0.08	0.25	0.08	0.18
CaO	-	0.04	-	-	-	-	-	-	-	-
Na ₂ O	0.45	0.10	0.31	0.40	0.43	0.38	0.42	0.22	0.34	0.26
K ₂ O	9.27	9.60	8.99	8.44	8.48	9.14	8.88	9.54	8.61	9.18
H ₂ O*	5.00	5.00	5.00	5.00	5.00	4.00	5.00	4.00	5.00	5.00
Total	99.87	99.67	99.61	97.34	97.87	99.83	98.08	100.07	96.76	98.31
Cations on basis of [22(O)] L.H.S.	2.67	2.62	2.67	2.61	2.64	[5.50] 2.75	[5.40] 2.63	[5.52] 2.74	[5.44] 2.62	[5.48] 2.68
Fe ³⁺	1.33	1.38	1.34	1.39	1.36	[2.50] 1.26	[2.60] 1.37	[2.45] 1.27	[2.56] 1.38	[2.52] 1.32
Fe ²⁺	0.29	0.15	0.25	0.17	0.22	[0.72] 0.35	[0.79] 0.28	[0.59] 0.24	[0.59] 0.14	[0.62] 0.21
Mg	0.08	0.16	0.09	0.09	0.07	[0.21] 0.11	[0.15] 0.07	[0.22] 0.11	0.68[0.18] 0.09	0.62[0.18] 0.09
Mn	0.12	2.68	0.13	2.65	0.18	2.66	0.19	2.70	0.17	2.69
Mg	0.85	1.11	1.02	1.03	0.98	[2.44] 1.22	[2.30] 1.12	[2.21] 0.88	[2.29] 0.86	[1.65] 0.80
Mn	1.34	1.09	1.11	1.22	1.24	[1.97] 0.98	[2.09] 1.02	[2.19] 1.08	1.98[2.55] 1.12	1.99[2.67] 1.30
Ca	0.004	0.04	0.01	0.01	0.01	[0.01] 0.01	[0.01] 0.01	[0.07] 0.02	[0.01] 0.01	[0.02] 0.01
Na	-	0.003	-	-	-	-	-	-	-	-
Na	0.06	0.94	0.02	0.95	0.05	0.90	0.06	0.89	0.06	0.89
K	0.88	0.93	0.86	0.85	0.82	[1.79] 0.89	[1.79] 0.87	[1.85] 0.90	[1.76] 0.85	[1.80] 0.88
2+	n.d.	n.d.	n.d.	n.d.	n.d.	n.d.	n.d.	n.d.	0.551	0.566
Mg/Mg+Fe _{TOT}	0.580	0.469	0.480	0.500	0.516	0.422	0.446	0.471	0.472	0.559
Mn/Mn+Mg+Fe _{TOT}	n.d.	n.d.	n.d.	n.d.	n.d.	0.002	0.002	0.007	0.002	0.005

^YFe₂O₃, FeO determined from Fe₂O₃/FeO ratios of biotites from similar rocks given in the literature.

*H₂O was not determined. H₂O contents used are those which give acceptable totals and are within the range given in Deer, Howie & Zussman (1962).

Abbreviations: m(matrix biotite); c(coarse biotite plates).

TABLE E

STAUROLITE ANALYSES AND FORMULAE

Sample A405/	E4E	M24	BC38	BC37a	BC34a
SiO ₂	26.40	26.55	26.62	26.04	26.16
Al ₂ O ₃	51.42	51.82	51.83	51.16	52.40
TiO ₂	0.52	0.38	0.58	0.61	0.55
Fe ₂ O ₃ ^Y	1.50	1.50	1.50	1.50	1.50
FeO ^Y	11.83	11.44	12.20	12.30	13.65
MgO	1.76	1.92	1.98	1.64	1.77
MnO	0.42	0.74	0.43	0.57	0.49
CaO	-	0.02	-	0.02	-
Na ₂ O	0.08	0.07	0.05	-	0.03
K ₂ O	-	-	-	0.01	-
H ₂ O*	2.5	2.5	2.5	2.5	2.5
TOTAL	96.48	97.07	97.80	96.58	97.57
Si	7.87	7.88	7.86	7.80	7.99
Al	17.07	17.11	17.02	17.07	17.83
Ti	0.12	0.08	0.12	0.14	0.13
Fe ³⁺	0.03	0.03	0.03	0.03	0.03
Fe ²⁺	2.96	2.83	3.02	3.08	3.11
Mg	0.79	0.85	0.87	0.74	0.81
Mn	0.11	0.18	0.11	0.14	0.13
Ca	-	0.01	-	0.01	-
Na	0.04	0.04	0.03	-	0.02
K	-	-	-	0.004	-
Mg/Mg+Fe _{TOT}	0.209	0.228	0.222	0.192	0.205

^Y Fe₂O₃ set at 1.5% from survey of staurolites from similar rocks given in the literature, in particular Deer, Howie & Zussman (1962).

* H₂O not determined. H₂O contents used are those which give acceptable totals and are within the range of H₂O in similar staurolites.

TABLE F

MUSCOVITE ANALYSES AND FORMULAE.

Sample A405/	BC38(m)	BC38(c)	M21'(m)	M21'(c)	E4E(m)	BC34a(m)	BC37a(c)	E2A(m)	BC42(m)	BC42(c)	
SiO ₂	44.09	44.74	45.65	45.36	46.45	44.52	44.55	47.10	48.28	51.41	
Al ₂ O ₃	32.23	34.01	34.13	35.48	32.61	33.76	33.74	35.77	35.75	37.35	
TiO ₂	0.52	0.42	0.42	0.33	0.40	0.37	0.43	0.65	0.48	0.30	
Fe ₂ O ₃ ^Y	1.91	1.33	1.39	1.24	1.23	1.28	0.95	1.32	1.48	1.17	
FeO ^Y	1.91	1.33	1.39	1.24	1.23	1.28	0.95	1.32	1.48	1.17	
MgO	1.53	0.5	0.69	0.56	0.49	0.64	0.49	0.54	0.63	0.43	
MnO	0.02	-	-	0.01	-	-	-	-	-	0.01	
CaO	-	-	-	-	-	-	-	0.01	-	-	
Na ₂ O	1.40	1.46	1.29	1.37	1.34	1.27	1.18	0.42	0.96	0.91	
K ₂ O	8.99	8.95	9.61	9.46	8.82	9.07	9.35	7.07	8.51	6.88	
H ₂ O*	5.00	5.00	5.00	5.00	5.00	5.00	5.00	5.00	3.00	3.00	
Total	97.76	97.89	99.70	100.22	97.82	97.58	97.08	99.51	100.76	102.88	
Cations on basis of 24 anions	Si	6.13	6.17	6.20	6.12	6.40	6.17	6.20	6.29	6.55	6.71
	Al	1.87	1.83	1.80	1.88	1.50	1.83	1.80	1.71	1.45	1.29
	Al	3.12	3.39	3.35	3.46	3.41	3.38	3.44	3.60	3.93	4.14
	Ti	0.05	0.04	0.04	0.03	0.04	0.04	0.04	0.06	0.05	0.03
	Fe ³⁺	0.20	0.13	0.15	0.13	0.13	0.13	0.10	0.13	0.15	0.11
	Fe ²⁺	0.23	0.16	0.16	0.14	0.14	0.15	0.11	0.14	0.17	0.13
	Mg	0.32	0.10	0.14	0.11	0.10	0.13	0.10	0.10	0.13	0.09
	Mn	0.003	-	-	0.001	-	-	-	-	-	0.001
	Ca	-	-	-	-	-	-	-	0.002	-	-
	Na	0.38	0.39	0.34	0.36	0.36	0.34	0.32	0.11	0.25	0.24
K	1.59	1.57	1.66	1.62	1.55	1.61	1.67	1.20	1.47	1.15	
Mg/Mg+Fe _{TOT}	0.427	0.254	0.310	0.298	0.265	0.320	0.324	0.277	0.292	0.267	

Abbreviations: m(matrix muscovite)
c(coarse muscovite plates)

^YFe₂O₃, FeO Determined from Fe₂O₃/FeO ratios in muscovites from similar rocks given in Deér, Howie & Zussman (1962).

* H₂O contents used are those which give acceptable totals and are within the range given in Deér, Howie & Zussman (1962).

TABLE G

DISTRIBUTION COEFFICIENTS FOR GARNET-BIOTITE, STAUROLITE-BIOTITE PAIRS

Sample A405/	$K_{D_{Mg-Fe}}^{G-Bi}$	$K_{D_{Mg-Fe}}^{G-Bi}$	$K_{D_{Mg-Fe}}^{G-Bi}$	$K_{D_{Mn}}^{G-Bi}$	$K_{D_{Fe-Mg_{TRANS}}}^{Bi-G}$ (after Saxena 1969)		'C'	CORRECTED $K_{D_{Mg}}^{G-Bi}$ $(=0.7(Mn/Mn+Mg+Fe^{2+})^G + K_{D_{Mg}}^{G-Bi})$ $X_{Mg} = \frac{Mg}{Mg+Fe^{2+}}$ (after Albeé, 1965)	Sample A405/	$K_{D_{Mg-Fe}}^{St-Bi}$ $X_{Mg} = \frac{Mg}{Mg+Fe_{TOT}}$
	$X_{Mg} = \frac{M_g}{Mg+Fe_{TOT}}$	$X_{Mg} = \frac{M_g}{Mg+Fe^{2+}}$	$X_{Mg}^G = \frac{Mg}{Mg+Fe_{TOT}+Mn+Ca}$ $X_{Mg}^{Bi} = \frac{Mg}{Mg+Fe_{TOT}+Mn}$	$X_{Mn} = \frac{Mn}{Mn+Mg+Fe}$	$X_{Fe} = \frac{Fe_{TOT}}{Mg+Fe_{TOT}}$	$X_{Fe} = \frac{Fe^{2+}}{Mg+Fe^{2+}}$				
M24	0.172	0.137	0.119	64.97	-0.6285	-0.6426	1.67	0.30	M24	0.233
E2A	0.216	-	0.173	73.18	-0.4888	-	-	-	BC38	0.267
E4E	0.207	0.144	0.155	115.80	-0.5538	-0.5705	1.68	0.28	BC34a	0.258
E4B	0.214	0.160	0.145	48.98	-0.5722	-0.5767	1.88	0.34	E4E	0.294
Average	0.199	0.147	0.148	81.93	-0.5688	-0.5966	1.74	0.31	BC37a	0.256
									Average	0.262

TABLE H

ANALYSES OF CALC-SILICATES (including an AMPHIBOLITE)

Sample A405/	MCS2a	MCS2c	BC45	BC18 Marinoan, Unit 1	BC40 Marinoan, Unit 3	E9S (Amphibolite)
Assemblage	Q, Pl, S, Bi (viii)	Pl, H, S, D (vi)	Q, Pl, H, E (v)	Q, Pl, S, Bi, C (viii)	Q, Pl, H	Pl, H, E (tr)
SiO ₂	57.51	55.79	64.75	60.16	78.76	46.96
Al ₂ O ₃	16.32	15.57	12.68	9.53	8.05	20.93
(Fe ₂ O ₃)	(n.d.)	(0.93)	(2.36)	(n.d.)	(0.81)	(2.11)
Total Fe as Fe ₂ O ₃	6.56	4.26	5.75	4.01	4.65	7.01
(FeO)	(n.d.)	(3.00)	(3.05)	(n.d.)	(3.46)	(4.41)
MnO	0.09	0.09	0.21	0.14	0.21	0.15
MgO	4.57	4.96	4.17	3.28	0.92	7.96
CaO	3.70	9.48	9.90	9.72	4.18	12.90
Na ₂ O	1.99	1.98	0.79	1.57	0.85	1.09
K ₂ O	5.85	4.35	0.65	2.77	0.07	0.13
TiO ₂	0.75	0.75	0.70	0.66	1.79	0.63
P ₂ O ₅	0.22	0.32	0.19	0.15	0.25	0.06
Ignition loss	0.70	0.82	1.04	7.38	0.07	0.87
Total	98.27	98.37	100.81	99.33	99.79	98.68
Oxidation ratio" After Chinner (1960)	n.d.	38.27	60.75	n.d.	31.89	48.90
H ₂ O	n.d.	n.d.	n.d.	0.95	n.d.	n.d.
Si/Al (as SiO ₂ /Al ₂ O ₃)	3.52	3.58	5.11	6.31	9.78	2.24
Ca/Al (as CaO/Al ₂ O ₃)	6.23	0.61	0.78	1.02	0.52	0.62

Abbreviations: Q(Quartz); Pl(Plagioclase); H(Hornblende); D(Diopside); E(Epidote); S(Scapolite); Bi(Biotite).

n.d. = not determined.

TABLE I

HORNBLLENDE ANALYSES AND FORMULAE

Sample A405/	BC45	MCS2c	BC40	E9S	
SiO ₂	47.42	51.51	42.26	46.14	
TiO ₂	0.32	0.12	0.40	0.58	
Al ₂ O ₃	9.03	3.53	15.67	12.48	
Fe ₂ O ₃ ^Y	4.03	3.84	6.53	3.26	
FeO ^Y	9.07	8.64	9.79	7.34	
MnO	0.42	0.14	0.77	0.14	
MgO	12.80	14.96	9.22	13.65	
CaO	12.18	12.31	10.88	11.86	
Na ₂ O	0.79	0.60	1.47	1.03	
K ₂ O	0.80	0.32	0.33	0.17	
H ₂ O*	2.00	2.00	2.00	2.00	
Total	99.66	98.61	99.77	99.15	
Cations on the basis of 24 anions	Si	6.99	7.55	6.29	6.72
	Al	1.01	0.45	1.71	1.28
	Al	0.48	0.13	0.88	0.75
	Ti	0.04	0.01	0.05	0.06
	Fe ³⁺	0.44	0.42	0.73	0.35
	Fe ²⁺	1.11	1.06	1.22	0.89
	Mn	0.05	0.02	0.10	0.02
	Mg	2.81	3.27	2.05	2.97
	Ca	1.92	1.94	1.74	1.85
	Na	0.23	0.18	0.43	0.30
K	0.14	0.05	0.06	0.04	

^YFe₂O₃, FeO Calculated using Fe₂O₃/FeO ratios of similar hornblendes given in Deer, Howie & Zussman (1962) vol. 2.

* H₂O values (assigned to give acceptable totals) are within the range given for Hornblendes of similar composition.

TABLE J

ANALYSES OF STRATOTYPE MARINO GROUP SEDIMENTARY ROCKS

AND THEIR PROPOSED METAMORPHIC EQUIVALENTS (given in brackets).

Sample A405/	MS1b maroon shale	MS2 maroon siltstone	MS3a calc- siltstone	(BC18) Unit 1	MS3b calc- siltstone	MS4a shale	(BC27') Unit 2	MS4a' shale	MS4b silty fine sandstone	(BC33a) Unit 2	MSS fine sandstone	(BC43) Unit 3
Major minerals present	Q,Pl,C,Cl	Q,Pl,C	Q,Pl,C	Q,Pl,S,Bi,C	Q,Pl,C	Q,Pl,C,Cl	Q,Pl,Bi,M	Q,Pl,C,Cl	Q,Pl,C,Cl	Q,Pl,Bi	Q,Pl,C	Q,Pl,Bi
SiO ₂	56.26	70.18	50.44	60.16	45.98	61.06	60.70	60.41	57.03	78.01	70.23	72.27
Al ₂ O ₃	11.29	7.28	9.13	9.53	8.54	11.06	15.82	11.00	5.27	9.38	8.11	11.55
(Fe ₂ O ₃)	(2.79)	(n.d.)	(1.46)	(n.d.)	(0.58)	(1.63)	(3.64)	(1.58)	(0.82)	(1.37)	(0.89)	(2.34)
Total Fe as Fe ₂ O ₃	4.92	2.79	4.29	4.01	3.58	4.47	8.27	4.55	2.68	4.67	4.60	6.82
(FeO)	(1.92)	(n.d.)	(2.55)	(n.d.)	(2.70)	(2.56)	(4.17)	(2.68)	(1.67)	(2.97)	(3.34)	(4.03)
MnO	0.21	0.19	0.12	0.14	0.10	0.11	0.12	0.11	0.13	0.08	0.09	0.12
MgO	5.70	1.21	3.36	3.28	2.52	3.46	3.71	3.34	1.60	1.48	1.62	2.17
CaO	5.96	7.33	14.43	9.72	18.00	6.93	2.57	7.56	15.61	1.71	5.00	1.41
Na ₂ O	1.79	2.65	1.71	1.57	1.67	1.84	2.15	1.83	1.39	2.81	2.09	3.65
K ₂ O	3.18	1.49	2.15	2.77	2.19	2.48	3.50	2.46	1.08	1.20	1.81	1.69
TiO ₂	0.65	0.41	0.67	0.66	0.58	0.76	1.08	0.76	1.24	2.38	0.74	0.97
P ₂ O ₅	0.18	0.15	0.17	0.15	0.18	0.17	0.22	0.17	0.08	0.26	0.11	0.05
Ignition loss	10.50	7.16	14.59	7.38	16.38	8.21	1.38	8.52	13.45	0.36	5.08	0.87
Total	100.64	100.80	101.05	99.33	99.71	100.53	99.80	100.71	99.25	101.97	99.42	100.71
H ₂ O	n.d.	n.d.	2.17	0.95	1.87	n.d.	1.63	2.72	1.37	n.d.	1.52	n.d.
Oxidation ratio	74.40	n.d.	53.38	n.d.	30.05	56.01	63.58 (av. unit 2 meta- shales = 54.57)	51.55	49.55	53.73	34.77	53.73
Si/Al (as SiO ₂ /Al ₂ O ₃)	4.98	9.64	5.52	6.31	5.38	5.52	3.84	5.49	10.82	8.32	8.66	6.26
Ca/Al (as CaO/Al ₂ O ₃)	0.53	1.01	1.58	6.97	2.11	0.63	0.16	0.69	2.96	0.18	0.62	0.12

Abbreviations: Q(Quartz); Pl(Plagioclase); C(Calcite); Cl(Clays); Bi(Biotite), M(Muscovite); n.d. = not determined.

TABLE K

ROCK ANALYSES OF TABLE J PRESENTED AS LOSS FREE

Sample A405/	MS1b Maroon shale	MS2 Maroon siltstone	MS3a Calc- siltstone (BC18) Unit 1	MS3b Calc- siltstone	MS4a Shale (BC27) Unit 2	MS4a Shale	MS4b Silty fine sandstone (BC33a) Unit 2	MS5 Fine sandstone (BC43) Unit 3				
SiO ₂	62.86	75.59	59.06	64.95	55.00	66.51	61.56	66.02	65.85	78.32	74.00	72.93
Al ₂ O ₃	12.62	7.85	10.69	10.29	10.22	12.05	16.04	12.02	6.09	9.42	8.55	11.65
Total Fe (AsFe ₂ O ₃)	5.50	3.01	5.02	4.33	4.28	4.87	8.39	4.97	3.09	4.69	4.85	6.88
Mno	0.24	0.20	0.14	0.15	0.12	0.12	0.12	0.12	0.15	0.08	0.09	0.12
MgO	6.37	1.30	3.93	3.54	3.01	3.77	3.76	3.65	1.85	1.49	1.71	2.19
CaO	6.65	7.90	16.90	10.50	21.53	7.55	2.61	8.26	18.02	1.72	5.27	1.42
Na ₂ O	2.00	2.86	2.00	1.70	2.00	2.00	2.18	2.00	1.60	2.82	2.20	3.68
K ₂ O	3.55	1.61	2.52	2.99	2.62	2.70	3.55	2.69	1.25	1.20	1.91	1.71
TiO ₂	0.73	0.44	0.78	0.71	0.69	0.83	1.10	0.83	1.43	2.39	0.78	0.98
P ₂ O ₅	0.20	0.16	0.20	0.16	0.21	0.18	0.22	0.19	0.09	0.26	0.12	0.05
Total	101.42	101.11	100.94	99.33	99.28	100.53	99.51	100.76	99.40	102.38*	99.61	101.62*

* High totals due to high SiO₂ value which results from devitrification of SiO₂-rich samples.

TABLE L

ANALYSES OF SOME MINERALS FROM CALC-SILICATES AND AN AMPHIBOLITE

Rock A405/ Mineral	E9S (Amphibolite) Plagioclase (bytownite)	E9S Hornblende (common)	BC45 Hornblende (common)	BC45 Epidote	MCS2c Hornblende (common) γ	MCS2c Scapolite (dipyre)	MCS2c Diopside (salite)	BC40 Plagioclase (bytownite)	BC40 Hornblende (tchermakitic)
SiO ₂	47.07	46.14	47.42	37.86	51.51	54.10	52.35	49.06	42.26
Al ₂ O ₃	35.01	12.48	9.03	25.21	3.53	23.59	0.85	34.63	15.67
Fe ₂ O ₃ *	trace	3.26	4.03	10.14	3.84	0.10	1.98	trace	6.53
FeO*	0.11	7.34	9.07	1.01	8.64	trace	5.94	0.07	9.79
MnO	0.03	0.14	0.42	0.14	0.14	-	0.10	-	0.77
MgO	0.04	13.65	12.80	0.07	14.96	0.01	13.58	0.01	9.22
CaO	17.31	11.86	12.18	23.31	12.31	8.85	21.72	15.70	10.88
Na ₂ O	1.69	1.03	0.79	0.02	0.60	8.59	0.33	2.53	1.47
K ₂ O	0.03	0.17	0.80	-	0.32	0.96	0.05	0.02	0.33
TiO ₂	-	0.58	0.32	0.20	0.12	0.01	0.02	0.01	0.40
H ₂ O [⊕]	-	2.00	2.00	2.00	2.00	0.10	0.3	-	2.00
(CO ₃ , F, Cl, SO ₃) [⊕]	-	-	-	-	-	4.00	-	-	-
Total	101.44	99.15	99.66	99.09	98.61	100.43	97.73	102.09	99.77

* Only total Fe determined by analysis; Fe²⁺, Fe³⁺ estimated from analyses by Deere, Howie & Zussman (1962) on minerals of similar compositions.

γ Analysis closest to that of common hornblende which is rich in Fe, poor in Mg.

⊕ Values within the range for minerals of similar composition.

Table M

COMPARISON WITH A NUMBER OF AREAS OF CRITICAL MINERALS AND MINERAL ASSEMBLAGES OF THE AMPHIBOLITE FACIES DEVELOPED AT SIMILAR GRADES⁺ TO THE NAIRNE-MT. BARKER CREEK AREA.

SHIOJIRI - TAKATO AREA, JAPAN. (low-pressure series- Miyashiro, 1973)		CENTRAL ABUKUMA PLATEAU, JAPAN. (low-intermediate pressure series- Miyashiro, 1973)		NAIRNE-MT. BARKER CREEK AREA (lower-grade rocks to the west, higher grades to the east.)		ERROL QUADRANGLE, NE APPALACHIANS, U.S.A. (Green, 1963; Thompson & Norton, 1968; Miyashiro, 1973).		NORTHERN MICHIGAN, U.S.A. (James, 1955; Miyashiro, 1973).		BURKE AREA, northern APPALACHIANS, U.S.A. (near intermediate pressure areas of NW and N-central Vermont-Woodland, 1963; Albee, 1965).			
Metapelites		Metapelites	Metabasites, Calc-silicates*	Metapelites	Metabasites, Calc-silicates*	Metapelites		Metapelites	Metabasites	Metapelites			
BIOT. AND ZONE Ch A SILLIM. ZONE K C Si Al		ZONE B Ch A Py MnO 10% Pl blue-green Ac MnO <10% (int. & calcic) Cpx green & brown CaHb (cs)		BIOT. ZONE AND ZONE STAUROLITE St F A Al ? Pl ? calcic blue-green & green ? Ep (cs)		STAUROLITE ZONE A Al F Si SILLIM. ZONE St		STAUROLITE ZONE St A Si SILLIM. ZONE Al		calcic Pl (An 80-100) green Ep Andesine green & brown Hb		F St Si A Al C A	
Stauroilite absent (possibly due to inapprop. bulk compositions or unfavourable oxygen fugacities)				Almandine garnets have around 5-10% MnO--similar to garnets from rocks of similar grade in the Central Abukuma Plateau, Japan.		Cordierite absent in regionally metamorphosed rocks, possibly due to inappropriate bulk compositions --(Hess, 1969)				Rare kyanite-only local-adjacent to granites. Early disappearance of stauroilite may be due to inapprop. bulk compositions or oxygen fugacity			
Abbreviations: Ca=calcite; Ch=chlorite; Cpx=clinopyroxene; A=andalusite Al=almandine; Py=pyralspite; C=cordierite; St=stauroilite; F=fibrolite Si=sillimanite; Hb=hornblende; Pl=plagioclase; Ep=epidote; Ac=actinolite K=K-feldspar						* "cs" signifies minerals from calc-silicates which are either not observed in metabasites or have differing ranges. † indicated by the horizontal dashed lines.							

TABLE N

AGE	ROCK GROUP	ROCK UNIT		
LOWER CAMBRIAN	KANMANTOO ³ GROUP	Tapanappa Formation		
		Talisker Calc-siltstone (106m)		
		Backstairs Passage Formation (1670m)		
		Carrickalinga Head Formation		
PRECAMBRIAN	ADELAIDE	Nairne Fault		
		Mt. Barker Quartzite Unit 4 (to 38m)		
		Unit 3 (440m)		
		Unit 2 (260m)		
		Unit 1 (390m) H.A*		
		SUPERGROUP	MARINO GROUP ²	Brighton Limestone (55m) E.A*
				Tapley Hill Formation (840m)
			STURT Belair Sub-group	Sturt Tillite (58m)
				Unit 5 (60m) ?
				Unit 4 (70m)
	TORRENS GROUP ¹	Unit 3 (55m)		
		Unit 2 (165m)		
		Unit 1 (60m)		
		Unit 7 (1020m)		
		Unit 6 (215m)		
		Unit 5 (205m)		
		Unit 4 (875m)		
	Unit 3 (255m)			
	Unit 2 (1980m)			
	Unit 1 Stoneyfell Quartzite (54m)			

- 1 Thicknesses estimated from pipeline excavations (except Br.LS)
- 2 Thicknesses measured in Mt. Barker Creek (incl. Brighton Limestone)
- 3 As 2; only base of uppermost unit examined
- 4 A disconformity at this level is proposed in the type area (Coats. 1967): no evidence of this break was found in this study.

TABLE 0

Correlation of the major tectonic elements generally used in the interpretation of the metamorphic history of the Mount Lofty Ranges (after Fleming, 1971) with those used in the Middleton area by Daily and Milnes (1973) and those of the present study of the Nairne - Mt. Barker Creek area.

Fleming(1971)	Daily and Milnes(1973)	This study
not generally recognized	pre-"S ₁ " bedding plane schistosity with accompanying mineral streaking L' ₁	F ₁ , S ₁
"F ₁ " , "S ₁ "	main phase of "F ₁ ", "S ₁ "	F ₂ , S ₂
"F ₂ " , "S ₂ "	"F ₂ " , "S ₂ "	F ₃ , S ₃
"F ₃ " , "S ₃ "	not observed	F ₄ *

* F₄ crenulations possibly post-date F₃ crenulations but the former are of very restricted development and their relationship is not certain.

APPENDIX I

DESCRIPTION OF THE SEQUENCE ALONG PART OF MT. BARKER CREEK

(Supplemented by Stratigraphic Column, Fig. A)

The major boundaries in the subdivision of the sequence described below are indicated. Reference to Map 1 shows the localities of these boundaries, these being marked by letters corresponding to those given below. Lesser boundaries are indicated by numbers corresponding to observation points recorded during the traverse along Mt. Barker Creek. Representative samples are indicated and their localities shown on Map 1, again by numbers corresponding to the recorded observation points.

STURT GROUP

(1) Upper levels of Tapley Hill Formation

- 0- 42 m Fine biotite schists grading to very micaceous metasiltstones. Well laminated and well bedded. Very dark grey where least weathered, with paler laminae which are calcareous (A405/BC1; locality 1).
- 42- 66 m Contact (A). Gradational contact. Increasing proportion of non-laminated, coarser metasiltstones and fine feldspathic metasandstones upwards. Contact placed at first metasandstones (locality 2).
- 66- 78 m Fine to medium-grained feldspathic metasandstones and arkoses. Pebbles to 0.5 cm in some coarser horizons. Weathered, non-calcareous. (A405/BC2; locality 3).
- 78-107 m Dark grey micaceous fine to medium-grained feldspathic metasandstones and minor metasiltstones, some containing scapolite. (A405/BC3, BC3(1) respectively, locality 4). Some horizons are very well laminated (A405/BC3(2)). The less micaceous beds appear to have the best developed lamination. Bands (to 30 cm) of very coarse, poorly sorted feldspathic metasandstones and arkoses are present. Bedding is poor and most outcrops are featureless. Grains are generally well rounded. (A405/BC4; near locality 4). Pebbles to 0.75 cm occur, these being restricted to horizons under 1.5 m thick.

APPENDIX I (cont'd)

(2) Brighton Limestone Equivalent

107-167 m Contact (B) obscured by soil (at 107 m). Lowest lithologies encountered are interbedded quartz-mica schists with variable calcite content. Calcite proportion increases over few metres, passing into a white coarsely crystalline massive marble with thin interbedded units of calcareous schist with laminae of calcite (to 2 cm). These units are usually laminated and lenticular, at most 40 cm thick (A405/BC5(1), BC6; locality 7). Units of almost pure marble are dominant throughout, reaching up to 10 m in thickness (A405/BC5; locality 6). Impure marbles (to 1 m) containing minor calc-silicates and quartz are grey and weakly laminated (A405/BC5(2); locality 7), these being most common near the base. Discordant calcite veins (to 20 cm) occur in the otherwise featureless massive marble units. Locality 8a marks the uppermost outcrop of Brighton Limestone Equivalent, approximately 55 m above the inferred base. This is probably close to the top, based on observations from float just to the north. Locality 11 is the inferred upper boundary, approximately 60 m above the base. The contact with overlying Marino Group is presumed conformable.

MARINO GROUP

(1) Unit 1 (392 m)

0- 57 m Predominantly well laminated feldspathic quartz-micaschists and metasiltsstones (A405/BC7; near locality 11), mainly as float. Lithologies gradually become less micaceous and coarser up sequence.

57-81 m Metasiltsstones and minor quartz-micaschists with well laminated horizons (A405/BC8; locality 12).

81-99 m Common interbeds of resistant weakly laminated, slightly feldspathic metasiltsstones, increasing to dominant lithology up sequence (A405/BC9; locality 14). Occasional well laminated horizons are present (A405/BC9(2); locality 14).

(99-179 m) Hallett Arkose Equivalent

99-141 m Gradation from lithologies below to mostly well laminated metasiltsstones (A405/BC11; near locality 17) with interbeds of less micaceous resistant metasiltsstones which are weakly laminated. Minor quartz-mica schists are present, grading into less micaceous metasiltsstones. Some horizons are calcareous (A405/BC12;

APPENDIX I (cont'd)

- 99-141 m (cont'd) near locality 17). Along strike to north, intervals of very feldspathic metasiltstone become common.
- 141-154 m Lithologies as at 141 m persist up sequence.
- 154-179 m Metasiltstones less micaceous and weakly to non-laminated, passing into fine feldspathic metasandstones. A moderate lamination is developed in some horizons and some rocks are calcareous. (A405/BC11(2); locality 19).
- 179-188 m Metasiltstones are generally well laminated and calcareous (A405/BC13; locality 21). Rocks are finer than the underlying strata. Cross-bedding with sets up to 40 cm near locality 21.
- 188-199 m Common pale very calcareous laminae (to 4 cm) in the metasiltstones (A405/BC14; locality 22).
- 199-250 m Interbedded less micaceous metasiltstones in the sequence of laminated, more pelitic metasediments. The interbeds are also calcareous but weakly laminated and contain scapolite. These become the dominant lithology up the sequence, well laminated units being less than 2.5 m thick. Samples of typical scapolite-bearing and scapolite-free lithology are A405/BC15(1) and A405/BC15 respectively (locality between 23 and 24).
- 250-259 m Non-laminated dark grey resistant fine metasiltstones.
- 259-272 m Dark grey weakly laminated fine metasiltstones, slightly calcareous in parts (A405/BC16; locality 26) with common scapolite porphyroblasts in some beds (to 5 cm).
- 272-327 m Weakly laminated fine metasiltstone with interbeds of more micaceous metasiltstones grading to quartz-micaschists. Abundant scapolite and minor hornblende occur in some beds (A405/BC17(2); locality 27), however most rocks are free of these minerals and scapolite is restricted to occasional thin laminae in general (A405/BC17, locality 27), or sometimes sparsely distributed in broader bands (to 20 cm). The abundance of scapolite-bearing laminae in some horizons results in a well laminated rock. Commonly scapolite beds are very lenticular, even on hand specimen scale (e.g. A405/BC17). Along strike, just over 0.6 km to the south, the equivalent interval consists of predominantly scapolite and hornblende-rich metasiltstones. Hornblende is

APPENDIX I (cont'd)

272-327 m (cont'd)

common in some horizons (which are typically lenticular) which pass into calc-silicates with minor mica and quartz (A405/BC23; locality 42). Rocks are commonly calcareous and well laminated. Beds with little scapolite are rare and under 2 cm thick (A405/BC23(1); locality 43).

327-333 m

Very well laminated metasiltsstones with common scapolite (+ minor hornblende) rich beds (to 3 cm thick). Scapolite-rich beds form over 50% of rock (A405/BC18; locality 29) and are often lenticular, down to hand specimen scale (A405/BC18). Occasional cross-cutting veins filled with scapolite and minor diopside occur (A405/BC18(1); locality 29).

333-347 m

Scapolite-rich beds a minor proportion of the metasiltsstones which are weakly laminated except in certain thin horizons (to 0.5 m, rarely to 1 m) where scapolite-rich beds (to 10 cm) are abundant, with a corresponding improvement in lamination. Along strike about 0.6 km to the south, the equivalent interval is richer in scapolite and hornblende on the whole. The well developed lamination encountered in some horizons to the north is largely destroyed by the abundance and grain size of the calc-silicate minerals (A405/BC24; locality 46). Minor folds of similar style occur in which the scapolite porphyroblasts are obviously extended along the axial plane schistosity (S_2) while the relative abundance of scapolite and hornblende follows the bedding. The intertonguing on all scales between scapolite and hornblende-rich metasiltsstones (grading to calc-silicates) and metasiltsstones which are poor in these minerals makes a fine subdivision of this interval impractical. The total scapolite-hornblende-bearing interval is approximately the same thickness in the south (localities 42-41) as in the north of Mt. Barker Creek (88 m; localities 26-30). Cross-bedding (with sets to 1 m) occurs at locality 33.

(347-392 m) (b) "Upper Arkose" Equivalent

Contact (at locality 30) sharp. An abrupt disappearance of scapolite and a coarsening of lithologies marks the base of the "Upper Arkose", which in the Marino Group stratotype overlies calcareous green and grey very fine siltstones and shales. The metamorphosed equivalents in Mt. Barker Creek (near location 30) are fine pale grey micaceous metasandstones (to micaceous

APPENDIX I (cont'd)

quartzites) which are slightly feldspathic, poorly bedded and generally non-laminated (A405/BC19, locality 31). The minor thin metasiltstone interbeds are weakly laminated. At locality 36, the lower contact is gradational over a few metres passing from scapolite-bearing metasiltstone to scapolite-free metasiltstones (A405/BC21) and very fine micaceous metasediments. Occasional thin interbeds (to 30 cm) of quartz micaschist occur (A405/BC22(1); locality 39). The metasediments are coarser in the vicinity of these localities (occasionally to medium-grained) but still only slightly feldspathic (A405/BC22). Rare arkose bands (medium-grained, to 5 cm thick) appear further south (A405/BC25(1); locality 48). Medium-grained feldspathic metasediments to 1 m thick (A405/BC25) are present to within a few metres of the top. Above, lithologies become finer and more pelitic, passing into weakly laminated metasiltstones (A405/BC26; locality 48).

(2) Unit 2 (263 m)

392-604 m Contact (C) gradational.

Weakly to well laminated metasiltstones grading to quartz-micaschists with lesser micaschist interbeds. Quartz-biotite segregations (to 4 cm) are present in some horizons and are developed along the bedding but partially deformed by the schistosity (A405/BC27(1); locality 49). Over about 4 m, the strata become well laminated, consisting of thinly interbedded (less than 1 cm) quartz-mica schists and micaschists with occasional (to 1 m) less micaceous metasiltstone interbeds which are sometimes cross-bedded on a small scale. The micaschists and some quartz-micaschists commonly contain abundant andalusite porphyroblasts, to 1 cm across (A405/BC27,28). The schistosity is sub-parallel or inclined at a very low angle (20°) to bedding in the schists and is deformed about the porphyroblasts (which are distributed along the bedding). A crenulation is commonly developed on schistosity surfaces. This is sub-parallel to a biotite lineation which is usually seen on bedding and schistosity surfaces and is consistently oriented down-dip (A405/BC29; locality 52). Higher in the sequence, quartz-biotite segregations are more common, forming distinct white lenses in the rocks (A405/BC30; locality 54), in beds up to 10 cm thick which can persist for over 20 m of strike length. Staurolite is common in some schists near the top of this sequence (A405/BC37; locality 74).

APPENDIX I (cont'd)

- (604-655 m) Transition to lithologies above.
- 604-620 m Above 604 m (locality 60) andalusite and micaschists less common. Increasing proportion of laminated quartz-micaschists and less micaceous metasiltsstones. Thin (to 30 cm) units of resistant metasiltsstone. Horizons to 4 m contain no andalusite. Quartz-biotite segregations absent. Very tight similar folds in quartz-micaschists at locality 61 (A405/BC31).
- 620-655 m Resistant metasiltsstones more common (A405/BC33), to 50 cm thick. Well developed staurolite crystals at locality 63 (A405/BC34). At locality 78, note a new layering forming parallel to the schistosity.
- (3) Unit 3 (441 m)
- (655-731 m) Member (a)
- 655-680 m Contact (D) gradational
Resistant metasiltsstones to 0.75 m thick become common. Some have been boudinaged, occasionally resulting in isolated lenses. The rocks are generally weakly to well laminated and typically non-calcareous. Higher in the sequence these massive units are over 1 m thick. Traces of andalusite (A405/BC38, locality 79) occur in the few schists.
- 680-697 m (localities 66-67; 80-81). A sudden increase in the proportion of resistant metasiltsstone to very fine metasandstone units at localities 66 (and 80 to the south) results in dominantly massive outcrops (A405/BC35) with thin more micaceous interbeds of metasiltsstones (grading to quartz-micaschists) which typically weather deeply. The resistant units show evidence of boudinaging and at locality 66, minor faulting is evident. It appears that some of the lenticular form of these units is of original sedimentary origin. Andalusite is absent.
- The lithologies become gradually more micaceous up the sequence, although the rocks are still dominantly massive metasiltsstones. The interbedded quartz-micaschists are less than 2.5 m thick and grade into less micaceous metasiltsstones. Numerous thin pegmatites (to 4 cm) are present in this interval, consisting of quartz + plagioclase ± muscovite.

APPENDIX I (cont'd)

- 697-709 m (localities 81-82). More pelitic interval. Dominantly metasiltsstones (A405/BC36) grading to quartz-micaschists in some horizons. Rocks are generally weakly to well laminated. Some interbedded less micaceous metasiltsstones occur, being usually less than 1.5 m thick (A405/BC40). Quartz-biotite segregations (to 6 cm) are common in some beds.
- 709-731 m (localities 82-83). Predominantly quartz-micaschists and very micaceous metasiltsstones with common andalusite in some horizons (A405/BC39). The less micaceous, more resistant metasiltsstone units are rare (to 0.75 m) in upper levels.
- (731-880 m) Member (b)
Contact (E) marks a gradational change to dominantly more pelitic strata.
- 731-799 m (localities 83-86). Very micaceous metasiltsstones grading to quartz-micaschists. Small scale similar folds are common at locality 83-84. Quartz-biotite segregations to 15 cm thick are present. In the upper 22 m of this interval, less micaceous metasiltsstones become more common. These grade into more pelitic lithologies and a recognition of distinct units is often impossible. Most rocks are laminated.
- 799-824 m (localities 86-87). Massive, resistant metasiltsstones grading to fine metasandstones with thin (to 1 m) more micaceous interbeds (to quartz-micaschists). Most rocks are laminated (A405/BC41).
- 824-880 m (localities 87-89). Metasiltsstones grading to quartz-micaschists with thin micaschist interbeds. Occasional less micaceous resistant metasiltsstone interbeds, ranging from 10 cm to 1 m in thickness. Minor andalusite occurs in thin (to 2 cm) micaschists (A405/BC42). Resistant metasiltsstones rare in upper 10 m and are less than 10 cm thick.
- (880-921 m) Member (c)
Contact (F) marks a thick unit consisting of common interbeds of resistant metasiltsstone in more pelitic metasiltsstones. The interbeds are generally less than 1.5 m thick and are often boudinaged. In the upper levels the resistant units are only up to about 40 cm thick, however these commonly grade vertically and laterally into the enclosing more micaceous rocks and distinct beds are generally absent. The least mi-

APPENDIX I (cont'd)

(880- 921 m) Member (c) (cont'd)

caceous rocks (A405/BC43; locality 90) are only weakly laminated, however with increasing mica content, lamination improves considerably.

(921-1018 m) Member (d)

Contact (G). Above, the lithologies are more micaceous.

921- 954 m (localities 90a-91). Very micaceous metasiltsstones with occasional interbeds of weakly laminated less micaceous metasiltsstones, typically less than 10 cm in thickness.

954-1018 m (localities 91-94). Occasional andalusite schist units (usually to 30 cm thick) consisting of interbedded mica-schists and quartz-micaschist. Some schistose units to 4 m thick are present, however these grade into metasiltsstones. Small-scale similar folds (A405/BC44) are common in some micaschists. Quartz-biotite segregations (occasionally folded) occur in some beds. They are usually less than 6 cm thick. At locality 93 are andalusite porphyroblasts to 1.5 cm across.

(1018-1096 m) Member (e)

Contact (H) marking a dominantly less pelitic interval above characterized by the abundance of resistant metasiltsstone interbeds.

1018-1056 m (localities 94-95). Interbeds of resistant metasiltsstone become more common up through the sequence, being less than 10 cm thick in the lower levels but reaching 40 cm (rarely 50 cm) in the upper levels. The thicker beds tend to grade into more micaceous metasiltsstones and do not have sharp boundaries. Most of these rocks are weakly laminated or non-laminated.

1056-1096 m (localities 95-97). Common horizons of thinly interbedded very micaceous metasiltsstones (grading to quartz-micaschists) with less micaceous metasiltsstone interbeds which are usually less than 15 cm thick. At locality 96 are small-scale folds in one such horizon which indicate refolding of earlier south-plunging folds by NE-plunging folds. Some kink structures are present nearby in quartz-mica schists.

APPENDIX I (cont'd)

- (4) Unit 4 (av. 22 m). Contact (I). This is a variable sequence consisting of layered calc-silicates and metasiltsstones with a highly variable content of calc-silicate minerals (hornblende and scapolite). A continuous range of lithologies is present, from calc-silicates to metasiltsstones (grading to quartz-mica schists). Because of the wide vertical and lateral variations in this interval, the sequence is best represented as a number of annotated stratigraphic columns, these being given in Figure 4. Their localities in Mt. Barker Creek are shown on Map 1 as are the locations of samples collected. Lower Contact (I) placed at first appearance of calc-silicate minerals.
- (5) Mt. Barker Quartzite. Contacts sharp. A lenticular massive ortho-quartzite, reaching a maximum of 11 m in thickness in the vicinity of Mt. Barker Creek. The variation in this unit is also best described with annotated stratigraphic columns (Fig. 4). The lower and upper contacts are sharp. Although the enclosing lithologies are generally weathered and do not normally outcrop at the boundaries, the quartzite is uniform in lithology up to its upper and lower limits.

KANMANTOO GROUP

- (1) (?) Carrickalinga Head Formation (Upper Member)
- Metasiltsstones with scapolite-rich beds grading into calc-silicates and marbles at certain levels. This unit is very thin in the vicinity of Mt. Barker Creek (0 - 9.5 m). The variation in thickness along Mt. Barker Creek and the relationships with the underlying and overlying strata is shown in the five stratigraphic sections measured (Fig. 4).
- (2) Backstairs Passage Formation (1673 m)
- (0 - 382 m) (a) Basal Member
- Contact with underlying strata variable (refer to Fig. 4).
- 0 - 84 m (localities 99, 130a-132). Grey massive fine (and occasionally medium-grained) metasandstones and lesser resistant metasiltsstones. Rocks weakly laminated in general although there are some well laminated horizons to 4 m (A405/BC48; locality 99). Occasional thin horizons (to 10 cm) are very well laminated and well bedded (flaggy). These are typically more micaceous, with

APPENDIX I (cont'd)

0 - 84 m (cont'd)

some beds passing into quartz-micaschists. Occasional less micaceous metasiltsstones are also flaggy but not as well laminated. The rocks become imperceptibly less micaceous up the sequence (A405/BC48(1); locality 100). Small to medium scale cross-bedding is developed in some metasandstone units.

84 - 121 m (localities 132-133). Predominantly well laminated very micaceous fine metasandstones and metasiltsstones (A405/BC53(1)) passing upwards into less laminated strata with well laminated horizons decreasing in thickness to under 1 m. Occasional less micaceous metasandstones are present but their boundaries are indistinct (A405/BC53(2)). Minor thin bands of very micaceous metasiltsstone (to quartz-mica schist) occur. These are generally less than 40 cm in thickness, however one such band at locality 133 is 3 m thick.

121- 189 m (localities 133-135). Lithologies less micaceous as a whole. Resistant metasiltsstones grading to softer, more micaceous metasiltsstones. Minor fine metasandstones (A405/BC54(1)), grading into metasiltsstones. Most strata are weakly laminated with thin (to 1 m) well laminated horizons (A405/BC54). Usually the more micaceous metasiltsstones exhibit the better lamination, however, some units (to 0.75 m) are very poorly laminated (A405/BC55). Up the sequence, well laminated horizons become thicker, reaching 5 m at some levels. At locality 134, cross-bedding is developed in fine metasandstones. Amplitude of the sets is 0.75 m.

189- 225 m (localities 135-137). Laminated very micaceous metasiltsstones, grading imperceptibly to more resistant less micaceous metasiltsstones. Distinct resistant units are less than 1 m in thickness and typically less well laminated. These occasionally grade into fine metasandstones.

225- 244 m (localities 137-138). Weakly laminated resistant metasiltsstones grading into fine metasandstones. Well laminated horizons occur, but are of minor significance, being less than 1.5 m in thickness. Thin (to 0.75 m) interbeds of very micaceous metasiltsstones and lesser quartz-micaschists (to 30 cm) are present.

244- 273 m (localities 138-140). Very micaceous metasiltsstones grading into resistant, less micaceous rocks. Generally weakly laminated with some well laminated horizons. Minor thin (to 50 cm) interbeds of fine metasandstones in the lower levels (A405/BC56).

APPENDIX I (cont'd)

273-303 m (localities 140-141). Fine metasandstones grading into metasiltstones in some horizons. Generally weakly laminated (A405/BC57) with thin (to 1 m) well laminated metasiltstones which sometimes grade into quartz-micaschists. Often, however, thin (to 0.75 m) quartz-micaschist units are poorly laminated. Cross-bedding of medium scale is present in some metasandstones.

303-357 m (localities 141-142). Resistant metasiltsstones which are generally weakly laminated. Thin horizons approach quartz-micaschists and are usually better laminated. Rare fine metasandstone interbeds are less than 50 cm thick and grade into metasiltsstones. The base of this interval is dominantly more pelitic than the bulk of strata, consisting of approximately 6 m of very micaceous metasiltsstones and minor quartz-micaschists which are fairly laminated.

357-382 m (localities 142-143). Resistant metasiltsstone interbeds (10 cm-75 cm) in more micaceous metasiltsstones.

(382-1616m) (b) Middle Member

Contact is placed at the first appearance of medium-grained metasandstones.

382-438 m (localities 143-145). Predominantly micaceous fine metasandstones grading to medium-grained metasandstones in some horizons (A405/BC59). The fine metasandstones also grade into metasiltsstones with no sharp boundaries between the units. Lamination is weak in most rocks, but some horizons are fairly well laminated. Metasiltsstones pass into quartz-micaschists in some horizons, these being usually less than 0.5 m thick.

438-463 m (localities 145-146). Fine to medium-grained metasandstones. Most horizons are laminated, with very well laminated units (to 0.75 m) which are more micaceous. Well laminated fine metasandstone and metasiltsstone units are also present (to 1 m). Slumping (mainly from the SE) is present at some intervals (e.g. locality 145). Small to medium scale cross-bedding is common, with sets of up to 40 cm. Large scours to depths of 15 cm are present in some laminated intervals, these being overlain by less laminated, coarser metasandstones (A405/BC60).

463-491 m (localities 146-147). More micaceous interval. Predominantly micaceous fine metasandstones grading to metasiltsstones and quartz-micaschists which are poorly laminated. Minor medium-grained metasandstones occur but grade into finer lithologies (A405/BC61).

APPENDIX I (cont'd)

- 491- 636 m (localities 147-153). Pass into coarser lithologies resembling interval 438-463 m. Medium-grained metasandstones and meta-arkoses become thicker (to 2 m) and more common up the sequence. These units are typically laminated and often cross-bedded. They imperceptibly grade into finer metasandstones higher in the sequence and individual units are difficult to distinguish except where these are interbedded with units of laminated fine metasandstones and metasiltsstones (to 1 m) which are often flaggy. The greater proportion of metasandstones and meta-arkoses become weakly laminated (A405/BC62; locality 148) up the sequence.
- 636- 668 m (localities 153-154). Fine metasandstones grading to metasiltsstones which are weakly laminated in general. At locality 154 is a 5 m thick metasiltsstone unit which is well laminated for about 3 m.
- 668-1418 m (localities 154-187). Sequence of predominantly well laminated to weakly laminated fine to medium-grained metasandstones and meta-arkoses with thin (to 1 m) units of more micaceous, flaggy metasandstones and metasiltsstones (grading to quartz-micaschists). Cross-bedding at low angles (to 20⁰) is very common, sets being usually less than 0.5 m but occasionally to 1 m in thickness. Slumping on a small scale is common at certain intervals (e.g. localities 164, 170, 176), the direction of slumping being primarily from the SE. A chaotic slump unit over 2 m in thickness at the 848 m level could be followed along strike for over 100 m (localities 170-172). Sample typical meta-arkose A405/BC63 (locality 184).
- 1418-1436 m (localities 187-188). Lithologies slightly finer in this interval. They are weakly to moderately laminated metasiltsstones with fine to medium-grained metasandstone interbeds (generally laminated) which are usually less than 1 m in thickness.
- 1436-1616 m (localities 188-202). Resembling interval 668-1418 however very micaceous metasiltsstones (to quartz-micaschists) are absent. Fine to medium-grained metasandstones and meta-arkoses form the dominant rock type (A405/BC64; locality 188). In the vicinity of locality 192 (approximately 1500 m level) low angle (10-30⁰) cross-stratification on a large scale is very common, resulting in fluctuations in readings on bedding orientation. Sets are usually less than 50 cm thick but very extensive laterally. At the 1515 m level (locality 193), ripple marks are well developed. At locality 197 are small folds in metasandstones. Quartz-biotite segregation

APPENDIX I (cont'd)

1436-1616 m (cont'd)

has occurred in some hinges. At the 1570 m level is a 50 cm unit of very micaceous metasiltstone (A405/BC65). A similar unit of 40 cm thickness occurs at 1593 m. Quartz-micaschists reappear in this unit, grading into less micaceous metasiltstone.

(1616-1673 m) (C) Upper Member

Contact is sharp.

1616-1673 m (localities 202-206). Predominantly non-laminated fine to medium-grained very micaceous feldspathic metasediments grading into metasiltstones in some horizons. Occasional thin horizons (to 1 m) are well laminated in the lower few metres. Quartz-biotite segregations are common in some intervals. Outcrops are typically rounded and featureless (A405/BC65; locality 202).

(3) Talisker Calc-Siltstone Equivalent (106 m)

Contact is gradational over several metres.

1673-1684 m (localities 206-207). Metasiltstones grading to fine metasediment units (to 1.5 m) and quartz-micaschists (A405/BC67). Over several metres the lithologies become more micaceous in general and very pelitic metasiltstones are the dominant rock type with minor less micaceous, resistant metasiltstone interbeds, to 50 cm thick.

1684-1696 m (localities 207-208). Quartz-micaschists and micaschists (A405/BC68). Rocks are commonly crenulated in the more micaceous beds.

1696-1741 m (localities 208-209). Fine micaceous metasediments and resistant metasiltstones which are weakly to non-laminated in general (A405/BC69). Minor more micaceous metasiltstone horizons occur, some rocks being almost quartz-micaschists (A405/BC69(1)).

(1741-1779 m) Nairne Pyrite Member

(Contacts (on Map 1) bound predominantly sulphide-rich strata).

1741-1752 m (localities 209-210). Pyritic very micaceous metasiltstones grading to quartz-micaschists and micaschists. Typical oxidised, gossanous outcrops (A405/BC70).

1752-1779 m (localities 210-211). Fine micaceous metasiltstones which are weakly to well laminated and pyritic. Rocks are partly oxidized but some pyrite remains. Jarosite veins are common in the more oxidized zones (A405/BC70(1)).

APPENDIX I (cont'd)

(4) Tapanappa Formation

Contact is sharp.

1779-1872 m (localities 211, 221-226). Micaceous fine to medium-grained feldspathic metasandstones which are weakly laminated in general but have occasional thin (to 30 cm) well laminated horizons. Finer, more micaceous intervals occur, these being metasiltsstones which grade into quartz-micaschists. The sequence becomes finer at higher levels, lithologies passing into fine metasandstones (A405/BC73(1)) and metasiltsstones. Occasional quartz-biotite segregations are up to 5 cm thick (A405/BC73). Above approximately the 1837 m level, metasandstones become more common (A405/BC74). These are weakly to moderately laminated in parts, however lamination is generally poor. Thin units (to 40 cm) of laminated very micaceous metasiltsstone (to quartz-micaschist) are often present.

1872-1902 m (localities 226-229). Predominantly very micaceous fine metasandstones which are poorly laminated in general (A405/BC74(1)). Thin horizons of better laminated, more micaceous metasandstones and metasiltsstones are still present. Fine to medium-grained metasandstones occur, usually less than 20 cm in thickness.

1902-1919 m (localities 229-231). Weakly laminated fine to medium-grained metasandstones with thin moderately laminated intervals. Minor metasiltsstone (to quartz-mica schist) units occur (e.g. lower 4 m). Small-scale slumping and cross-bedding is evident in some intervals (localities 229-230). Metasandstone beds are up to 2.5 m thick and are commonly interbedded with thin quartz-micaschists (to 30 cm). Occasional current ripples (very low angle) and some minor cut-and-fill structures are present.

1919-1943 m (localities 231-232).
Very micaceous fine metasandstones and metasiltsstones (A405/BC75) which grade into quartz-micaschists in some thin horizons.

1943-1963 m (localities 232-233)
Thinly interbedded fine metasiltsstones and micaschists. These are oxidized and pale yellow to red-brown in colour and were probably sulphide-rich (A405/BC76).

1963-1974 m (localities 233-234). Metasiltsstones grading to quartz-micaschists. Poorly laminated but the outcrop is very weathered.

APPENDIX I (cont'd)



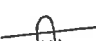



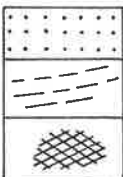
1974-1981 m (localities 234-235). Sulphide bearing fine metasilstones or metashales. Gossanous outcrop (A405/BC77).

1981-1991 m (locality 235-236). 2.5 m of quartz-micaschists passing upwards into fine to medium-grained metasandstones and metasilstones. Most rocks are weakly laminated.









APPENDIX II

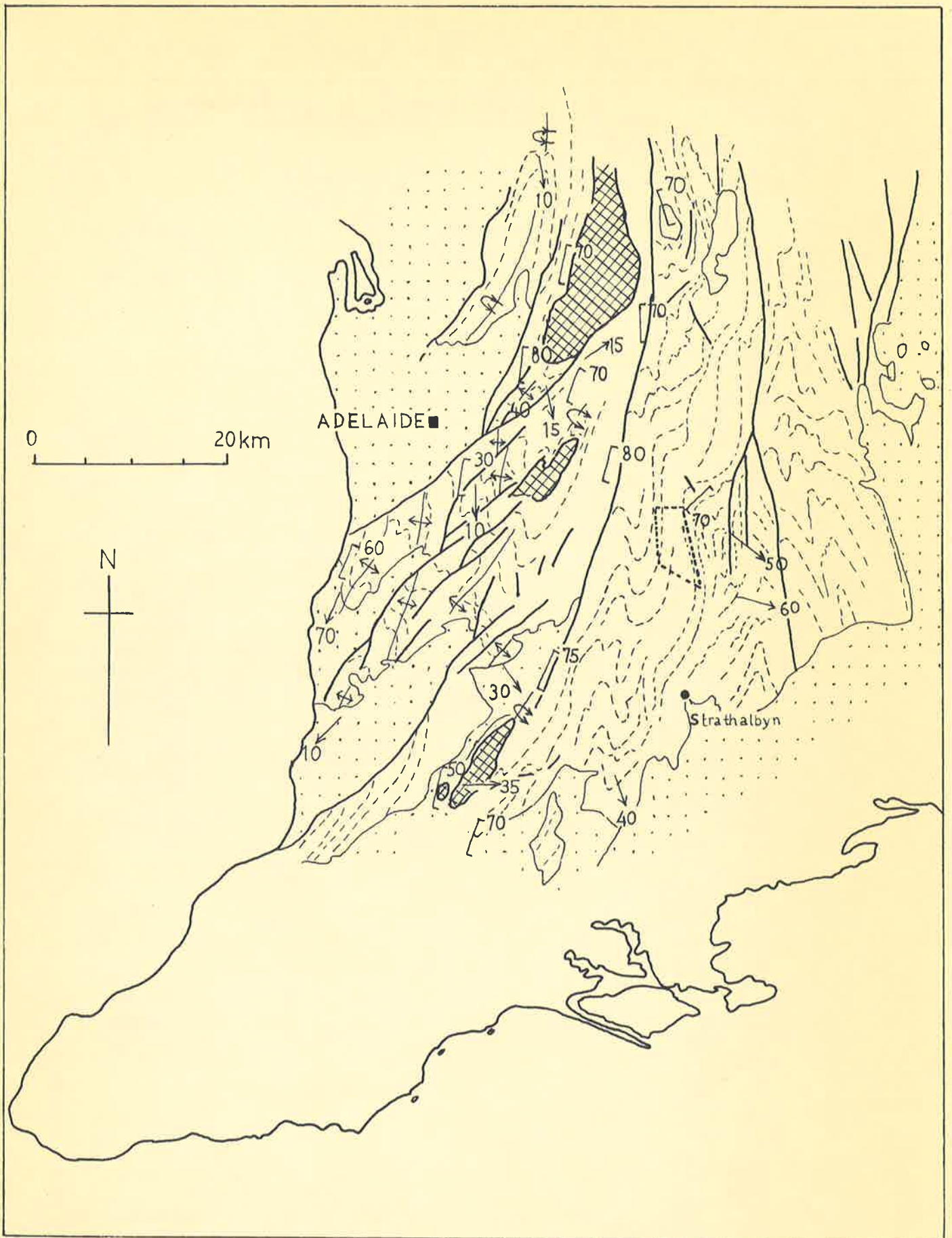
Structural maps of the Mt. Lofty Ranges in the vicinity of the Nairne-Mt. Barker Creek area (outlined) after Offler and Fleming (1968) and Fleming (1971).

A. Occurrence and orientation of F_1 structures

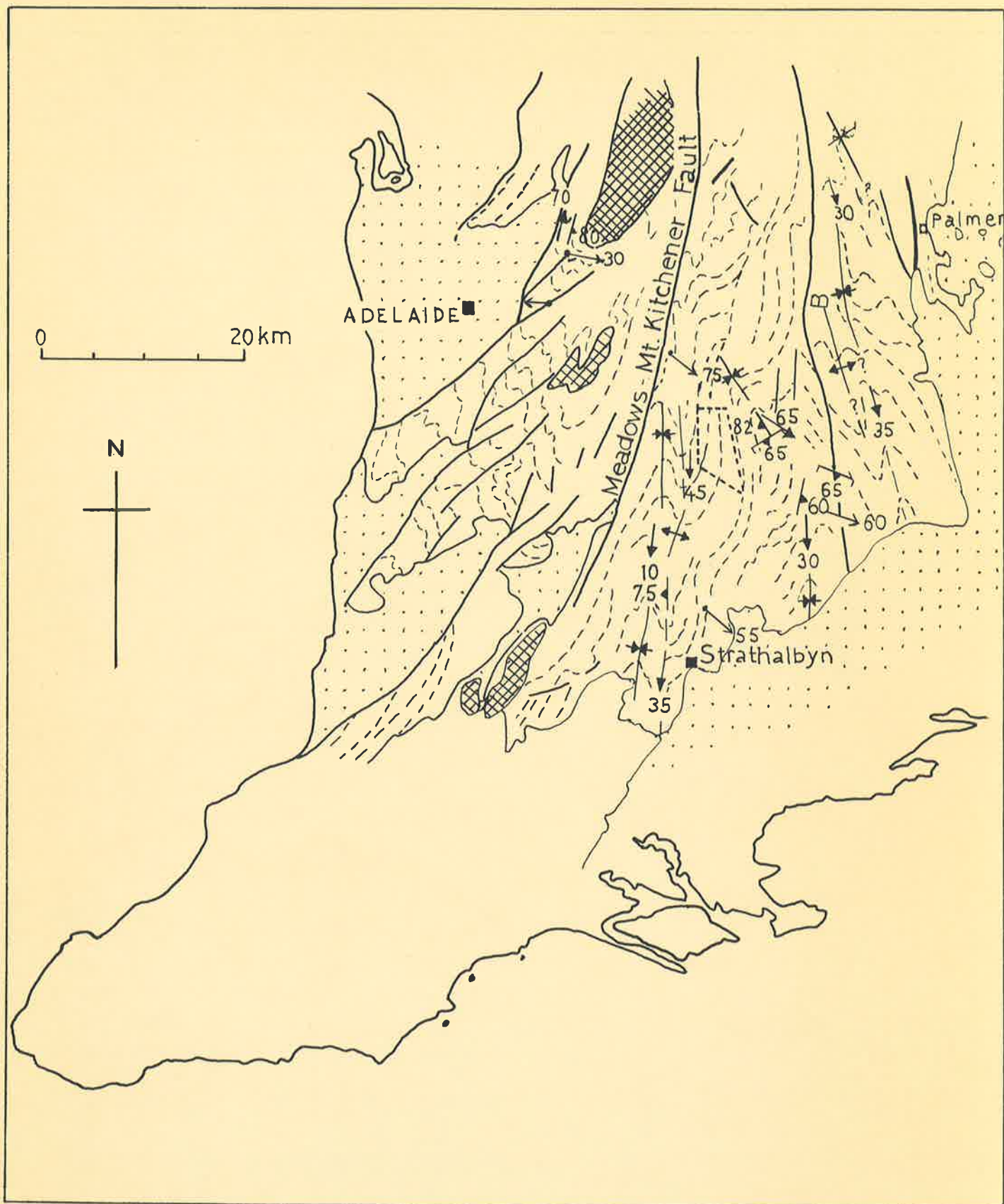
Symbols:		anticline
		syncline
		overturned anticline
		fault
		cleavage, schistosity S_1
		fold axis, F_1
		Post-Cambrian structural trends in Cambrian, Upper Precambrian Precambrian

B. Occurrence and orientation of F_2 and F_3 structures

Symbols:		F_2 anticline
		F_2 syncline
		crenulation cleavage, S_2
		F_2 fold axis
		F_3 anticline
		F_3 syncline
		crenulation cleavage, S_3
		F_3 fold axis.



A

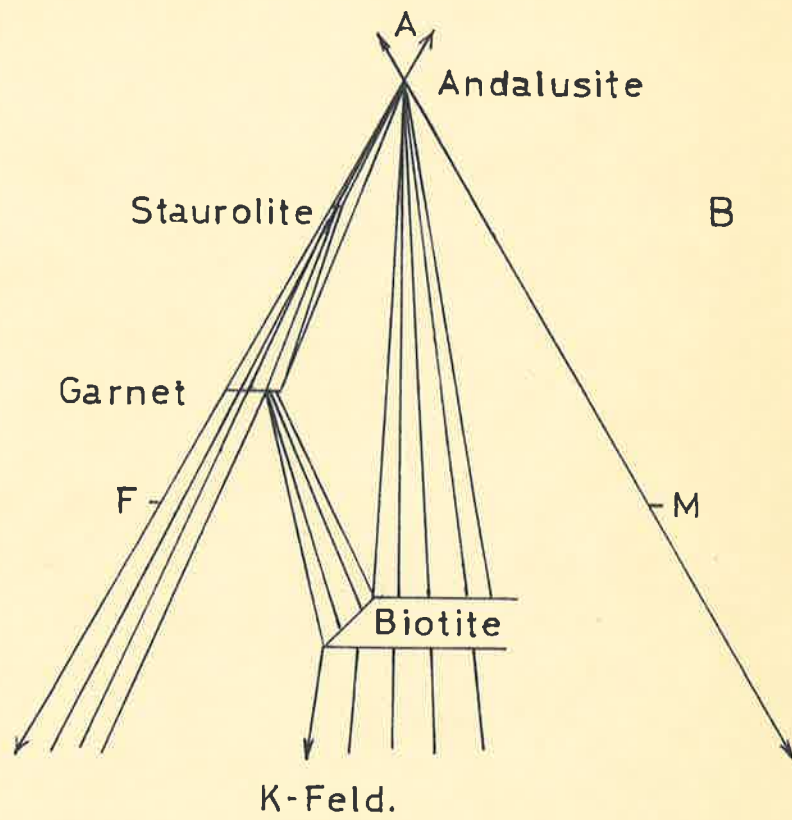
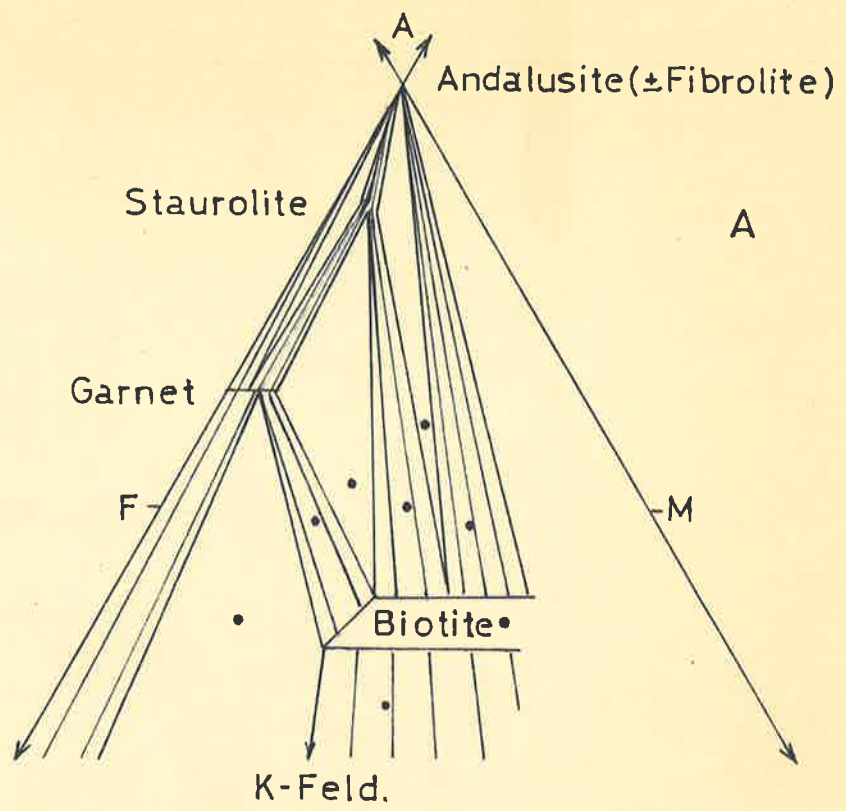


B

APPENDIX III

AFM plots of rocks in the Dawesley-Kanmantoo Area
after Fleming, 1971.

- A. Mineral assemblages in pelitic and semipelitic schists
- B. Andalusite + staurolite + garnet + biotite assemblages,
staurolite possibly having lower Mg/Mg+Fe ratio than
garnet.



APPENDIX IV

(A) Summary of the various textural associations observed in the Mt. Lofty Ranges, and in particular the Dawesley-Kanmantoo area relating to the direct and indirect transformation of andalusite to fibrolite (after P.D. Fleming, Ph.D. thesis, 1971, pp. 115-116).

1 Rare. Small clumps of elongate sillimanite prisms in andalusite porphyroblasts, lying approximately parallel to the andalusite cleavage.

2 Common. Fibrolite closely associated with biotite and quartz often forming mats, tufts and small sprays of needles. Nearest andalusites commonly have embayments filled by biotite and/or have portions of their boundaries indistinct when shared with biotite. Plagioclase and muscovite are not directly associated with these textures.

3 Common. Muscovite plates filling embayments in andalusite and adjacent biotite. Small granules of andalusite, grains of opaques and rare patches of biotite occur as islands within the muscovite. The granules of andalusite are in optical continuity with neighbouring andalusite porphyroblasts as are often biotite crystals and patches. Some quartz inclusions occur in muscovite. The edges of muscovite plates away from andalusite merge into fibrolite and xenoblastic biotite mats containing little or no quartz. Individual small prisms of fibrolite occur near the edge of the muscovite plates.

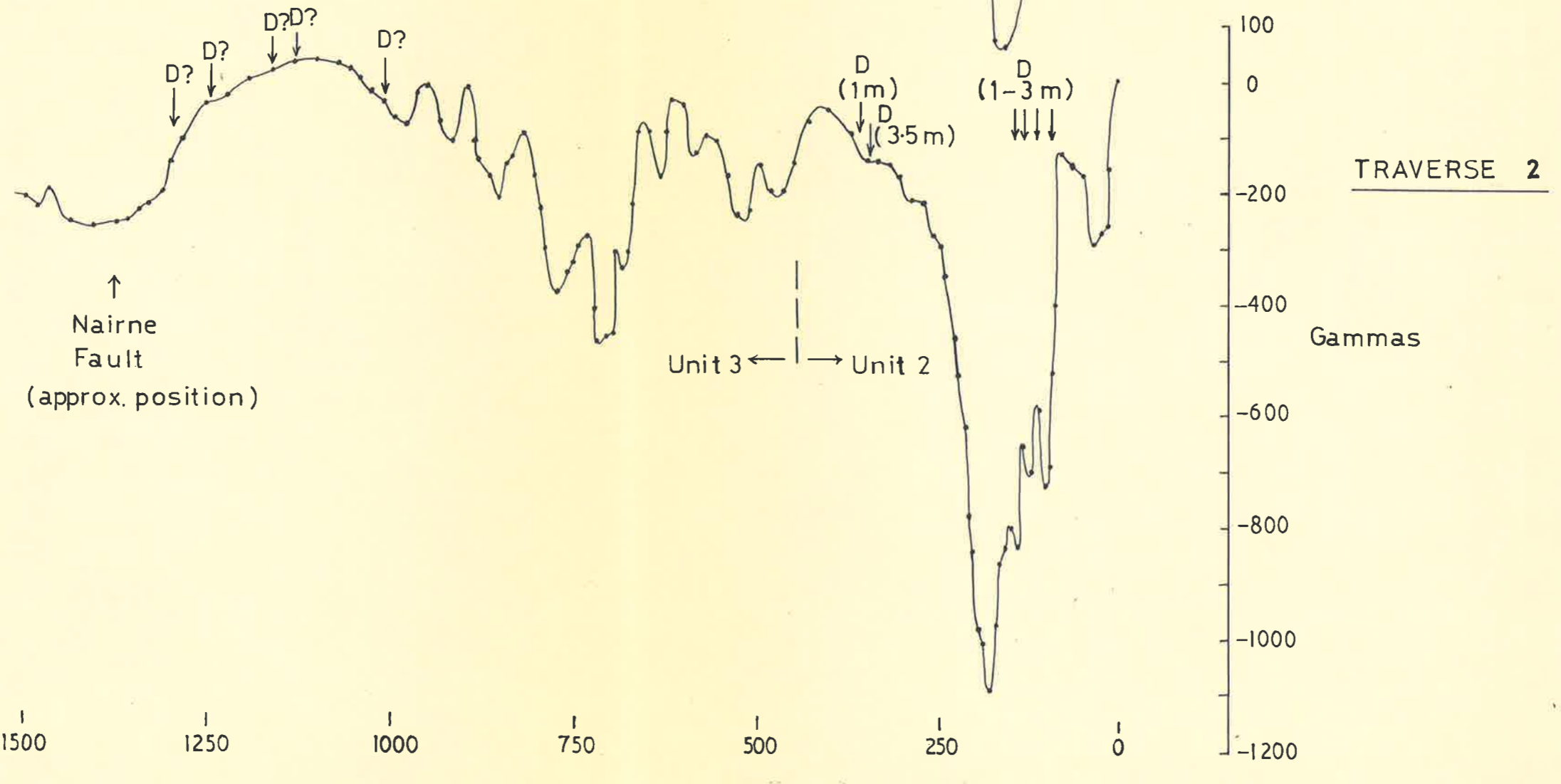
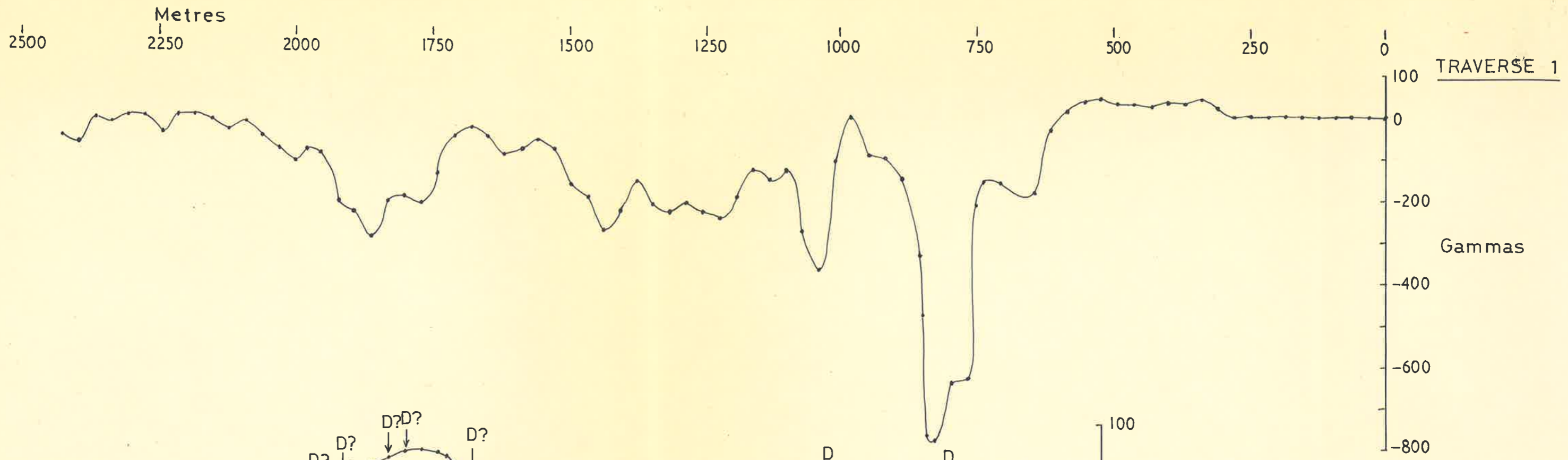
4 Similar to 3. Muscovite plates may also contain intimately associated biotite, fibrolite and quartz.

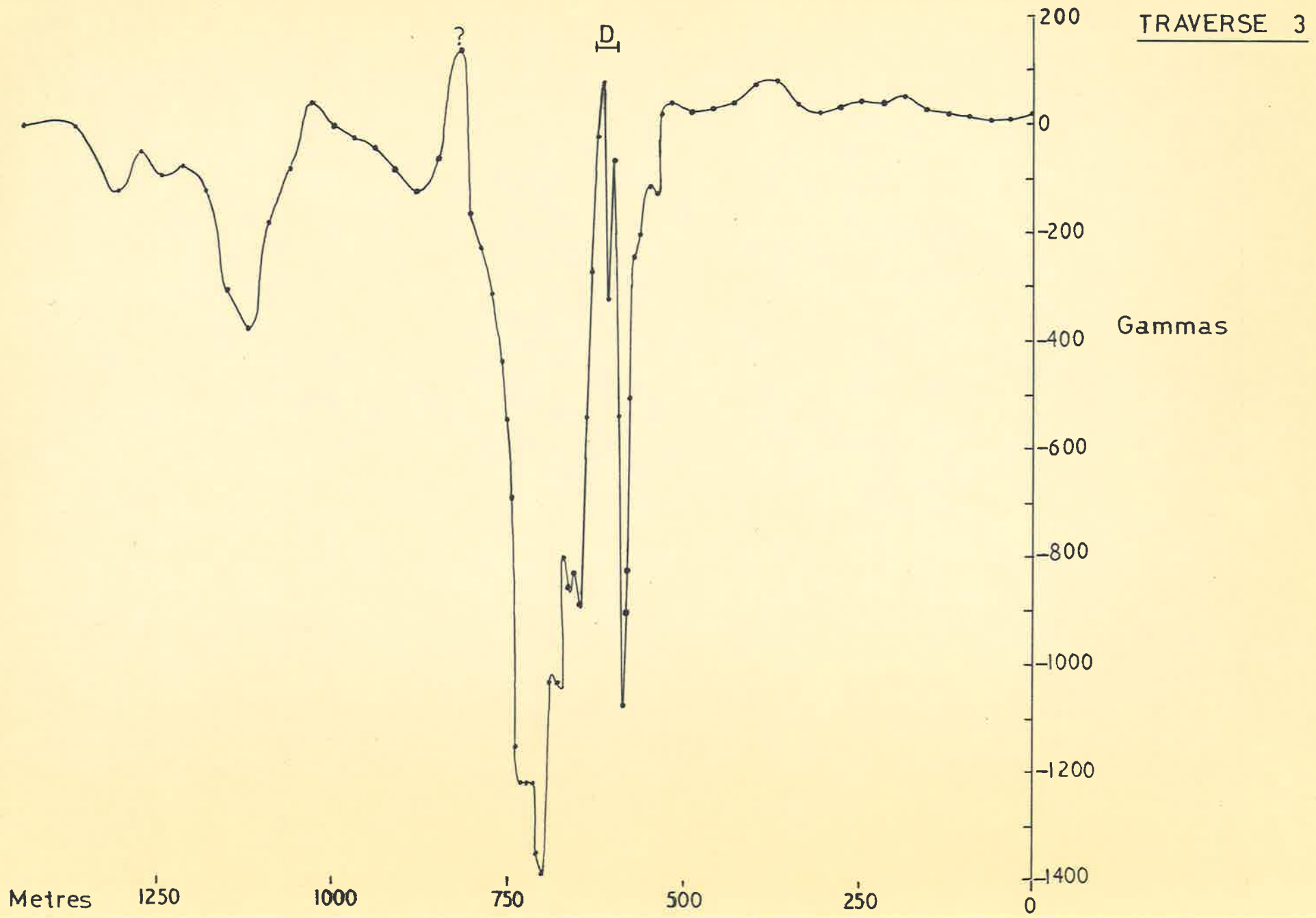
5 Fibrolite + biotite mats, tufts occurring near andalusite porphyroblasts which show little evidence of embayment or replacement by other minerals. Some mats continuous with aligned biotites in the matrix schistosity and contain no quartz.

APPENDIX V

Magnetic survey over Marino Group metasediments and metadolerite dykes in the vicinity of Nairne. The three traverses (T1, T2, T3) are shown on map 1.

Traverse 2 is situated 30 m north of the Mannum-Onkaparinga River pipeline and is parallel to it. Exposures of metadolerite dykes in the pipeline excavations are projected onto the line of traverse 2, and denoted 'D'. Inferred positions of dykes determined from float material alongside the excavations are denoted 'D?'. These positions are highly suspect. Traverse 1 is situated to the north of traverse 2 and runs perpendicular to the strike of the metasediments, and approximately perpendicular to the trend of the dykes. Traverse 3 is also perpendicular to strike, passing over a naturally outcropping dyke approximately 1 km due south of Nairne.





REFERENCES

- Abele, C., & McGowran, B. (1959): The geology of the Cambrian south of Adelaide (Sellick Hill to Yankalilla). *Trans. R. Soc. S. Aust.* 82, 301-320.
- Albe , A.L. (1965): Distribution of Fe, Mg and Mn between garnet and biotite in natural mineral assemblages. *J. Geol.* 73, 155-164.
- Albe , A.L. (1968): Metamorphic zones in Northern Vermont. In E-anZen, W.S. White, J.B. Hadley & J.B. Thompson (Eds.) "Studies of Appalachian Geology", 329-341 *Interscience*.
- Althaus, E. (1967): The triple point Andalusite-Sillimanite-Kyanite. *Contr. Mineral. Petrol.* 16, 29-44.
- Atherton, M.P. (1965): Composition of garnet in regionally metamorphosed rocks. In W.S. Pitcher & G.W. Flinn (Eds.) "Controls of Metamorphism," Chapt. 15. Oliver-Boyd, Edinburgh.
- Beger, R.M., Burnham, C.W. & Hays, J.F. (1970): Structural changes in sillimanite at high temperature [abs.] *Geol. Soc. Am. Abs with Program* 2, 490-491.
- Binks, P.J. (1966): Geology of the Horrocks Pass area. *Quart. geol. Notes, geol. Surv. S. Aust.* 20, 9-11.
- Butler, B.C.M. (1967): Chemical study of minerals from the Moine Schists of the Ardnamurchan area, Argyllshire, Scotland. *J. Petrology* 8, 233-267.
- Cameron, W.E. & Ashworth, J.R. (1972): Fibrolite and its relationship to sillimanite. *Nature Phys. Sci.* 235, 134-136.
- Campana, B., & Horwitz, R.C. (1956): The Kanmantoo Group of South Australia considered as a transgressive sequence. *Aust. J. Sci.* 18 (4), 128-129.
- Carmichael, D.M. (1969): On the mechanism of prograde metamorphic reactions in quartz-bearing pelitic rocks. *Contr. Mineral. Petrol.* 20, 244-267.
- Chakraborty, K.R. & Sen, S.K. (1967): Regional metamorphism of pelitic rocks around Kandra, Singbhum, Bihar. *Contr. Mineral. Petrol.* 16, 210-232.
- Chinner, G.A. (1960): Pelitic gneisses with varying ferrous-ferric ratios from Glen Clova, Scotland. *J. Petrology.* 1, 178-217.

REFERENCES (cont'd)

- Chinner, G.A. (1961): The origin of sillimanite in Glen Clova, Angus. *J. Petrology* 2, 312-323.
- Chinner, G.A. (1962): Almandine in thermal aureoles. *J. Petrology* 3, 316-340.
- Chinner, G.A. (1965): The kyanite isograd in Glen Clova, Angus, Scotland. *Miner. Mag.* 34, 132-143.
- Cloos, E. (1947): Study of oolite deformation, South Mountain Fold, Maryland. *Bull. geol. Soc. Am.* 58, 843-918.
- Coats, R.P. (1967): The "Lower Glacial Sequence" - Sturtian type area. *Quart. geol. Notes, geol. Surv. S. Aust.* 23, 1-3.
- Daily, B. (1963): The fossiliferous Cambrian succession on Fleurieu Peninsula, South Australia. *Rec. S. Aust. Mus.* 14, 579-601.
- Daily, B. (1976): New data on the base of the Cambrian in South Australia. *Izv. Akad. Nauk. Ser. geol.* 3, 45-52 (translation from Russian).
- Daily, B. & Milnes, A.R. (1971): Stratigraphic notes on Lower Cambrian fossiliferous metasediments between Campbell Creek and Tunkalilla Beach in the type section of the Kanmantoo Group, Fleurieu Peninsula, South Australia. *Trans. R. Soc. S. Aust.* 95, 199-214.
- Daily, B. & Milnes, A.R. (1972): Revision of the stratigraphic nomenclature of the Cambrian Kanmantoo Group, South Australia. *J. geol. Soc. Aust.* 19, 197-202.
- Daily, B. & Milnes, A.R. (1973): Stratigraphy, structure and metamorphism of the Kanmantoo Group (Cambrian) in its type section east of Tunkalilla Beach, South Australia. *Trans. R. Soc. S. Aust.* 97, 213-251.
- Deer, W.A., Howie, R.A. & Zussman, J. (1962): Rock forming minerals. Longmans, Green & Co. Ltd., London.
- Engel, A.E.J. & Engel, C.G. (1958): Progressive metamorphism and granitization of the major paragenesis, northwest Adirondack Mountains, New York. *Bull. geol. Soc. Am.* 69, 1369-1414.
- Ernest, W.G. (1960): The stability relations of magnesioriebeckite. *Geochim. cosmochim. Acta.* 19, 10-40.
- Ferguson, C.C. & Harte, B. (1975): Textural patterns at porphyroblast margins and their use in determining the time relations of deformation and crystallization. *Geol. Mag.* 112, 467-480.

REFERENCES (cont'd)

- Fleming, P.D. (1971): Metamorphism and folding in the Mt. Lofty Ranges, South Australia, with particular reference to the Dawesley-Kanmantoo area. Ph.D. thesis, Univ. Adelaide (unpub.).
- Fleming, P.D. & Offler, R. (1968): Pre-tectonic crystallization in the Mt. Lofty Ranges, South Australia. *Geol. Mag.* 105, 356-359.
- Forbes, B.G. (1976). Precambrian Geology. In Twidale, C.R., Tyler, M.J. and Webb, B.P., (Eds) "Natural History of the Adelaide Region." 5-10. (*R. Soc. S.Aust.*)
- French, B.M. and Eugester, H.P. (1965): Experimental control of oxygen fugacities by graphite gas equilibria. *J. geophys. Res.* 70, 1529-1539.
- Ganguly, J. (1968): Analysis of the stabilities of chloritoid and staurolite and some equilibria in the system $\text{FeO-Al}_2\text{O}_3\text{-SiO}_2\text{-H}_2\text{O-O}_2$. *Am. J. Sci.* 266, 277-298.
- George, R.J. (1967): Metamorphism of the Nairne Pyrite Deposit. Ph.D. Thesis, Univ. Adelaide. (unpubl.)
- Green, J.C. (1963): High level metamorphism of pelitic rocks in northern New Hampshire. *Am. Miner.* 48, 991-1023.
- Green, T.H. & Vernon, R.H. (1974): Cordierite breakdown under high-pressure, hydrous conditions. *Contr. Mineral. Petrol.* 46, 215-226.
- Guidotti, C.V. (1968): Prograde muscovite pseudomorphs after staurolite in the Rangeley-Oquossoc areas, Maine. *Am. Miner.* 53, 1368-1376.
- Guidotti, C.V. (1969): A comment on "Chemical study of minerals from the Moine schists of the Ardnamurchan area, Argyllshire, Scotland", by B.C.M. Butler, and its implications for the Phengite Problem. *J. Petrology.* 10, 164-170.
- Harry, W.T. (1950): Aluminium replacing silicon in some silicate lattices. *Miner. Mag.* 29, 142-149.
- Heath, G.R. (1963): Stoneyfell Quartzite: descriptive stratigraphy and petrography of the type section. *Trans. R. Soc. S. Aust.* 87, 159-165.

REFERENCES (cont'd)

- Heckel, P.H. (1972): Ancient shallow marine environments. In Rigby, J.K. & Hamblin, W.K. (Eds.) "Recognition of Ancient Sedimentary Environments." Spec. Publs. *Soc. econ. Palaeont. Miner., Tulsa.* 16, 226-276.
- Hensen, B.J. & Green, D.H. (1973): Experimental study of the stability of cordierite and garnet in pelitic compositions at high pressures and temperatures. III Synthesis of experimental data and geological applications. *Contr. Mineral. Petrol.* 38, 151-166.
- Hess, P.C. (1969): The metamorphic paragenesis of cordierite in pelitic rocks. *Contr. Miner. Petrol.* 24, 191-202.
- Hietanen, A. (1956): Kyanite, andalusite, and sillimanite in the schists in Boehls Butte quadrangle, Idaho. *Am. Mineral.* 41, 1-27.
- Hietanen, A. (1969): Distribution of Fe and Mg between garnet, staurolite and biotite in aluminium-rich schist in various metamorphic zones north of the Idaho Batholith. *Am. J. Sci.* 267, 422-456.
- Holdaway, M.J. (1971): Stability of andalusite and the aluminium silicate phase diagram. *Am. J. Sci.* 271, 97-131.
- Hollister, L.S. (1969): Metastable paragenetic sequence of andalusite, kyanite, and sillimanite, Kwoiek area, British Columbia. *Am. J. Sci.* 267, 352-370.
- Horwitz, R.C., Thomson, B.P. & Webb, B.P. (1959). The Cambrian-Precambrian boundary in the eastern Mt. Lofty Ranges region, South Australia. *Trans. R. Soc. S.Aust.* 82, 205-218.
- Horwitz, R.C. & Thomson, B.P. (1960): Milang map sheet, Geological Atlas of South Australia, 1:63,360 series (Geol. Surv. S.Aust: Adelaide).
- Hoschek, G. (1967): Untersuchungen zum Stabilitätsbereich von Chloritoid und Staurolith. *Contr. Mineral. Petrol.* 14, 123-162.
- Hoschek, G. (1969): The stability of staurolite and chloritoid and their significance in metamorphism of pelitic rocks. *Contr. Mineral. Petrol.* 22, 208-232.
- Hounslow, A.W. & Moore, J.M. (1967): Chemical petrology of Grenville schists near Fernleigh, Ontario. *J. Petrology.* 8, 1-28.
- Howchin, W. (1929): On the probable occurrence of Sturtian tillite near Nairne and Mount Barker. *Trans. R. Soc. S.Aust.* 53, 27-32.

REFERENCES (cont'd)

- Hsu, L.C. (1968): Selected phase relationships in the system Al-Mn-Fe-Si-O-H: A model for garnet equilibria. *J. Petrology*, 9, 40-83.
- James, H.L. (1955): Zones of regional metamorphism in the Precambrian of northern Michigan. *Bull. geol. Soc. Am.* 66, 1455-1488.
- Kleeman, A.W. & Skinner, B.J. (1959): The Kanmantoo Group in the Strathalbyn-Harrogate region, South Australia. *Trans. R. Soc. S. Aust.* 82, 61-71.
- Kretz, R. (1959): Chemical study of garnet, biotite and hornblende from gneisses of southwestern Quebec, with emphasis on distribution of elements in coexisting minerals. *J. Geol.* 67, 371-402.
- Kretz, R. (1960): The distribution of certain elements among coexisting calcic pyroxenes, calcic amphiboles and biotites in skarns. *Geochim. cosmochim. Acta.* 20, 161-191.
- Kretz, R. (1961): Some applications of thermodynamics to coexisting minerals of variable composition. Examples: orthopyroxene-clinopyroxene and orthopyroxene-garnet. *J. Geol.* 69, 361-387.
- La Ganza, R.F. (1959): Origin of the Nairne pyrite deposit (a discussion). *Econ. Geol.* 54, 333-335.
- Leslie, W.C. (1962): Geology of the Delamere area, South Australia. B.Sc. Honours thesis, Univ. Adelaide. (unpubl.)
- Link, P.K. (1976): Facies and palaeogeography of Late Precambrian Sturtian glacial sediments, Copley area, northern Flinders Ranges and in the Sturt Gorge near Adelaide, South Australia. B.Sc. Honours Thesis, Univ. Adelaide (unpubl.)
- Love, R.J. (1972): The geochemistry of the Tapley Hill Formation and Sturt Tillite, near Darlington, South Australia. B.Sc. Honours thesis, Univ. Adelaide (unpubl.).
- Lyons, J.B. & Morse, S.A. (1970): Mg,Fe partitioning in garnet and biotite from some granitic, pelitic and calcic rocks. *Am. Miner.* 55, 231-245.
- Madigan, C.T. (1927): The geology of the Willunga scarp. *Trans. R. Soc. S. Aust.* 51, 398-409.
- Marlow, P.C., (1975): Structural investigations near Macclesfield, South Australia. M.Sc. thesis. Univ. Adelaide (unpubl.).

REFERENCES (cont'd)

- Mawson, D. (1949): A third recurrence of glaciation evidenced in the Adelaide System. *Trans. R. Soc. S. Aust.* 73, 117-121.
- Mawson, D. & Sprigg, R.C. (1950): Subdivision of the Adelaide System. *Aust. J. Sci.* 13, 69-72.
- Milnes, A.R., Compson, W. and Daily, B., (1977): Pre- to syn-tectonic emplacement of Early Palaeozoic granites in southeastern South Australia. *J. geol. Soc. Aust.* 24, 87-106.
- Milton, C. & Eugester, H.P. (1959). Mineral assemblages of the Green River Formation. In P.H. Abelson (Ed). "Researches in Geochemistry," 118-150. Wiley, New York.
- Misch, P. (1971): Porphyroblasts and "crystallization force": some textural criteria. *Bull. geol. Soc. Am.* 82, 245-252.
- Miyashiro, A. (1953): Calcium-poor garnet in relation to metamorphism. *Ibid.* 4, 179-208.
- Miyashiro, A. (1961): Evolution of metamorphic belts. *J. Petrology.* 2, 277-311.
- Miyashiro, A. (1964): Oxidation and reduction in the earth's crust with special reference to the role of graphite. *Geochim. Cosmochim. Acta.* 28, 717-729.
- Miyashiro, A. (1973): "Metamorphism and Metamorphic Belts". George Allen & Unwin Ltd.
- Mount, T.J. (1975): Diapirs and diapirism in the Adelaide "Geosyncline" South Australia. Ph.D. Thesis, Univ. Adelaide (unpubl.)
- Offler, R. (1963): Structural geology of the Strathalbyn anticline, South Australia. *Trans. R. Soc. S.Aust.* 87, 199-208.
- Offler, R. & Fleming, P.D. (1968): A synthesis of folding and metamorphism in the Mount Lofty Ranges, South Australia. *J. geol. Soc. Aust.* 15, 245-266.
- Pain, A.M. (1968): A study of the metadolerite dyke swarm in the Woodside district of South Australia. B.Sc. Honours thesis, Univ. Adelaide (unpubl.)
- Perchuk, L.L. (1967): The biotite-garnet geothermometer. Dokl (Proc.) Akad. Sci. U.S.S.R. *Geol. Sci. sect.* 177, 131-134.

REFERENCES (cont'd)

- Pettijohn, F.J. (1975): "Sedimentary Rocks", 3rd ed. Harper and Row, New York.
- Phinney, W.C. (1963): Phase equilibria in the metamorphic rocks of St. Paul Island and Cape North, Nova Scotia. *J. Petrology* 4, 90-130.
- Pitcher, W.S. & Read, H.H. (1960): The aureole of the main Donegal Granite. *Q. Jl geol. Soc. Lond.* 116, 1-36.
- Poole, L.E. (1969): The structural geology of an area south of Kanmantoo, South Australia. B.Sc. Honours thesis. Univ. Adelaide. (unpubl.)
- Ramsay, J.G. (1967): "Folding and Fracturing of Rocks". McGraw-Hill, New York.
- Rast, N. (1965): Nucleation and growth of metamorphic minerals. In W.S. Pitcher & G.W. Flinn (Eds) "Controls of Metamorphism," 73-102. Oliver & Boyd, Edinburgh.
- Reineck, H.E. & Singh, I.B. (1973): "Depositional Sedimentary Environments." Springer-Verlag, New York.
- Richardson, S.W. (1968): Staurolite stability in part of the system Fe-Al-Si-O-H. *J. Petrology* 9, 467-488.
- Richardson, S.W. (1970): The relation between petrogenic grid, facies series, and geothermal gradient in metamorphism. *Fortschr. Miner.* 47, 65-76.
- Richardson, S.W., Gilbert, M.C. & Bell, P.M. (1969): Experimental determination of kyanite-andalusite and andalusite-sillimanite equilibria; the aluminium silicate triple point. *Am. J. Sci.* 267, 259-272.
- Saxena, S.K. (1969): Silicate solid solutions and geothermometry. 3. Distribution of Fe and Mg between coexisting garnet and biotite. *Contr. Miner. Petrol.* 22, 259-267.
- Schreyer, W. & Seifert, F. (1969): High pressure phases in the system $MgO-Al_2O_3-SiO_2-H_2O$. *Am. J. Sci.* 267, 407-443.
- Schreyer, W. & Yoder, Jr. H.S. (1964): The system Mg-cordierite- H_2O and related rocks. *Neus Jb. Miner. Abh.* 101, 271-342.
- Scott, S.D. (1976): Application of the sphalerite geobarometer to regionally metamorphosed terrains. *Am. Miner.* 61, 661-670.

REFERENCES (cont'd)

- Seifert, F. & Schreyer, W. (1970): Lower temperature stability limit of Mg cordierite in the range 1-7kb water vapour pressure : a redetermination. *Contr. Miner. Petrol.* 27, 225-238.
- Sen, S.K. & Chalkraborty, K.R. (1968): Magnesium-iron exchange equilibrium in garnet-biotite and metamorphic grade. *Neus Jb. Miner. Abh.* 108, 181-207.
- Shaw, D.M. (1956): Geochemistry of pelitic rocks, Part III, major elements and general geochemistry. *Bull. geol. Soc. Am.* 67, 919-934.
- Shido, F. (1958): Plutonic and metamorphic rocks of the Nakoso and Iritono districts in the central Abukuma Plateau. Tokyo Univ. Fac. Sci. *J. Sec. 2*, 11, 131-217.
- Skinner, B.J. (1958): The geology and metamorphism of the Nairne Pyritic Formation, a sedimentary sulphide deposit in South Australia. *Econ. Geol.* 53, 546-562.
- Sprigg, R.C. (1942): The geology of the Eden-Moana Fault Block. *Trans. R. Soc. S. Aust.* 66, 185-214.
- Sprigg, R.C. & Campana, B. (1953): The age and facies of the Kanmantoo Group. *Aust. J. Sci.* 16, 12-14.
- Sprigg, R.C. & Wilson, A.F. (1954): Echunga Map Sheet, Geological Atlas of South Australia, 1:63,360 series (Geol. Surv. S. Aust.: Adelaide).
- Sprigg, R.C., Whittle, A.W.G. & Campana, B. (1951): Adelaide Map Sheet, Geological Atlas of South Australia, 1:63,360 series (Geol. Surv. S. Aust.: Adelaide).
- Spry, A. (1963): The origin and significance of snowball structure in garnet. *J. Petrology*, 4, 211-222.
- Spry, P.G. (1976): Base metal mineralization in the Kanmantoo Group, South Australia. The South Hill, Bremer and Wheel Ellen areas. B.Sc. Honours thesis, Univ. Adelaide. (unpubl.).
- Strens, R.G.J. (1968): Stability of Al_2SiO_5 solid solutions. *Miner. Mag.* 36, 839-849.

REFERENCES (cont'd)

- Thompson, J.B. & Norton, S.A. (1968): Palaeozoic regional metamorphism in New England and adjacent areas. In E-an Zen, W.S. White, J.B. Hadley & J.B. Thompson (Eds). "Studies of Appalachian Geology, Northern and Maritime", 319-327. *Interscience*.
- Thomson, B.P. (1966): Stratigraphic relationships between sediments of Marinoan age - Adelaide region. *Quart. geol. Notes, geol. Surv. S. Aust.* 20, 7-9.
- Thomson, B.P. (1969): ADELAIDE Map Sheet, Geological Atlas of South Australia, 1:250,000 series. (Geol. Surv. S. Aust.: Adelaide).
- Thomson, B.P. (1969): The Kanmantoo Group and Early Palaeozoic Tectonics. In L.W. Parkin (Ed.) "Handbook of South Australian Geology", 97-108 (Government Printer, Adelaide.)
- Thomson, B.P., Daily, B., Coats, R.P. & Forbes, B.G. (1976): Late Precambrian and Cambrian geology of the Adelaide "Geosyncline" and Stuart Shelf, South Australia. 25th International Geological Congress, Australia, Excursion 33a guidebook.
- Thomson, B.P. & Horwitz, R.C. (1961): Cambrian-Precambrian unconformity in Sellick Hill-Normanville area of South Australia. *Aust. J. Sci.* 24, 40.
- Thomson, B.P. & Horwitz, R.C. (1962): BARKER Map Sheet, Geological Atlas of South Australia, 1:250,000 series. (Geol. Surv. S. Aust.: Adelaide).
- Tozer, C.F. (1955): The mode of occurrence of sillimanite in the Glen District, Co. Donegal. *Geol. Mag.* 92, 310-320.
- Turner, F.J. (1968): "Metamorphic petrology: Mineralogical and field aspects." McGraw-Hill, New York.
- Turner, F.J. & Weiss, L.E. (1963): "Structural analysis of metamorphic tectonites." McGraw-Hill, New York.
- Velde, B. (1965): Phengite micas : synthesis, stability and natural occurrence. *Am. J. Sci.* 263, 886-913.
- Willoughby, D.R. (1960): The geology and structural analysis of the northern part of Hallett Cove. B.Sc. Honours thesis. Univ. Adelaide (unpubl.)
- Wiltshire, R.G. (1975): The structural geology of the Old Boolcoomata area, South Australia. Ph.D. thesis, Univ. Adelaide (unpubl.)

REFERENCES (cont'd)

- Winkler, H.G.F. (1967): "Petrogenesis of Metamorphic Rocks". Springer-Verlag, New York.
- Woodland, B.G. (1963): A petrographic study of thermally metamorphosed pelitic rocks in the Burke area, northeastern Vermont. *Am. J. Sci.* 261, 354-375.
- Woodland, B.G. (1965): The geology of the Burke quadrangle, Vermont: *Bull. Vt. geol. Surv.* 28.
- Yoder, Jr., H.S. & Tilley, C.E. (1962): Origin of basalt magmas: an experimental study of natural and synthetic rock systems. *J. Petrology* 3, 342-352.
- Zen, E-an. (1969): The stability relations of the polymorphs of aluminium silicate : a survey and some comments. *Am. J. Sci.* 267, 297-309.